"POLYPROPYLENE/METAL OXIDE NANOCOMPOSITES: FIBER SPINNING AND EVALUATION"

Thesis submitted to

Cochin University of Science and Technology

in partial fulfilment of the requirements

for the award of the degree of

Doctor of Philosophy

Saisy K Esthappan

Department of Polymer Science and Rubber Technology
Cochin University of Science and Technology
Kochi- 682 022, Kerala, India

May 2012

"POLYPROPYLENE/METAL OXIDE NANOCOMPOSITES: FIBER SPINNING AND EVALUATION"

Ph. D Thesis

Author

Saisy K Esthappan
Department of Polymer Science and Rubber Technology
Cochin University of Science and Technology
Cochin- 682 022, Kerala, India
E-mail: saisyk@gmail.com

Guide:

Dr. Rani Joseph
Professor
Department of Polymer Science and Rubber Technology
Cochin University of Science and Technology
Cochin- 682 022, Kerala, India
E-mail: rani@cusat.ac.in

May 2012

Department of Polymer Science and Rubber Technology
Cochin University of Science and Technology
Cochin- 682 022, Kerala, India

Dr. Rani Joseph
Professor

Mob: +91 9446467850
E-mail: rani@cusat.ac.in

Certificate

This is to certify that this thesis entitled **"POLYPROPYLENE /METAL OXIDE NANOCOMPOSITES: FIBER SPINNING AND EVALUATION"** is a report of the original work carried out by **Ms. Saisy K Esthappan** under my supervision and guidance in the Department of Polymer Science and Rubber Technology, Cochin University of Science and Technology, Cochin-22. No part of the work reported in this thesis has been presented for any other degree from any other institution.

Dr. Rani Joseph
(Supervising Guide)

Cochin-22

Declaration

I hereby declare that the thesis entitled **"POLYPROPYLENE/METAL OXIDE NANOCOMPOSITES: FIBER SPINNING AND EVALUATION"** is the original work carried out by me under the supervision of **Prof. Rani Joseph,** Department of Polymer Science and Rubber Technology, Cochin University of Science and Technology, Cochin-22 and has never been included in any other thesis submitted previously for the award of any degree.

Cochin – 22
23/05/2012

Saisy K Esthappan

Dedicated to

My beloved Parents.....

Acknowledgements

First, let me bow before the Almighty God for being with me in every moment and giving me the strength to overcome all the hurdles. Without His blessings, I would not have been able to complete this thesis.

I would like to express my profound debt of gratitude to my supervising guide Prof. Rani Joseph for proper guidance, motivation and freedom throughout my research work. I am grateful to Prof. Eby Thomas Thachil, Head of the Department, Polymer Science & Rubber Technology and former head Prof. Thomas Kurian for giving necessary facilities and support during the research.

I would like to express my sincere thanks to Prof. K .E George, Prof. Sunil Narayanan Kutty, Prof. Philip Kurian, Jaya Teacher for the whole hearted cooperation throughout my research work. I express my gratitude to all the teaching and non-teaching staff of Department of Polymer Science & Rubber Technology for their support during these years.

I am grateful to Dr. Nasim, Associate Director, DMSRDE Kanpur for providing me all facilities during fiber drawing experiments. My sincere thanks to Dr. Mukesh Kumar Sinha, Dr. Anuraag Srivastav, Mrs. Priyanka Katiyar, Mr.Brij Kishore, Textile Department, DMSRDE Kanpur for their support to overcome all hurdles during the preparation of fibers. I am grateful to Dr. Shiny Palaty (Department of Chemistry, Bharat Mata College, Thrikkakara) for her support.

I am very thankful to my dear friend Vinayasree for being with me to share my pains and her concern during the days in Athulya hostel. At this moment I remember Nimisha and Sherin Antony for their love and caring . There are no words to express my gratitude to Bijesh K for his sincere friendship, timely help and caring.

I would like to express my deep sense of gratitude to Vidya G and Dr. Nimmi K P for their valuable help, support, motivation, love and caring. I will cherish the days spent with Asha Krishnan, Nisha Nandakumar and Cimi daniel for their sincere friendship and support extended to me. At this moment I remember Vijutha Chechi, Ayswarya E P, Misha Hari , Julie Jose, Jilu Varghese for their friendship that made the days I spent in the Athulya hostel a memorable one. I thank all my friends in Athulya hostel for their help and love.

I am immensely thankful to Renju chechi for her love, motivation and care. I am also thankful to Chinmayi and Sinuchettan. I am indebted to Pramila teacher and Ajalesh B Nair for their selfless help, consideration and love. I would like to express my gratitude to Syama P, Devi P V and Mary for their nice friendship.

I am gratefully acknowledge Sinto chettan for his valuable help, support, encouragement, advices and suggestions. I am also thankful to Suma teacher, Zeena chechi and Jenish Paul for their caring, love and support especially during conference days. I am grateful to Bipin sir and Dr. Anna Dilfi K F for their remarkable help to start my work. I would like to express my gratitude to Abhilash chettan especially for valuable suggestions during thesis preparation. I am grateful to Denny teacher and Preetha teacher for their prayers and affection. I would like to express gratitude to Sreejesh P R for his support during fiber preparation. I extend my gratitude to Manoj Sir, Jolly Sir, Neena George, Treasa Sunitha George, Newly chechi, Leny teacher, Sona Narayanan, Jabin teacher, Muralidharan M A, Vidhya Francis, Teena Thomas, Resmi V C, Shadhiya M A, Dr. Anoop Aanad, Vineetha Varkey, Dr. Saritha Chandran, Jayesh G, Dr. Ranimol Stephen, July Chechi, Binu Sir for the help rendered to me. I am also thankful to Sreedevi teacher, Sobha teacher, Midhun, Neena, Neethu, Divya and Soumya.

I am gratefully acknowledge Ms. Jelmi E J (Amritha Viswa Vdhyapeetham Coimbatore), Sunil paul, Eldho Elias (M G University Kottaym), Dr. Aby C P (Toyo University, Japan), Geetha Chechi (Dept. of Physics, CUSAT), Ullas G Kalappura (Dept.of electronics) for the valuable help during the anaslysis of samples. I would like to express my gratitude to Saritha G Bhat, Sherin, Rekha (Biotechnolgy, CUSAT) for the help during antibacterial studies. I express my gratitude to STIC, CUSAT for characterisation of the samples.

I would like to thank my parents for their love, prayers, care, patience and support, without which this thesis would not be a reality. I am grateful to my sister for her love, support and for being my best friend. I am also thankful to my brother, sister in law and our dear Elva.

Finally, I would like to thank all those who inspired, guided and accompanied me during the course of my life……..

Saisy K Esthappan

Preface

Polypropylene (PP) has been getting much attention over the years due to its excellent properties and low cost. It is used to make plastic bottles, fiber for clothing, components in cars etc. Properties of PP can be modified by using nanofillers to make it useful for engineering applications. Among various fillers, metal oxide nanoparticles exhibit a large variety of properties and can also be used as a reinforcing filler. Zinc oxide (ZnO) and titanium dioxide (TiO_2) are attracting attention due to its many significant physical and chemical properties like high chemical stability, low dielectric constant, high luminous transmittance, intensive ultraviolet absorption, antibacterial activity etc.

In the present work synthesis and characterization of ZnO and TiO_2 nanoparticles were done. Antibacterial properties of these materials were also studied. PP/metal oxide nanocomposites were prepared by melt mixing method and various properties were studied. PP/metal oxide nanocomposite fiber were prepared by melt spinning method and properties were evaluated. The thesis includes eight chapters:

Chapter 1 is an introduction and a review of the literature on polymer nanocomposites. Objectives of the present work are also discussed.

Chapter 2 describes synthesis, characterization and antibacterial properties of nano ZnO. This chapter discussed the preparation of ZnO particles by changing the preparation medium and properties are compared with commercially available ZnO. Chapter 3 describes properties of PP/ZnO composites films prepared by melt mixing and compression moulding. Effect of particle size of ZnO on various properties such as

mechanical, dynamic mechanical, processability, transparency, thermal and crystallization was described. Morphology, elemental composition and crystal structure of neat PP and composites are given in this chapter. Properties of composites after thermal ageing and photo ageing are also discussed. Chapter 4 describes preparation of PP/ZnO composite fibers through melt spinning and evaluation of its properties.

In chapter 5 crystal structure and particle size of TiO_2 prepared by sol gel and wet synthesis is discussed. Elemental composition and thermal stability are given in this chapter. Antibacterial properties of TiO_2 prepared by wet synthesis and commercially available TiO_2 are also reported. Chapter 6 focus on properties of PP/ TiO_2 composite films prepared through melt mixing and compression moulding. Effect of particle size of TiO_2 on the properties of PP are described in this chapter. Various properties of the composites after thermal and photo ageing are also discussed. Chapter 7 reports the melt spinning of PP/ TiO_2 nanocomposite fibers and evaluation of its properties. Chapter 8 is the summary and conclusion, future outlook of the study.

CONTENTS

.....ꕥ.....

INTRODUCTION

Contents

Nanotechnology is attracting worldwide attention due to its huge potential for wide range of applications. New physical and chemical properties arise when size of materials becomes smaller and smaller. Among various nanoparticles, metal oxide nanoparticles are attracting attention due to their applications in electronics, optoelectronics and used in different products such as sunscreens, toothpaste etc. Polymers have become extremely important in modern industrial society. They are used to make everything, from plastic bottles and fibers for clothing to components in automotives. Polypropylene (PP) has been getting attraction over the years due to its good performances, such as high mechanical properties and low cost.

The current research aims to investigate synthesis of zinc oxide (ZnO) and titanium dioxide (TiO_2) nanoparticles and the possibile use of these nanoparticles for fabricating PP based nanocomposites and fibers and thereby imparting several properties to PP. In this chapter, a concise introduction to PP, composites, nanocomposites, fibers and nanomaterials are given.

1.1 Composites

Throughout the history of human civilization, modification have been done in materials of construction. Earlier, mud was combined with straw to improve the performance and strength of the composite structure to build some of humankind's monuments. Hence, the use of inexpensive materials to upgrade the performance of commodity materials is not a new idea. Today, cost-effective materials have been continuously developed and expanded for various materials of construction.

Composites are materials with two or more distinct components that combine to give characteristics superior to those of the individual components. A polymer alone can not provide all the superior properties like strength, thermal stability, flame retardancy, UV stability etc. Additives are used to enhance properties of polymer. Mineral fillers, metals and fibers have been incorporated to plastics and elastomers to make composites. The effect of fillers on properties of the composites depends on their concentration, particle size, shape and on their interaction with the polymer. A composite material can be defined as a macroscopic combination of two or more distinct materials, having recognizable interface between them. Composites are made up of continuous and discontinuous phase. The discontinuous phase that is stiffer and stronger than the continuous phase is called the reinforcement and the so called continuous phase is referred to as the matrix. The constituents retain their identity; they do not dissolve or merge completely into one another. Composites provide design fabricator, equipment manufactures and consumers with sufficient flexibility to meet the demands presented by various environments and special requirements. Depending on the size of the fillers, composites can be classified into microcomposites and nano composites. In microcomposites the size filler particle is above 100nm and in nanocomposites

size of filler is below 100nm. Nanocomposites attracted great attention after the growth of nanotechnology.

1.1.1 Nanocomposites

The term nanocomposites describe a two phase material where at least one of the phases is in nanometer range. Nanotechnology is one of the most promising areas for technological development. In material research, the development of polymer nanocomposites contain significantly less amount of filler and there is a great retention of the inherent processability of the neat polymer. Polymer nanocomposites exhibit improvement in properties like mechanical strength, thermal stability, flame retardancy, chemical resistance, surface appearance, electrical conductivity etc.

These enhancements in performance are observed at lower concentration of nano filler [1-6]. Polymer nanocomposites are also developed for electronic application such as thin film capacitors in integrated circuits and solid polymer electrolytes for batteries. It is a field of wide research interest with remarkable technological promise [7-10].

Other applications of nanocomposites include enhancement in barrier property by the addition of small amount of nano fillers [11,12]. Remarkable effects on the transparency and haze characteristics of films have also been reported by the presence of nano sized fillers. Modification in crystallization behaviour in smaller spherulitic domain dimensions has shown by the addition of nano particles in to thermoplastic matrix. Nano reinforced polymers have shown a substantial enhancement in properties over existing polymer and composites.

The nanocomposites have found applications in various fields such as engine cover, timing belt cover, oil reservoir tank and fuel hose in automobile

industries [13]. Nanocomposites of nylon 6- clay hybrid show significant increase in modulus and heat distortion temperature. First example of industrial use of polymer-clay nanocomposites is timing belt covers made from nylon 6-clay by injection moulding [14,15]. Nanocomposites also find applications in the various fields such as interior and exterior body parts of automotives due to their improved dimensional stability, for use in multi layer polyethylene terephthalate bottles, tyre cords for radial wires, food grade drinking containers, electric component, sensors, sensitive areas like high corrosive environment, artificial bio implants etc. Among the various polymers, PP is one of the best matrix for nanocomposite preparation due to its wide range of applications compared to other polymers.

1.2 Polypropylene

PP was produced commercially about 55 years ago after the development of a suitable stereo-specific catalyst, which enabled the polymer to have the kind of structural characteristics useful for rigid products. The production of PP is expected to abide into the next millennium as raw materials in an expanding number of end-use products for the automotive and film industries. Earlier, the performance of PP was considered only between polyethylene and polystyrene. But, later, there is significant competition to substitute engineering polymers as materials of construction by PP base resins.

The substantial enhancement in PP usage is due to a combination of many factors besides a good physical and chemical properties. Because of appropriate melt rheology and thermal behaviour, PP-based materials are usually processable in various equipments ranging from injection moulding to some designed for use in other industries like calendaring and air-quenched blow film equipment. Additionally, lowest density among commodity plastics of approximately 0.90 g/cm^3, abide market diffusion of PP at the current rate

of growth is almost ensured on the basis of good mechanical properties at reduced cost. Because many major companies are designing their products, PP exist as the main product with the broadest design flexibility and simplicity of recycling. Its good thermal stability, low density, chemical and environmental inertness add to its attractiveness as the material of construction. PP became one of the most important thermoplastics used in a wide range of products like textiles, pipes, automotive parts, appliances and packaging materials. By the late 1970s, global demand of PP was less than 5,000 kton; 25 years later, demand has increased to 40,000 kton. With an expected annual growth of about 6%, it remains one of the fastest growing polymers over the years.

Due to the enhanced performance, there is an intense competition between the commercial polymers today. Polymer selection for any specific design is depends on their properties. The most common design characteristics are cost, temperature performance, toughness-stiffness balance, chemical resistance, electrical properties, long-term dimensional stability and environmental resistance. However, a polymer can often be selected according to their specific gravity, colourability, wear resistance, recyclability, material unification, foamability, mouldability, flammability, weldability, biodegradability etc.

Competitive penetration of PP into other applications has primarily taken place in polyethylene, polystyrene, polyvinyl chloride, thermoplastic polyester, nylon-6 or -6/6, and sometimes directly into metals or thermoset polymers like phenolic or reinforced reaction injection moulded urethane. Replacement of these polymers by PP is due to wide material design options, chemical resistance, heat resistance, recyclability, processability, economics and aesthetics [16].

1.2.1 Classification of PP based on stereo regularity

Stereochemical isomerism is possible in PP because propylene monomers can link together such that the methyl groups can be located in one spatial arrrangement or another in the polymer. If the methyl groups are all on one side of the chain, they are referred to as isotactic, and if they are on alternate sides of the chain, they are called syndiotactic PP. In these, each chain has a regular and repeating symmetrical arrangement of methyl groups that form different unit cell crystal types in the solid state. A random arrangement of methyl groups along the chain has no symmetry, and PP with this type of arrangement is known as atactic PP. Schematic representation of tacticity of PP is given in figure1.1.

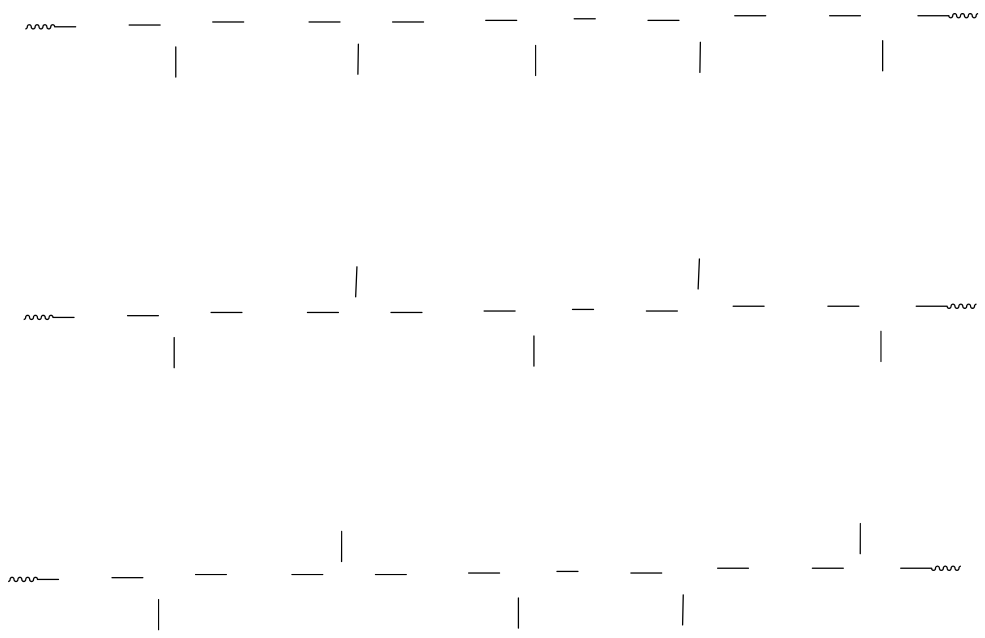

Figure 1.1: Schematic representation of Stereo isomers of PP

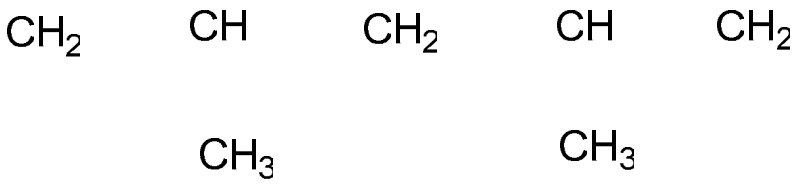

Isotactic PP (iPP) has excellent physical, mechanical and thermal properties when it is used in room-temperature applications [17]. It is stiff and has high melting point, low density and relatively good resistance to impact compared to others. These properties can be change by altering tacticity amount and distribution, the average chain lengths, the incorporation of a comonomer such as ethylene into the polymer chains and the incorporation of an impact modifier into the resin.

Atactic material is a soft, sticky, gummy material and used in sealants and other applications where its stickiness is preferred. Isotactic is crystalline whereas syndiotactic is far less crystalline and not a large volume commercial material.

The properties of PP in the melt state come from the average length of the polymer chains and the breadth of the distribution of the polymer chain lengths. In solid state, the main properties of the PP depends on the type and amount of crystalline and amorphous regions formed from the polymer chains. Semi crystalline PP consists of both crystalline and amorphous phases. The relative content of each phase depends on structural and stereo chemical characteristics of the polymer chains and the conditions under which the polymer is converted into final products such as fibers, films etc.

1.2.2 PP fibers and fabrics

A large volume of PP can be classified as fibers and fabrics. The advantages of PP fibers and fabrics are low specific gravity, which means greater bulk per given weight strength, chemical resistance and strain resistance. PP fibers and fabrics vary depending upon the manufacturing process as slit film, continuous filaments, staple fibers, bulked continuous filaments, monofilament, non woven fabrics and carpets [16].

1.2.2.1 Slit-film

In slit-film production, wide web extruded film, which is oriented in the machine direction by virtue of the take-up system, is slit into narrow tapes. These tapes are woven into fabrics for different end uses. Usually, non controlled rheology homopolymer of about 2- 4 g/l0 min is used for this. Higher flow rate resins allow higher extrusion speeds, but lower MFR resins result in a higher tenacity at a given draw ratio. An important application of slit-film is in carpet backings. Today, more carpet backing is produced from PP than from the natural jute fibers, which at one time were dominant. Jute suffers, from its unsteady supply situation, being affected by weather. Furthermore, PP is not subject to damaging moisture absorption and mold attack in high humidity. Slit-film also used in many other applications such as twine, woven fabrics for feed and fertilizer sacks, sand bags and bulk container bags, tarpaulins, mats, screens for erosion prevention and geotextiles to stabilize soil beds. Fibrillated slit-film is used as a face yarn in outdoor carpets and mats.

1.2.2.2 Continuous filament fibers

Continuous filament (CF) fibers are more conventional fibers than slit-film fibers in that each strand results from extrusion through its own die hole. PP homopolymer is extruded through small holes in a die called a spinneret, each spinneret containing somewhere around 150 holes each and spinning speeds are often high. The resulting filaments are very fine, being on the order of 5 denier per filament (dpf; a denier being defined as 1 g/9000 m). Therefore, to reduce viscosity, relatively high melt flow rate of PP, and high process temperatures are used. Extrusion takes place through several spinnerets at the same time. CF fibers are not crimped or texturized as produced. Such bulking can be imparted in a secondary process or the CF fiber yarns can be used as is, often in combination with other types of yarns.

1.2.2.3 Bulked continuous filament

Bulked continuous filament (BCF) processes are similar to CF processes, except that in BCF, a texturizer is an integral part of the process, to impart bulk to the fibers, through crimps or kinks. Commonly, BCF fibers are of 20 dpf, with yarns being in the vicinity of 2000 denier. PP homopolymer with melt flow rates (MFRs) in the range of 12-20 MFR and normal molecular weight distribution is typically used. BCF yarns are mainly used as carpet face yarns and in fabrics for upholstery.

1.2.2.4 Monofilament

As the name implies, single filaments are extruded; the molten filaments are cooled and solidified in a water bath and then drawn. Typically, monofilaments are fairly large, being on the order of 250 dpf. Rope and twine are produced by twisting bundles of monofilament together. PP rope and twine are strong and moisture resistant, making them very useful in marine applications.

1.2.2.5 Nonwoven fabrics

Nonwoven fabrics account for more PP usage than any other single fiber application. There are three types of nonwoven fabrics: thermo bonded, from staple fibers; spun bonded; and melt-blown. The fabrics from each process differ from each other in properties and appearance, and often combinations of two types are used together. Spun bonded fabrics are strong, whereas melt-blown fabrics are soft and have high bulk. Nonwoven fabrics are used in several areas, probably the most well known being for the liners in disposable diapers. At the other extreme, civil engineering fabric and tarpaulins are also produced from nonwoven fabrics.

1.2.2.5.1 Staple fibers

Staple fibers are short fibers, ranging from less than an inch to a little less than a foot in length, depending on the application. Staple fibers are spun fibers that are produced in either of two somewhat different processes. In the long-spin traditional process, fiber is spun similarly to CF fibers, wound undrawn in a tow in one step and then drawn, crimped and cut in a second step. The other staple fiber process is known as the short-spin or compact spinning process. This is a one-step process with relatively slow spinning speeds of about 300 ft/min, but one in which the spinnerets have an extremely large number of holes (>50,000). Overall, the process is more economical than the traditional process. Staple fibers can be carded and drawn into spun yarns in the same way as natural fibers, or they can be used in nonwoven fabrics. The PP resins used are usually homopolymers with MFRs from 10-30 g/10 min, depending on the application.

1.2.2.5.2 Spun bonded fabric

In this process, molten filaments are air quenched and then drawn by air at high pressure. To form a fabric, the filaments are then deposited on a moving porous belt to which a vacuum is applied underneath. Bonding of the fibers is accomplished by passing the fabric through heated calender rolls.

1.2.2.5.3 Melt-blown fiber/fabric

In the melt-blown process, polymer is extruded through a special melt-blowing die. The die feeds high-temperature air to the exiting filaments at a high velocity, and, in addition, the exiting filaments are quenched with cool air. In the process, drawn solidified filaments are formed very close to the die. Formation of the fabric is accomplished by blowing the filaments onto a moving screen. The melt blowing process requires resins that have very high melt flow rates, on the order of 500 g/ 10 min or higher. A resin of

narrow molecular weight distribution is also desirable. The fibers formed in the melt-blown process are very fine and allow for the production of lightweight uniform fabrics that are soft but not strong. Fabrics from fine melt-blown fibers can be used in medical applications because they allow the passage of water vapor but prevent the penetration of liquid water and aqueous solutions.

1.2.2.6 Carpets

PP carpets are commercially used on a large scale. For residential carpeting, dyebility and deep pile construction have been desirable. PP cannot readily be dyed, and therefore PP fibers are colored via the addition of pigments during extrusion. Pigmented fibers have a somewhat different appearance compared with dyed fibers, such as those from wool, nylon, and polyester. PP fibers have also been less resilient in deep pile than those from wool or nylon. However, with advances in technology in PP resins, fiber, and carpet construction, PP usage in residential carpets is steadily growing. Commercial carpets are of short pile, dense construction, and therefore resilliency of PP fibers is not an issue. Furthermore, for the same reason that PP cannot be dyed, it resists· staining and soiling. Since muted tones are desirable for commercial carpeting, the colors available from pigmentation are ideal. Also, pigmented fibers are more colorfast and fade less in sunlight. Moreover in pigmented fibers, the color does not just reside on the surface, it is distributed uniformly throughout; therefore, fiber breakage in rough treatment does not result in loss of color.

1.2.3 Applications of PP fibers

Even though synthetic fibers are in use since 1930s, it has replaced most of the natural fibers used today [18]. One of the most widely used of these fibers is iPP. iPP fibers show a wide range of properties and it is suitable for

various applications. These properties are dependent on the structure of the polymer and processing conditions. Hence, studying the structure development of iPP fibers during their formation gives information on the effect of various processing conditions on fiber structure and morphology. Even though PP is recently introduced synthetic fiber, its late entry contributed to be of advantage as the markets and fiber manufacturing technologies were already in place. PP can be used in any of the extrusion lines with only minor modifications. Due to the excellent properties and the processability of PP, some of the synthetic and natural fibers are replaced by PP. Recently, PP fibers are used in carpet, hygiene, medical, home furnishing, geotextile, packaging, filtration, agriculture, apparel applications etc.

Increase in production of PP fibers with maintaining high quality are the keys for its growth in market. PP fibers with different tenacities are produced according to market requirements. General textile fibers have tenacities between 4.0 - 6.0 g/den. High tenacity fibers up to 8.0 g/den are produced for the use in industrial applications such as ropes, nets etc [18,19]. PP fiber is one of the lightest synthetic fibers that are usually found in many products [20]. PP is one of the largely used polymer for producing man–made fibres especially for technical applications. PP fibres can withstand temperatures up to 140^0C before melting at about 170^0C. The density of PP is less than that of water, hence it float as ropes, nets, etc. Textile fibers are generally used in apparel, upholstery and carpets. Flame retardancy is an important and necessary property for some applications such as curtains, floor coverings etc. In accordance with the rapid developments in science and technology, the applications of textile fibers have also expanded to technical fields also. Fibers are now extensively used in the field of technical textiles such as military applications, safety and protective garments, automotive and aerospace

applications, electronic and optical devices, geotechnical applications and as additives to enhance polymer properties [20-23].

1.2.4 PP based nanocomposites

PP is extensively used in textiles, furniture, automobiles, electrical equipment and in packing industry [24]. It has good mechanical, thermal and electrical properties and shows excellent resistance to moisture, grease and oils. PP does not show stress-cracking problems and compared to polyethylene, it shows excellent electrical and chemical resistance at higher temperatures. Addition of nanoparticles in to polymer matrix could show dielectrics with new and enhanced properties. Extensive reserach have been conducted to broaden the applicability of PP by increasing its strength and toughness [25-27]. A Reinforcement of PP with small amount of nanoparticles could improve the mechanical properties and flame resistance and may enhance dielectric properties.

Variety of particulate fillers are successfully used in PP to enhance its performance, and to widen its application to fields where other engineering thermoplastics have been used. Most commonly used fillers in PP are talc, calcium carbonate, glass fiber, mica, silica, glass beads, clay, carbon nanotubes (CNTs) etc. Factors that affect the properties of the composites are particle size, specific surface area, hardness, chemical composition, interface chemistry, filler morphology and degree of purity of fillers. When the particle size is reduced, there is an improvement in strength and modulus with a decrease in deformability.

Several studies have reported improvements in mechanical, thermal, electrical and flammability properties of PP with the incorporation of different nano-sized fillers like clay, $CaCO_3$ etc [28-35]. Mechanical properties of PP

are also increased by melt mixing with particulate fillers such as talc, mica, clay [36-39] and glass, jute, aramid, and carbon fibers fillers [40-44] and also by melt blending with other polymers [45-48]. Single wall carbon nanotubes (SWNTs) are also good candidates for reinforcing various polymer matrices due to their high tensile strength and modulus [49-51]. Extensive investigations have been done to modify PP by the incorporation of various fillers [52-85].

Jianguo Tand et al studied the effects of organic nucleating agents and ZnO particles on the crystallization of iPP [86]. Crystallization behaviour and mechanical properties of iPP composites with crosslinked styrene- butadiene nanoparticles contain sodium benzoate was studied by Zhang et al. [87]. Enhancement of stiffness of these nanocomposites is due to high nucleation density and the crystallization kinetics of iPP proceed faster in the presence of ultrafine elastomeric particles with length scales below 100 nm [87]. Gui et al [88] reported that nucleation density of iPP is increased with the addition of an organic phosphorus nucleating agent. Inorganic nanoparticles are also added as nucleating agents for iPP [89].

Research has revealed that the morphology of PP, is affected by the presence of fillers like carbon, glass, poly(ethylene terephthalate) and polyimide [90-96]. Nano reinforcement enhances the mechanical and other properties including changes in polymer crystallization behaviour is reported [97-103]. Research has shown that nanostructured vapour grown carbon nanofibers [99], polyhedral silsesquioxane [100] and montmorillonite clay [101] enhance the crystallization rate of PP. Changes in the crystallization behaviour of thermoplastics in presence of carbon nanotubes and nanofibers have been reported [99,104-106]

Abdolhosein et al studied the thermal and structural behaviours of PP/SWNTs by melt processing method [107].The influence of $CaCO_3$ filler component on the thermal decomposition process of PP/LDPE/DPA ternary blend was studied by Fatih Dogan et al [108]. S. Reyes et al found carbon nanoparticles as effective nucleating agents for PP [109]. Thermal and spectroscopic characterization of PP/CNT composites were studied by B.B Marosfoi et al [110].

1.2.5 PP nanocomposite fibers

Applications of PP fibers can be broadened by modifying the properties of fiber such as high mechanical performance, flame retardancy, chemical resistance, UV resistance, electrical conductivity, soil resistance, water repellency, antistatic and antibacterial properties etc by suitable additives. Additives such as antioxidants, processing stabilizers and light stabilizers are added to increase mechanical properties of PP which resulted in market growth of PP. Without suitable additives PP fibers would not be used for durable applications such as carpets or geotextiles. Now a day, new additives are used to increase the functionality of PP fibers to enter new markets. Substitution of other synthetic and natural fibers is also possible by the addition of fillers in PP .They are widely used for producing household materials and also used in various applications such as filters, protective clothing , reinforcement for tyres, rubber goods and composites.

Furthermore, the properties of fiber can be enhanced by melt mixing with particulates and fibrous materials as well as by melt blending with other polymers. CNT and montmorillonite modified polymer nanocomposite fibers were reported in literature [111-125].

The use of nanotechnology in textile industry has been attracting worldwide attention. This is mainly due to the fact that conventional methods used to enhance the various properties to fabrics often do not give permanent effects and will lose those properties after laundering. Nanoparticles can increase the durability of treated fabrics with respect to conventional materials due to their large surface area and high surface energy. Washfastness is also required for textile and it is related with the adhesion of nanoparticles to the fibers. Nanoparticles can be applied by dipping the fabrics in a solution containing a specific binder to increase the wash fastness.

Organic and inorganic particles are used in polymers to modify these materials for high-technology applications. Nanotechnology leads to preparation of nanoscale systems and particles for various end uses such as nanocomposite fibers. PP is naturally hydrophobic and has almost zero water absorption, which forces moisture to pass through its structure in vapour form, enhances the moisture transport process and maintaining dry feeling. Most baby nappies and other incontinence products are padded with it for this reason. It is used in combination with a fibre that is naturally hydrophilic. A pre-treated or naturally hydrophilic polyester (Sorbtec/Coolmax type) outer layer will pull moisture through the hydrophobic PP inner layer to give extremely good comfort performance as in the Lowe Alpine's Dual Fiber Dryflo products.

New application areas are recognized due to the continuous growth of high strength PP fiber in textile market. Flame retardant fiber for wall coverings, upholstery, commercial carpeting etc are developed recently. The main problem for flame retardant PP fiber are processibility, UV stability and economics. Recent advances in flame retardant technology have significantly

improved processibility but stability and cost is not favourable. Light stability of PP composite fibres are important for textile products for light-weight summer fabric as well as for leisure and sport wear. Moreover, thermal stability of the PP composites is required for spinning the fiber. So for increasing the stability, processability without sacrificing the flame retardancy, inorganic nanomaterials can be used.

1.3 Nanomaterials

Nanomaterials are commonly found in nature for millions of years, produced by living things or volcanic activity. Nano-effects are widely observed from non reflective moth's eyes to extraordinarily efficient nano-lenses in crystalline sponges. The teeth of Coral- grazing parrot fish sconsist of bundles of nanofibers make it strong and durable. People have taken the advantage of nanotechnology for centuries. In the fourth-century A.D. Roman glassmakers were produced glasses containing nanosized metals. An artifice from this period called Lycurgus cup depicts the death of King Lycurgus, is made from soda lime glass containing silver and gold nanoparticles. The beautiful colours of the windows of medieval cathedrals are due to the presence of metal nanoparticles present in the glass. As the size of gold particles change it can appear as red, blue or gold colour and it is used in stained glass and ceramics. Photography developed in the eighteenth and nineteenth centuries depends on production of silver nanoparticles sensitive to light. Computer chips have been made using nanotechnologies for the last 20 years. Chemists have been making polymers with nanoscale subunits for decades. The word nano comes from a Greek word means dwarf or extremely small. One nanometer spans 3-5 atoms lined up in a row. The sizes of atoms to bacteria is schematically shown in figure 1.2.

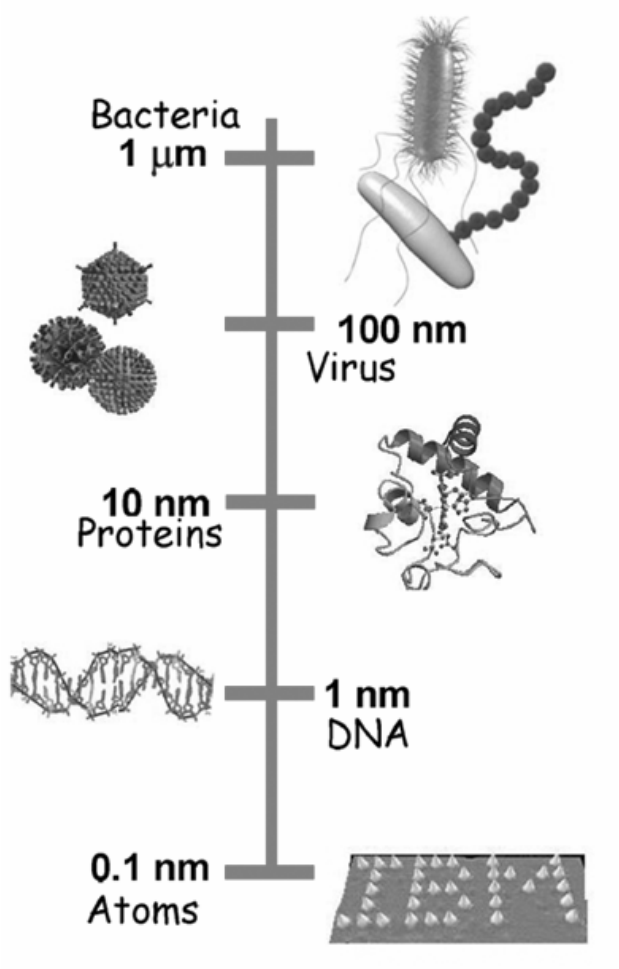

Figure 1.2: Schematic representation of size of objects

Nanomaterials can be classified in to three depending upon their nanometer dimension. Thin (nano) films used in computer chips and fuel cell applications represent one-dimensional nanomaterials. Carbon nanotubes, oxide-based nanotubes, biopolymers such as DNA, nanowires made of silicone, gallium nitride and indium phosphide represent two-dimensional nanomaterials. Nanoparticles exist in three dimensions having diameters less than 100 nm. This includes engineered particles such as the fullerenes and quantum dots.

In the mid- 1980s a new class of material-hollow carbon spheres called buckyballs or fullerenes was discovered. This was motivated the research that led to fabrication of carbon nanofibres, with diameters below 100 nm. In 1991 S. Iijima of NEC in Japan reported the first production of carbon nanotubes [126]. Synthesis of nanoparticles of carbon-rods, fibres, tubes with single walls or double walls, open or closed ends and straight or spiral forms have been reported. They have a capacity to carry an electric current a thousand times more than copper wires and to have twice the thermal conductivity of diamond. They are used as reinforcing particles in nanocomposites. Table 1.1 lists relative dimensions of objects in the nanoscale [127].

Table 1.1: Relative dimensions of objects in nanoscale

Object	Relative dimensions (nm)
Hydrogen atom	0.1
Typical bond between two atoms	0.15
Water molecule	0.3
C_{60} Fullerene	1
Helix of DNA	2.5
Cell membranes	8
Dendrimers	10
Virus	100
Red Blood Cell	7,000
Human hair	80,000
Dust mite	200,000
Head of pin	1,000,000

Nanomaterials have attracted great attention because they enhance the performance of the materials [128-131]. Some unique properties such as magnetic, optical, mechanical and electronic that abruptly change with changes

in the size of the material at the nanoscale. The term nanoparticle covers a wide range of chemical and other entities which can be metallic, mineral, polymer-based or a combination of materials. Nanoparticles include metal (Au, Pt, Pd, Cu etc.), semiconductor (CdS, CdSe, ZnS etc.), metal and metal oxide (FeO_3, Al_2O_3, ZnO, TiO_2 etc.). They have wide range of uses such as catalysts, drug delivery mechanisms, dyes, sunscreens, filters and much more.

1.3.1 Preparation of nanomaterials

There are two general ways to produce nanomaterials. The first is to start with a bulk material and then break it into smaller pieces using mechanical chemical or other form of energy (top down). Second is to synthesize the material from atomic or molecular species via chemical reactions, allowing for the precursor particles to grow in size (bottom-up). Schematic representation of top down and bottom up approach is shown in figure 1.3.

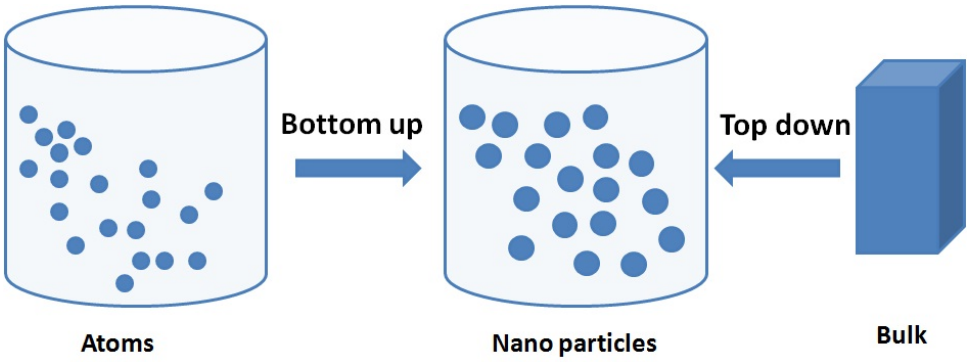

Figure 1.3: Schematic representation of preparation of nanoparticles

Both approaches can be done in either gas, liquid, supercritical fluids, solid states or vacuum. Most of the manufacturers are concentrated in the ability to control a) particle size b) particle shape c) size distribution d) particle composition e) degree of particle agglomeration. Different techniques for

preparing nanoparticles have been reported such as sol– gel technique [132], microemulsion synthesis [133], mechanochemical processing [134], spray pyrolysis and drying [135], RF plasma synthesis [136], supercritical-water processing [137], self-assembling [138], vapour transport process [139],sonochemical or microwave-assisted synthesis [140], direct precipitation [141] homogeneous precipitation [142],chemical co-precipitation [143,144], chemical vapour deposition [145],thermal decomposition [146,147], hydrothermal synthesis [148,149], solid-state reaction [150], spray pyrolysis [151], microemulsion precipitation [152-156] and chemical vapour deposition method [157]. Some of the above methods are discussed below.

1.3.1.1 Sol-gel process

Sol gel technique is used for the preparation of colloidal nanoparticles from liquid phase. Now a day it has been used for the production of advanced nanomaterials and coatings. Sol-gel processes are usually adapted for oxide nanoparticles. The main advantages of sol- gel techniques are low temperature of processing and versatility.

1.3.1.2 Hydrothermal synthesis

This method includes crystallizing substances from high-temperature aqueous solutions at high vapour pressures. The crystal growth is performed in an apparatus consisting of a steel pressure vessel called autoclave, in which a nutrient is supplied along with water. A gradient of temperature is maintained at the opposite ends of the growth chamber so that the hotter end dissolves the nutrient and the cooler end causes seeds to take additional growth.

1.3.1.3 Aerosol-based processes

Aerosols can be defined as solid or liquid particles in a gas phase, where the particles can range from molecules up to 100 μm in size. Spraying of the

precursor chemicals onto a heated surface or into the hot atmosphere results in precursor pyrolysis and formation of aerosol particles. For example CdS nanoparticles were produced by generating aerosol micro-droplets containing Cd salt in the atmosphere containing hydrogen sulphide.

1.3.1.4 Chemical vapour deposition (CVD)

CVD consists in activating a chemical reaction between the substrate surface and a gaseous precursor. Activation can be achieved either with temperature or with a plasma. Plasma allows decreasing significantly the process temperature compared to the thermal CVD process. This method is used to produce carbon nanotube.

1.3.1.5 Atomic or molecular condensation

Metal containing nanoparticles is produced mainly by this method. A bulk material is heated in vacuum to produce a stream of vapourized and atomized matter, which is directed to a chamber containing either inert or reactive gas atmosphere. Rapid cooling of the metal atoms due to their collision with the gas molecules results in the condensation and formation of nanoparticles. Metal oxide nanoparticles are produced when a reactive gas like oxygen is used.

1.3.1.6 Gas-phase condensation

Gas-phase condensation uses a vacuum chamber that consists of a heating element, the metal to be made into nano-powder, powder collection equipment and vacuum hardware. The process utilises a gas, which is typically inert, at pressures high enough to promote particle formation, but low enough to allow the production of spherical particles. Metal is introduced onto a heated element and is rapidly melted. The metal is quickly taken to temperatures far above the meltingpoint, but less than the boiling point, so that an adequate vapour pressure is achieved. Gas is continuously

introduced into the chamber and removed by the pumps, so the gas flow moves the evaporated metal away from the hot element. As the gas cools the metal vapour, nano sized particles are formed.

1.3.1.7 Supercritical fluid synthesis

Supercritical fluid means the fluid which is forced into supercritical state by regulating its temperature and pressure. This is used to form nanoparticles by a rapid expansion of a supercritical solution. Supercritical fluid method is currently developed at the pilot scale in a continuous process.

1.3.1.8 Mechanical processes

These include grinding, milling and mechanical alloying techniques. Large particles are physically powdered into small particles. The advantages of these techniques are that they are simple and require low-cost equipment. However, there can be difficulties such as agglomeration of the powders, broad particle size distributions and contamination from the process equipment itself. It is commonly used for inorganic materials and metals, but not organic materials.

1.3.2 Nanostructure morphologies

A variety of morphologies including prismatic forms [158], bipyramidal dumbbell-like [159], ellipsoidal [160], spheres [161], nanorods [162], nanowires [163], whiskers [164], nanotubes [165] and columnar hexagonal-shaped nanomaterials [166] are obtained when the method of preparation changes. Some of them are shown in figure 1.4[167].

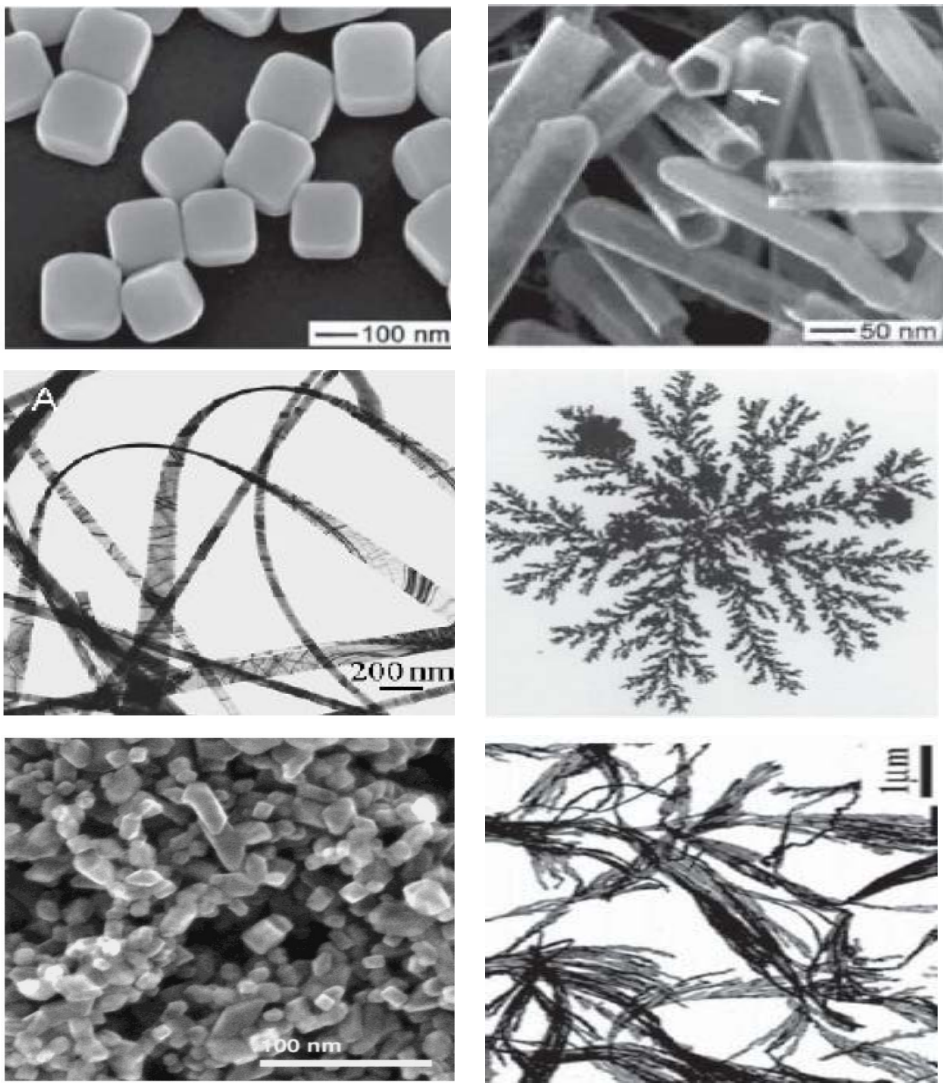

Figure 1.4: Different morphologies of nanoparticles

1.3.3 Titanium dioxide

Titanium dioxide (TiO_2) exist in three different crystalline forms. They are rutile, anatase and brookite [168-170]. The most common form is rutile which is also the equilibrium phase at all temperatures. The metastable anatase and brookite phases get converted convert in to rutile upon heating. Rutile, anatase and brookite all contain six coordinated titanium. Titanium is in

octahedral coordination with O atom as TiO_6 units in all the three forms. The different lattice structures arise due to the difference in arrangements of TiO_6 octahedra which is due to the difference in Ti-O bond length and angle. The rutile and anatase lattices are tetragonal with $P4_2$ /mnm and $I4_1$/amd space groups, respectively, and brookite is orthorhombic with Pbca symmetry[171]. A series of Ti_n O_{2n-1}($4 \leq n \leq 10$) daughter-structures are also formed by shear operations on a rutile mother–structure to accommodate nonstoichiometry [172]**.** Unit cell of rutile and anatase is given in figure 1.5 [173].

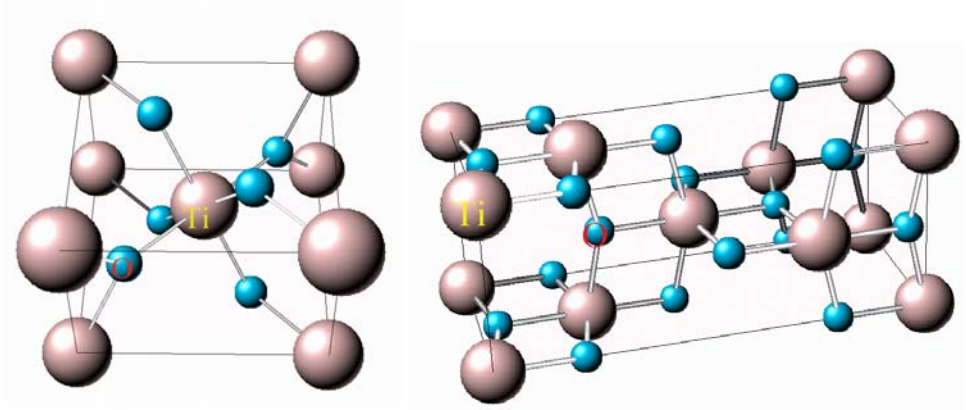

Figure 1.5: Unit cell of rutile and anatase crystal structure of TiO_2

TiO_2 is one of the whitest materials which has gained a nickname as titanium white. Hence, it is included in many cosmetic preparations to reflect light away from the skin. It is a main component of sun block to deter the absorption of ultraviolet (UV) rays from the sun, the concentration of which determines the product's Sun Protection Factor. TiO_2 is used as pigment to improve the white color of certain food materials such as dairy products and candy. It also lends brightness to toothpaste and some medications. It is also used as a food additive and flavor enhancer in various non-white foods, including dried vegetables, nuts, seeds, soups and mustard. Since TiO_2 reflects light so well, it is suitable for use as a protective coating for many products

like automobile parts and optical mirrors. Due to its refractive ability, it is a component of paints used to coat cars, boats, and airplanes. TiO_2 is also used in a number of construction and building materials. In plastic industry TiO_2 is used as a coating to absorb UV light and make the material durable. TiO_2 is the most widely used white pigment due to its brightness and high refractive index (n = 2.7), in which it is surpassed only by a few other materials. Approximately 4 million tons of pigmentary TiO_2 are consumed annually in the world. When deposited as a thin film, it is an excellent reflective optical coating for dielectric mirrors and some gemstones like "mystic fire topaz". TiO_2 is used to mark the white lines on the tennis courts of the All England Lawn Tennis and Croquet Club, best known as the venue for the annual grand slam tennis tournament, Wimbledon [174].

TiO_2 normally have electronic band gaps greater than 3.0eV and high absorption in the UV region. TiO_2 nanomaterials are very stable, nontoxic, cheap and can impart antifogging functions on various glass products, i.e., mirrors and eye glasses, having super hydrophilic or super hydrophobic surfaces. Feng et al observed that reversible super hydrophilicity and super hydrophobicity could be switched back and forth for TiO_2 nanorod films. Stain proofing, self cleaning properties can also be imparted on various types of surfaces due to the superhydrophilic or super hydrophobic surfaces. TiO_2 nanomaterials have also been used as sensors for various gases and humidity because of the electrical or optical properties which change upon adsorption [175]**.** Sakamoto et al. observed both absorption and scattering significantly affected the shielding capability of spherical TiO_2 in the UV range of 350-375nm and its absorption capability played an important role in shielding at shorter wavelengths than 350nm. The high UV shielding effect at short wavelengths was due to the high absorption capability of nano-sized TiO_2.

Among the polymorphs, anatase is used as a photocatalyst and catalyst support in industrial processes [176-180]. Usually, large surface areas are required for catalyst supports to disperse a catalyst-active material effectively to enhance the number of active sites. As the catalyst is used at high temperature, high-thermal stability and large surface area is also important. Hence, synthesis of TiO_2-photocatalyst with high thermal stable anatase phase is one of the key issues in smart coating for building materials application [181-183].

TiO_2 is widely used in plastics and other applications for its UV resistant properties where it acts as a UV absorber, efficiently transforming destructive UV light energy into heat. In ceramic glazes, TiO_2 acts as an opacifier. TiO_2 is found in sunscreen with a physical blocker due to its high refractive index, its strong UV light absorbing capabilities and its resistance to discolouration under ultraviolet light. This improves its stability and helps to protect the skin from UV light. Sunscreens designed for infants or people with sensitive skin are often based on TiO_2 or ZnO, as these mineral UV blockers cause less skin irritation than chemical UV absorber ingredients.

1.3.4 Zinc oxide

ZnO crystallizes in two main forms, hexagonal wurtzite and cubic zinc blende. The wurtzite structure is most stable and common. The zinc blende form can be stabilized by growing ZnO on substrates with cubic lattice structure. In both forms, the zinc and oxide centers are tetrahedral. In addition to the wurtzite and zinc blende forms, ZnO can be crystallized in the rocksalt structure at a relatively high pressures of about 10 GPa [184]. Hexagonal and zincblende forms have no inversion symmetry. Various lattice symmetry properties result in piezoelectricity of the hexagonal wurtzite and cubic zincblende and pyroelectricity of hexagonal wurtzite.

Point group of hexagonal structure is 6mm (Hermann-Mauguin notation) or C_{6V} (Schoenflies notation), and the space group is P63mc or C6v4. The lattice constants are a = 3.25 Å and c = 5.2 Å; their ratio 1.60 is close to the ideal value for hexagonal cell c/a = 1.633[185]. Bonding in ZnO is largely ionic with the corresponding radii of 0.074 nm for Zn^{2+} and 0.140 nm for O^{2-}. This property accounts for the preferential formation of wurtzite rather than zinc blende structure [186] as well as the strong piezoelectricity of ZnO. Because of the polar Zn-O bonds, zinc and oxygen planes are electrically charged. To maintain electrical neutrality, those planes reconstruct at atomic level in most relative materials, but not in ZnO, its surfaces are atomically flat, stable and exhibit no reconstruction. This anomaly of ZnO is not fully explained yet [187]. The wurtzite and zinc blende structure is given in figure 1.6[188].

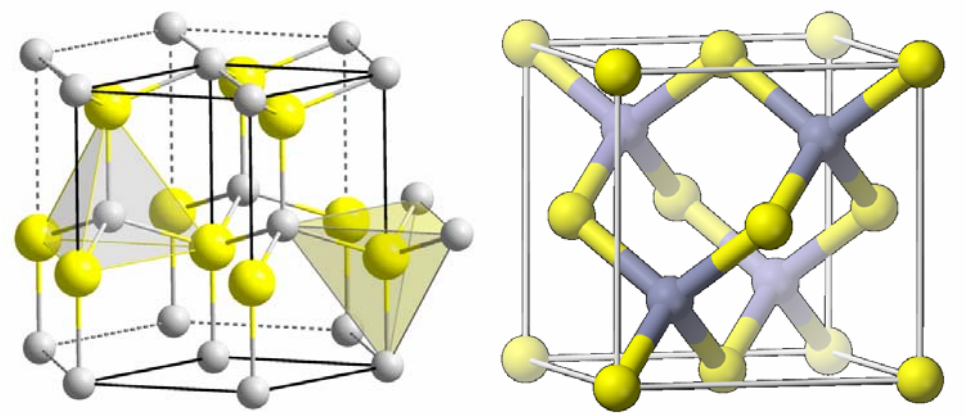

Figure 1.6: Unit cell structure of wurtzite and zinc blende of ZnO

Nano-ZnO as a functional inorganic filler has been widely used in functional devices, catalysts, pigments, optical materials, cosmetics and UV absorbers[189-197]. After Sawai et al [198,199] was observed that ZnO powder had antibacterial activity against some bacteria strains in 1995, more and more investigations have shown that ZnO as an antibacterial agent. Now a

day, there have been some reports regarding the antimicrobial activity of ZnO nanoparticles [200]. It has been observed that ZnO nanoparticles have higher antibacterial affects on microorganism like S Aureus than other metal oxide nanoparticles [201]. Similarly, Tam et al [202] have investigated antibacterial activity of ZnO nanorods prepared by hydrothermal method. ZnO showed good activity against E Coli and B. Atrophaeus, but it was more effective in the later. It was reported that the ZnO nanoparticles treated fabric showed higher antibacterial activity when compared with ZnO bulk treated fabrics whereas the neat fabrics showed no antibacterial activity.

Introduction of nano ZnO into polymers can enhance the mechanical properties of the polymers because of a strong interfacial interaction between polymers and nanoparticles but also endow polymers with some other functional capabilities, such as photostabilization and protect matrix resins from environmental degradation and increase the toughness [203-206]. Moreover, its smaller diameter and relatively lower quantity of addition would have little influence on the transparency of the products [207].

ZnO is a good stabiliser as it shows a steep transmission cut-off at 385 nm, which extends well into the far-IR. There are some reports on the use of nano ZnO for UV stabilization of polyolefins [208]. It was reported that nano ZnO gives superior resistance to degradation compared to organic HALS at their appropriate loading levels. UV absorbing efficiency of nano ZnO is increased with decrease in particle size and helps to reduce the loading in the polymer when compared to a larger particle size. As particles with dimensions well below the wavelength of light and above the level of appreciable quantum confinement have negligible loss from scattering [209]. It has been reported that 20–50 nm unagglomerated ZnO, even at very high loading levels (up to 60 wt%), effectively absorbs UV radiation and remains transparent in the visible

region [210]. Hence, the incorporation of nano ZnO should result in a marked reduction in hindered amine light stabilisers stabiliser loading and this helps to reduce the cost of the end product and also reduces any adverse effects of the stabiliser on the aesthetic properties of the material.

ZnO-based semiconductor devices are also important for the integration on a single chip. So far, a variety of applications of nano ZnO like biosensors, UV detectors and FED are under way. ZnO has been proposed to be a more promising UV emitting phosphor than GaN due to its larger exciton binding energy. This leads to a reduced UV lasing threshold and gives higher UV emitting efficiency at room temperature [211]. Surface acoustic wave filters using ZnO films have already been used for video and radio frequency circuits. Piezoelectric ZnO thin film has been developed into ultrasonic transducer arrays operating at 100 MHz [212]. Bulk and thin films of ZnO have reported high sensitivity for toxic gases [213-216]. Moreover, hole mediated ferromagnetic ordering in bulk ZnO by introducing Mn as dopant has been predicted theoretically and reported recently [217,218]. Vanadium doped *n*-type ZnO films also shows a Curie temperature above room temperature [219].

1.4 Objectives of the work

The study has been undertaken to prepare nano ZnO and nano TiO_2 and to study the effect of particle size of ZnO and TiO_2 on the various properties of PP and its fiber. Salient objectives of the research work are:

- To investigate the effect of various preparation medium on the particle size and morphology of ZnO.
- To compare the antibacterial property of ZnO prepared in chitosan medium and commercial ZnO using gram positive and gram negative bacteria.

- To investigate effect of ZnO prepared in chitosan medium and that of commercial ZnO on the mechanical, thermal, crystallization, processability and transparency of PP.
- To explore the UV and thermal stability of PP in presence of ZnO.
- To investigate the effect of reinforcement and thermal stability of fibers prepared from PP/ZnO nanocomposites.
- To synthesize TiO_2 by sol gel and wet synthesis method, its characterization by XRD, SEM, TEM etc and to evaluate the antibacterial property of commercial and TiO_2 prepared by wet synthesis.
- To study the effect of particles size of TiO_2 on the properties of PP/TiO_2 composite.
- To fabricate and characterize the fiber prepared from PP/TiO_2 composites.

References

[1] Chou Chai-jing, Read AE, Garcia-Meitin EL Bosnyak CP, Annual Technical Conference Proceedings, Society of Plastics Engineers, 2002, 48, 1452.

[2] Mohammad M Hasan, Yuanxin Zhou, Hassan Ivlahfuz, Shaik Jeelani, Materials Science and Engineering: A, 2006, 429, 181.

[3] Ling Y, Omachinski S, Logsdon J, Whan Cho J, Lan T, 2004, Nano-Effects in In Situ Nylon-6Nanocomposites. Retrieved February 28, 2005 from http://www.nanocor.com/tech_papers/antec2001.asp.

[4] Eggnog Zeynep, Cokmak Miko, Batur Celal, Annual Technical Conference Proceedings, Society of Plastics Engineers, 2002, 48, 1519.

[5] Garcia-Rejon A, Derdouri A, Denault J, Bureau MN, Cole K, Annual Technical Conference Proceedings, Society of Plastics Engineers 2002, 48, 410.

[6] Gilman Jeffrey W, Kashiwagi Takashi, Lichtenhan Joseph D, Nanocomposites: A Revolutionary New Flame Retardant Approach, 42nd International SAMPE Sumposium, 1997, 1078.

[7] Goettler Lloyd A, Lysek Bruce A, Annual Technical Conference Proceedings, Society of Plastics Engineers, 1999, 45, 3972.

[8] Kressler jorg, Thomann, Ralf Annual Technical Conference Proceedings, Society of Plastics Engineers 1998, 44, 2400.

[9] Lew CY, Murphy WR, McNally GM. Annual Technical Conference Proceedings, Society of Plastics Engineers 2002, 48, 1530.

[10] Dahman Sam J, Annual Technical Conference Proceedings, Society of Plastics Engineers, 2000, 46, 2407.

[11] Miller Joshua, Greene Joseph, Annual Technical Conference Proceedings, Society of Plastics Engineers, 2002, 48, 3594.

[12] McConaughy Shawn D, Annual Technical Conference Proceedings, Society of Plastics Engineers, 2002, 48, 3587.

[13] Liang Shen, Yijian Lin, Qiangguo Du, Wei Zhong. Composites Science and Technology 2006, 66, 2242.

[14] Hedenqvist MS, Backman A, Gallstedt M, Boyd RH, Gedde UW. Composites Science and Technology 2006, 66, 2350.

[15] Gonzalez I, Eguiazabal JI, Nazabal, J. Composites Science and Technology 2006, 66, 1833.

[16] Hand book of Polypropylene and Polypropylene composites edited by Harutun G. Karian, Marcel Dekker, Inc,New York, Basel,1999.

[17] Kissel W J, Meyer J A, Handbook of Polypropylene and Polypropylene Composites, Haruton G. Karian RheTech, Inc, 11.

[18] Gupta V B, Mondal S A, and Bhuvanesh Y C, J. Appl. Polym. Sci., 1997, 65, 9, 1773.

[19] Joshi M , Viswanathan V, J. Appl. Polym. Sci., 2006, 102, 3, 2164.

[20] Noumowe A, Cement and Concrete Research 2005,35,2192.

[21] Schultze-Gebhardt F, Herlinger K H ,Ullmann's Encyclopedia of Industrial Chemistry, Wiley-VCH, Weinheim, 2002, 10.

[22] Elias H G, An Introduction to Polymer Science, Wiley-VCH, Weinheim, 1997.

[23] Stibal W, Schwarz R, Kemp U, Bender K, Weger F, Stein M, Ullmann's Encyclopedia of Industrial Chemistry, Wiley-VCH: Weinheim, 2002,3.

[24] Karger-Kocsis J, Polypropylene an a-z reference. Kluwer, Academic, London,1999.

[25] Kotek J, Kelnar I, Studenovsky M, Baldrian J , Polymer ,2005, 46,4876.

[26] Schimanski T, Peijs T, Lemstra PJ, Loos J, Macromolecules, 2004 37,1810.

[27] Thio YS, Argon AS, Cohen RE, Polymer, 2004,45,3139.

[28] Liu Z, Gilbert MJ, J Appl Polym Sci 1996,59,1087.

[29] Lee YJ, Manas-Zloczower I, Feke DL, Polym Eng Sci 1995,35,1037.

[30] Mansour SH, Abd-El-Messieh SL,J Appl Polym Sci, 2002,83,1167.

[31] Luyt AS, Molefi JA, Krump H, Polym Degrad Stab 2006,91,1629.

[32] Zhou Y, Rangari V, Mahfuz H, Jeelani S, Mallick PK, Mater Sci Eng 2005,402,109.

[33] Wang Y, Wang J, Polym Eng Sci, 1999, 39, 190.

[34] Lei SG, Hoa SV, Ton-That MT, Compos Sci Technol, 2006, 66,1274.

[35] Nilufer Erdem, Aysun A Cireli, Umit H Erdogan, Journal of Applied Polymer Science, 2009, 111, 2085.

[36] Velasco JI, De Saja JA, Martinez AB. J Appl Polym Sci 1996,61,125.

[37] Liu X, Wu Q. Polymer 2001, 42, 10013.

[38] Qiu W, Mai K, Zeng H. J Appl Polym Sci 2000,77,2974.

[39] Chiang WY, Yang WD, Pukanszky B, Polym Engng Sci 1994,34,485.

[40] Kuhnert I, Fischer HD, Muras J. Kunstoff 1997, 42,29.

[41] Wu C-M, Chen M, Karger-Kocsis, J. Polymer Bull 1998, 41,239.

[42] Assouline E, Pohl S, Fulchiron R, Gerard J-F, Lustiger A, Wagner HD, Marom G, Polymer 2000,41,7843.

[43] Hobbs SY, Nat Phys Sci 1971, 234,12.

[44] Campbell D, Qayyum MM. J Polym Sci, Polym Phys Ed 1980,18,83.

[45] Duvall J, Sellitti C, Myers C, Hiltner A, Baer E, J Appl Polym Sci,1994,52,195.

[46] Ikkala OT, Holsti-Miettinen RM, Seppala I, J Appl Polym Sci 1993, 49,1165.

[47] Gupta AK, Purwar SN, J Appl Polym Sci 1984,29,1595.

[48] Zhang X, Xie F, Pen Z, Zhang Y, Zhang Y, Zhou W, Eur Polym J,2002,38,1.

[49] Yakobson BI, Smalley RE. Am Sci 1997,85,324.

[50] Yu MF, Files BS, Arepalli S, Ruoff RS. Phys Rev Lett, 2000,84,5552.

[51] Baughman RH, Zakhidov AA, de Heer WA. Science 2002,297,787.

[52] Assouline E, Lustiger A, Barber A H, Cooper C A, Klein E, Wachtel E, Wagner H D, J Polym Sci: Part B: Polym Phys, 2003, 41, 520.

[53] Nagarajan K, Levon K, Myerson A S, J Therm Anal Calor, 2000, 59, 497.

[54] Yuksekkalayci C, Yilmazer U, Orbey N, Polym Eng Sci, 1999, 39, 1216.

[55] Fujiyama M, Wakino T, J Appl Polym Sci, 1991, 42, 2739.

[56] Smith T L, Masilamani D, Bui L K, Brambilla R, Khanna Y P, Gabriel K A, J Appl Polym Sci, 1994, 52, 591.

[57] Macauley N J, Harkin-Jones E M A, Murphy W R, Polym Eng Sci, 1998, 38, 516.

[58] Khanna Y P, Macromolecules, 1993, 26, 3639.

[59] Feng Y, Jin X, Hay N J, J Appl Polym Sci 1988, 69, 2089.

[60] Zhang R, Zhang H, Lou X, Ma D, J Appl Polym Sci, 1994, 51, 51.

[61] Kim Y C, Kim C Y, Polym Eng Sci, 1991, 31,1009.

[62] Shepard T A, Delsorbo C R, Louth R M, Walborn J L, Norman D A, Harvey N G, Spontak R J, J Polym Sci Part B Polym Phys, 1997, 35, 2617.

[63] Smith T L, Masilamani D, Bui L K, Khanna Y P, Bray R G, Hammond WB, Carran S,Bellers J J, Binder-Castelli S, Macromolecules 1994, 27, 3147.

[64] Kim C Y, Kim Y C, Kim S C, Polym Eng Sci, 1993, 33, 1445.

[65] Avella M, DellErba R, Martuscelli E, Ragosta G, Polymer, 1993, 34, 2951.

[66] Bauer, T.; Thomann, R.; Muelhaupt, R. Macromolecules 1998, 31, 7651.

[67] Velasco JI, De Saja JA, Martinez AB, J Appl Polym Sci, 1996,61,125.

[68] Liu X, Wu Q. Polymer, 2001,42,10013.

[69] Qiu W, Mai K, Zeng H, J Appl Polym Sci, 2000,77,2974.

[70] Chiang WY, Yang WD, Pukanszky B, Polym Engng Sci 1994,34,485.

[71] Kuhnert I, Fischer HD, Muras J, Kunstoff, 1997,42,29.

[72] Wu C-M, Chen M, Karger Kocsis J, Polymer Bull 1998,41,239.

[73] Assouline E, Pohl S, Fulchiron R, Gerard J F, Lustiger A, Wagner HD, Marom G, Polymer, 2000,41,7843.

[74] Hobbs SY, Nat Phys Sci, 1971,234,12.

[75] Campbell D, Qayyum MM, J Polym Sci, Polym Phys Ed 1980,18,83.

[76] Duvall J, Sellitti C, Myers C, Hiltner A, Baer E, J Appl Polym Sci 1994,52,195.

[77] Ikkala OT, Holsti Miettinen RM, Seppala I, J Appl Polym Sci, 1993, 49,1165.

[78] Gupta AK, Purwar SN, J Appl Polym Sci, 1984,29,1595.

[79] Zhang X, Xie F, Pen Z, Zhang Y, Zhang Y, Zhou W, Eur Polym J 2002,38,1.

[80] Thostenson ET, Ren Z, Chou T W. Composites Sci Technol, 2001, 61,1899.

[81] Fornes TD, Yoon PJ, Keskkula H, Paul DR, Polymer, 2001,42,9929.

[82] Fu BX, Yang L, Somani RH, Zong SX, Hsiao BS, Phillips S, Blanski R, Ruth P, J Polym Sci Part B: Polym Phys, 2001,39,2727.

[83] Lozano K, Barrera EV, J Appl Polym Sci, 2001,79,125.

[84] Kumar S, Doshi H, Srinivasrao M, Park JO, Schiraldi DA, Polymer, 2002,43,1701.

[85] Ma J, Zhang S, Qi Z, Li G, Hu Y, J Appl Polym Sci, 2002,83,1978.

[86] Jianguo Tang, Yao Wang, Haiyan Liu, Laurence A, Belfiore, Polymer, 2004, 45, 2081.

[87] Zhang M L, Liu Y Q, Zhang X H, Gao J M, Huang F, Song ZH, Wei GS, Qiao J L, Polymer 2002,43,5133.

[88] Gui QD, Xin Z, Zhu WP, Dai G. J Appl Polym Sci 2003;88(2),297–301.

[89] Privalko V P, Karaman V M, Privalko E G, Walter R, Friedrich K, Zhang MQ, Rong MZ,J Macromol Sci—Phys, 2002,B41,487.

[90] Thomason J L, Van Rooyen A A, J Mater Sci, 1992, 27, 889.

[91] Tan J K, Kitano T, Hatakeyama T, Crystallization of carbon fibre reinforced polypropylene, J Mater Sci, 1990, 25, 3380.

[92] Varga J, Karger Kocsis J, J Mater Sci Lett, 1994, 13, 1069.

[93] Janevski A, Bogoeva Gaceva G,J Appl Polym Sci, 1998, 69,381.

[94] Sukhanova T E, Lednicky F, Urban J, Baklagina Y G, Mikhailov G M,Kudryavtsev V V,J Mater Sci, 1995, 30, 2201.

[95] Janevski A, Bogoeva Gaceva G, Mader E, J Appl Polym Sci, 1999,74, 239.

[96] Avella M, Martuscelli E, Sellitti C, Gargagnani E, J Mater Sci,1987,22, 3185.

[97] Thostenson ET, Ren Z, Chou T W, Composites Sci Technol, 2001,61,1899.

[98] Fornes T D, Yoon P J, Keskkula H, Paul DR, Polymer, 2001,42,9929.

[99] Lozano K, Barrera EV, J Appl Polym Sci, 2001,79,125.

[100] Fu B X, Yang L, Somani R H, Zong S X, Hsiao B S, Phillips S, Blanski R, Ruth P, J Polym Sci Part B: Polym Phys, 2001, 39,2727.

[101] Ma J, Zhang S, Qi Z, Li G, Hu Y,J Appl Polym Sci, 2002,83,1978.

[102] Kumar S, Doshi H, Srinivasrao M, Park J O, Schiraldi D A, Polymer 2002,43,1701.

[103] Zhang M, Liu Y, Zhang X, Gao J, Huang F, Song Z, Wei G, Qiao J, Polymer, 2002,43,5133.

[104] Arup R Bhattacharyya, Sreekumar T V, Tao Liua, Satish Kumara, Lars M Ericson, Robert H. Hauge, Richard E. Smalley, Polymer 2003,44 , 2373.

[105] Grady B P, Pompeo F, Shambaugh R L, Resasco D E,J Phys Chem B, 2002, 106 , 5852.

[106] Sandler J, Broza G, Nolte M, Schulte K, Lam Y M, Shaffer M S P, journal of macromolecular science, Part B—Physics,2003, B42, 479.

[107] Abdolhosein Fereidoona, Morteza Ghorbanzadeh Ahangaria, Seyfolah Saedodin, Journal of Macromolecular Science, Part B Physics, 2008, 48,196, 2008.

[108] Fatih Dogan, Kamil Sirin, Ismet Kaya, Mehmet Balcan, Polym Adv Technol, 2010,21,512.

[109] Reyes de Vaaben S, Aguilar A, Avalos F, Ramos de Valle LF, Journal of Thermal Analysis and Calorimetry, 2008,93, 947.

[110] Marosfoi B B, Szabo A, Gy Marosi, Tabuani D,Camino G, Pagliari S, Journal of Thermal Analysis and Calorimetry, 2006, 86, 669.

[111] Guan G H, Li C C, Zhang D, J Appl Polym Sci, 2005, 95,1443.

[112] Yoon K H, Polk M B, Min B G, Schiraldi D A, Polym Int , 2004, 53, 2072.

[113] Chang J H, Kim S J, Im S, Polymer, 2004, 45, 5171.

[114] Chang J H, Kim S J, Joo Y L, Im S,Polymer 2004, 45,919.

[115] Ergungor Z, Cakmak M, Batur C, Macromol Symp,2002,185, 259.

[116] Ibanes C, David L, De Boissieu M, Seguela R, Epicier T, Robert G, J Polym Sci Part B: Polym Phys, 2004, 42, 3876.

[117] Usuki A, Kato M, Okada A, Kurauchi T, J Appl Polym Sci,1997, 63, 137.

[118] Mlynarcikova Z, Borsig E, Legen J, Marcincin A, Alexy P,J Macromol Sci Pure Appl Chem, 2005, 42, 543.

[119] Mlynarcikova Z, Kaempfer D, Thomann R, Mulhaupt R, Borsig E, Marcincin, A. Polym Adv Technol 2005, 16, 362.

[120] Palikova S, Thomann R, Reichert P, Mulhaupt R, Marcincin A, Borsig E, J Appl Polym Sci, 2003, 89, 604.

[121] Rottstegge J, Zhang X Q, Zhou Y, Han C C, Wang D J, J Appl Polym Sci, 2007, 103, 218.

[122] Zhang X Q, Yang M S, Zhao Y, Zhang S M, Dong X, Liu X X, Wang D J, Xu D F, J Appl Polym Sci, 2004, 92,552.

[123] Saeed K, Park S Y, Haider S, Baek J B, Nanoscale Res Lett, 2009,4,39.

[124] Mun1 M K, Kim J C, Chang J H, Polym Bull, 2006, 57,797.

[125] Janowska G, Mikolajczyk T, Olejnik M J, Therm Anal Calorim, 2008, 92, 495.

[126] Fakhrul Razi A, Atieh MA, Gitlin N, Chuah TG, El Sadig M, Biak BRA, Composite Structures, 2006, 75, 496.

[127] Aswathy K V , Ph.D thesis, Nano zinc oxide –a novel modifier for thermoplastics, 2007.

[128] Uyeda R, Prog Mater Sci, 1991, 35, 1.

[129] Siegel RW, Nanostruct Mater, 1993, 3, 1.

[130] Gleiter H, Nanostruct Mater 1992, 1, 1.

[131] Kear B H, Keem L E, Siegel R W, Spaepen F, Taylor K C, Thomas E L, Tu KN, Research Opportunities for Materials with Ultrafine Microstructures vol. NMAB454, National Academy, Washington, DC, 1989.

[132] T Tsuzuki, McCormick P G, Scripta Mater,2001, 44, 1731.

[133] Singhal M, Chhabra V, Kang P, Shah D O, Mater Res Bull,1997, 32, 239.

[134] Okuyama K, Lenggoro I W, Chem Eng Sci,2003, 58, 537.

[135] Sato T, Tanigaki T,Suzuki H, Saito Y, Kido O, Kimura Y, Kaito C, Takeda A, Kaneko S, J Cryst Growth ,2003,313,255..

[136] Viswanathan R, Lilly G D, Gale W F, Gupta R B, Ind Eng Chem Res, 2003, 42 ,5535.

[137] Koh Y W, Lin M, Tan C K,Foo Y L, Loh K P, J. Phys Chem B,2004,108,11419.

[138] Yu W D, Li X M, Gao X D, Cryst Growth Des,2005,5, 151.

[139] Hu X L, Zhu Y J, Wang S W , Mater Chem Phys, 2004,421.

[140] Wang J M, Gao L, Inorg Chem Commun, 2003,6,877.

[141] Kim J H, Choi W C, Kim H Y, Kang Y, Park Y K, Powder Technol,2005, 153, 166.

[142] Wang L N, Muhammed M, J Mater Chem, 1999, 9, 2871.

[143] Rodriguez Paez J E, Caballero A C, Villegas M, Moure C, Duran P, Fernandez J F, J Eur Ceram Soc,2001, 21,925.

[144] Purica M, Budianu E, Rusu E, Danila M, Gaurila R, Thin Solid Films, 2002, 403, 485.

[145] Rataboul F, Nayral C, Casanove M J, Maisonnat A, Chaudret B, J Organomet Chem, 2002,307,643644 .

[146] Audebrand N, Auffredic J P, D Louer, Chem Mater,1998,10, 2450.

[147] Yang Y, Chen H, Zhao B, Bao X, J Cryst Growth, 2004,263, 447.

[148] Liu B, Zeng H C, J Am Chem Soc,2003,125, 4430.

[149] Lu C H, Yeh C H, Ceram Int, 2000, 26, 351.

[150] Zhu Y, Zhou Y, Appl Phys A, 2008, 92, 275.

[151] Tani T, Madler L, Pratsinis S E, J Nanopart Res, 2002, 4, 337.

[152] Hingorani S, Pillai V, Kumar P, Multani M S, Shah D O, Mat Res Bull, 1993, 28, 1303.

[153] Hingorani S, Shah D O, J Mater Res,1995,10,461.

[154] Shingal M, Chhabra V, Kang P, and Shah D O, Mat Res Bull, 1997,32, 239.

[155] Lim B P, Wang J, Ng N C, Chew C H, Gan L M, Ceram Int, 1998, 24, 205.

[156] Inoguchi M, Suzuki K, Kageyama K, Takagi H, Sakabe Y, J Am Ceram Soc, 2008, 91,3850.

[157] Lyu S C et al, Chemical Physics Letters, 2002, 363,134.

[158] Li W J, Shi E W, Zhong W Z and Yin Z , J Cryst Growth, 1999,203,186.

[159] Wang B G, Shi E W and Zhong W Z ,Cryst Res Technol, 1998 ,33, 937.

[160] Lu C H,Yeh C H , Ceram Int, 2000, 26, 351.

[161] Neves M C, Trindade T, Timmons A M B, Pedrosa de Jesus J D, Mater Res Bull 2001, 36, 1099.

[162] Pal U , Santiago P , J. Phys Chem B, 2005, 109, 15317.

[163] Vayssieres L, Adv Mater, 2003, 15, 464

[164] Hu J Q, Li Q, Wong N B, Lee C S and Lee S T , Chem Mater, 2002, 14, 1216.

[165] Sun Y, Fuge G M, Fox N A, Riley D J and Ashfold M N R,Adv. Mater. 2005 ,17, 2477.

[166] Ni Y H, Wei X W, Ma X , Hong J M, J. Cryst. Growth, 2005, 283, 48.

[167] 203.199.213.48/1041/1/Physical_and_chemical_metods.pdf

[168] Bragg W L, Atomic Structure of Minerals Cornell University Press, Ithaca, 1937, 102.

[169] Clark J G, The Chemistry of Titanium and Vanadium ,Elsevier, NewYork, 1968, 66.

[170] Dachille F, Simons P Y, Roy R, Am. Mineral. 53, 1929.

[171] Mo S D, Ching W Y, Phys. Rev. B, 51, 13023,1995.

[172] Kosuge K, Chemistry of Non-stoichiometric Compounds Oxford University Press, Oxford, UK, 1994, 121.

[173] http://cst-www.nrl.navy.mil/users/sullivan/TiO2/TiO2_rutile.gif

[174] Wikipedia, the free encyclopedia ,http://en.wikipedia.org/wiki/ Titanium_ dioxide

[175] Xiaobo Chen, and Samuel S. Mao, Chem. Rev., 2007, 107, 2891.

[176] Matsuda S, Kato A, Applied Catalysis, 1983, 8,149.

[177] Yu J, Yu J C, Leung M K P et al, Journal of Catalysis, 2003,217,69.

[178] Ma G B, Zhu J M, Ming N B, Journal of Metastable and Nanocrystalline Materials, 2005, 235.

[179] Wang H, Wu Y, Xu B Q, Applied Catalysis B, 2005, 59, 139.

[180] Dhage S R, Gaikwad S P, Ravi V, Bulletin of Materials Science,2004,27, 489.

[181] Parkin I P,Palgrave R G, Journal of Materials Chemistry, 2005,15,1689.

[182] Wang X, Yu J C, Ho C, Hou Y, Fu X, Langmuir, 2005,21,2552.

[183] Yu J G, Su Y R, Cheng B, Advanced Functional Materials, 2007, 17,1984.

[184] Rossler U, ed. (1999), Landolt-Bornstein, New Series, Group III, Vol. 17B, 22, 41B, Springer, Heidelberg.

[185] Claus Franz Klingshirn, Bruno K. Meyer, Andreas Waag, Axel Hoffmann, Johannes M M Geurts (1 August 2010), Springer, 9–10, ISBN 978-3-642-10576-0. Retrieved 9 December 2011.

[186] Baruah S, Dutta J, Sci Technol Adv Mater, 2009, 10, 013001, doi:10.1088/1468-6996/10/1/013001.

[187] Wang Z S, Huang C H, Huang Y Y et al., Chemistry of Materials, 2001, 13, 678.

[188] http://en.wikipedia.org/wiki/Zinc_oxide#Structure

[189] Baruwati B, Kumar D K, Manorama S V, Sensors and Actuators B: Chemical, 2006,119, 676.

[190] Li Y K, Li G R, Yin Q R, Materials Science and Engineering B, 2006, 130, 264.

[191] He Y J, Yu X Y, Li T L et al., Powder Technology, 2006, 166, 72.

[192] Li YQ, Fu S Y, Mai Y W, Polymer, 2006, 47, 2127.

[193] Usui H, Shimizu Y, Sasaki T et al., Journal of Physical Chemistry B, 2005, 109,120.

[194] Dang Z M, Fan L Z, Zhao S J, et al., Materials Science and Engineering B, 2003, 99, 386.

[195] Iwasaki T, Satoh M, Masuda T et al. , Journal of Materials Science, 2000, 35, 4025.

[196] Zhao H X, Li R K Y, Polymer, 2006, 47, 3207.

[197] Tjong S C, Liang G D, Bao S P, J Appl Polym Sci, 2006,102, 1436.

[198] Sawai J, Igarashi H, Hashimoto A, Kokugan T, Shimizu M, J Chem Eng Jpn, 1995, 28, 288.

[199] Sawai J, Saito I, Kanou F, Igarashi H, Hashimoto A, Kokugan T, Shimizu M, J Chem Eng Jpn, 1995, 28, 352.

[200] Yadav A, Prasad V, Kathe A A, Raj S, Yadav D, Sundarmoorthy C, Vigneshvaran N, BullMarter Sci., 2006, 29, 641.

[201] Jones N, Ray B, Ranjit K T, Manna A C,2007, FEMS Microbiology Letters, 279, 71.

[202] Tam K H , Djurisic A B, Chan C M N, Xi Y Y , Tse C W, Leung Y H, Chan W K, Leung F C C,Thin Solid Films, 2008, 516, 6167.

[203] Li Q, Chen S L, Jiang WC, J Appl Polym Sci, 2007, 103, 412.

[204] Guo Z, Wei S, Shedd B, Scaffaro R, Pereira T, Hahn HT, J. Mater. Chem., 2007,17,806.

[205] Xu B, Zhong M Q, Sun L, Xiang S F, Xu L X, Gaofenzi Cailiao Kexue Yu Gongcheng, Polym. Mater. Sci. Eng., 2007, 23,137.

[206] Ren X C, Cai X F, Zhao H J, Chen S Y, Dan Y, Effect of light-shield agents on the structural and properties of ageing POM. Sichuan Daxue Xuebao (Gongcheng Kexue Ban) J. Sichuan Univ. (Eng. Sci. Edition), 2007, 39(3), 107.

[207] Li S, Toprak MS, Jo Y, Suk D, Jon K, Do K, Muhammed M , Adv.Mater. 2007,19, 4347.

[208] Ammala A, Hill A J, Meakin P, Pas S J, Turney T W, Journal of Nanoparticle Research, 2002,4, 167.

[209] Kyprianidou Leodidou T, Margraf P, Caseri W, Suter UW,Walther P, Polymers for Advanced Technologies ,1996,8,505.

[210] Hill A J, Hannink R H J, Nanostructure Control of Materials, Woodhead Publishing Ltd., Cambridge, 2006.

[211] Yang P, Yan H, Mao S, Russo R, Johnson J, Saykally R, Morris N, Pham J, He R, Choi H J, Adv. Mater.,2002, 12, 323.

[212] Ito Y, Kushida k, Sugawara K,Takeuchi H, IEEE Trans, Ultrasonics, Ferroelectrics, and Frequency Control,1995, 42, 316.

[213] Ryu H W, Park B S, Akbar S A, Lee W S, Hong K H, Jin Seo Y, Shin D C, Park J S, Choi G P, Sens. Actuator B, 2003,96, 717.

[214] Sberveglieri G, Sens. Actuator B,1995, 23, 103.

[215] Trivikrama Rao G S, Tarakarama Rao D, Sens. Actuator B,1999, 55, 166 .

[216] Cheng X L, Zhao H, Huo L H, Gao S, Zhao J G, Sens. Actuator B,2004, 102, 248.

[217] Dietl T, Semicond. Sci. Technol, 2002,17, 377.

[218] Sharma P, Gupta A, Rao K V, Owens F J, Sharma R, Ahuja R, Osorio J M, Johansson B, Gehring G A, Nat. Mater,2003, 2, 673 .

[219] Saeki H, Tabata H, Kawai T, Solid State Commun,2001, 120, 439.

.....ഠോര....

SYNTHESIS,CHARACTERIZATION AND ANTIBACTERIAL PROPERTIES OF ZINC OXIDE NANOPARTICLES

Contents

Zinc oxide nanoparticles were prepared by reacting zinc chloride and sodium hydroxide in different mediums such as chitosan, poly vinyl alcohol, ethanol and starch. The materials were characterized by scanning electron microscopy (SEM), x-ray diffraction (XRD) studies, transmission electron microscopy (TEM) and thermogravimetric analysis (TGA). Elemental analysis was done by energy dispersive X-ray Analysis (EDAX). Antibacterial properties were studied using Bacillus aereus (gram positive) and Escherichia coli (gram negative) bacteria. The above studies were also carried on commercially available zinc oxide (CZO). Zinc oxide nanoparticles prepared using chitosan medium (NZO) showed lowest crystallite size in XRD. Morphology of the particle was changed by changing the reaction medium. XRD showed hexagonal wurtzite crystal structure of ZnO. TEM analysis showed particle size of the smallest particle of NZO is 35 nm and highest as 67 nm. Thermogravimetric studies (TGA) indicated improved thermal stability of NZO than CZO particles. Antibacterial studies showed excellent resistance of CZO and NZO to Bacillus aereus and Escherichia coli.

2.1 Introduction

Nano zinc oxide has a wide range of applications in various fields due to its unique and superior physical and chemical properties compared with bulk ZnO. The large specific surface area, high pore volume, low toxicity, nanostructured properties and low cost of nano ZnO [1] make it a promising candidate particularly in catalysts [2], chemical absorbents [3], as polymer additives [4], antiwear additives for oil lubricants [5] and advanced ceramics [6]. Zinc oxide nanoparticles have optical, electrical and photochemical activity [7], it can be used as photocatalysts [8], solar energy conversion cells [9,10],Ultra Violet (UV) detectors and UV emitting devices [11], chemical sensors sensitive to chemicals such as alcohol and benzene [12], and gas sensing materials for many gases such as ammonia, hydrogen and ozone [13-15]. Zinc oxide with direct band gap of about 3.37 eV at room temperature is a good material suitable for generating UV light [16]. ZnO with exciton binding energy of about 60 meV can ensure an efficient exciton emission at room temperature and low excitation energy [17, 18]. Thin films and nanoscale coating of ZnO particles on suitable substrates is important for its potential applications as substrates for functional coatings, printing, UV inks, e-print, optical communications (security papers), protection, portable energy, sensors, photocatalytic wallpaper with antibacterial activity etc [19-33]. The powder is widely used as an additive into numerous materials and products including plastics, ceramics, glass, cement, rubber, lubricants, paints, ointments, adhesives, sealants, pigments, source of Zn nutrient in foods, fire retardants etc[34]. The films of ZnO, indium tin oxide and cadmium oxide have been investigated in recently as transparent conducting oxide due to their good optical and electrical properties in combination with large band gap, abundance in nature, optical transmittance in visible region and non toxicity. Because the optical, electrical and magnetic properties of ZnO are markedly influenced by its

particle size, morphology and structure [35-37]. ZnO nanoparticles can be obtained by physical and chemical routes. However, chemical methods are more suitable for industrial scale production [35] due to its low efficiency and cost in obtaining nanoparticles with uniform size and morphology [36]. Different techniques for preparing ZnO nanoparticles have been reported such as, sol– gel technique [36], microemulsion synthesis [38], mechanochemical processing [37], spray pyrolysis [39], thermal decomposition of organic precursor [40], RF plasma synthesis [41], supercritical-water processing [42], self-assembling [43], vapour transport process [44], sonochemical or microwave-assisted synthesis [45], direct precipitation [46] homogeneous precipitation [47],chemical co-precipitation [48,49], chemical vapour deposition [50],thermal decomposition [51,52], hydrothermal synthesis [53,54], solid-state reaction [55],spray pyrolysis [56], and microemulsion precipitation [57-61]. Different ZnO nano structures such as nanospheres, nanorods, nanowires, nanotubes and flower-like nanostructures are obtained from these techniques. Variety of morphologies including prismatic forms [62], bipyramidal dumbbell-like [63], ellipsoidal [64], spheres [65], nanorods [66, 67], nanowires [67], whiskers [68], nanotubes [69], nanorings [70] and columnar hexagonal shaped ZnO [71] have been investigated.

LI Yan et al reported the formation of nest like ZnO by solvothermal synthesis [72].Tengfa Long et al studied the formation of ZnO nanorods and nanodisks from zinc chloride aqueous solution [73]. Yoshie Ishikawa et al prepared ZnO nanorods by pulsed laser ablation technique in water media at high temperature [74]. Ameer Azam etal used low temperature synthesis using micromechanical route [75].

The above methods require complex equipment and complicated operations. So, it is a challenge to search for a simple route to prepare metal

oxides nanoparticles with a high yield. We have used precipitation technique for the preparation of zinc oxide nanoparticles. In this work ZnO was prepared using zinc chloride and sodium hydroxide in different mediums such as chitosan, ethanol, polyvinyl alcohol (PVA) and starch. Compared with the above-mentioned methods, this method has four advantages: (1) it is very cheap and facile because of not requiring any complex equipment and complicated operations (2) the reaction is environmentally friendly since the byproducts are chitosan and sodium chloride (3) the reaction is safe and quick and (4) the high yield. Prepared ZnO was characterized by TEM, SEM, XRD and TGA. Antibacterial properties of ZnO was studied using a gram positive and gram negative bacteria.

2.2 Experimental

2.2.1 Materials

Chitosan samples were supplied by M/s. Indian Sea Foods, Cochin, Kerala (Viscosity 304 cps) and degree of deacetylation is 80.79%. PP homopolymer (REOL H200MA) was supplied by M/s. Reliance Industries limited. PVA, starch, ethanol, NaOH and $ZnCl_2$ was supplied by alpha chemicals, Cochin.

2.2.2 Methods

2.2.2.1 Preparation of zinc oxide

Zinc oxide nanoparticles were prepared by reacting zinc chloride and sodium hydroxide in different mediums such as chitosan, poly vinyl alcohol, ethanol and starch. In this method zinc chloride (5g in 500 ml 1% acetic acid in water) was added to chitosan (5g in 500ml 1% acetic acid in water) with vigorous stirring using mechanical stirrer. This was allowed to react for 24 hours. During this period stabilization of the complex take place. Then sodium hydroxide (25g in 500ml 1% acetic acid in water) was added drop wise from

burette to the above solution with stirring using mechanical stirrer. The whole mixture was allowed to digest for 12 hours at room temperature. This was to obtain homogeneous diffusion of OH^- and Cl^- to the matrix. The precipitate formed was washed several times with distilled water until complete removal of sodium chloride and dried at 100^0C. Then it was calcined at 550^0C for four hours. Figure 2.1 shows the schematic representation of preparation zinc oxide nanoparticles in chitosan medium. The experiment was repeated using other mediums such as poly vinyl alcohol, ethanol and starch.

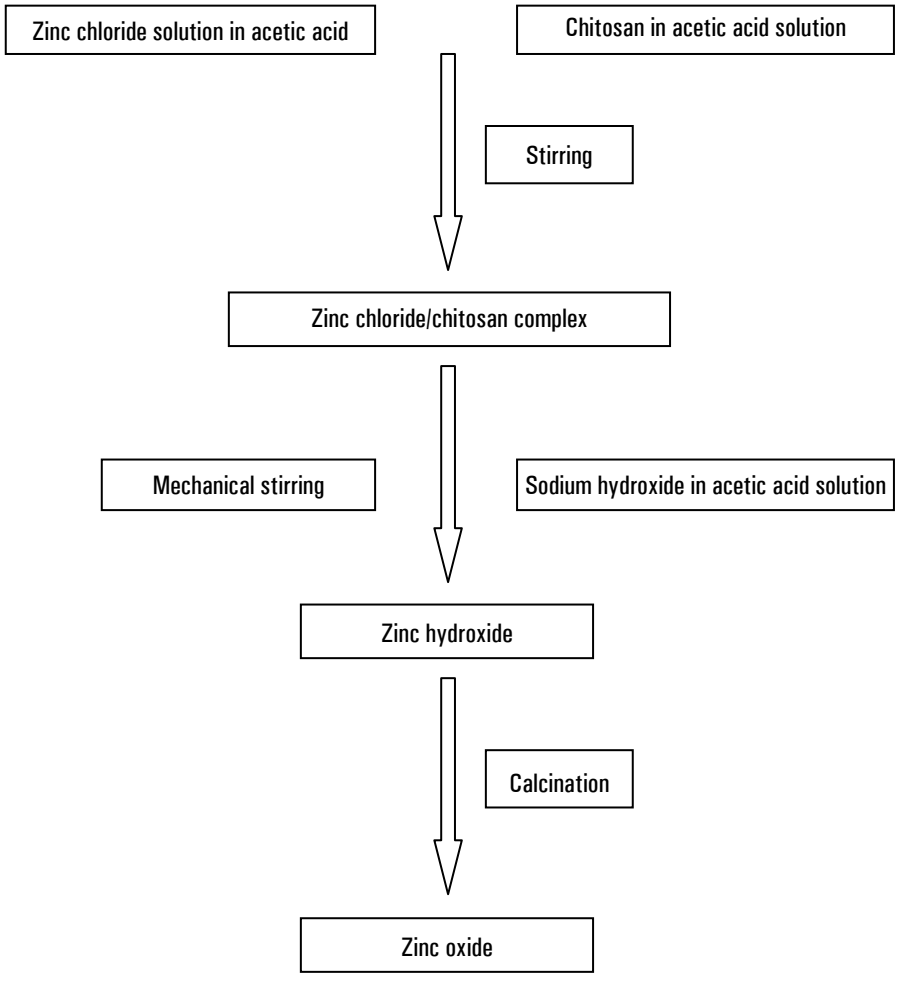

Figure 2.1: Schematic representation of preparation of zinc oxide

2.2.2.2 X-ray diffraction analysis

XRD is used to determine the size and shape of the unit cell for any compound most easily using the diffraction of x-rays. X-ray diffraction studies are used for the finger print characterization of crystalline materials and their structure determination. Each crystalline solid has its unique characteristics. Once the material has been identified, it is used to determine its structure, i.e. how the atoms packed together in the crystalline state and what the interatomic distances and angle are, etc.

XRD studies were done using Rigaku Geigerflex at wavelength CuK_a=1.54 A^0. Particle size was calculated using Debye Sherrer equation:

$$CS = 0.9\lambda/\beta\cos\Theta \quad \text{----------} \quad (2.1)$$

where CS is the crystallite size, β is the full width at half-maximum ($FWHM_{hkl}$) of an hkl peak at 2Θ value, 2Θ is the scattering angle.

2.2.2.3 Scanning electron microscopy

Scanning electron microscopy is used to gather information about topography, morphology, composition and micro structural information of materials. In SEM, electrons are thermoionically emitted from a tungsten or lanthanum hexa boride cathode and are accelerated towards an anode; alternatively electrons can be emitted via field emission. The electron beam, which has an energy ranging from a few hundred eV to 100keV, is focused by one or two condenser lenses in to a beam. Characteristic X-rays are emitted when the primary beam causes the ejection of inner shell electrons from the sample and are used to determine the elemental composition of the sample. The back scattered electrons emitted from the sample can be used alone to form an image or in composition with the characteristic X-rays.

These signals are monitored by photomultiplier tubes and magnified. An image of the investigated microscopic region of the specimen is observed in cathode ray tube and is photographed.

In this work, morphology of the ZnO was studied using scanning electron microscope (JOEL model JSM 6390LV). The powder was mounted on a metallic stub and an ultrathin coating of gold is deposited by low vacuum sputter coating. This is done to prevent the accumulation of static electric fields at the specimen due to the electron irradiation during imaging and to improve contrast. The SEM can produce high resolution images of the sample surface.

2.2.2.4 Transmission electron microscopy

In TEM, a beam of electrons is transmitted through an ultra thin specimen, interacting with the specimen as it passes through. An image is formed by the interaction of the electrons transmitted through the specimen. The image is magnified and focused into a fluorescent screen, on a layer of photographic film, or to be detected by a sensor such as a CCD camera. TEM gives significantly higher resolution images than light microscopes, due to the small de Broglie wavelength of electrons. This helps the user to examine fine detail even as small as a single column of atoms, which is tens of thousands times smaller than the smallest resolvable object in a light microscope.

In this work, TEM studies were carried out on JEM-2200-FS, Field Emission Transmission Electron Microscope, JEOL, Japan.

2.2.2.5 Energy Dispersive Analysis by X-rays

EDAX is a widely used technique to analyze the chemical composition of a material under SEM by detecting the X-rays produced as the result of the

electron beam interactions with the sample. When the sample is bombarded by the electron beam, the electrons are ejected from atoms comprising the sample surface. The resulting electron vacancies are filled by electrons from a higher state and an x-ray is emitted to balance the energy difference. EDS x-ray detector measures the relative abundance of X-rays against their energy. The detector is typically a lithium-drifted silicon solid-state device. As the incident x-ray hits the detector, creates a pulse of charge that is proportional to the energy of x-ray. The pulse charge is converted to a pulse voltage by using a charge sensitive preamplifier. The signal is pass to a multichannel analyzer where the pulses are sorted by the tension. The energy determined by measuring the voltage per incident x-ray is sent to a computer for display and further data evaluation. The spectrum of x-ray energy versus counts is measured to determine the elemental composition of the sample volume. Very light elements such as hydrogen do not emit X-rays and are impossible to detect because of the low-energy transitions occur. In this work elemental composition of the ZnO was studied using scanning electron microscope (JOEL model JSM 6390LV).

2.2.2.6 Thermogravimetric analysis

Thermogravimetric analysis (TGA) measures the weight change in a material as a function of temperature and time, in a controlled environment. This can be very useful to investigate the thermal stability of a material. It is suitable for use with all types of solid materials, including organic and inorganic materials. The material is heated to very high temperature so that one of the components decomposes into a gas, which dissociates into the air. If the compounds in the mixture remain are known, then the percentage by mass can be determined by taking the weight of what is left in the mixture and dividing it by the initial mass. From the mass of the original mixture and the total mass of impurities liberating upon heating, the stoichiometric ratio

can be used to calculate the percent mass of the substance in a sample. TGA is commonly employed in research to determine the characteristics of materials such as polymers, to determine degradation temperatures, absorbed moisture content of materials, the level of inorganic and organic components in materials and solvent residues. Thermogravimetric analyzer (TGA Q-50, TA instruments) was used to study the effect of TiO_2 on the thermal stability of PP. Approximately 10 mg of the samples were heated at a rate of 20^0 C/min from ambient to 800^0C.

2.2.2.7 Antibacterial properties

Bacterial nutrient medium (nutrient broth) was used to cultivate the gram positive [Bacillus aereus (NCIM No:2155)] and gram negative bacteria [Escherichia coli (NCIM No:2343)] respectively. Control nutrient broth as such was inoculated with the bacteria. NZO and CZO was dispersed at a concentration of 0.1mg/ml in the test media, prepared and commercially available. The test organisms were inoculated in the tubes and they were allowed to grow over night. Next day, the culture was serially diluted and plated on to the nutrient agar plates. The colonies formed were counted the next day. The result was expressed as CFU.

2.3 Results and Discussion

2.3.1 X-ray Diffraction

The XRD pattern of ZnO prepared in different mediums such as chitosan, PVA, starch and ethanol is given in figures 2.2-2.5 respectively. Figure 2.6 represents the XRD of commercial zinc oxide. These figures show the characteristics peaks of hexagonal crystal structure. The peaks obtained are correspond to (100), (002), (101), (102), (110), (103), (112), (201), (004), (202), (104) planes. The (101) plane is most prominent. Hexagonal wurtzite structure of ZnO belongs to the space group P63mc1

and lattice parameters a = 3.2539 Å and c = 5.2098 Å. The crystallite size of ZnO calculated using Debye Sherrer equation is given in table 2.1. Least crystallite size is obtained for ZnO prepared in chitosan medium (NZO). The influence of chitosan matrix is important in forming the nanoparticles of the zinc oxide. The stability of the complex formed between the particle and the surrounding polymer matrix and the proper diffusion of the reacting species are the most important criteria for the formation of nanoparticles.

Table 2.1: Crystallite size of ZnO prepared in different mediums

Medium	Crystallite size(nm)
Chitosan	13.4
Polyvinyl alcohol	28.29
Starch	25.01
Ethanol	21.4
Commercial ZnO	29.2

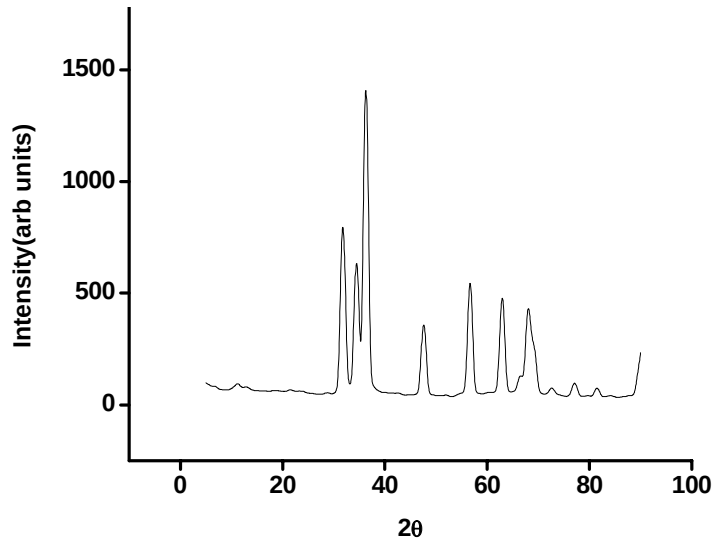

Figure 2.2: XRD pattern of ZnO prepared in chitosan medium

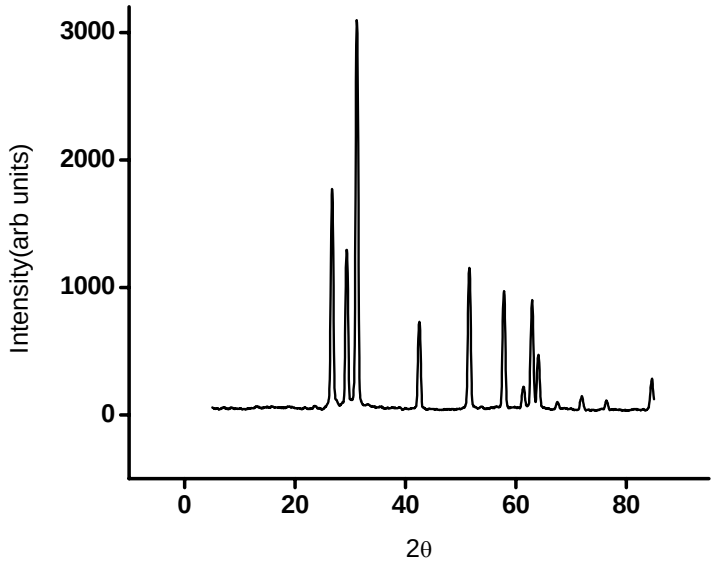

Figure 2.3: XRD pattern of ZnO prepared in polyvinyl alcohol medium

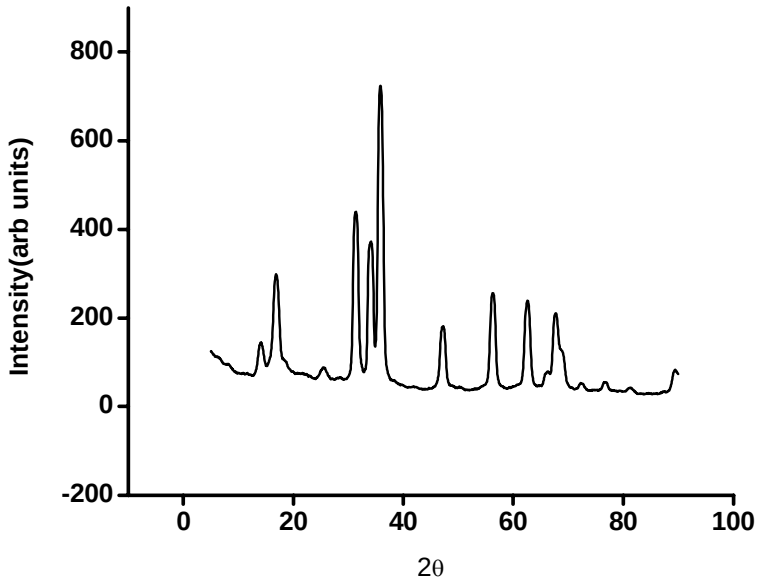

Figure 2.4: XRD pattern of ZnO prepared in Ethanol medium

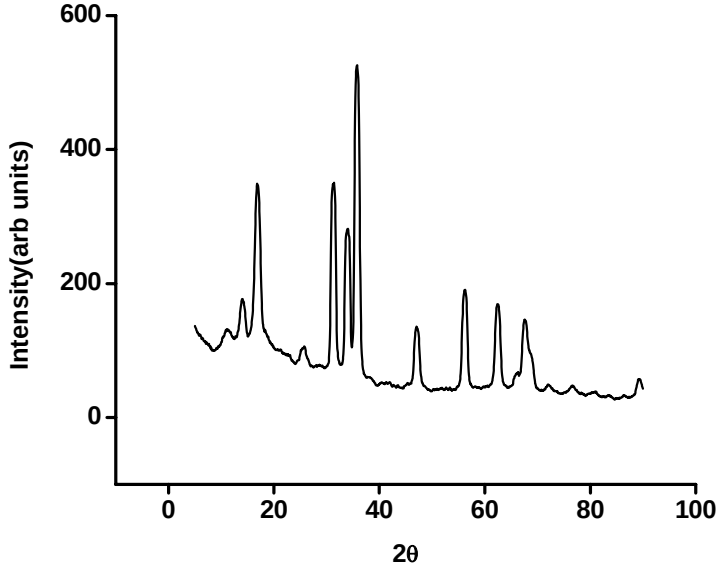

Figure 2.5: XRD pattern of ZnO prepared in starch medium

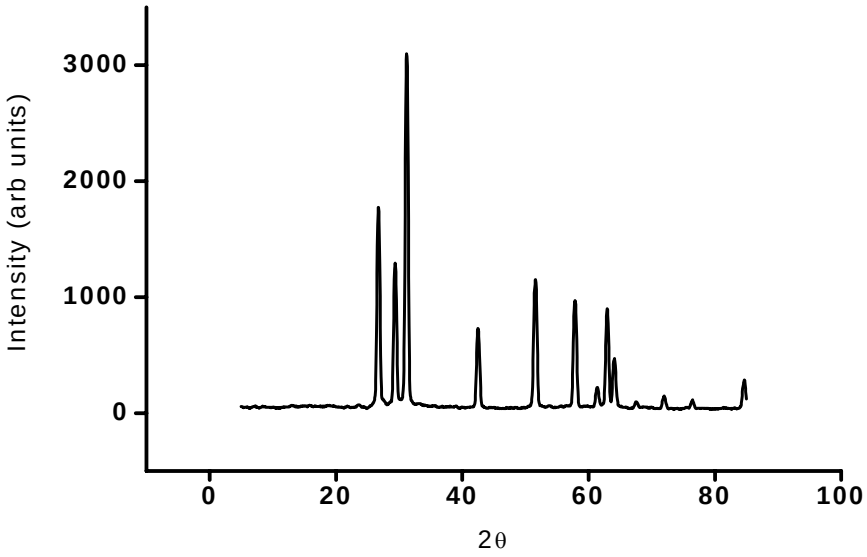

Figure 2.6: XRD pattern of commercial ZnO

2.3.2 Scanning Electron Micrographs

SEM photographs of ZnO prepared in different mediums and commercial ZnO are shown in figure 2.7. From the SEM images, it is clear that by changing the medium, morphology of the particles also changes. ZnO prepared in chitosan medium (NZO) shows spherical morphology while in ethanol medium flower like morphology is obtained. In PVA and starch medium large particles are observed. In chitosan medium small particles are observed and majority of the particles have a uniform nanostructure.

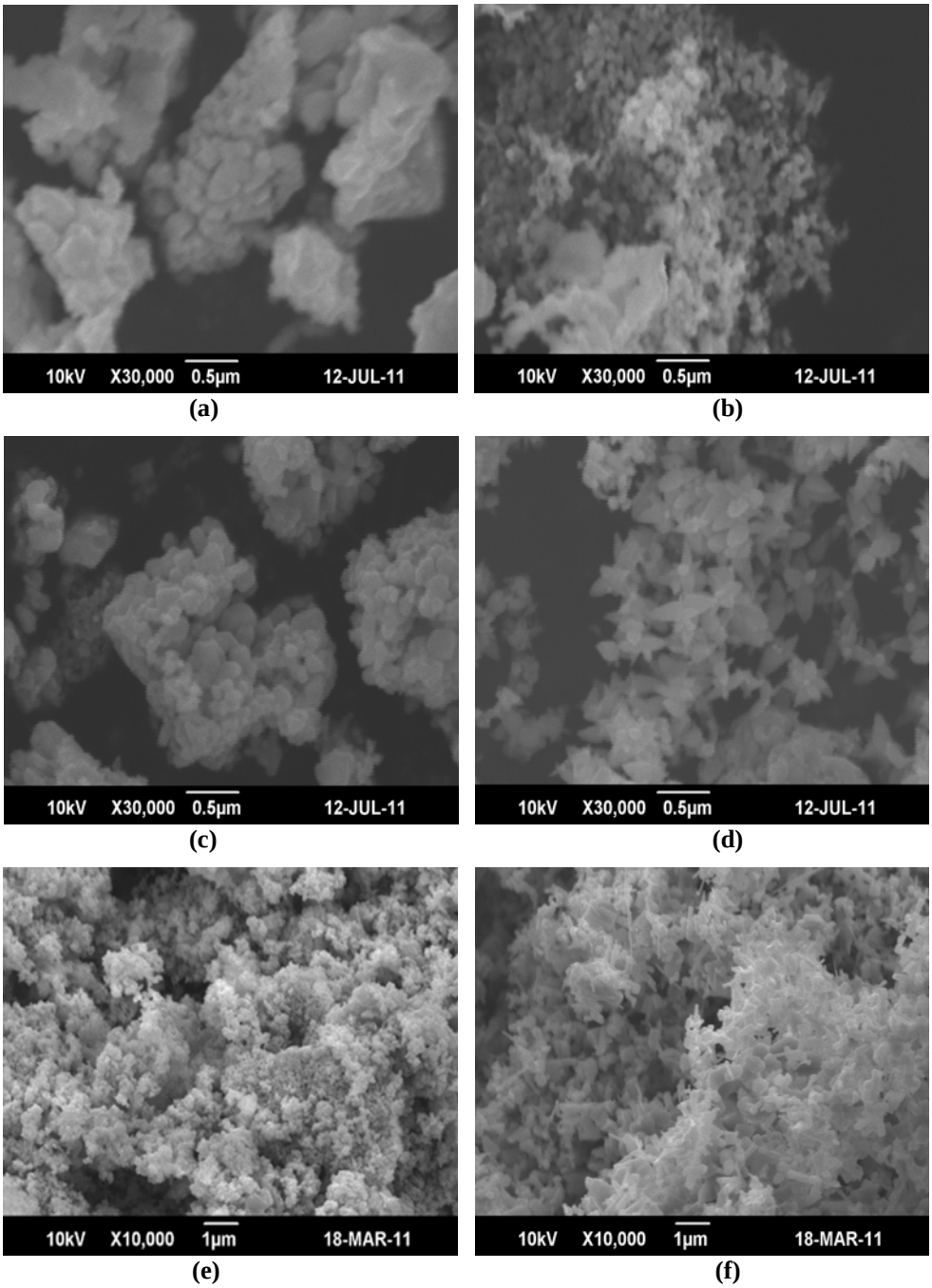

Figure 2.7: Scanning electron micrographs of ZnO prepared in (a) starch (b) chitosan (c) PVA (d) ethanol (e) chitosan (10,000 magnification) (f) commercial ZnO

The influence of chitosan matrix is very important in forming nanoparticles of zinc hydroxide and ZnO subsequently on calcination. Chitosan is a class of materials prepared by deacetylation of chitin to various extents, is of particular interest because it contains both -NH_2 and –OH groups. Also, the P^{Ka} associated with the amine groups is unusually low, so that a significant portion of them are in the –NH_2 form in a weakly acidic media (P^H 5.5-6.5) and has several advantageous. Amine chemistry, including metal complexation can occur in a phase in which the precursors combined and it makes possible to carry out reactions at the amine sites without using basic conditions in which the $ZnCl_2$ components themselves can be dissolved. Schematic representation of structure of chitosan is shown in figure 2.8.

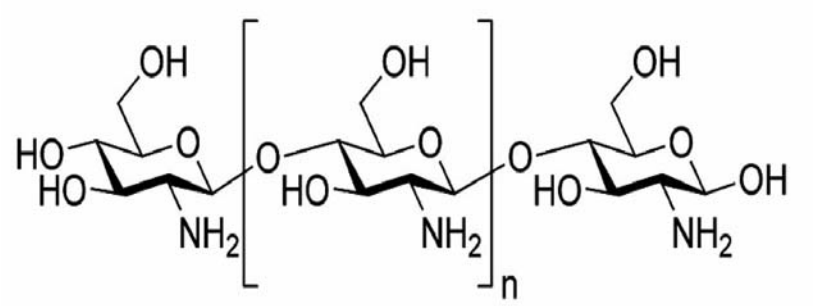

Figure 2.8: Schematic representation of structure of chitosan

The stability of the complex formed between the $ZnCl_2$ and the surrounding polymer matrix and the proper diffusion of the reacting species are the most important criteria for the formation of nanoparticles.

2.3.3 Trnsmission electron microscopy

Transmission electron microscopy (TEM) gives an idea about the size and shape of the particles on the scale of atomic diameters. Figure 2.9 shows the TEM images of ZnO prepared in chitosan medium (NZO). It can be observed that most of the particles are in nano-meter scale and are mostly of elongated spherical

shape. Figure 2.10 shows the particle size distribution of ZnO nanoparticles from TEM images. Most of the particles in the range of 45-60nm.

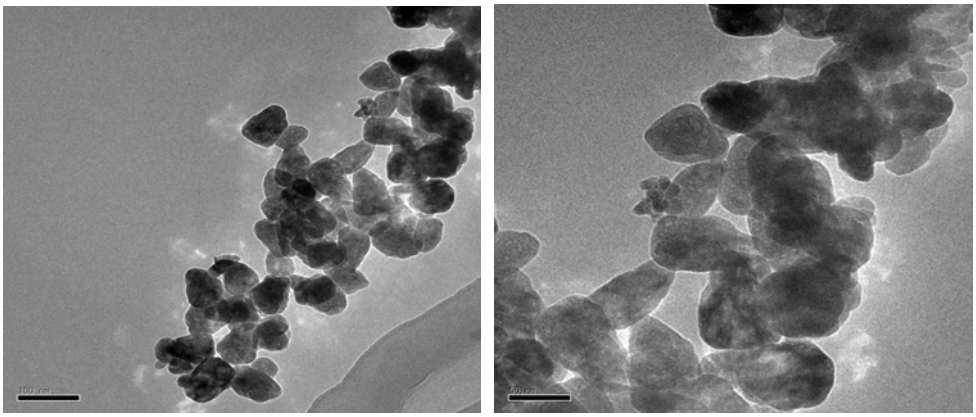

Figure 2.9: Transmission electron micrographs of ZnO nanoparticles

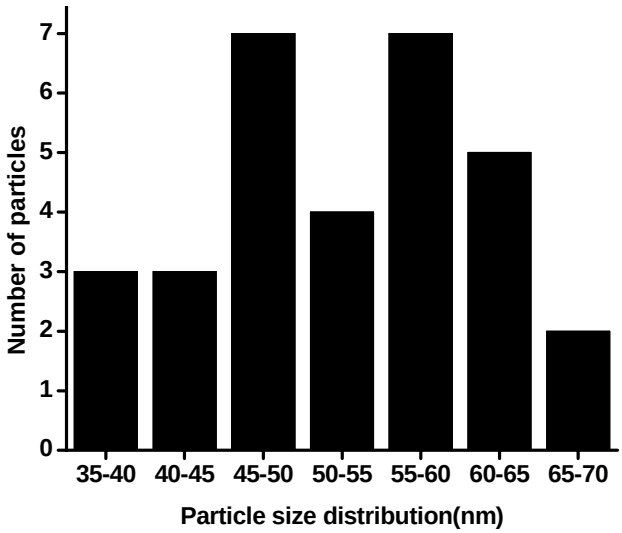

Figure 2.10: Particle size distribution of ZnO nanoparticles

2.3.4 Themogravimetric analysis

Thermogravimetric studies were carried out to investigate the degradation behaviour of NZO and CZO. Figure 2.11 shows the thermal behaviour of NZO and CZO from 30^0C to 900^0C in nitrogen atmosphere. Degradation of

NZO take place at higher temperature when compared to that of CZO. In the thermogram of CZO more degradation peaks are observed. This may be due to the impurities in the CZO. The degradation of NZO take place at higher temperature than CZO particles. This indicates significant improvement in thermal stability with decreasing the particle size of ZnO.

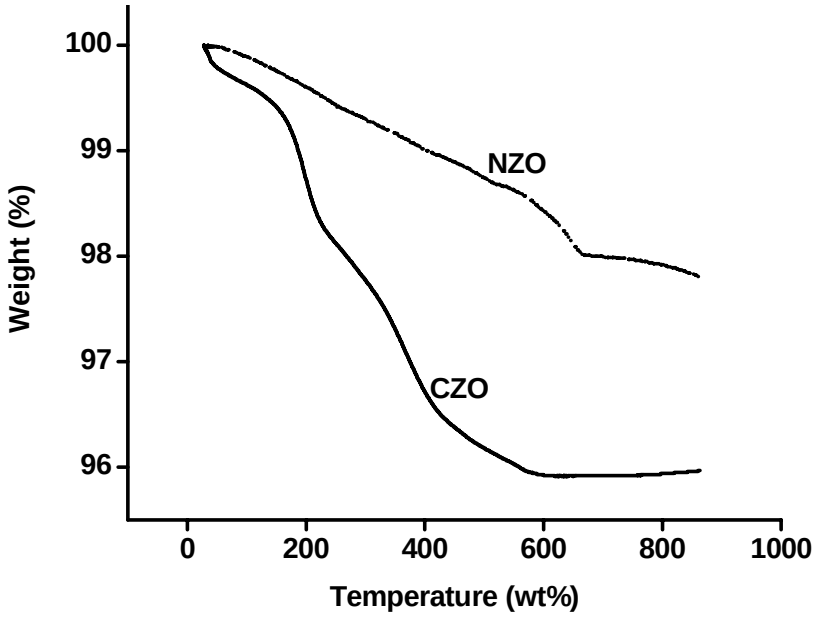

Figure 2.11: Thermogram of NZO and CZO

2.3.5 Energy Dispersive Analysis by X-rays

The energy dispersive X-ray spectrum of zinc oxide nanoparticles is shown in the figure 2.12. It is a key tool for identifying the chemical composition of a specimen. EDAX shows only peaks of zinc and oxygen. From figure 2.12 it is clear that prepared ZnO is free from impurities like chitosan and other materials.

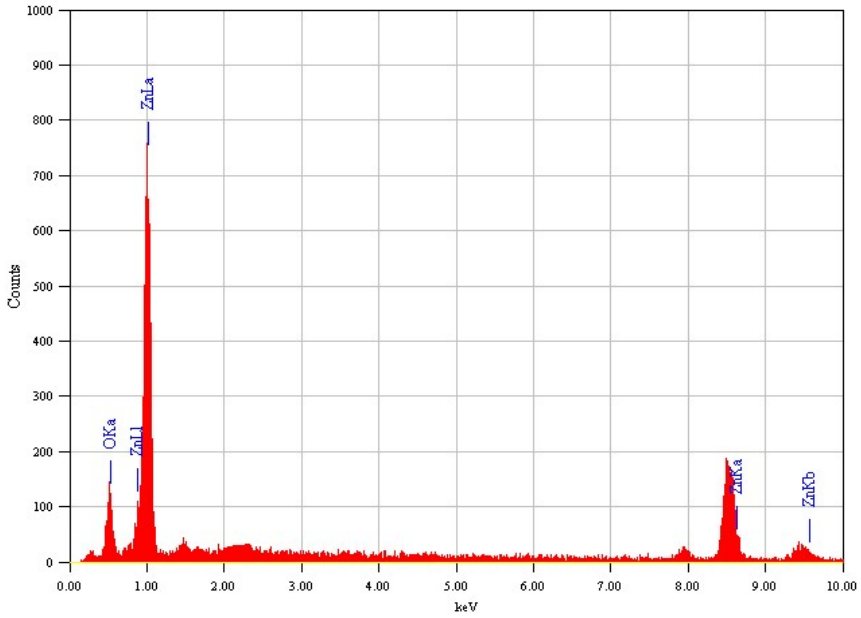

Figure 2.12: Energy dispersive X-ray spectrum of ZnO prepared in chitosan medium

2.3.6 Antibacterial properties of zinc oxide

2.3.6.1 Reduction in colony forming units (CFU)

Antibacterial properties of CZO and NZO in Escherichia coli (NCIM No: 2343) is shown in table 2.2. Percentage reduction in E- coli is 99.96% for CZO and for 99.98% for NZO. Zinc oxide shows good resistant to Escherichia coli. From the table it is clear that particle size of ZnO has no significant role in the antibacterial properties of ZnO.

Table 2.2: Colony forming unit using Escherichia coli (NCIM No: 2343)

Sample	Colony forming unit	% of reduction
Control	$9x\ 10^{8}$	
CZO	$3.19x10^{5}$	99.96
NZO	$1.37x10^{5}$	99.98

Table 2.3 shows antibacterial properties of CZO and NZO in to Bacillus aereus (NCIM No: 2155). Zinc oxide shows good resistant to Bacillus aereus irrespective of the particle size.

Table 2.3: Colony forming unit using Bacillus aereus (NCIM No:2155)

Sample	Colony forming unit	% of reduction
Control	$75x\ 10^{6}$	
CZO	$1.34x10^{6}$	98.66
NZO	$8x10^{5}$	98.94

2.4 Conclusion

Zinc oxide nanoparticles were prepared by precipitation method in different mediums. X-ray diffraction analysis indicates least crystallite size is obtained when chitosan is used as the medium. From X-ray diffraction analysis it is clear that all ZnO particles are in hexagonal wurtzite crystal structure. Scanning electron micrographs show formation of spherical particles of ZnO prepared in chitosan medium. Flower like morphology is observed for ZnO prepared in ethanol medium. EDAX shows the absence of side products or impurities after calcination. TGA analysis shows the better thermal stability of NZO compared to that of CZO. TEM studies showed that the particle size of smallest particle of NZO is 22nm. CZO and NZO show excellent resistance to Bacillus aereus and Escherichia coli. Reduction in particle size has no role in the antibacterial properties.

References

[1] Franklin N M, Rogers N J, Apte S C, Batley G E, Gadd G E, Casey P S, Environ Sci Tech,2007, 41, 8487.

[2] Jung H, Choi H, Appl Catal B, 2006,66, 288 .

[3] Sayyadnejad M A, Ghaffarian H R, Saeidi M, Int J Environ Sci Tech, 2008,5,565.

[4] Carrion F G, Sanes J, Bermudez M D, Wear, 2007, 262, 1504.

[5] Hernandez Battez H, Gonzalez R, Viesca J L, Fernandez J E, Dlaz Fernandez J M, Machado A, Chou R, Riba J, Wear, 2008,265, 422.

[6] Rao K J, Mahesh K, Kumar S, Bull. Mater. Sci., 2005, 28, 19.

[7] Kumpika T, Thongsuwan W, Singjai P, Thin solid Films, 2008,516, 5640.

[8] Park S B, Kang Y C, J. Aerosol Sci., 1997, 28, S473.

[9] Rao A R , Dutta V, Nanotechnology, 2008, 19, 445712.

[10] Wei D, Unalan H E, Han D, Zhang Q, Niu L, Amaratunga G, Ryhanen T, Nanotechnology,2008, 19, 424006.

[11] Carrey J, Carrere H, Khan M L, Chaudret B, Marie X, Respaud M, Semicond. Sci. Technol.,2008,23,025003.

[12] Ge C, Xie C, Hu M, Gui Y, Bai Z, Zeng D, Mater. Sci. Eng. B, 2007,141, 43.

[13] Rout C S, Hegde M, Govindaraj A, Rao C N R, Nanotechnology, 2007,18, 205504.

[14] Rout C S, Raju A R, Govindaraj A, Rao C N R, Solid State Commun, 2006,138, 136.

[15] Kenanakis G, Vernardou D, Koudoumas E, Kiriakidis G, Katsarakis N, Sens. Actuators B, 2007, 124,187.

[16] Singhal M, Chhabra V, Kang P, Shah D O, Mater. Res. Bull., 1997, 32, 239.

[17] Feldmann C, Adv. Fundam. Mater., 2003,13,101.

[18] Kitano M, Shiojiri M, Powder Technol., 1997,93, 267.

[19] Ozgur U, Alivov Y I, Liu C, Teke A, Reshchikov M A, Dogan S, Avrutin V, Cho S J, Morkoc H, J. Appl. Phys., 2005, 98, 041301.

[20] Yamamoto O, Int. J. Inorg. Mater., 2001, 3, 643.

[21] Yamamoto O, Komatsu M, Sawa J, Nakagawa Z E, J. Mater. Sci : Mater. Med., 2004, 15, 847.

[22] Sawai J, Shoji S, Igarashi H, Hashimoto A, Kokugan T, Shimizu M, Kojima H, Ferment J, Bioeng., 1998, 86, 521.

[23] Pearton S J, Norton D P, Ip K, Heo Y W , Steiner T, J. Vac. Sci. Technol.B, 2004, 22, 932.

[24] Brayner R, Ferrari Iliou R, Brivois N, Djediat S, Benedetti M F, Fievet F, Nano Lett., 2006, 6, 866.

[25] Jing L Q, Sun X J, Shang J, Cai W M, Xu Z L, Du Y G, Fu H G, Sol. Energy Mater. Sol. Cells, 2003, 79, 133.

[26] Shen W F, Zhao Y , Zhang C B, Thin Solid Films, 2005, 483, 382.

[27] Bae S H, Lee S Y, Jin B J,Im S, Appl. Surf. Sci., 2001, 169, 525.

[28] Niesen T P, De Guire M R, J. Electroceram., 2001, 6, 169.

[29] Bachari E M, Ben Amor S, Baud G, Jacquet M, Mater. Sci. Eng. B, 2001, 79, 165.

[30] Ibanez R U, Barrado J R R, Martin F, Brucker F, Leinen D, Surf. Coat. Technol., 2004, 675,188.

[31] Golego N, Studenikin S A, Cocivera M, J. Electrochem. Soc., 2000, 147, 1592.

[32] Chaudhuri S, Bhattacharyya D, Maity A B, A K Pal, Surf. Coat. Adv. Mater., 1997, 246, 181.

[33] Bahnemann D, Sol. Energy, 2004, 77, 445.

[34] Anne Aimable, Maria Teresa Buscaglia, Vincenzo Buscaglia, Paul Bowen, Journal of the European Ceramic Society, 2010, 30, 591.

[35] Fotou G P, Pratsinis S E, Chem. Eng. Commum., 1996,151, 251.

[36] Mondelaers D, Vanhoyland G,Van den Rul H, Haen J D,Van Bael M K, Mullens J, Van Poucke L C, Mater. Res. Bull., 2002, 37, 901.

[37] Tsuzuki T, McCormick P G, Scripta Mater., 2001, 44, 1731.

[38] Singhal M, Chhabra V, Kang P, Shah D O, Mater. Res. Bull., 1997, 32 , 239.

[39] Okuyama K, Lenggoro I W, Chem. Eng. Sci., 2003, 58, 537.

[40] Rataboul F, Nayral C, Casanove M J, Maisonnat A, Chaudret B, J. Organomet. Chem. 2002, 307, 643644 .

[41] Sato T, Tanigaki T, Suzuki H, Saito Y, Kido O, Kimura Y, Kaito C, Takeda A, Kaneko S, J. Cryst. Growth, 2003, 313, 255.

[42] Viswanathan R, Lilly G D, Gale W F, Gupta R B, Ind. Eng. Chem. Res., 2003, 42 ,5535.

[43] Koh Y W, Lin M, Tan C K, Foo Y L, Loh K P, J. Phys.Chem. B, 2004,108,11419.

[44] Yu W D, Li X M, Gao X D, Cryst. Growth Des., 2005, 5 , 151.

[45] Hu X L, Zhu Y J, Wang S W, Mater. Chem. Phys., 2004,421.

[46] Wang J M, Gao L, Inorg. Chem. Commun., 2003, 6, 877.

[47] Kim J H, Choi W C, Kim H Y, Kang Y, Park Y K, Powder Technol.,2005, 153, 166.

[48] Wang L N, Muhammed M, J. Mater. Chem., 1999, 9, 2871.

[49] Rodriguez-Paez J E, Caballero A C, Villegas M, Moure C, Duran P, Fernandez J F, J. Eur. Ceram. Soc., 2001, 21, 925.

[50] Purica M, Budianu E, Rusu E, Danila M, Gaurila R, Thin Solid Films,2002, 403, 485.

[51] Audebrand N, Auffredic J P, Louer D, Chem. Mater., 1998,10, 2450.

[52] Yang Y, Chen H, Zhao B, Bao X, J. Cryst. Growth, 2004,263, 447.

[53] Liu B, Zeng H C, J. Am. Chem. Soc. , 2003, 125, 4430.

[54] Lu C H, Yeh C H, Ceram. Int., 2000, 26, 351.

[55] Zhu Y, Zhou Y, Appl. Phys. A, 2008, 92, 275.

[56] Tani T, Madler L, Pratsinis S E, J. Nanopart. Res., 20020, 4, 337.

[57] Hingorani S, Pillai V, Kumar P, Multani M S, D. O. Shah D O, Mat. Res. Bull., 1993, 28, 1303.

[58] Hingorani S, Shah D O, J. Mater. Res., 1995, 10, 461.

[59] Shingal M, Chhabra V, Kang P, Shah D O, Mat. Res. Bull., 1997,32, 239.

[60] Lim B P, Wang J, Ng S C, Chew C H, Gan L M, Ceram. Int., 1998, 24, 205.

[61] Inoguchi M, Suzuki K, Kageyama K, Takagi H, Sakabe Y, J. Am. Ceram. Soc., 2008, 91, 3850.

[62] Li W J, Shi E W, Zhong W Z and Yin Z , J. Cryst. Growth, 1999, 203, 186.

[63] Wang B G, Shi E W, Zhong W Z , Cryst. Res. Technol., 1998, 33, 937.

[64] Lu C H , Yeh C H , Ceram. Int., 2000, 26, 351.

[65] Neves M C, Trindade T, Timmons A M B, Pedrosa de Jesus J D, Mater. Res. Bull. 2001, 36, 1099.

[66] Pal U and Santiago P *J. Phys. Chem.* B,2005, 109, 15317.

[67] Vayssieres L , *Adv. Mater.,2003,* 15, 464

[68] Hu J Q, Li Q,Wong N B, Lee C S and Lee S T , Chem. Mater.,2002, 14, 1216.

[69] Sun Y, Fuge G M, Fox N A, Riley D J and Ashfold M N R,Adv. Mater. 2005, 17, 2477.

[70] Gui Z, Liu J, Wang Z Z, Song L, Hu Y, Fan W C and Chen D Y , J. Phys. Chem. B, 2005, 109, 1113.

[71] Ni Y H, Wei X W, Ma X and Hong J M, J. Cryst. Growth, 2005, 283, 48.

[72] LI Yan, FENG Hui-yun, ZHANG Nan, LIU Chuan-sheng, Trans. nonferrous Met.Soc. China, 2010, 20, 119.

[73] Tengfa Long, Shu Yin , Kouta Takabatake ,Peilin Zhnag ,Tsugio Sato, Nanoscale Res Lett 2009, 4,247.

[74] Yoshie Ishikawa, Yoshiki Shimizu, Takeshi Sasaki, Naoto Koshizaki , Journal of Colloid and Interface Science,2006, 300, 612.

[75] Ameer Azam, Faheem Ahmed, Nishat Arshi, Chaman M, Naqvi A H, International Journal of Theoretical & Applied Sciences, 2009, 12.

.....ꕥ.....

POLYPROPYLENE/ZINC OXIDE NANOCOMPOSITES THROUGH MELT MIXING

Contents

PP/ ZnO nanocomposites were prepared using 0-5wt% of zinc oxide by melt mixing. It was then compression moulded in to films. The composites were prepared using ZnO prepared in chitosan medium (NZO) and commercial ZnO (CZO). Mechanical properties of the composites increased by the addition of ZnO. Transparency of the composite films were improved by reducing the particle size of ZnO. Melt flow index studies revealed that NZO increased the flow characteristics of PP while for CZO decreased. Differential scanning calorimetric studies indicated an increase in degree of crystallinity by the addition of ZnO. X-ray diffraction studies indicated α-form of isotactic polypropylene. Thermogravimetric studies showed an improvement in thermal stability of PP on addition of ZnO. An increase in storage modulus, loss modulus and tan δ values of the composites was observed in dynamic mechanical analysis. Limiting oxygen index values showed an increase on addition of NZO. Uniform dispersion of the ZnO was observed in the scanning electron micrographs of the tensile fractured surface of composites. Mechanical, morphology and IR studies were carried out after thermal and UV ageing. NZO filled films showed better properties compared to CZO filled films.

3.1 Introduction

Polymer nanocomposites have attracted great attention due to their enhanced mechanical strength and thermal properties at low filler loadings [1-8]. This was attributed to the unique characteristics of the nanofillers [9]. Now a days, nanostructured versions of conventional inorganic fillers are used in plastic composites. Much effort has been done to enhance the properties of polymers by adding inorganic nanofillers such as SiO_2 [10], ZnO [11,12] and $CaCO_3$[13]. Recently, nanocomposites based on PP matrix constitute a major challenge for industry since they represent the route to substantially improve the mechanical and physical properties of PP [14-16]. PP is one of the most widely used thermoplastic polymers due to its good physical and mechanical properties as well as the ease of processing at a relatively low cost. There is a number of investigations on the PP nanocomposites filled with different types of fillers such as carbon nanotubes [17-19], nanoclay [20,21], talc, mica and fibrous fillers etc. Reinforcement at nanoscale to increase mechanical and other properties including changes in the polymer crystallization behaviour is being studied [22]. There are many articles related to the crystallization behaviour of PP and PP composites [23–27]. The crystallization behaviour of reinforced PP composites with flax fiber, sisal fiber, pine fiber, glass fiber, hemp fiber, jute fiber and wood has been reported [28–33].

The enhanced properties are due to the synergistic effects of nanoscale structure and interaction of fillers with polymers. The size and structure of the dispersed phase significantly influence the properties of polymer nanocomposites [34-36]. The key factors for the preparation of improved performance are the fine and a homogeneous dispersion of the nano powders and a strong interface adhesion between matrix and nanofillers.

Various approaches have been taken for the preparation of nanocomposites by in situ polymerization, solution mixing, melt mixing etc [37-40]. Among these, melt mixing of the polymeric matrix with the filler is the most convenient and economical way of obtaining composite. Nano zinc oxide has attracted increased attention as one of the multifunctional inorganic nanoparticles, due to its significant properties, such as high chemical stability, low dielectric constant, large electromechanical coupling coefficient, high luminous transmittance, high catalytic activity, intensive ultraviolet and infrared adsorption [41,42]. In this work, we investigated the morphology, mechanical, dynamic mechanical, crystallization, transparency, thermal and flow properties of the PP/ZnO nanocomposites prepared by melt mixing. Mechanical, morphology and IR studies were carried out after UV and thermal ageing.

3.2 Experimental

3.2.1 Materials

Isotactic PP homopolymer (REPOL H200MA) with melt flow index of 25 g/min was supplied by M/s.Reliance Industries limited.

3.2.2 Methods

3.2.2.1 Preparation of PP/ZnO composites: Compression moulding

The melt compounding was performed using a Thermo Haake Polylab system operating with counter rotating screws at 40 rpm for 8 min at 170^0C (figure 3.1) with a capacity of $60cm^3$. The polymer and the ZnO have been charged to the mixing chamber. A mixing time of 8 min was fixed since the torque stabilized to constant values during this time. The stabilization of torque related to the attainment of a stable structure. Composites of different concentrations (0-5wt%) of ZnO were prepared. The hot mix immediately pressed after mixing using a hydraulic press. The samples were then made in to films using compression moulding at 180^0C for 6 min in an electrically heated hydraulic press.

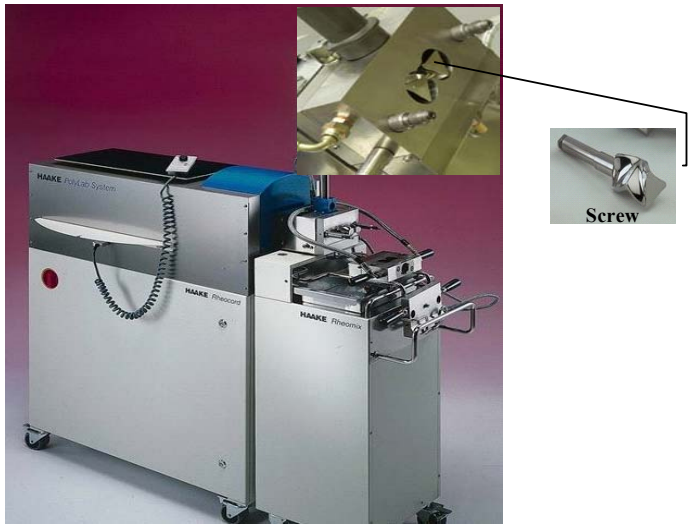

Figure 3.1: Thermo Haake Polylab system

3.2.2.2 Mechanical properties of PP/ZnO composites

Mechanical properties of the compression moulded samples of PP and PP/ZnO composites were studied using a Universal testing machine (UTM, Shimadzu, model-AG1) with a load cell of 10 kN capacity. The specimens used were rectangular strips of dimensions 10 × 1 cm. The gauge length between the jaws at the start of each test was adjusted to 40 mm and the measurements were carried out at a cross-head speed of 50 mm/min (ASTM D 882).

3.2.2.3 Dynamic mechanical analysis (DMA)

In DMA, the viscoelastic properties of a material are characterized by applying a sinusoidal deformation to the material at a single or at multiple frequencies and monitoring the response of the material. Response of a viscoelastic material to an imposed deformation will depend on how fast or slow the deformation is applied to the sample. When characterizing a material by DMA, the time of the deformation is determined with respect to the frequencies, as frequency is the inverse of time (frequency = 1/time). High frequencies are analogous to short times and low frequencies to long times.

Dynamic mechanical analyser (DMA Q-800, TA Instruments) was used to study the effect of ZnO on the viscoelastic properties of PP. The tests were carried out on rectangular shaped specimens of dimensions 3 ×1 cm by temperature sweep (temperature ramp from 30^0C to 150^0C at 3^0C/min) method at a constant frequency 1 Hz. The dynamic storage modulus, loss modulus and tan δ (ratio of loss modulus to storage modulus) were measured.

3.2.2.4 Scanning electron microscopy

The morphology of the tensile fractured surface of PP and composites was studied using scanning electron microscope (JOEL model JSM 6390 LV).

3.2.2.5 Thermogravimetric analysis

Thermogravimetric analyzer (TGA Q-50, TA instruments) was used to study the effect of ZnO on the thermal stability of PP. Approximately 10 mg of the samples were heated at a rate of 20^0 C/min from ambient to 800^0C in nitrogen atmosphere.

3.2.2.6 Differential Scanning Calorimetry

Differential Scanning Calorimetry (DSC) is used for studying the thermal behaviour of a material as a function of temperature as they go through physical and chemical changes with absorption or evolution of heat. It is used to study the thermal transitions, including phase changes, crystallization, melting, glass transitions of a material as a function of temperature. Heat flow, i.e, heat of absorption (endothermic) or heat of emission (exothermic), is measured as a function of temperature or time of the sample and compared with that of a thermally inert reference. The materials as they undergo changes in chemical and physical properties, which are detected by transducers , then changes in to electrical signals that are collected and give thermogram. In this work, DSC measurements were performed on a DSC Q100 differential scanning

calorimeter. Indium was used for temperature and enthalpy calibration (T_m = 156.63 °C, ΔH_m = 28.47 J/g) and analysis were carried out in nitrogen atmosphere. Samples of about 5–10 mg sealed in aluminum pans were heated from 30^0C to 200^0C at a heating rate of 10^0C/min in nitrogen atmosphere. When the temperature reached 200^0C, samples were maintained for 1 min to eliminate the thermal history and then cooled at a rate of 10^0C/min. The crystallization exotherm and subsequent melting curves of the samples were recorded in the range from 35^0C to 200^0C.

The degree of crystallinity of the samples (Xc) was calculated according to Equation

$$X_c=\Delta H_c/(\Delta H^0_c(1-Wm))x100 \quad \text{---------- (3.1)}$$

Where ΔH_c is the enthalpy of crystallization, ΔH^0_c is the theoretical specific enthalpy of crystallization of 100% crystalline PP, which was taken as 207.1 J/g [43] and Wm is the weight percentage of ZnO.

3.2.2.7 Melt flow index (MFI) measurements

MFI is a measure of the ease of flow of the melt of a thermoplastic polymer. It is defined as the mass of polymer, in grams, flowing in ten minutes through a capillary of a specific diameter and length by a pressure applied via prescribed alternative gravimetric weights for alternative prescribed temperatures as per ASTM D 1238. MFI of the composites were studied using CEAST melt flow modular line indexer (ITALY) at 190^0C and 2.16 and 5 kg wt. Preheating time of 6 minute is given before each experiment. The weight of the substance extruded in 10 min in grams is measured.

3.2.2.8 Limiting Oxygen Index (LOI)

The advanced LOI chamber accurately determines the relative flammability of plastics and other materials. Flamability of nanocomposites was characterized

by burning test, which gives a quantitative measure of rate of burning of polymeric samples. Test was conducted according to ASTM D 635. Sample dimensions were 150X12.7X3.2mm^3. The test specimens were burned in a precisely controlled atmosphere of nitrogen and oxygen. Test samples were placed vertically in the flammability apparatus. The free end of the specimen was exposed to gas flame. Flammability of materials was determined by measuring the minimum oxygen concentration that will support combustion.

3.2.2.9 X-ray diffraction studies

X-ray diffraction studies were carried out using Rigaku Geigerflex at wavelength CuK_a=1.54 A^0.

3.2.2.10 Thermal ageing

Thermal ageing was carried out in a hot air oven at 100^{0}C for 24 hours. Mechanical, morphology and IR studies were carried out after thermal ageing.

3.2.2.11 Photo ageing

In the present study, the PP film samples were exposed under a 30-watt shortwave UV lamp at a distance of 30 cm for 48 hours. Mechanical, morphology and IR studies were carried out after photo ageing.

3.2.2.12 Infrared (IR) spectroscopy

Infrared spectroscopy is one of the most powerful analytical techniques used for chemical identification. The technique when coupled with intensity measurements may be used for quantitative analysis. One of the important advantages of IR spectroscopy is it provides information about the structure of a molecule quickly, without tiresome evaluation methods. This technique is based on the simple fact that a chemical substance shows selective absorption in the IR region giving rise to close-packed absorption bands called an IR

absorption spectrum, over a wide wavelength range. Various bands present in the IR spectrum correspond to the characteristic functional groups and bonds present in a chemical substance. Hence, an IR spectrum of a chemical substance is a fingerprint for its identification. IR spectrum (Thermo Nicolet, iS10 Fourier Transform Infrared, KBr Pellets transform mode) was used to study the degradation products after thermal and photo ageing.

3.3 Results and Discussion

3.3.1 Mechanical properties of PP/ ZnO composites

Figures 3.2 and 3.3 show variation in tensile strength and modulus of PP with ZnO content. The incorporation of ZnO in the PP matrix results in an increase in the tensile strength and modulus, reaches a maximum at 1.5wt% concentration of ZnO and then decreases. In the case of PP with NZO the tensile strength increased from 31.75 to 44.37 N/mm^2 and tensile modulus from 1105.35 to 1897.02 N/mm^2 at 1.5 wt% NZO. CZO filled PP shows an increase in tensile strength from 31.8 to 41.2 N/mm^2 at 1.5 wt% CZO and tensile modulus from 1105.75 to 1422.9 N/mm^2 at 0.5Wt% of CZO. The increase in properties may be due to the interface interaction between nanoparticles and a polymer matrix can transfer stress, which is beneficial for the improvement of the tensile strength of composite films. However, with increasing content of nanoparticles, aggregation occurs, which leads to a decrease in the contact area between the nanoparticles and polymer matrix and results in the formation of defects in the composites. Therefore, the effective interfacial interaction is reduced, and the tensile strength of the films decreased [44]. The mechanical properties also depend on the dispersion of nanoparticles in the matrix. The improvement of tensile modulus and strength of PP/ZnO nanocomposites is related to the inherent stiffness and quality of the dispersion of ZnO and also adhesion between the matrix and nanoparticles [45, 46]. Morphology and particle size of ZnO has a major role on the mechanical

properties of PP. Elongation at break (figure 3.4.) of PP decreased by the addition of low concentration of ZnO, at a higher concentration it is increased.

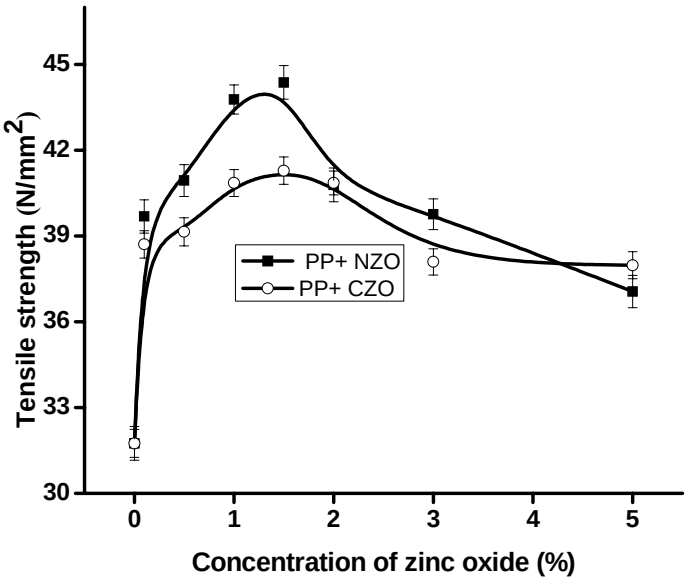

Figure 3.2: Effect of particle size of ZnO on tensile strength of PP/ZnO composites

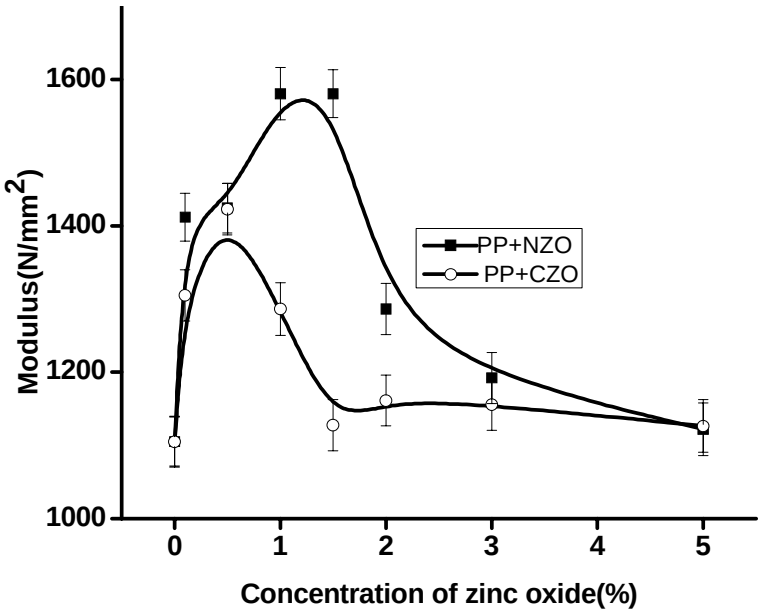

Figure 3.3: Effect of particle size of ZnO on modulus of PP/ZnO composites

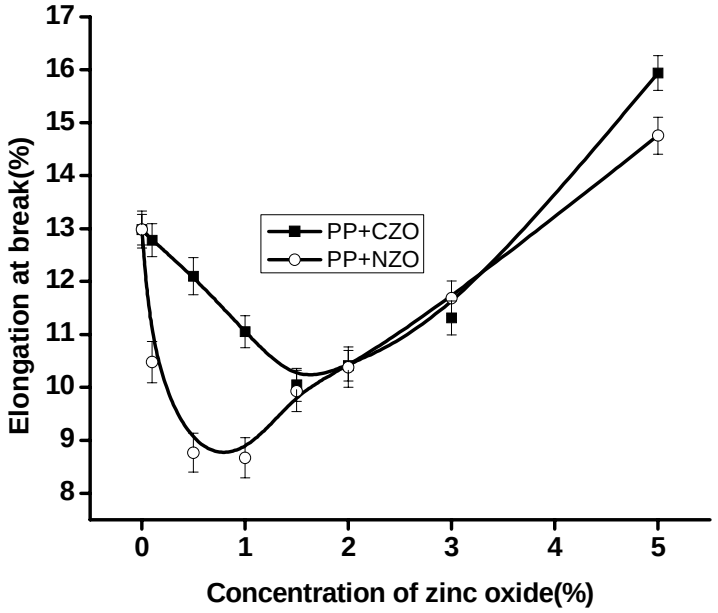

Figure 3.4: Effect of particle size of ZnO on elongation at break of PP/ZnO composites

3.3.2 Dynamical mechanical analysis of PP/ ZnO composites

Dynamic storage modulus is the most important property to assess the load-bearing capability of a material. It is usually used to study the relaxations in polymer materials. The ratio of loss modulus to storage modulus is known as mechanical loss factor (tanδ). This is a measure of the balance between elastic phase and the viscous phase in the polymeric structure. This is related to the impact properties of the material.

The storage modulus of neat PP and PP/ZnO nanocomposites as a function of temperature at 1Hz are shown in figure 3.5. Storage modulus of the PP is increased with the addition of ZnO. The increase in storage modulus is significant at low temperature like 40^0C. The increase may be due to the stiffening effects of ZnO and efficient stress transfer between the polymer matrix and nano ZnO.

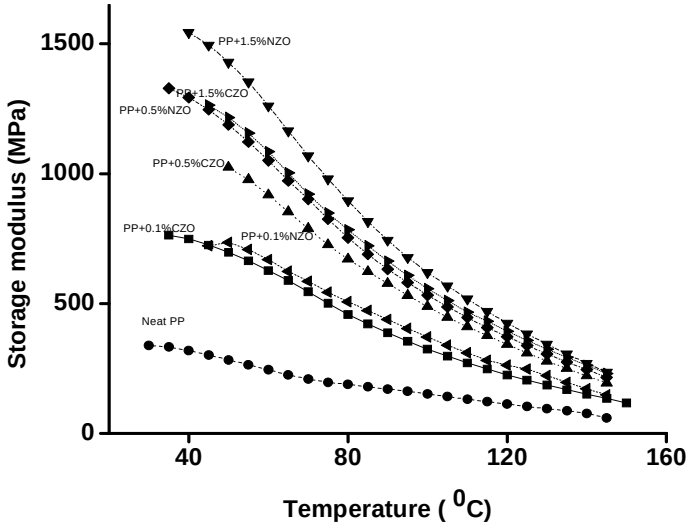

Figure 3.5: Effect of ZnO on storage modulus of PP/ZnO composites

The loss modulus of the PP and composites are given in figure 3.6. The loss modulus also increased substantially with ZnO concentration. The reinforcing effect of ZnO can be attributed to their specific interactions and the formation of a rigid percolating ZnO network within the polymer matrix. Maximum improvement is shown by PP with 1.5 wt% NZO. Composite of PP with NZO showed significant improvement compared to CZO.

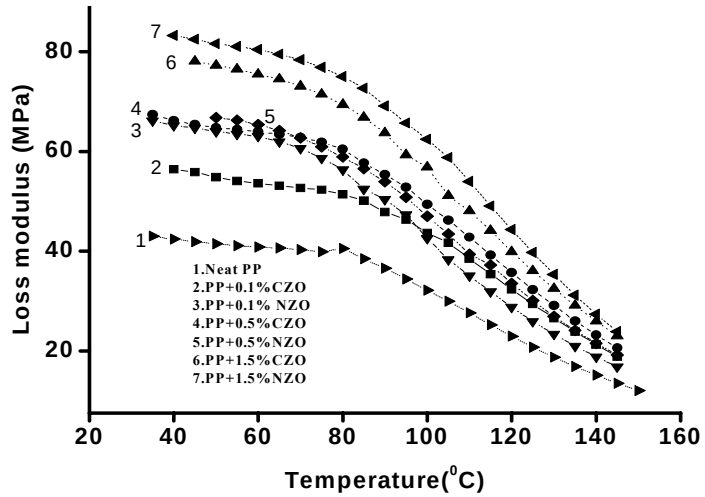

Figure 3.6: Effect of ZnO on loss modulus of PP/ZnO composites

The tanδ curves of PP and composites are shown in figure 3.7. It is evident from the figure that there is an increase in tanδ value on addition of ZnO. This indicates an increase in damping characteristics of the composites. It is obtained in many cases that the improvement of stiffness markedly decreases the ductility. But PP/ZnO composite showed increased stiffness without reduction in ductility.

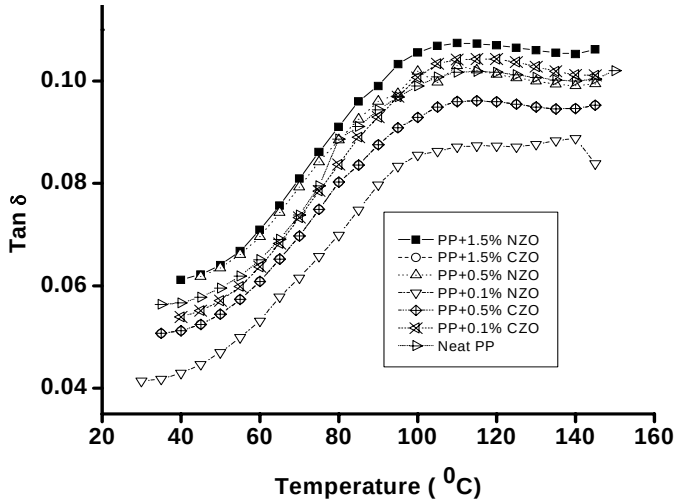

Figure 3.7: Effect of ZnO on tanδ values of PP/ZnO composites

3.3.3 Torque studies

Figure 3.8 indicates the variation of torque with mixing time for neat PP and PP/ ZnO composites. Torque is increased rapidly during initial mixing and then dropped to stabilize a line with higher mixing time.

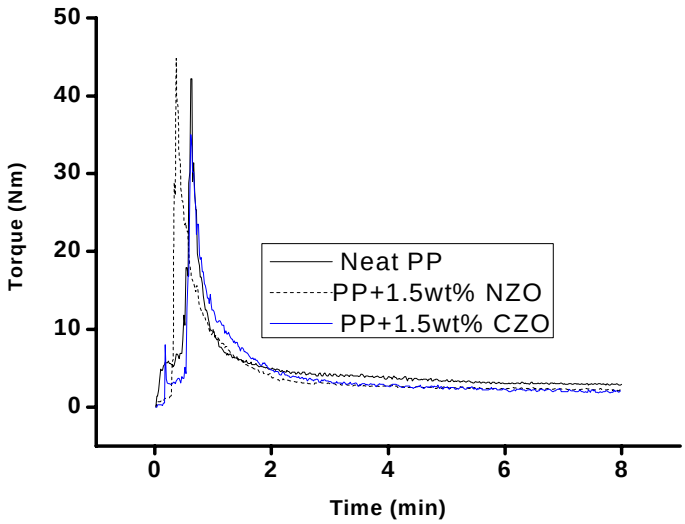

Figure 3.8: Variation of torque with time during mixing

This indicates good level of mixing at the specified conditions. Also the torque value of the PP/NZO composites are higher than that of neat PP and PP/CZO composites. This is mainly due to the increase in interfacial interaction between the nanoparticles and polymer [47].

3.3.4 X-ray diffraction analysis of Composites

XRD is a most commonly used technique to characterize the degree of dispersion of nanoparticles in the polymer. XRD plots of neat PP and PP/ZnO composites are given in figure 3.9. The peaks obtained are corresponding to the planes (110), (040), (130) represents α form of isotactic PP. Gopinath Mani et al observed the similar peaks in the XRD pattern of isotactic PP [48]. X-ray diffraction pattern of nanocomposites show sharp and highly intense peaks whereas neat PP shows less intense peaks. This may due to the development of crystallinity in the polymer. In both neat PP and PP with ZnO, the crystal plane of PP is monoclinic. The α-form is monoclinic, and is the most common and stable crystal form of iPP. A unit cell of α-form of iPP is shown in Figure 3.10.

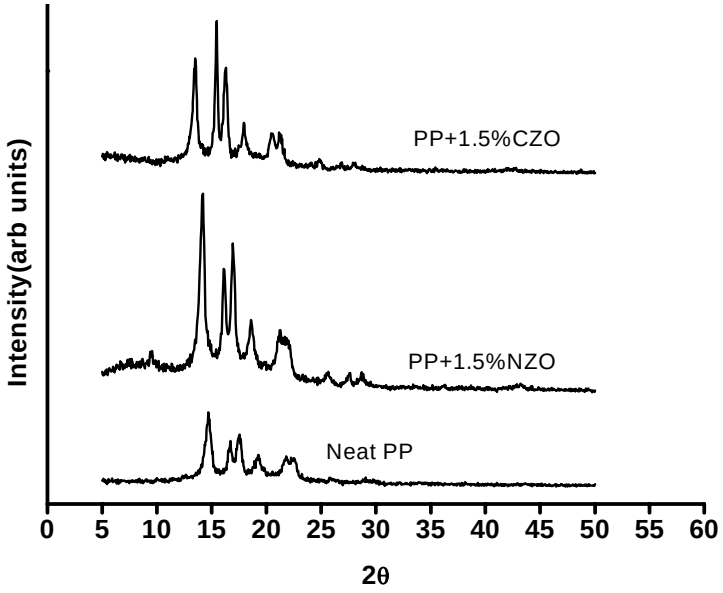

Figure 3.9: X-ray diffraction pattern of neat PP and ZnO filled composites

This contains twelve monomer units, and there are four chains passing through the unit cell, each of which has a 3_1 helical conformation [5]. The polymer chain axis or the helix axis is parallel to the c-axis of the unit cell, and the polymer chains are arranged in alternate layers of right hand and left hand helices along the b-axis of the unit cell as shown in Figure 3.8.2 [49].

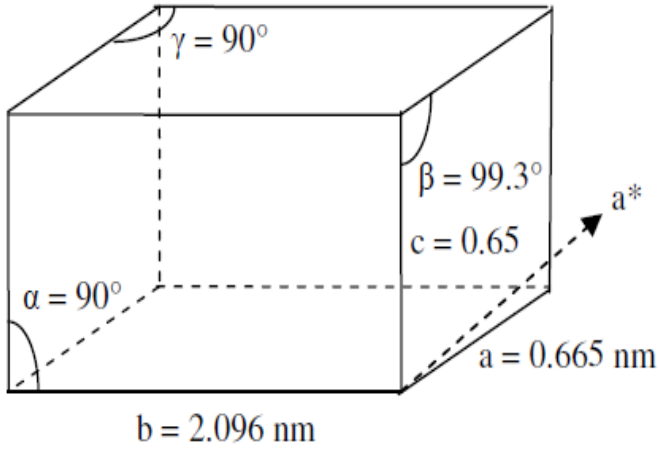

Figure 3.10: Schematic representation of unit cell of α-form isotactic polypropylene crystal

3.3.5 Scanning Electron Micrographs (SEM) of the nano composites

Figures 3.11a, 3.11b and 3.11c represents the SEM photographs of fractured surfaces of neat PP, composites of PP with NZO and CZO at 1.5 wt% respectively. The SEM of PP with 1.5wt% NZO shows formation of fiber like structure which results increase in mechanical properties. Uniform distribution of ZnO is observed in the SEM photographs. Figures 3.11d and 3.11e show SEM photographs of PP with NZO and PP with CZO at 5 wt% respectively. At higher percentage large particles are observed due to the agglomeration of the zinc oxide particles. This may be the reason for the decrease in mechanical properties at higher concentration.

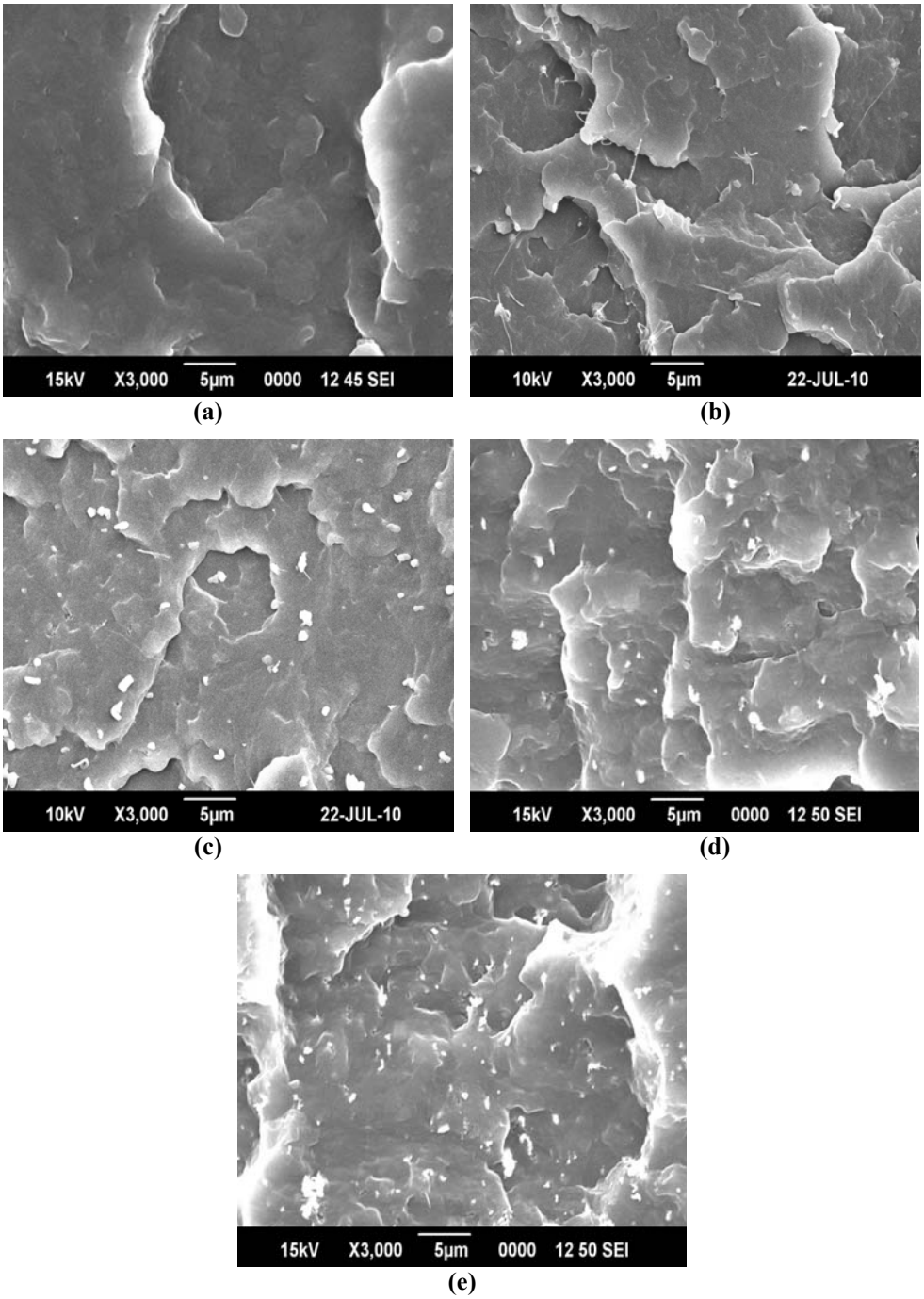

Figure 3.11: SEM images of fractured surface of a) neat PP b) PP+1.5wt% NZO c) PP+1.5wt% CZO d) PP+5wt% NZO e) PP+5wt% CZO filled composites

3.3.6 EDAX of the composites

EDAX is used for identifying the chemical composition of a specimen. Figure 3.12 represents the EDAX of neat PP, 1.5wt% NZO filled PP and 1.5wt% CZO filled PP.

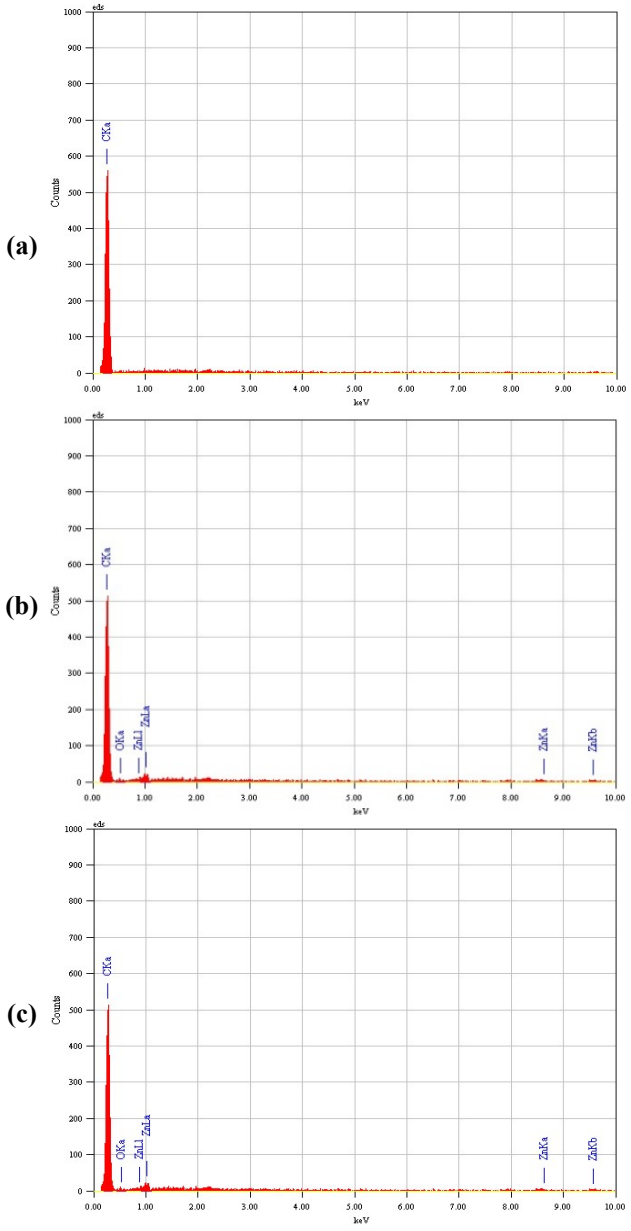

Figure 3.12: EDAX of a) neat PP b) PP+5wt%NZO c) PP+5wt%CZO composites

EDAX shows the presence of ZnO in the PP matrix. EDAX of the composites shows the peak compared to zinc and oxygen indicating the presence of ZnO in the composites. Lighter elements such as hydrogen cannot be observed in EDAX due to the beryllium window that isolates the cooled detector from the vacuum system. So the peak of hydrogen is not seen in the spectrum.

3.3.7 Thermogravimetric analysis (TGA)

Figure 3.13 represents the thermogram of neat PP and composites. The values are tabulated in table 3.1. Thermal stability of PP/ZnO composites are greater than neat PP. The properties studied by TGA indicate an improvement in thermal stability of PP by the addition of ZnO. Onset of degradation (temperature at which degradation starts) is increased by the addition of ZnO. The increase is significant when the particle size of ZnO decreases. Onset of degradation of neat PP is 391^0C where as 1wt% NZO added PP is 422.7^0C. The temperature at which maximum degradation takes place is increased by the addition of ZnO. Rate of degradation is decreased with filler loading. The increase in thermal stability of the composites may be due to the strong interaction between the ZnO and PP. TGA studies show that inorganic fillers, which are widely used industrially to improve the mechanical properties of polymer materials, have various effects on the thermal oxidation of PP. There are some reports on the increase in decomposition temperature of PP by the addition of nanosilica [49], clay [50] etc. Gilmann [51] suggested that the thermal stability of polymers in presence of fillers is due to the hindered thermal motion of polymer chains.

Table 3.1.Effect of ZnO particle size on the thermal stability of PP

Concentration of ZnO (%)	Temperature at which maximum degradation take place (^{0}C)		Onset of degradation (^{0}C)		End set of degradation (^{0}C)		Residue (%)		Rate	
	NZO	CZO	NZO	CZO	NZO	CZO	NZO	CZO	NZO	CZO
0	471.6	471.6	391.0	391.0	500.7	500.7	1.4	1.4	56.3	56.3
0.5	472.9	471.8	409.8	390.1	500.1	492.9	0.8	0.9	54.5	43.8
1	474.4	472.4	422.7	392.9	499.9	498.9	1.6	1.8	53.4	47.6
1.5	475.4	472.9	416.3	396.6	499.8	498.5	2.6	2.2	53.9	51.1
2	475.3	475.4	412.7	401.7	497.2	498.6	3.5	3.3	53.8	52.6
3	473.9	471.6	406.3	402.6	499.1	494.6	3.9	3.6	52.4	51.7

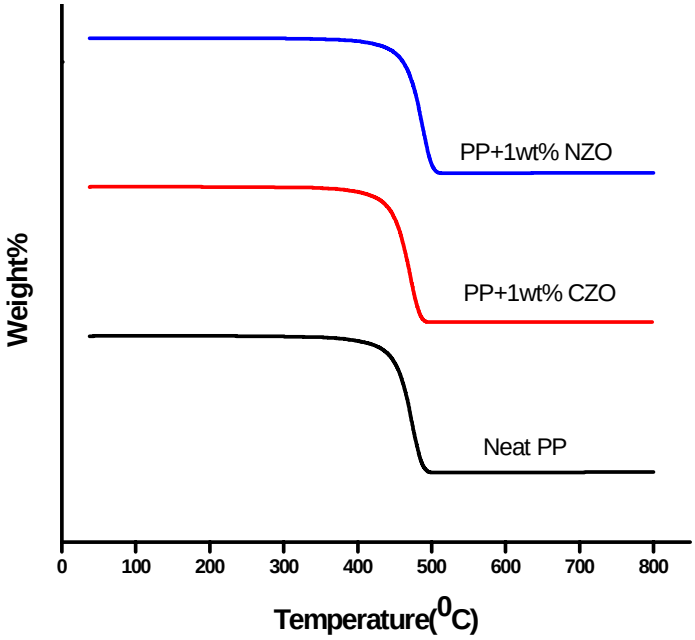

Figure 3.13: Thermogram of PP and PP/ZnO composites

3.3.8 Kinetic analysis of thermal decomposition

Coats–Redfern method was used to study the kinetics of thermal degradation of PP and PP/ZnO composites [52]. This method is an integral method and thermal degradation functions for the Coats–Redfern method are given in Table 3.2.

Table 3.2: The mechanisms of solid-state thermal degradation reaction and corresponding thermal degradation functions g(α).

$g(\alpha) = kt$	Symbol	Rate controlling process
Deceleratory αt curves		
(a) Based on diffusion mechanism		
α^2	D_1	One-dimensional diffusion
$\alpha+(1-\alpha)\ln(1-\alpha)$	D_2	Two-dimensional diffusion
$[1-(1-\alpha)^{1/3}]^2$	D_3	Three-dimensional diffusion
$1-(2/3)\alpha-(1-\alpha)^{2/3}$	D_4	Three-dimensional diffusion (Gistling-Brounshtein equation)
(b) Based on geometrical models		
$1-(1-\alpha)^{1/n}$	R_n	Phase-boundary reaction; n=1, 2 and 3 (one, two and three dimensional, respectively
(c) Based on 'order' of reaction		
$-\ln(1-\alpha)$	F_1	First order (Mampel equation)

Thermogravimetric function g(α) and activation energy(E) is obtained from the equation:

$$\ln [g(\alpha)/T^2] = \ln \{(AR/\Phi_E)(1–2RT/E)\} –E/RT \quad \text{---------- (3.2)}$$

where α is the decomposed fraction at any temperature and is given as:

$$\alpha = C_i–C/C_i–C_f$$

where C is the weight at the chosen temperature, C_i is the weight at initial temperature and C_f is the weight at final temperature, α, is the heating rate, E is the activation energy for decomposition. Activation energy (E) can be calculated from the slope of the curve and pre-exponential factor (A) using the intercept value of the plot of ln $[g(\alpha)/T^2]$ against the reciprocal of absolute temperature (1/T). The order of decomposition reaction was measured using the best linear fit of the kinetic curve and that gives the maximum correlation coefficient. The form of g(α), which best represents the experimental data gives the proper mechanism. From these calculations it is observed that the Mampel equation (–ln(1 – α)) fits in well. The linear correlation coefficients suggest that the F_1 model is the most appropriate to describe the experimental results (Table 3.2).

From the table 3.3 it is clear that the activation energy of PP increased with the addition of ZnO nanoparticles. Activation energy (E) obtained for neat PP is 126.52 kJ/mol, 1.5wt% NZO added PP is 136.84 kJ/mol. Significant increase in activation energy indicates high thermal stability. Representative plot of Coats–Redfern equation for neat PP, PP/1.5wt% NZO and PP/3wt% NZO is shown in figure 3.14.

Table 3.3: Apparent activation energy (E) and correlation coefficients (R) for neat PP and PP/ZnO composites by Coats–Redfern method.

Sample name	R	E
Neat PP	0.999	126.52
PP+0.5% NZO	0.999	134.73
PP+1.5% NZO	0.999	136.84
PP+3% NZO	0.999	133.61

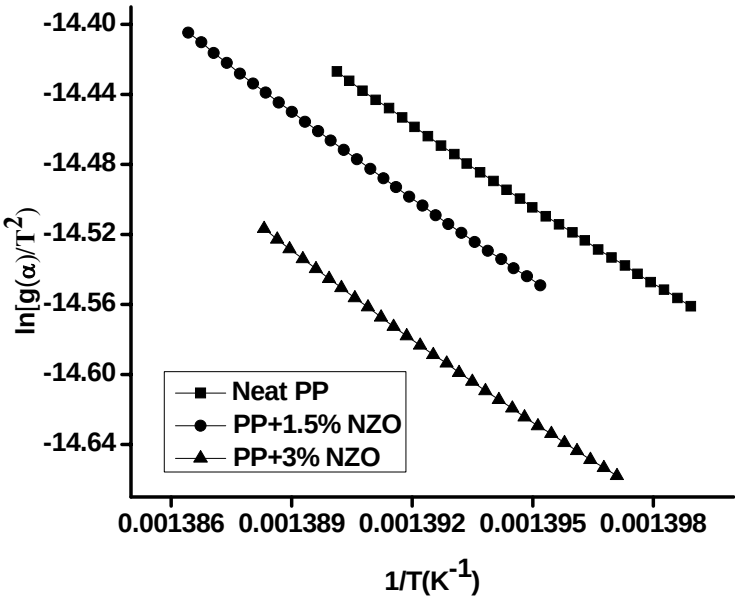

Figure 3.14: Representative plot of Coats–Redfern equation for neat PP and PP/ZnO nanocomposites

3.3.9 Differential Scanning Calorimetry (DSC)

DSC is one of most widely accepted techniques of thermal analysis for studying the crystallization characteristics of polymers and composites. DSC crystallization exotherms of neat PP and composite are shown in figure 3.15. From DSC crystallization exotherms, Tc (the temperature at the crossing point of the tangents of the baseline and the high-temperature side of the exotherm), Tcp (the peak temperature of the exotherm) and ΔH_c (enthalpy of crystallization) can be obtained is shown in table 3.4. Percentage crystallinity (Xc) was calculated using the Equation (3.1). It shows an increase in crystallinity by the addition of ZnO. Degree of crystallization of PP is increased by the addition of ZnO. Anoop Anand K [53] et al showed an improvement in the crystallization characteristics of Poly Ethylene Terpthalate by the addition of carbon nanotube. The Tc – Tcp values of the composites were smaller than that of neat PP, indicating that the addition of ZnO into PP increased the crystal growth rate (CGR) of PP.

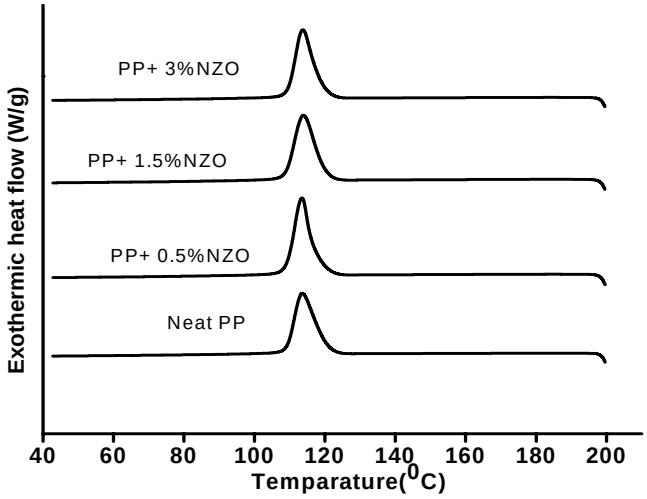

Figure 3.15: Cooling behaviour of neat PP and PP/ZnO composites

Table 3.4: Effect of ZnO on the crystallisation behaviour of PP/ZnO composites

Sample name	Tc (^{0}C)	Tcp (^{0}C)	Tc-Tcp	ΔH_c (J/g)	X_c(%)
Neat PP	120.6	113.6	7	81.7	39.4
PP+0.5%NZO	117.5	113.5	4	92.9	45.1
PP+1.5%NZO	119.24	113.9	6.2	93.86	46.0
PP+3%NZO	120.14	113.8	5.4	88.84	44.2

Melting behaviour of the composites are shown in figure 3.16 and values are tabulated in table 3.5. From the DSC curves, Tm (designed here as the temperature at the crossing point of the tangents of the baseline and the low temperature side of the curves), Tmp (the peak temperature of the curve), and ΔHm (heat of fusion) can be obtained. The maximum rate of melting (Tmp) occurred at 163.8^{0}C for pure PP and its Tm is 154.3^{0}C. The Tm value of PP with 1.5 wt% NZO was increased by about 3^{0}C compared with neat PP. In Figure 3.16, it can be seen that there is single peak observed for the curves of PP and composites indicates the melting of α-phase. However, PP with 3 wt% NZO shows a peak at low melting temperature indicates the presence of a small amount of β- phase.

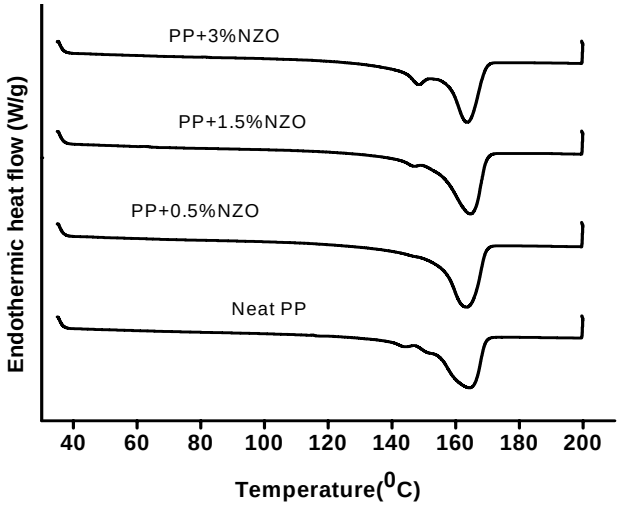

Figure 3.16: Melting behaviour of neat PP and PP/ZnO composites

Table 3.5: Effect of ZnO on the melting behaviour of PP

Sample name	Tm (^{0}C)	Tmp (^{0}C)	ΔH_m (J/g)
Neat PP	154.37	164.8	48.61
PP+0.5%NZO	155.68	163.69	60.29
PP+1.5%NZO	157.5	163.71	62.83
PP+3%NZO	154.3	164.8	45.47

3.3.10 Melt flow index (MFI)

MFI gives an idea about the flow characteristics of the thermoplastics. It depends on the molecular properties such as molecular weight and structure of polymers [54]. Figures 3.17a and 3.17b show the effect of ZnO on the MFI of PP at 5kg and 2.16kg respectively. MFI of PP is decreased by the addition of CZO indicate a decrease in flow characteristics of the polymers. In NZO filled PP, MFI is increased by the addition of low concentration of NZO indicates an increase in the flow properties of the polymers. Adding the low concentration of nanoparticles may provide a flow favouring orientation due to the small size of NZO as depicted in figure 3.18. An increase in MFI is reported when adding multi walled carbon nanotube to PP [55]. After adding 1wt% NZO to the PP

the MFI value decreases gradually. It indicates the structure of nanoparticles was interconnected to hinder the molecular motion of polymer chains [56].

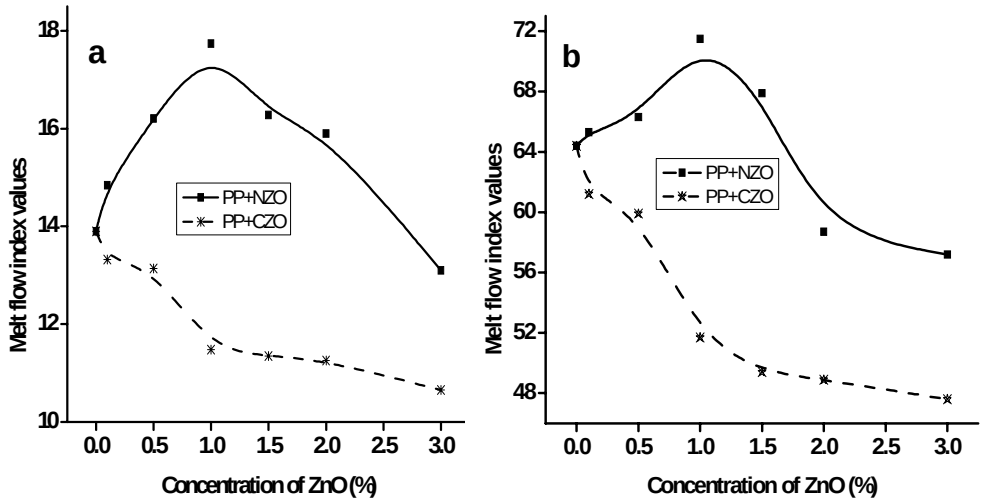

Figure 3.17: Effect of ZnO particle size on the melt flow index of PP using (a) 2.16kg and (b) 5 kg weight

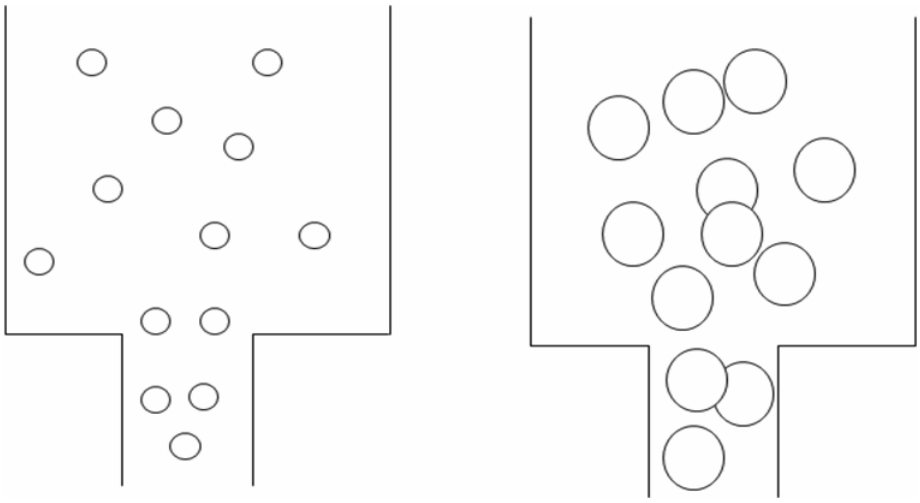

(a) **(b)**

Figure 3.18: Schematic representation of flow behaviour of a) PP/NZO and b) PP/CZO composites

3.3.11 Transparency of the films

The percentage transmittance of neat PP and composites is given in figure 3.19. By the addition of ZnO the transmittance of the film is decreased. NZO filled PP films show higher transparency when compared to CZO filled PP films. Photographs showing the transparency of the films are given in figure 3.20. From the figure it is evident that the composites based on NZO are much clearer than those containing CZO. This may be due to decrease in spherulite size of PP and also due to smaller ZnO particles in the composites.

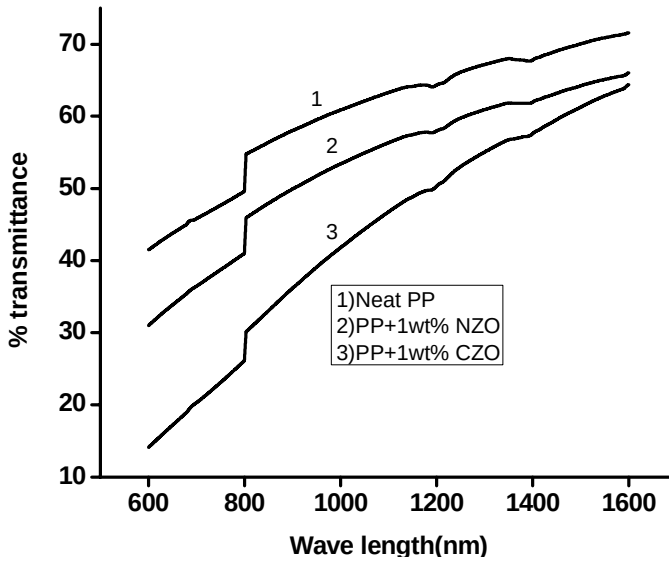

Figure 3.19: Visible-IR transmittance of neat PP and PP/ZnO composites

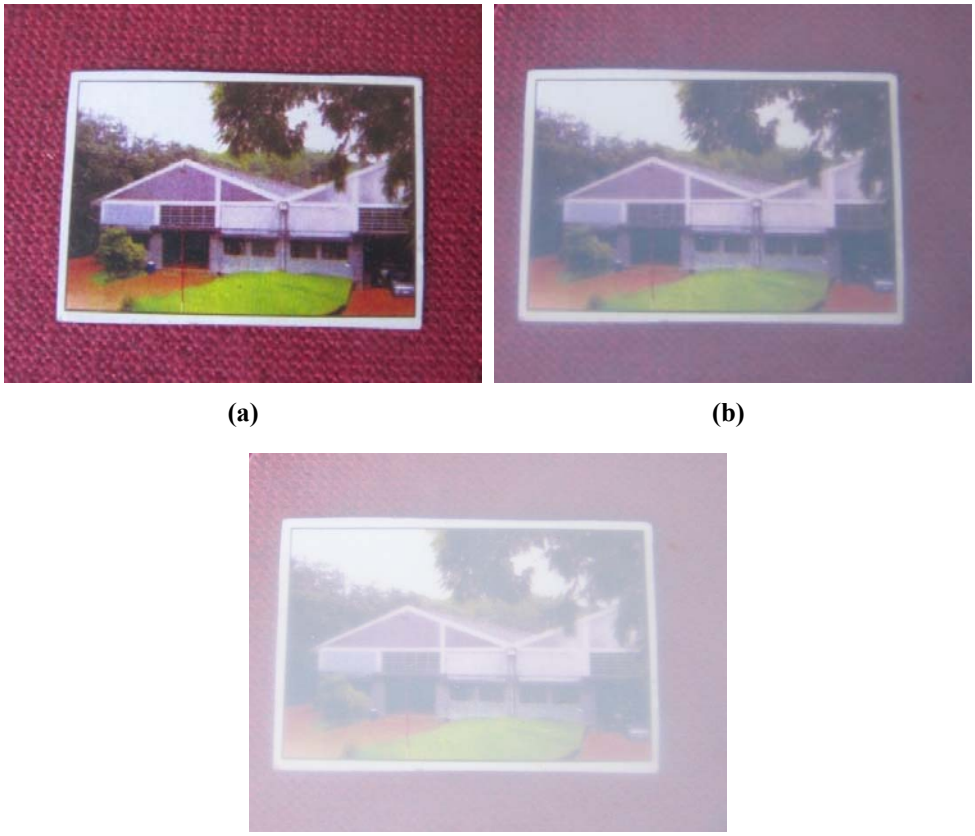

(a) **(b)**

(c)

Figure 3.20: Photographs of a) neat PP b) PP+1wt%NZO c) PP+1wt%CZO composite films

3.3.12 Limiting oxygen index (LOI)

Figure 3.21 represents the value of LOI of neat PP and nanocomposites. Incorporation of NZO in polymer for the fire retardant applications can avoid the toxicity of the degradation products compared with the more traditional additives such as halogenated products. In addition, the use of nanoparticles helps to reduce the weight of additives. LOI of PP is increased with the addition of ZnO. The enhancement in the flame retardancy is attributed to the good filler dispersion [57].

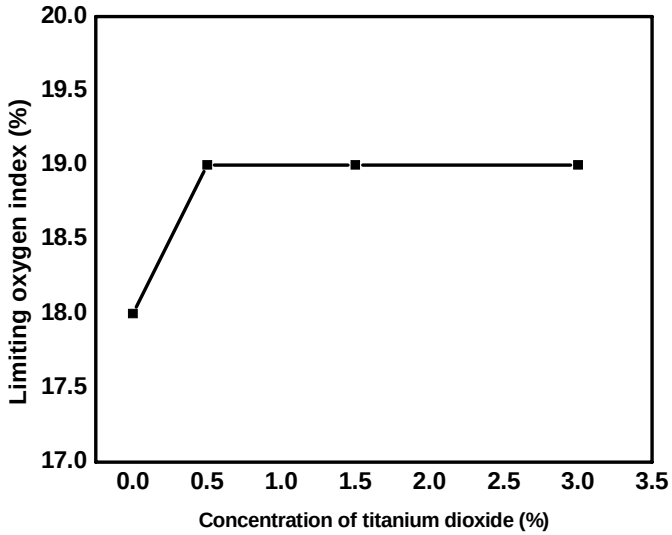

Figure 3.21: Effect of ZnO on limiting oxygen index of PP/ZnO composites

3.3.13 Thermal and Photo Ageing

PP can be easily degraded by a stimulus like elevated temperature and sunlight [58]. PP has tertiary carbon atoms and is known to be very vulnerable to oxidative degradation under the influence of temperature and sunlight. PP degradation chemistry has been recognized as free radical-chain reaction, which leads to polymer chain scission [59] as shown in figure 3.22. It is generally accepted that this chain scission causes brittleness. Degradation has a great influence on the mechanical properties and morphology of the composites.

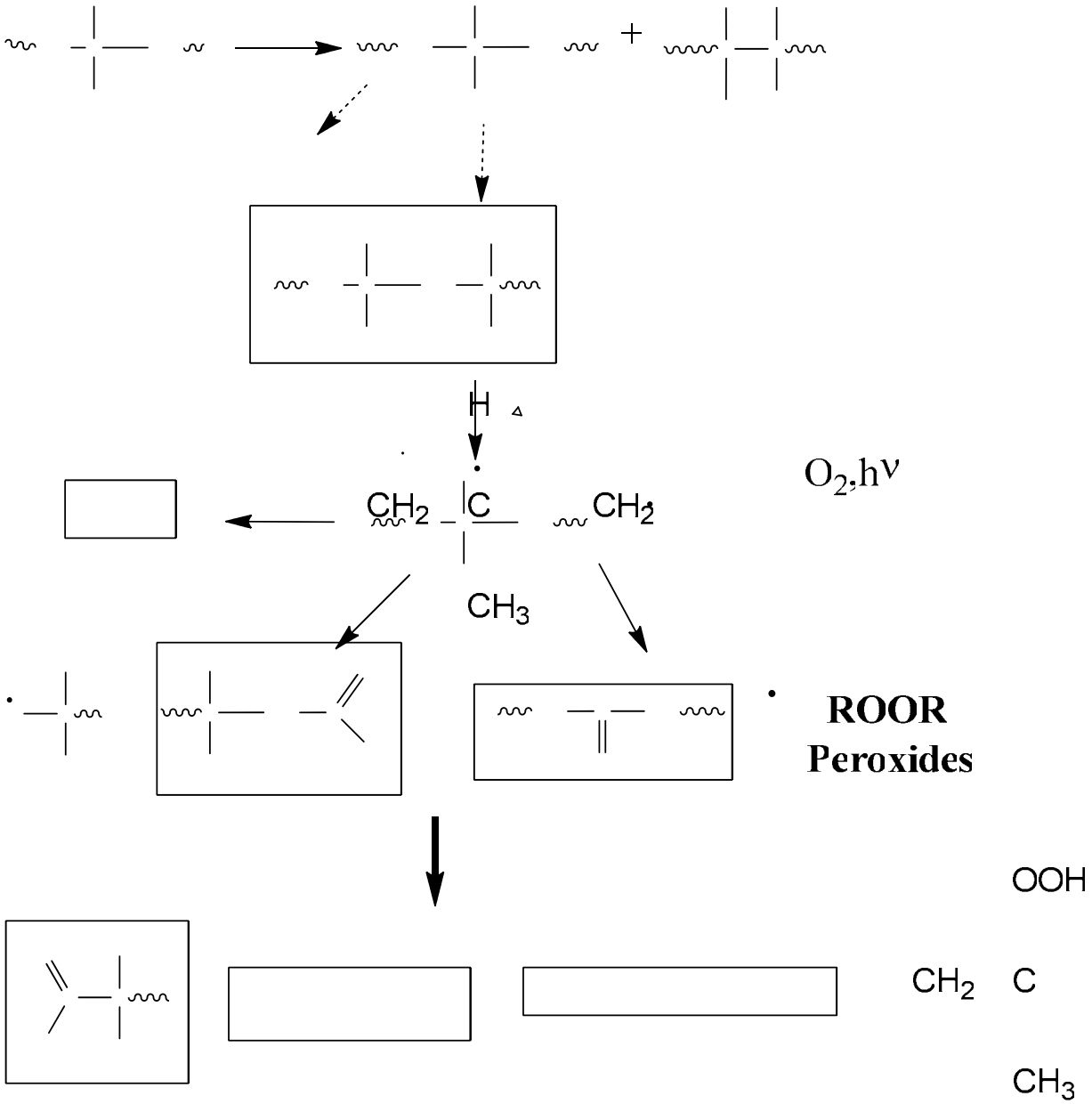

Figure 3.22: Mechanism of degradation of PP by light and heat

3.3.13.1 Thermal ageing

3.3.13.1.1 Mechanical properties of composites

Mechanical properties of the neat PP and composites, such as tensile strength and modulus were evaluated before and after 24 hours of thermal ageing and results are shown in figures 3.23 and 3.24. At all concentrations, composites based on CZO and neat PP degraded faster than those with NZO. This shows nano ZnO improves the thermal stability of the composites. Thermal ageing take place in oven is dependent on the presence of oxygen, which is actually the main factor responsible for PP degradation in the thermal environment [60]. In polymers, there will be a depth profile of degradation, with higher rate oxidation near the surface, due to the oxygen starvation in the sample interior. In this way, the diffusion of oxygen plays a major role in defining the extent of chemical degradation [61, 62]. In nanocomposite structures, oxygen molecules are concentrated more on the fillers, decreasing the diffusion path through the PP.

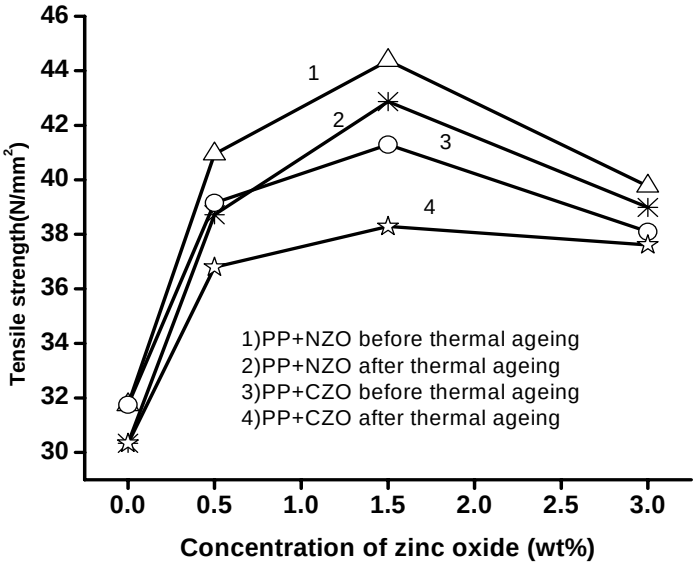

Figure 3.23: Effect of thermal ageing on tensile strength of PP/ZnO composites

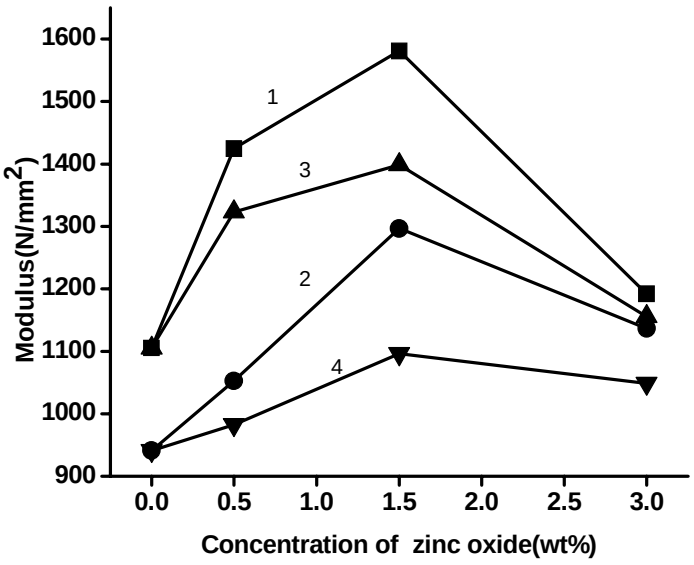

Figure 3.24: Effect of thermal ageing on tensile modulus of PP/ZnO composites.

3.3.13.1.2 Morphology of the fractured surface.

SEM images of the tensile fractured surfaces of the neat PP and its composites with 1.5wt% of ZnO after thermal ageing are shown in figure 3.25. As can be seen from figure, the nanoparticles are well dispersed in the polymer matrix resulting in improved mechanical properties of the polymer even after thermal ageing.

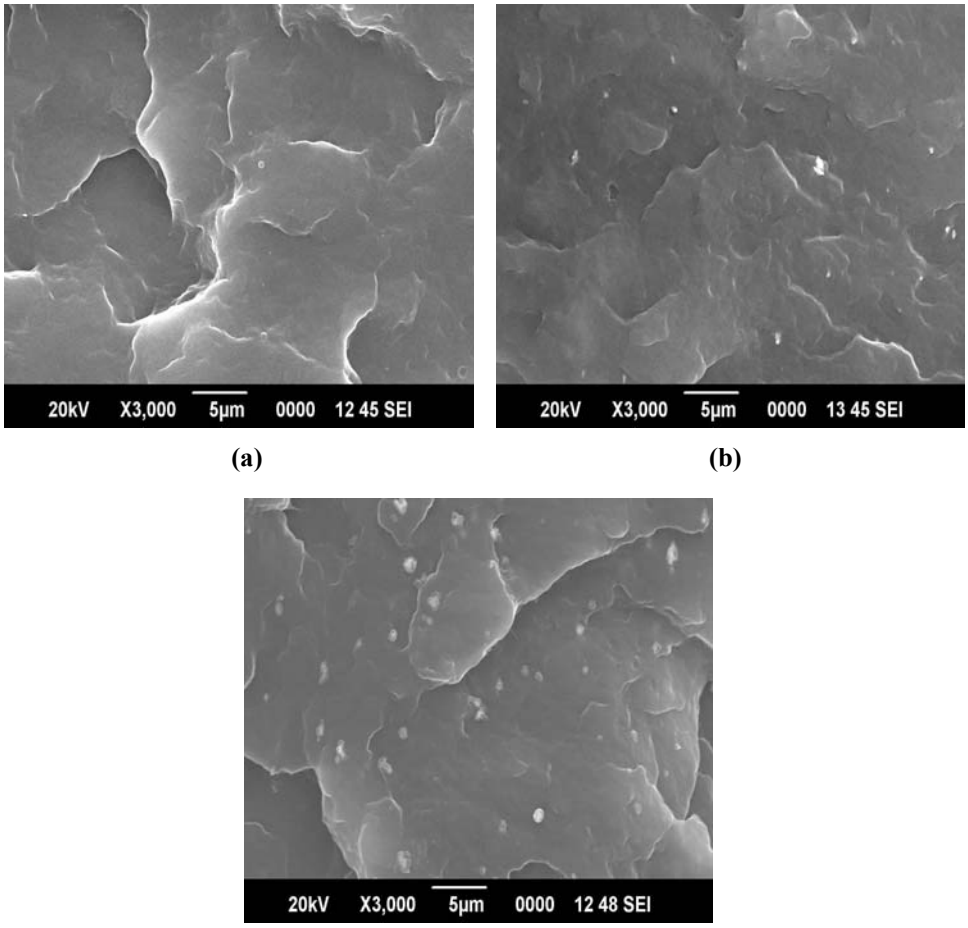

(a) **(b)**

(c)

Figure 3.25: Scanning electron micrographs of (a) neat PP (b) PP+1.5wt%NZO (c) PP+1.5wt%CZO composites after thermal ageing.

3.3.13.1.3 IR spectroscopy

Degradation products of neat PP and its composites with NZO after thermal ageing is studied by IR spectroscopy. IR spectrum of neat PP, PP with 0.5wt% NZO, 1.5wt% NZO and 3wt% NZO are shown in figure 3.26. The consequence of degradation of PP is the formation of hydroperoxides and carbonyl species like ketones, esters and acids as discussed in figure 3.22. These degradation products give absorption peaks in the wave number range 3200-3600 and 1600-1800 cm^{-1} in the spectrum. The peak in the range of

3200-3600 cm^{-1} indicating the hydroperoxide formation. The intensity this peak is less in case of PP composites with NZO when compared to neat PP. But at 3wt%, the intensity of this peak is increased slightly when compared to lower concentration of NZO filled PP. This indicates ZnO nanoparticles at lower concentration give better resistance to thermal degradation of PP. The IR peak in the range 1600-1800cm^{-1} corresponds to carbonyl group, the intensity of this decreases with increasing ZnO concentration, which supports the fact that incorporation of nano ZnO reduces the thermal degradation of PP. The characteristic peaks for PP in the wave number range of 2800-3000cm^{-1}, related to the asymmetric and symmetric C-H stretching vibration. The intensity of this peak increases in presence of ZnO compared to that of neat PP. This indicates improved resistance of PP to thermal degradation in presence ZnO nanoparticles and this is significant at low concentration. As the concentration increases agglomeration of ZnO particle take place and nanoeffect is reduced.

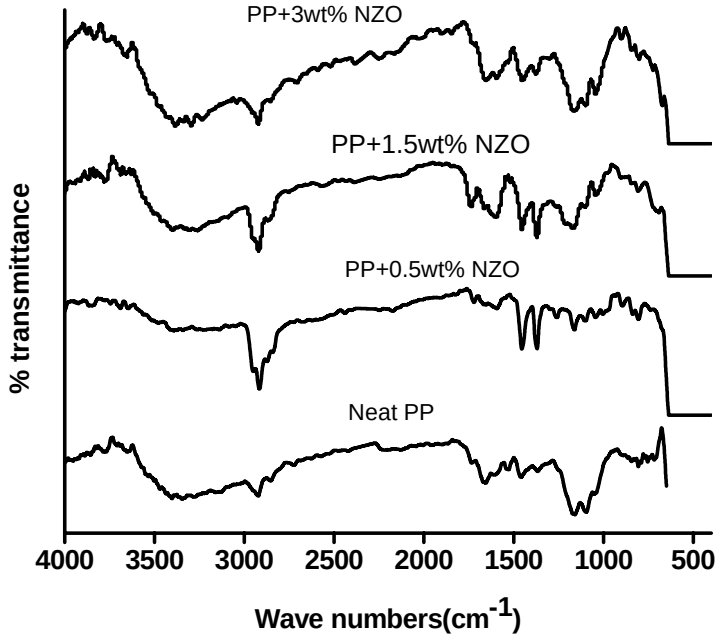

Figure 3.26: IR spectrum of PP/ZnO composites after thermal ageing

3.3.13.2 UV ageing

3.3.13.2.1 Mechanical properties of the composites

The mechanical properties of the neat PP and composites, such as tensile strength and modulus after 48 hours of UV irradiation are represented in figure 3.27 and figure 3.28 respectively. After UV irradiation, mechanical properties of the composites and neat PP decreased. However, properties of the composites are higher than that of neat PP even after photo ageing. Resistance of PP to photo-degradation embrittlement can be improved significantly with the addition of ZnO particles. Based on the tensile results, it can be summarized that the presence of ZnO particles reduce the effect of UV degradation.

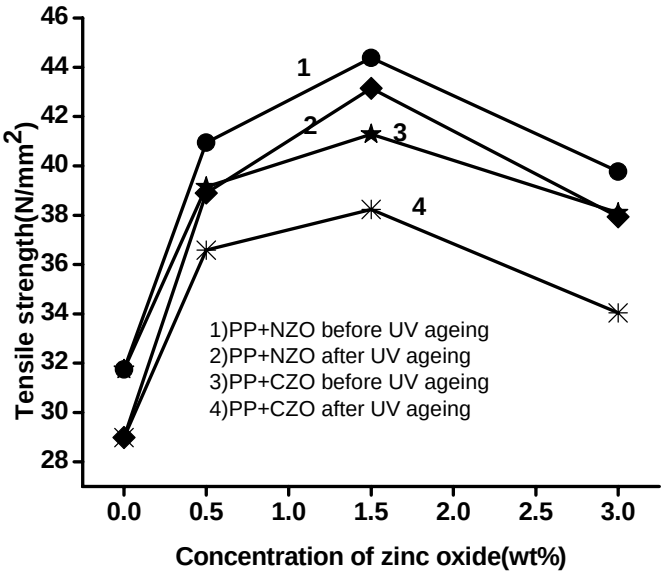

Figure 3.27: Effect of photo ageing on tensile strength of PP/ZnO composites.

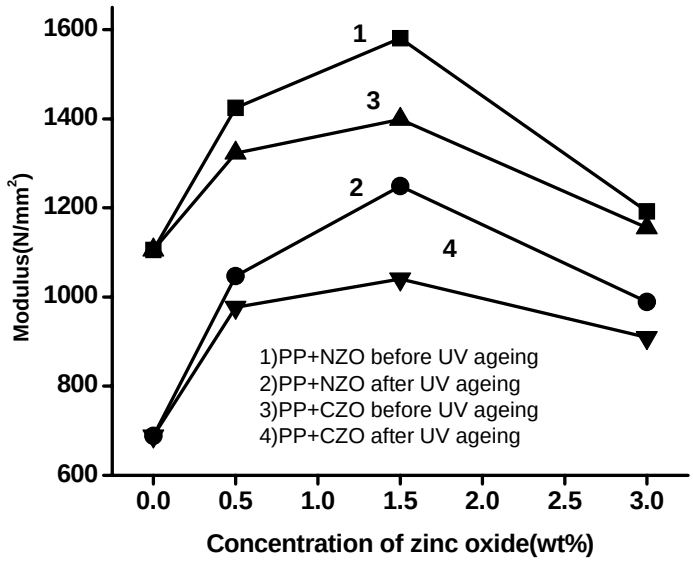

Figure 3.28: Effect of photo ageing on tensile modulus of PP/ZnO composites.

3.3.13.2.2 IR spectroscopy

Generally , photo-oxidation processes includes radical reactions, which are initiated mainly by two sources:(1) high energy photon collision (2) the presence of impurities such as trace metals left from the polymerisation processes [63]. Photo-oxidation of PP results in the formation of hydroperoxides and carbonyl species like ketones, esters and acids [64, 65]. Figure 3.29 represent the FTIR spectrum of neat PP, 1.5% NZO filled PP and 1.5% CZO filled PP after UV irradiation. In the IR spectrum of neat PP there is a broad peak in the range of 3200-3600 cm^{-1} indicate the formation of hydroperoxides, intensity of this peak decreases by the addition of TiO_2 especially in case of NZO. The striking information from the figure is that for the composites, the intensities of carbonyl peak is decreased. It thus can be deduced that ZnO nanoparticles play an important role in stabilizing the PP molecules and delay the photodegradation by acting as screens. The dominant screening mechanism

is that the ZnO nanoparticles absorb the UV radiation and thus reduce the UV intensity that can promote the oxidation of the PP chains [66].

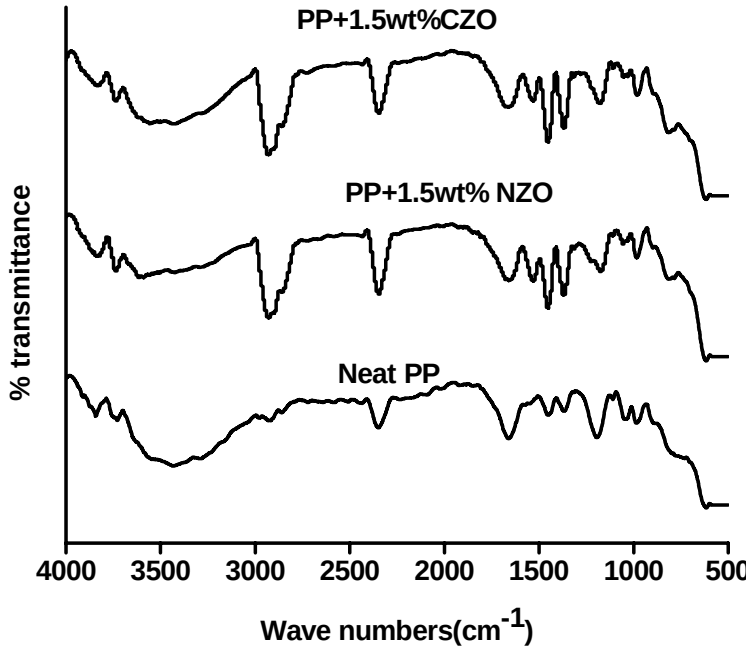

Figure 3.29: IR spectrum of PP/ZnO composites after photo ageing

3.3.13.2.3. Morphological studies

SEM examination was carried out to investigate the effect of UV radiation on the tensile fracture morphology of PP and the composites. Figure 3.30 shows the overviews of the fracture surface morphologies for PP, PP+1.5wt% CZO and PP+1.5wt% NZO tensile specimens after UV irradiation respectively. SEM photographs of neat PP and CZO filled PP shows damages after UV irradiation. It can be seen that small holes in the SEM of neat PP and CZO filled PP. These holes are caused by photo-degradation on the specimen surfaces. When examining the fractured surface of NZO filled PP composites such holes are not observed.

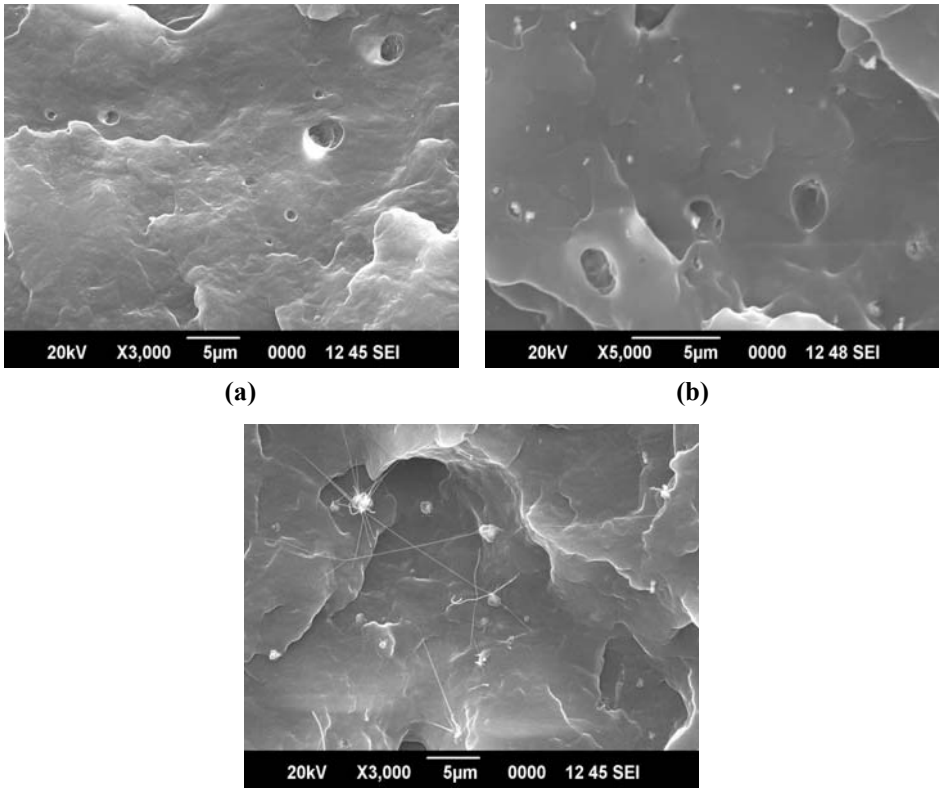

Figure 3.30: Scanning electron micrographs of (a) neat PP (b) PP+1.5wt% CZO and (c) PP+1.5wt% NZO added composites after photo ageing

3.4 Conclusion

PP/ZnO composites are prepared by melt mixing method. Mechanical and dynamic mechanical properties of PP are improved by the addition of ZnO. PP shows better thermal stability in presence of ZnO. Differential scanning calorimetric studies show increase in crystallinity of PP by ZnO addition. X-ray diffraction studies of neat PP and composites indicate the presence of α phase of monoclinic PP. Melt flow index increases by adding low concentration of NZO whereas CZO added PP shows a decrease in MFI. Transparency of the PP films is decreased by the addition of ZnO. PP with NZO filled film shows higher transparency when compared to CZO filled PP

films. Limiting oxygen index of PP is increased by the addition of ZnO. Mechanical, morphology and IR studies show improved performance of composites even after thermal and UV ageing when compared to neat PP. NZO filled PP shows better properties than CZO filled composites.

References

[1] Saujanya C, Radhakrishnan S, Polymer 2001, 42 , 6723.

[2] Mishra S, Sonawane S H, Singh R P, Bendale A, Patil K, Journal of Applied Polymer Science 2004, 94, 116.

[3] Ming Qiu Zhang, Min Zhi Rong, Hai Bo Zhang, Klaus Fried Rich., Polymer Engineering and Science, 2003, 43,490.

[4] Jiang-Ping He, Hua-Ming Li, Xia-Yu Wang, Yong Gao, European Polymer Journal 2006 ,42,1128.

[5] Alexandre M, Dubois P., Materials Science and Engineering Report 2000, 28, 1.

[6] Yang J, Lin, Y, Wang J, Mingfang Lai, Jing Li, Liu J, Xin Tong, Cheng H., J.Appl Polym Sci 2005, 98,1087.

[7] Garcia M, Van Vilet G, Jain S, Schrauwen BA, Sarkissov A, Van Zyl WE, Boukamp B, Rev Adv Mater Sci 2004,6,169.

[8] Dong Wook Chae, Byoung Chul Kim, Polym Adv Technol 2005, 16, 846.

[9] Jun Yang, Yuhan Lin,Jinfeng Wang, Mingfang Lai, Jing Li, Jingjiang Liu, Xin Tong, Huiming Cheng, Journal of Applied Polymer Science, 2005,98, 1087.

[10] Garcia M, Van Vilet G, Jain S, Schrauwen BA, Sarkissov A, Van Zyl WE, Boukamp B. Rev Adv Mater Sci, 2004,6,169.

[11] Dong Wook Chae, Byoung Chul Kim, Polym Adv Technol, 2005, 16, 846.

[12] Shu-Cai Li, Ya-Na Li, J of Appl Polym Sci, 2010,116,2965.

[13] Maurizio Avella, Maria Emanuela Errico, Gennaro Gentile, Macromol Symp 2007, 247, 140.

[14] Garcia-Lopez D, Merino J C, Pastor J M, J. Appl. Polym. Sci, 2003, 88, 947.

[15] Ellis T S, D Angelo J S, J Appl Polym Sci, 2003, 90, 1639.

[16] Luyt A S, Dramicanin M D, Antic Z , Djokovic V, Polymer Testing 2009,28, 348.

[17] Ha-da Bao, Zhao-xia Guo and Jian Yu, Chinese Journal of Polymer Science, 2009, 27, 393.

[18] Hesheng Xia,Qi Wang,Kanshe Li,Guo-Hua Hu, Journal of Applied Polymer Science, 2004,93, 378.

[19] Prashantha K, Soulestin J, Lacrampe M F, Claes M, Dupin G, Krawczak P, eXPRESS Polymer Letters 2008, 2, 735.

[20] Yong Tang, Yuan Hu, Lei Song, Ruowen Zong,Zhou Gui, Zuyao Chen, Weicheng Fan, 2003, 82,127.

[21] Pralay Maiti, Pham Hoai Nam, and Masami Okamoto, Naoki Hasegawa and Arimitsu Usuki, Macromolecules 2002, 35, 2042.

[22] Bhattacharya A R, Sreekumar T V, Tao Liu, Satish Kumar, Ericson M, Robert, Hauge H, Richard E S, Polymer 2003, 44, 2373.

[23] Ma L C, Li L P, Guo C G, J Therm Anal Calorim, 2010,101,1101.

[24] Maity J et al. , Compos Part A Appl Sci Manuf., 2008, 39,825.

[25] Svoboda P, Svobodova D, Slobodian P et al. , Polym Test., 2009; 28,215.

[26] Razavi-Nouri M, Ghorbanzadeh-Ahangari M, Fereidoon A et al., Polym Test., 2009, 28,46.

[27] Karger-Kocsis J, London: Chapman and Hall, 1995.

[28] Arbelaiz A, Fernandez B, Ramos JA et al., Thermochim Acta. 2006,440,111.

[29] Zafeiropoulos N E, Baillie C A, Matthews F L., Compos Part A Appl Sci Manuf., 2001,32,525.

[30] Girones J, Pimenta M T B, Vilaseca F et al., Carbohydr Polym. 2008,74,106.

[31] Pracella M, Chionna D, Anguillesi I, Kulinski Z, Piorkowska E, Compos Sci Technol., 2006, 66, 2218.

[32] Acha B A, Reboredo M M, Marcovich N E., Polym Int., 2006,55,1104.

[33] Devaux E, Gerard J F, Bourgin P, Chabert B. , Compos Sci Technol., 1993, 48,199.

[34] Maurizio Avella , Federica Bondioli , Valeria Cannillo, Emilia Di Pace, Maria Emanuela Errico , Anna Maria Ferrari , Bonaventura Focher , Mario Malinconico, Composites Science and Technology, 2006, 66, 886.

[35] Gojny F H, Wichmann M H G, Kopke U, Fiedler B, Schulte K, Composites Science and Technology ,2004, 64, 2363.

[36] Vera-Agullo J , Gloria-Pereira G , Varela-Rizo H , Jose Luis Gonzalez , Martin-Gullon I, Composites Science and Technology, 2009, 69, 1521.

[37] Oksman K, Mathew A P, Bondeson D, Kvien I, Composites Science and Technology, 2006 , 66,2776.

[38] Quang T N, Donald G B, Advances in Polymer Technology, 2006, 25, 270.

[39] Suriyan Rakmae, Yupaporn Ruksakulpiwat, Wimonlak Sutapun, Nitinat Suppakarn, Journal of Applied Polymer Science, 2011,122, 2433.

[40] Madhuchhanda Sarkar, Kausik Dana, Sankar Ghatak and Amarnath Banerjee, Bull. Mater. Sci., 2008, 31, 23.

[41] Johnson J C, Yan H, Schaller R D, Haber L H, Saykally R J, Yang P, J. Phys. Chem., 2001,105,11387.

[42] Rensmo H, Keis K, Lindstrom H, Sodergren S, Solbrand A, Hagfeldt A, and S E , Lindquist, J. Phys. Chem. B, 1997, 110, 2598.

[43] Wunderlich, B. Thermal Analysis, New York: Academic Press, 1990.

[44] Shu-Cai Li, Ya Na Li, Journal of Applied Polymer Science 2010,116, 2965.

[45] Kim J A, Seong D J, Kang T J, Youn J R, Carbon, 2006, 44, 1898.

[46] Zhang Y Q, Liu G R, Qiang H F, Li G Y, International Journal of Mechanical Sciences, 2006,48, 53.

[47] Sun Shuisheng, Li Chunzhong, Zang Ling, Du H L, Burnell-Gray J S, Polym J, 2006,42,1643.

[48] Gopinath Mani, Qinguo Fan, Samuel C U, Yiqi Yang, 2005,97, 218.

[49] Chgnati Srinivasa Reddy, Chapal Kumar Das., J of Appl Polym Sci ,2006, 102.

[50] Sangeetha Hambir, Neelima Bulakh, Jog J P, Polymer Engineering and Science, 2002,42,1800.

[51] Gilman J W, Applied Clay Science, 1999, 15, 31.

[52] Coats AW, Redfern J P. Nature 1964, 68, 201.

[53] Anoop Anand K, Sunil Jose T , Agarwal U S , Sreekumar T V, Bhawna Banwari, Rani Joseph, Polymer, 2006,47,3976.

[54] Yang W, Liu Z Y, Shan G F, Li Z M, Xie B H,Yang M B, Polym Test 2002, 24,490.

[55] Chin ChunTeng, Chen Chi M Ma,Yen Wei Huang, Siu Ming Yuen,Cheng Chih Weng, Cheng Ho Chen, Shun Fua Su, Composites: Part A, 2008, 39,1869.

[56] Lee S H, Kim M W, Kim S H,Youn J R, Eur Polym J, 2008, 44,1620.

[57] Kancheng mai, Zhengjun Li, yuxin qiu, Hanmin zeng, Journal of Applied Polymer Science, 2001,81, 2679.

[58] Kato Y, Carlsson D J, Wiles D M, J Appl Polym Sci 1969, 13,1447.

[59] Alam M S, Nakatani H, Ichiki T, Goss G S B, Liu B, Terano M , J Appl Polym Sci, 2002, 86,1863.

[60] Rapoport N Y, Berulava S I, Kovarskii A L, Musayelyan I N, Yershov YuA, Miller V B, Polym Sci U S S R (EnglmTrnasl), 1975, A17, 2901.

[61] Rabello M S,White J R, Polym Degrad Stab, 1997,56,55.

[62] Zanetti M, Bracco P, Costa L, Polym Degrad Stab, 2004,85,657.

[63] Allen N S, Edge M, Fundamentals of polymer degradation and stabilisation.London:Elsevier Applied Science, 1992[chapter4]

[64] Qin H, Zhang S, Liu H, Xie S, Yang M, Shen D, Polymer, 2005,46,3149.

[65] Morlat S, Mailhot B, Gonazalez D, Gardette J L, Chem Mater 2004, 16,377.

[66] Hongxia Zhao, Robert K Y Li, Polymer 47,2006,3207.

.....ഠ൦ര.....

POLYPROPYLENE/ZINC OXIDE NANOCOMPOSITE FIBERS THROUGH MELT SPINNING

Contents

PP/ZnO composites were prepared by melt mixing method. It was then spun in to fibers by melt spinning and subsequent drawing. Mechanical properties of the fibers were measured using Favimat tensile testing machine with a load cell of 1,200cN capacity. Thermal behaviour of the fibers was studied using differential scanning calorimetry and thermogravimetric analysis. Surface morphology and cross section of the fiber was studied using scanning electron microscopy. Mechanical properties of the PP fiber was improved by the addition of ZnO nanoparticles. Thermogravimetric analysis shows significant improvement in thermal stability of PP fiber. Improvement in crystallinity is observed by the addition of ZnO nanoparticles. Antibacterial properties of fiber was studied using Bacillus aereus (gram positive) and Escherichia coli (gram negative) bacteria.

4.1 Introduction

PP is a widely used thermoplastic for hygienic applications such as food packaging, surgical masks, diapers etc. It is also used for fibers and films. PP fibres have been widely used in apparel, upholstery, floor coverings, geotextiles, car industry, automotive textiles, various home textiles etc [1, 2]. Because of the low cost, high toughness, strength and resistance to chemicals, PP fibers find a broad spectrum of use in industrial and home furnishing sector [3]. PP comprises a major portion of the materials used for spun bound and melt blown fabrics in hygiene and medical products [4-16]. It has a relatively low melting point of 160-175^{0}C and it is an ideal polymer for making fibers. Three different crystalline forms of PP have been identified: α-monoclinic, β-trigonal and γ-orthorhombic. All the three forms are the helical conformation of the constituent PP chains. The α- form is the most stable and also the most important in making of PP fibers. Its monoclinic lattice has unit cell dimensions of a=0.665 nm, b=0.2096 nm, c=0.650 nm, $\alpha=\gamma=90^0$, $\beta=99.3^0$ and PP chains lie in the direction of the C – axis. The structure includes both left-handed and right handed helical PP chains and any given helix for the most part lies next to helices of the opposite chirality [17-19]. Isotactic α-PP also exhibits a lamellar branching, which is unique in polymer crystallography [20]. PP provides nearly half of base fiber for non-wovens fabrics [21]. Some synthetic and natural fibers are replaced by PP fibers are replaced by PP fibers due to its excellent properties and processability.

Modification of PP can improve the properties of the fiber. New materials are used today in PP fibers to increase the functionality and enter new markets. Conventional methods used to modify fibers and fabrics do not lead to permanent effects and lose their functions after laundering or wearing. However, because of their high surface energy, nanoparticles present better

affinity for fibers and fabrics and increase the durability of their function. Thus, the studies related to the modification of polymeric textile fibers and fabrics by nanoparticles has increased recently [22, 23]. Incorporation of fillers in polymer generally shows improvement in strength, thermal stability and crystallization behaviour of PP fibers [24-29]. Anton Marcin et al reported the positive influence of boehmite Disperal 40, organoclay Cloisite C15A, nano TiO_2 and MWCNT nanofillers in oriented PP composite fibers on their UV barrier properties at low content of the nanofiller [30]. Effect of silica particles on crystallization behaviour of PP fibers were studied by Natee Srisawat et al [31].

Melt spinning, electrospinning and wet spinning are the commonly used method for the production of fibers [32, 33]. Among these methods melt spinning is the least complex method and it involves forcing a polymer melt through a spinneret and in to air to cause the polymer to solidify. It does not involve any problems associated with the use of solvents and is therefore the preferred method provided that the polymer gives a stable melt. The homogenized melt is extruded the spinneret and solidify anywhere from a few centimetres from the spinneret plate to as far away as several meters.

This chapter reports the preparation of PP/ZnO nanocomposite fibers by melt spinning and drawing. Mechanical, thermal, morphological, x-ray diffraction analysis and antibacterial properties of these fibers were studied.

4.2 Experimental

4.2.1 Preparation of PP/ZnO nanocomposite fibers

PP/ZnO (0-3wt% of ZnO) composites were prepared by melt mixing method. The hot mix were then made into sheets using a hydraulic press and cut in to small pieces to prepare fibers. The fibers were spun using a small scale spinning machine manufactured by Bradford University Research Ltd.,

UK, using a single hole spinneret of 1 mm diameter at 175^0C with ram speed 3.10m/min and winding speed 35m/min. Subsequent drawing was done at 100^0C at a draw ratio of 1:6. Schematic representation of melt spinning machine is given in figure 4.1 and specifications are given below.

Spinneret	:	Single hole, dia = 1 mm, length = 7 mm
Cylinder temperature	:	175 (± 0.5) °C
Ram speed	:	3 .10 (± 0.02) mm/min
Winding speed	:	35(± 0.2) m/min
Filament type	:	mono filament

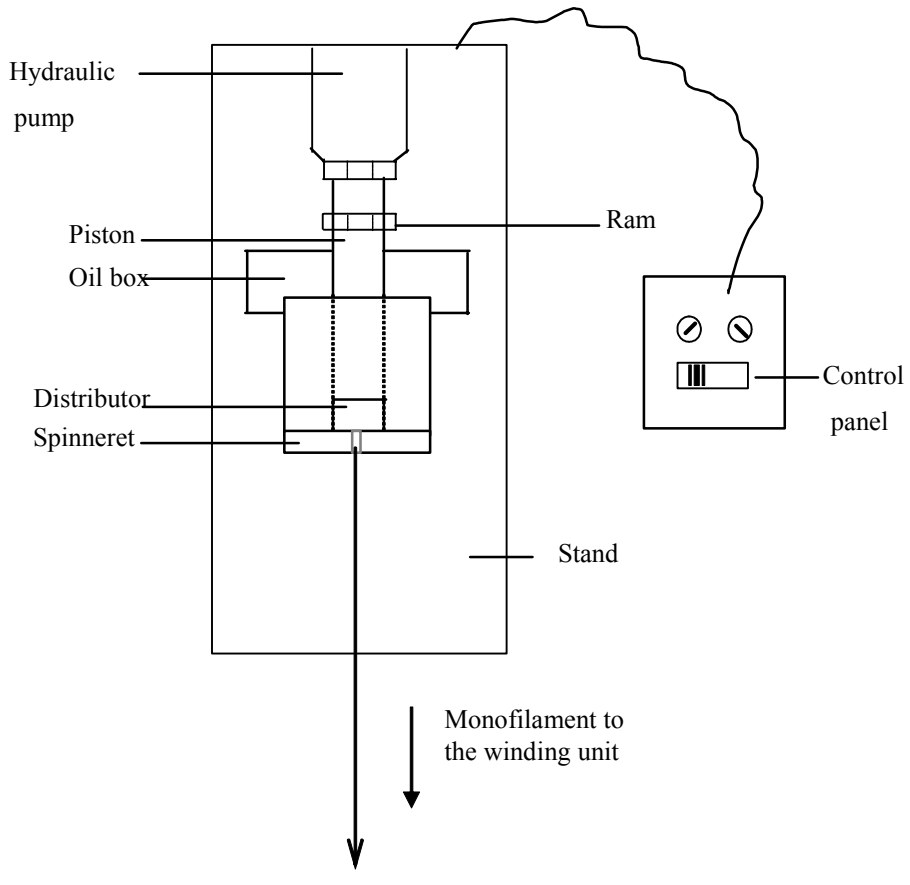

Figure 4.1: Schematic representation of laboratory scale melt spinning machine

The spun fibers were subsequently drawn using a laboratory single zone drawing machine, a schematic representation of which is given in figure 4.2. The specifications and conditions of drawing were as follows:

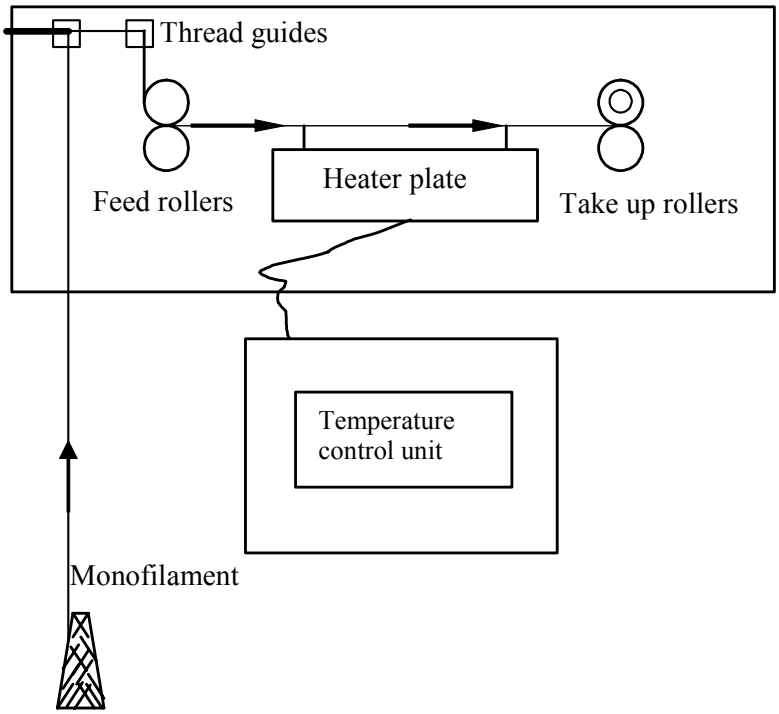

Figure 4.2: Schematic representation of the fiber drawing set-up

Draw ratio	:	1:6
Outer diameter of the rollers	:	11.2 cm
Length of the heating plate	:	20.5 cm
Heater temperature	:	100 ± 0.5 °C

4.2.2 Mechanical properties of the fibers

The mechanical properties of the fibers were studied by a Favimat fiber testing machine with a load cell of 1,200 cN capacity with guage length of 20 mm and test speed 20 mm/min. The pretension was set at 0.50 cN/tex and

the temperature was maintained at 25± 0^0 C. Ten measurements were taken to represent each data.

4.2.3 Thermogravimetric analysis

Thermogravimetric analyzer (TGA Q-50, TA instruments) was used to study the effect of ZnO on the thermal stability of PP fibers. Approximately 10 mg of the samples were heated at a rate of 20^0 C/min from ambient to 800^0C in nitrogen atmosphere. The corresponding weight changes were noted with the help of an ultrasensitive microbalance.

4.2.4 Differential scanning calorimetry

DSC studies were carried out using Q-50 TA instruments in nitrogen atmosphere. The samples were heated to 200^0C at a rate of 10^0C/min, isothermal for 1minute, followed by cooling to 40^0C at a rate of 10^0C/min. In DSC, the crystallization characteristics are studied from the heat flows associated with corresponding transitions as a function of temperature. The percentage crystallinity [34] of the samples was calculated using following equation:

$$X_c = [\Delta H_c/(\Delta H^0_c(1-Wm))]x100 \quad \text{----------} \quad (4.1)$$

where ΔHc is the enthalpy of crystallization of the tested fiber and ΔH^0c is the extrapolated value of enthalpy corresponding to 100% crystalline PP, which was obtained from literature as ΔH^0c =165J/g [35] and Wm is the weight fraction of ZnO in PP fiber.

4.2.5 Scanning electron microscopy

Scanning electron microscope JEOL JSM-6390 was used to study the surface morphology and cross section of fibers.

4.2.6 X-ray diffraction studies

X-ray diffraction studies of the fibers were carried out using Rigaku Geigerflex at wavelength CuK_a=1.54 A^0.

4.2.7 Antibacterial properties of fibers

Effect of bacterial medium on the fibers were studied by putting the fiber in bacterial medium containing Bacillus aereus (gram positive) and E- Coli (gram negative bacteria). Morphology of fibers were studied using SEM after ten days.

4.3 Results and Discussion

4.3.1 Mechanical properties of the fiber

Figure 4.3 is the photographs of PP fibers and PP/ZnO composite fibers after drawing at 100^0C and 1:6 draw ratio.

Figure 4.3: Photographs of neat PP and PP/ZnO composite fibers

Tenacity or strength of PP fibers is increased by the addition of ZnO, reaches maximum at 0.5wt% and then decreased. The increase in tenacity (figure 4.4) is 71.5wt% at 0.5wt% of NZO and 41.1% for 0.5 wt% CZO added PP fiber. The increase in modulus (figure 4.5) is about 38.567% for

0.5 wt% of NZO and 36.67% in case of 0.5wt% of CZO when compared to that of neat PP fiber. Increase in tenacity may be due to the good orientation of NZO in the fiber. The elongation at break (figure 4.6) of the PP fibers is increased in case of NZO filled fibers, reaches a maximum and decreases. This may be due to the increase in toughness of the fiber. In case of CZO filled PP fibers elongation at break decreases by the addition of CZO particles. Effect of ZnO on the time to rupture of fibers is given in figure 4.7. By the addition of ZnO time taken to rupture increases, indicate reinforcing effect of ZnO in PP fiber. Linear density (figure 4.8) of the PP fiber is increased by the addition of ZnO which indicates increase in fineness of fibers. Properties of the fiber depend on internal structure, degree of crystallinity and conditions of spinning [36].

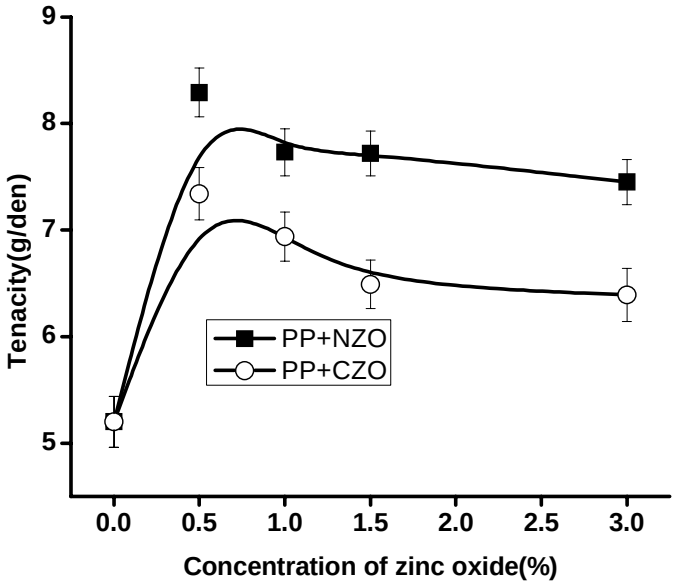

Figure 4.4: Effect of ZnO on tenacity of PP/ZnO composite fibers

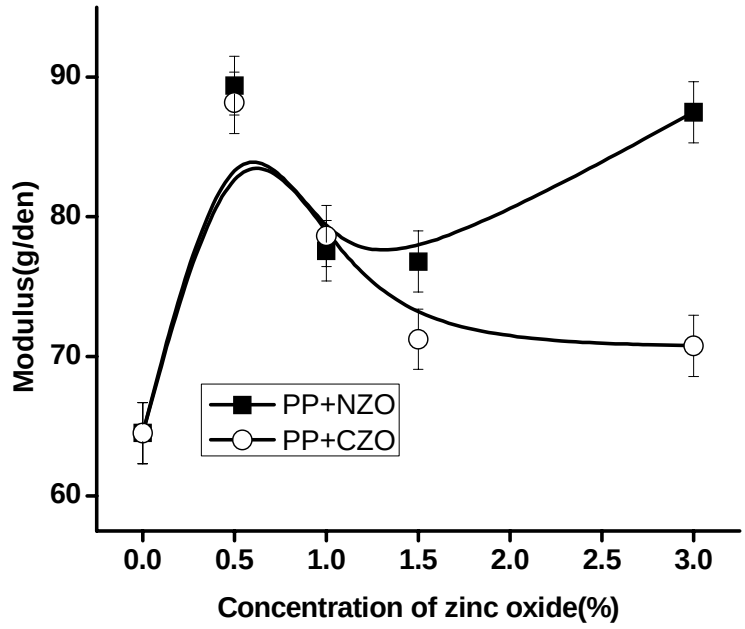

Figure 4.5: Effect of ZnO on modulus of PP/ZnO composite fibers

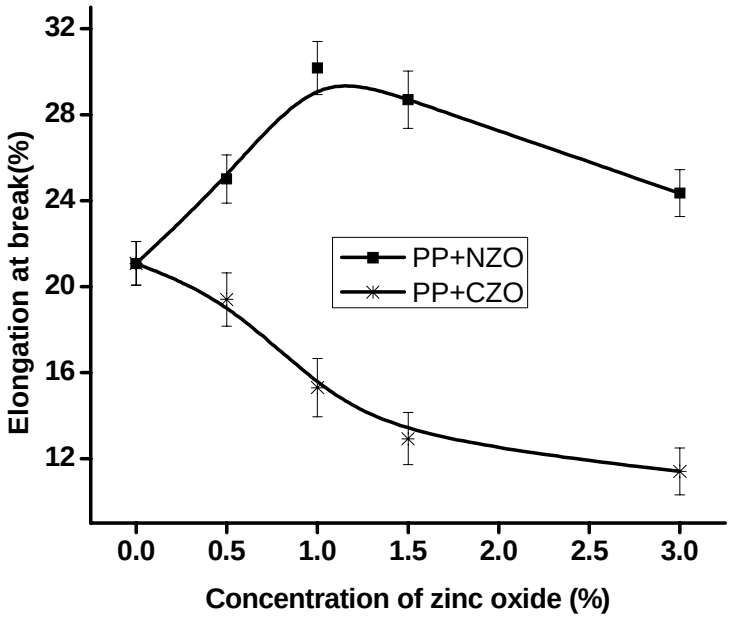

Figure 4.6: Effect of ZnO on elongation at break of PP/ZnO composite fibers

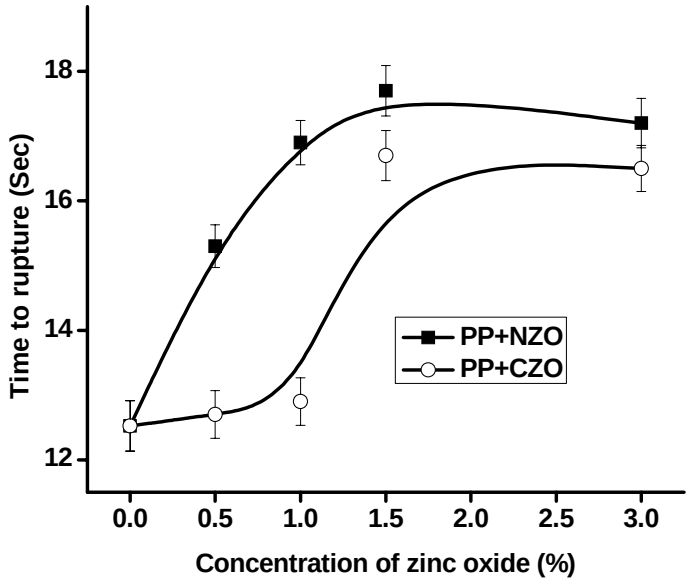

Figure 4.7: Effect of ZnO on time to rupture of PP/ZnO composite fibers

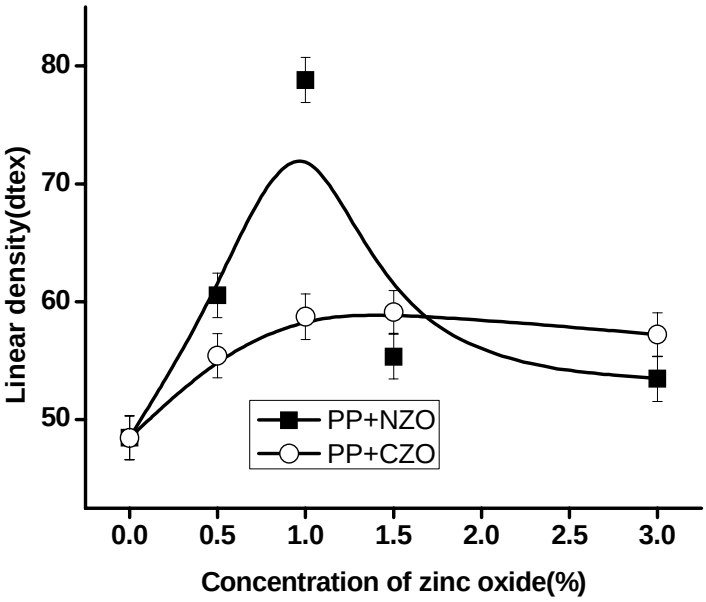

Figure 4.8: Effect of ZnO on linear density of PP/ZnO composite fibers

4.3.2 Thermogravimetric analysis of the fibers

The TGA and DTG curves, obtained under nitrogen atmosphere, of pure PP fiber and PP/NZO fibers are shown in figure 4.9 and 4.10 respectively and data is

tabulated in table 4.1. The thermograms of neat PP and composites fibers are found to be similar in nature. All fibers show single step decomposition and this is due to breakdown of polymer chains. TGA shows the shifting of thermograms towards higher temperature region with increase in concentration of NZO. This indicates degradation of composite fibers takeplace at higher temperature. The enhanced stability of the composite fibers with respect to the neat fibers may be due to the hindering of thermal motion of PP chains by nanoparticles [37],which restrict the degradation of polymer chains. Due to higher compactness of chains, takes much more time to attain the thermal equilibrium and degradation process occurred slowly. Onset of degradation is increased by 31.3^{0}C for fiber containing 3wt% NZO when compared to neat PP. The temperature at which maximum degradation take place is increased by 38.9^{0}C by the addition of 3wt% NZO. There are some recent reports on the increase in polymer stability by the addition of inorganic naoparticles [38-49].

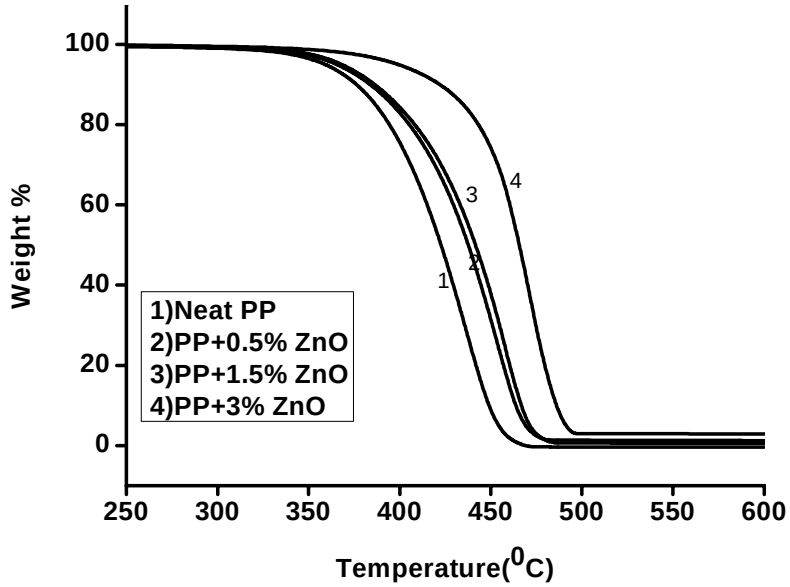

Figure 4.9: Thermogram of PP/ZnO nanocomposite fibers

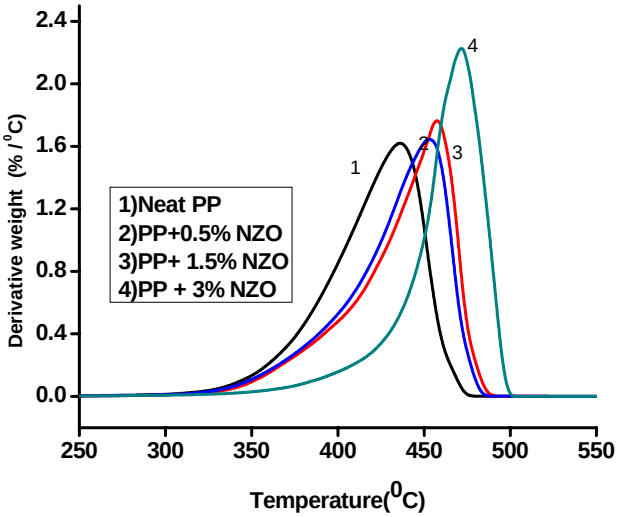

Figure 4.10: Differential thermogram of PP/ZnO nanocomposite fibers

Table 4:2: Thermogravimetric analysis of PP/ZnO nanocomposite fibers

Sample name	Onset temperature (^{0}C)	Endset temperature (^{0}C)	Residue (%)	Temperature at which maximum degradation(^{0}C)
Neat PP	324.9	473.66	0.3883	433.56
PP+0.5% NZO	337.84	486.87	0.5956	457.67
PP+1.5% NZO	342.72	488.28	1.255	458.39
PP+3% NZO	356.18	497.28	2.883	472.44

4.3.3 Kinetic analysis of thermal decomposition

Kinetics of thermal degradation of PP and PP/ZnO composites fibers is studied by Coats–Redfern method [50] and thermal degradation functions were listed in Table 3.3. Detailed description is given in section 3.3.8. From the table 4.3 it is clear that the activation energy of PP fiber is increased by the addition of NZO. Activation energy (E) obtained for neat fiber is 79.5 kJ/mol, 3% NZO added PP is 139.7 kJ/mol. Significant increase in activation energy indicates high thermal stability. Representative plot of Coats–Redfern equation for neat PP fiber, PP/1.5wt% NZO composite fiber and PP/3wt% NZO composite fiber is shown in figure 4.11.

Table 4.3: Apparent activation energy (E) and correlation coefficients (R) for neat PP and composite fibers by Coats–Redfern method.

Sample name	R	E
Neat PP fiber	0.999	79.57
PP+0.5% NZO fiber	0.999	93.125
PP+1.5% NZO fiber	0.999	96.64
PP+3% NZO fiber	0.999	139.71

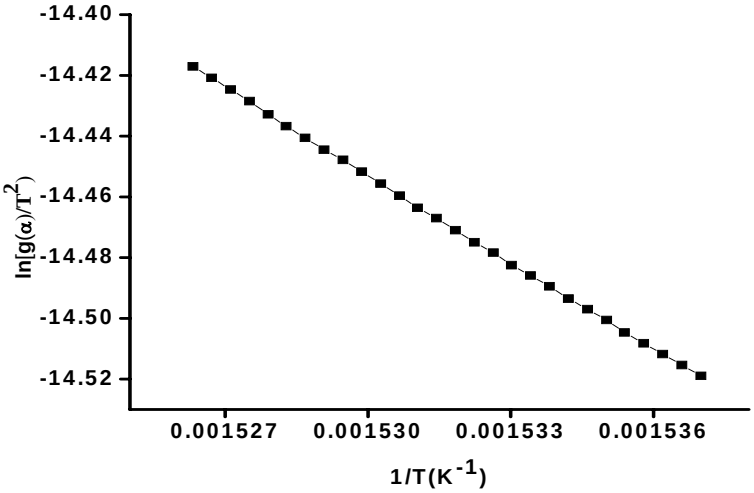

Figure 4.11.a: Representative plot of Coats–Redfern equation for neat PP fiber

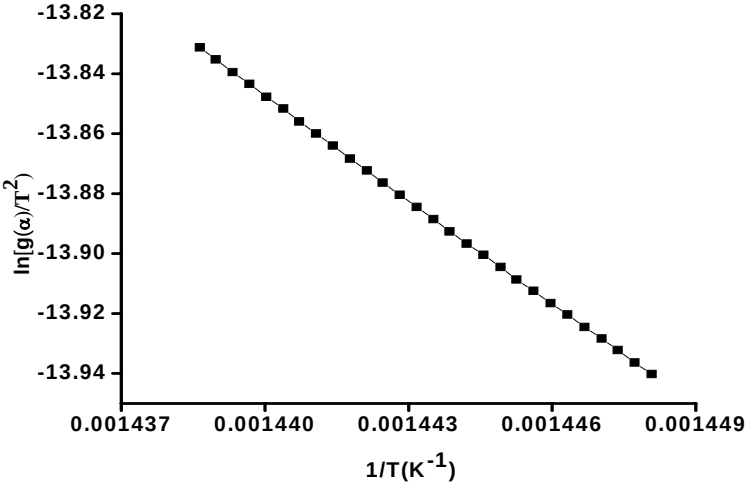

Figure 4.11.b: Representative plot of Coats–Redfern equation for PP+1.5wt% NZO fiber

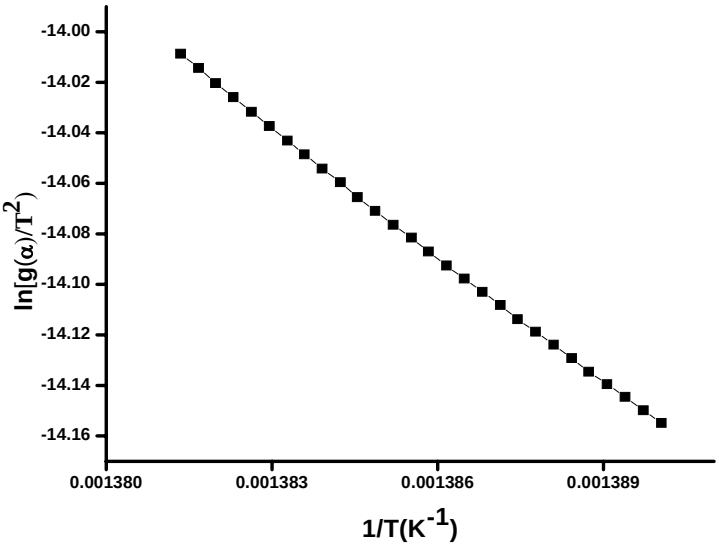

Figure 4.11.c: Representative plot of Coats–Redfern equation for PP+3% NZO fiber

4.3.4 Differential scanning calorimetry (DSC)

DSC curves of the neat PP and composite fibers are shown in figures 4.12 and 4.13. From DSC crystallization exotherms (figure 4.12), Tc (the temperature at the crossing point of the tangents of the baseline and the high-temperature side of the exotherm), Tcp (the peak temperature of the exotherm) and ΔH_c (enthalpy of crystallization) can be obtained is reported in table 4.4. Percentage crystallinity (Xc) of the fibers can be calculated from the Equation (4.1). Results indicate that there is no significant change in the crystallinity of PP fiber by the addition of NZO.

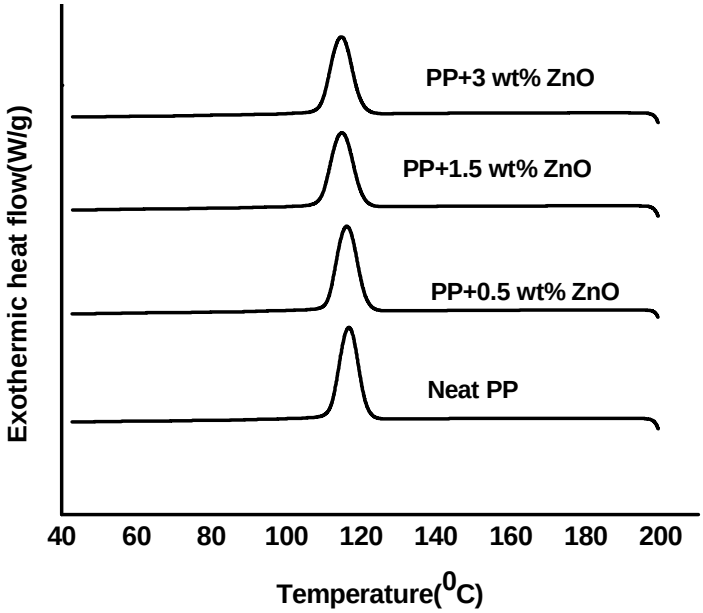

Figure 4.12: Cooling behaviour of neat PP and PP/NZO composite fibers

Table 4.4: Effect of NZO on the crystallization behaviour of PP/NZO fibers

Sample name	Tc(^{0}C)	Tcp(^{0}C)	Tc-Tcp	ΔH_c (J/g)	Xc (%)
Neat PP	121.43	116 .68	4.75	96.5	58.48
PP+0.5%NZO	121.32	116.12	5.2	94.37	57.48
PP+1.5%NZO	120.45	114.83	5.62	92.47	56.89
PP+3%NZO	120.12	114.67	5.45	93.67	58.52

Melting behaviour of fibers is shown in figure 4.13 and values are tabulated in table 4.5. From the DSC curves, Tm (designed here as the temperature at the crossing point of the tangents of the baseline and the low temperature side of the curves), Tmp (the peak temperature of the curve), and ΔHm (heat of fusion) can be obtained. The maximum rate of melting (Tmp) take place at 166.6^{0}C for PP fiber and its Tm is 151.5^{0}C. The Tm value of PP fiber with 3 wt% NZO is increased by about 2.1^{0}C compared with neat PP

fiber. In Figure 4.13, it can be seen that there is a small peak at lower melting temperature of PP fiber and 0.5% NZO filled PP fibers and a peak at higher melting temperature. However, PP fiber at high concentration of NZO shows only single peak at high melting temperature. The first peak, with lower melting temperature, indicates the presence of a small amount of β-phase, whereas the second peak indicates the melting of α-phase.

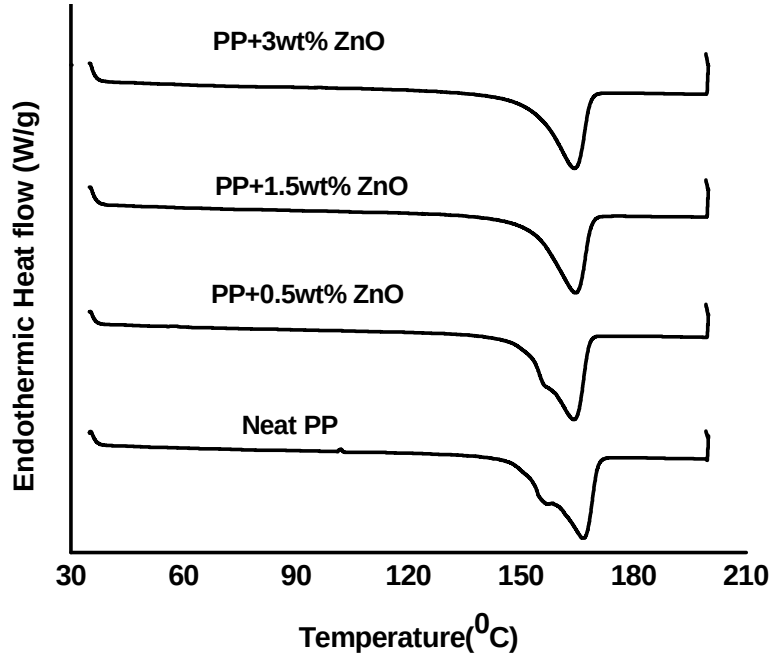

Figure 4.13: Melting behaviour of PP and PP/NZO composite fibers

Table 4.5: Effect of ZnO on the melting behaviour of PP/NZO fibers

Sample name	Tm (^{0}C)	Tmp (^{0}C)	ΔH_m (J/g)
Neat PP	151.53	166.66	89.5
PP+0.5%NZO	151.57	164.09	88.91
PP+1.5%NZO	153.02	164.54	72.17
PP+3%NZO	153.65	164.28	70.11

4.3.5 X-ray diffraction pattern of fibers

X-ray patterns of neat PP fibers and ZnO filled PP fibers are shown in Figure 4.14. Generally, iPP is a multicrystalline polymer and has five crystalline forms such as α, β, γ, δ and pseudohexagonal. The XRD study (Figure 4.14) shows ZnO do not affect the crystalline form of PP fibers. Same crystalline form is observed for both PP and composite fibers. The peaks observed corresponds to (110), (040) and (130) and (041) planes of PP, indicate the α–form of iPP.

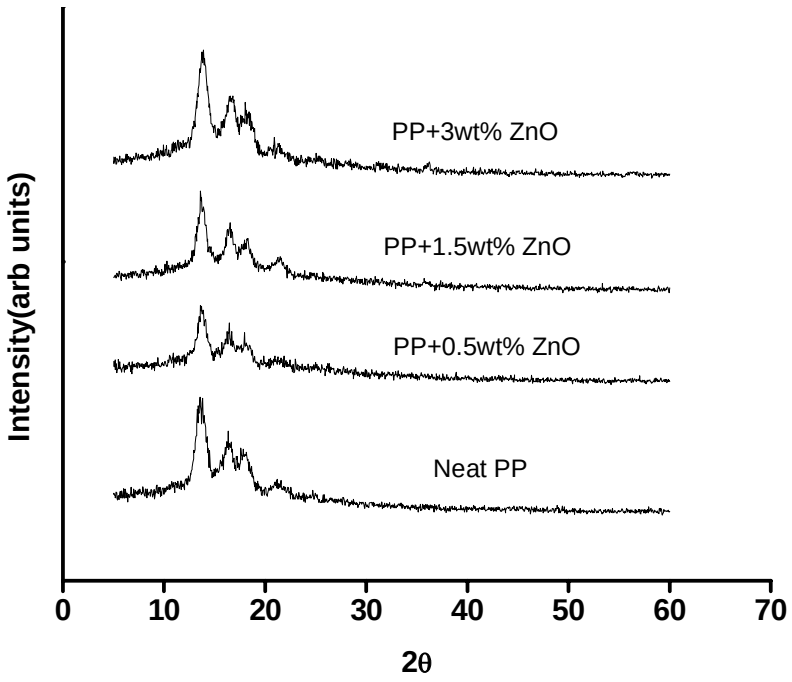

Figure 4.14: X-ray diffraction pattern of PP and PP/NZO composite fibers

4.3.6 Morphology of the fibers

SEM images of neat PP and PP/ZnO composite fibers are shown in figure 4.15. Smooth fiber surface is observed in the SEM of PP/NZO composites fiber compared to neat PP fiber and CZO filled PP fiber. The SEM

of cross section of the fibers is given in figure 4.16. Significant differnce is observed in the SEM of cross section of PP fibers, CZO filled fiber and NZO filled fiber. This morphological difference may be due to the difference in dispersion state and orientation of filler in PP fiber. NZO filled PP fiber shows good dispersion of filler.This also evident from improvement in mechanical properties compared to neat PP fiber.

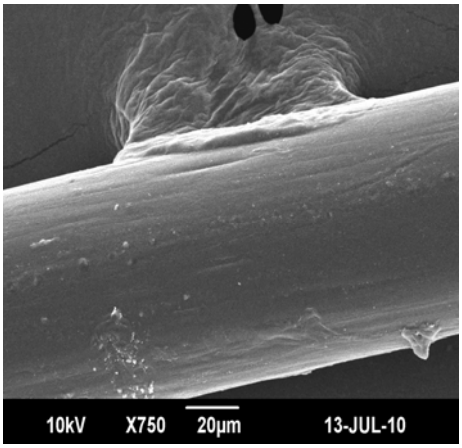

(a)

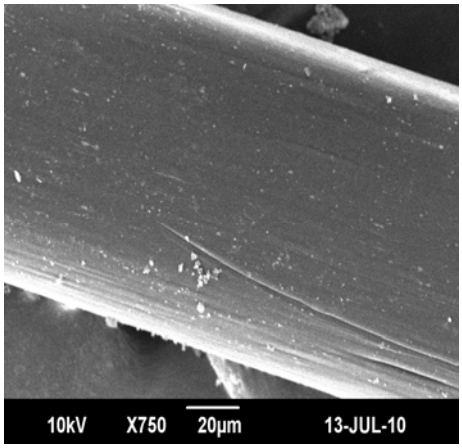

(b)

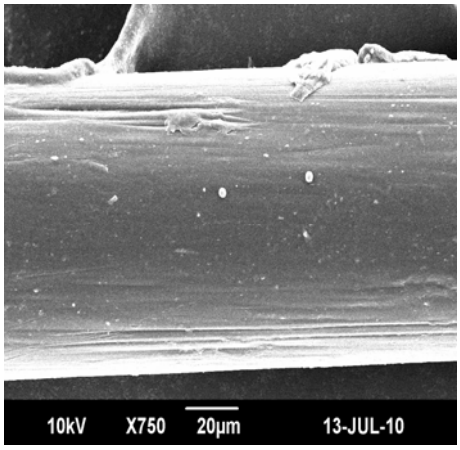

(c)

Figure 4.15: Scanning electron micrographs of (a) neat PP (b) PP+ 3wt% NZO (c) PP+ 3wt% CZO fibers

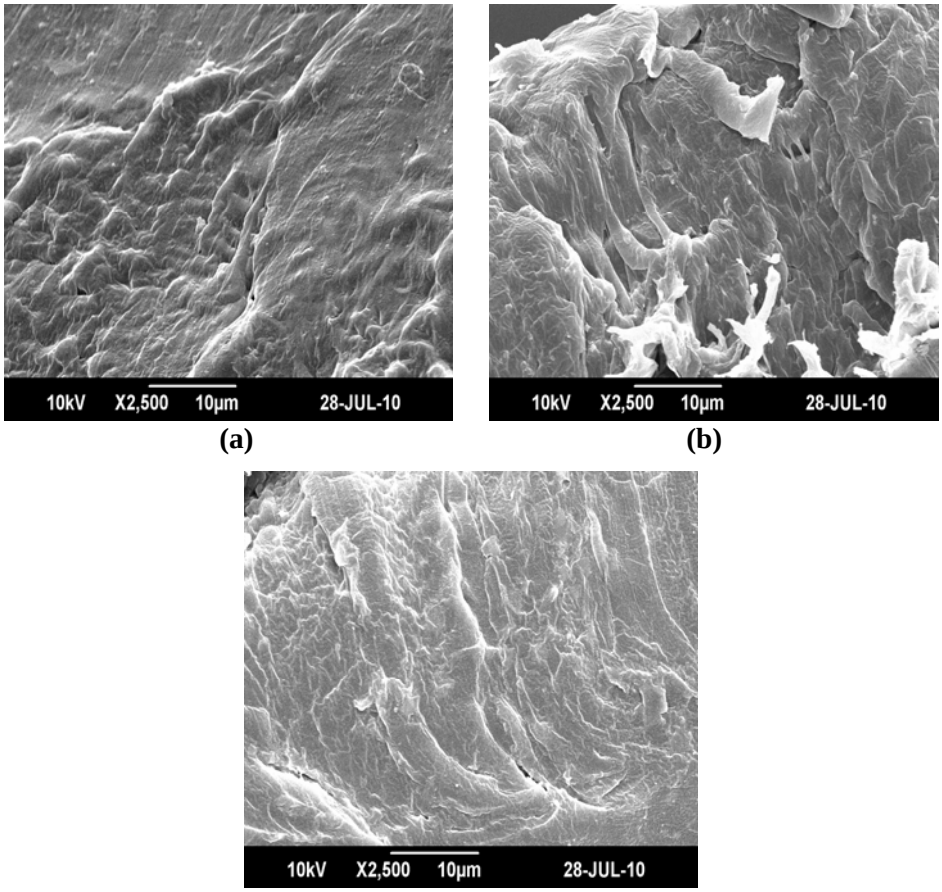

Figure 4.16: Scanning electron micrographs of cross section of (a) neat PP (b) PP+3wt% NZO(c) PP+ 3wt% CZO fibers

4.3.7 Antibacterial properties of fibers

ZnO shows excellent antibacterial properties and this is evaluated in chapter 2. The resistance of PP textiles to bacterial attack make it possible to use in medical field and defense clothings. Figure 4.17 shows the morphology of the fibers after putting them in bacterial medium for ten days in Bacillus aereus. Fiber surface is more smooth compared to morphology of fibers before bacterial attack (figure 4.15). Figure 4.18 shows the morphology of the fibers after putting them in bacterial medium for ten days in E-coli. Fiber morphology is not significantly changed by the attack of E-coli.

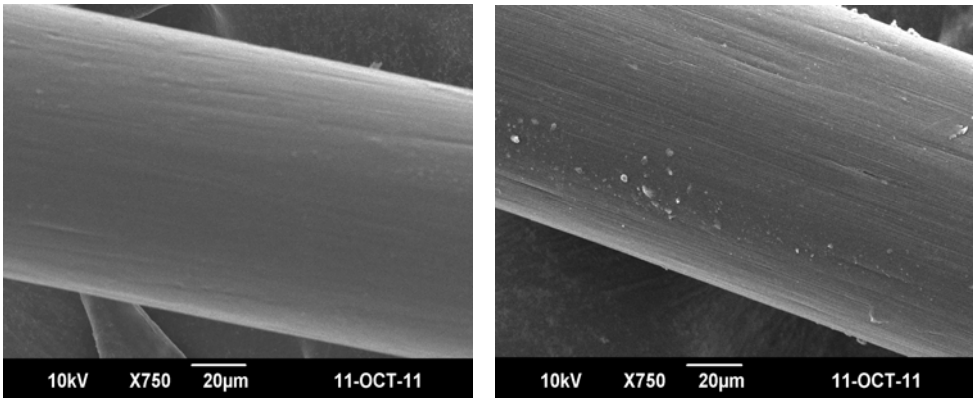

(a) **(b)**

Figure 4.17: Scanning electron micrographs of (a) neat PP (b) PP/3wt% NZO filled fibers after treating with Bacillus aereus

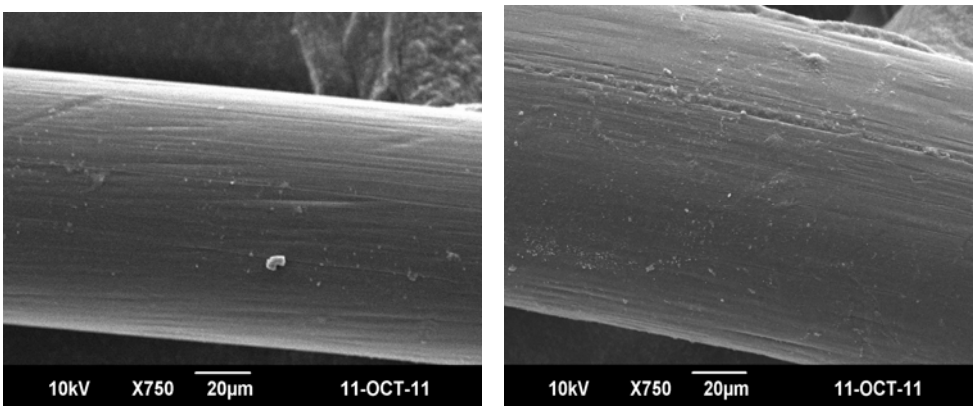

(a) **(b)**

Figure 4.18: Scanning electron micrographs of (a) neat PP (b) PP/3wt% NZO filled fibers after treating with E-Coli.

4.4 Conclusion

Melt spinning could be used for the preparation of neat PP fiber and PP/ZnO composite fiber. Mechanical properties of the fiber increased by the addition of ZnO. Significant improvement is shown by NZO filled PP fibers when compared to CZO filled PP fibers. Thermal stability of the PP fiber is increased significantly in presence of NZO. NZO has no significant effect on

the crystallinity of PP fiber. X-ray diffraction studies indicate similar crystal form of PP fiber and composite fibers. Morphology of the cross section of the neat fiber is different from the morphology of the CZO filled, NZO filled PP fiber indicate difference in dispersion and molecular orientation of filler in the fibers. PP fiber and NZO filled fiber are not attacked by bacteria.

References

[1] Gleixner G, Flame retardant PP fibres-lateat developments, Chem Fibers Int, 2001,51, 422.

[2] Karger Kocsis J, Polypropylene an a-z reference, Kluwer Academic, London,1999.

[3] Horrocks A R, Anand S C, Handbook of Technical Textiles, The Textile Institute, Woodhead Publisching Limited ,ISBN1 85573 3854, Cambridge, 2000.

[4] Floyd K L, The role of polypropylene in nonwovens, Plast Rubber Process. Appl,1984,4,317.

[5] Wei K Y, Vigo T L, Goswami B C, J.Appl.Polym.Sci.,1985, 30, 153.

[6] Nanjundappa R, Bhat G S, J.Appl. Polym. Sci., 2005, 98, 2355.

[7] Malkan S R, An overview of spun bonding and melt blowing Technologies, tappi J, 1995, 78, 185.

[8] Zhang D, Bhat G, Malkan S, Sun Q, Wadsworth L, J.tex.Inst., Part I 1998,89,289.

[9] Zhang D, Bhat G, Malkan S, wadsworth L, J.ther.Anal.,1997,49,161.

[10] Bhat G.S, Nanjudappa R, Kotra R, Thermochim.Acta, 2002,392.

[11] Bhat G S, Jangala P K, Spruiell J E, J.Appl.Polym.Sci., 2004, 92, 3593.

[12] Zhang D, Sun Q, Bhat G, Wadsworth L, J.Appl.Polym.Sci.,1998,69,421.

[13] Zhang D, Bhat G, Sanjiv M, Wadsworth L, Tex. Res. J,1998,68,27.

[14] Hoyle A G, Tappi J., 1990,73,85.

[15] Warner S B, Tex.Res.J.,1989, 59,151.

[16] Fraser W A, Whitwell J C, Miller B, Thermochimica Acta, 1974,8,105.

[17] Lotz B, Wittman J C, Lovinger A J, Polymer,1996, 37, 4979.

[18] Cheng S Z D, Janimak J J , Roguez J, Crystalline structure of PP homo and copolymers,in Polypropylene Structure Blendsand composites, vol 1, Structure and morphology,Karger-Kocsis J.(ed),Chapman and Hall, London, 1995,31.

[19] Iijima M, Sorbitol G, Macromoloecules 2000, 33, 520.

[20] Lotz B, Wittman J C, Lovinger A J, Polymer,1996,37,4979.

[21] Mei-fang Zhu, H.H.Yang, Polypropylene fibers in Handbook of fiber chemistry, Third edition, edited by Monachem Lewin,CRC press, Boca Raton FL,2006.

[22] Rottstegge J, QiaoY K, Zhang X, Zhou Y, Xu D, Han CC, Wang D, J Appl Polym Sci 2007; 103, 218.

[23] Marcincin A, Hricova M, Marcincin K, Legen J, Ujhelyiova A, Bonduel D, Claes M, Presented at Proceeding Book of International Conference, Futuro Textiles, Lille, France,2006, 135.

[24] Joshi M, Shaw M, Butola B S, Fibers and Polymers, 2004,5,59.

[25] Pavlokova S, Thomann R, Reichert P, Mulhaupt R, Marcincin A, Borsig E, J Appl Polym Sci, 2003, 89, 604.

[26] Chaowei Hao, Ying Zhao, Aihua He, Xiuqin Zhang, Dujin Wang, Qingfang Ma, Yizhuang Xu, Journal of Applied Polymer Science, 2010, 116, 1384.

[27] Chih-Wei Chiu , Chin-An Lin , Po-Da Hong, J Polym Res , 2011, 18,367.

[28] Xiuqin Zhang, Mingshu Yang, Ying Zhao, Shimin Zhang,Xia Dong, Xuexin Liu, Dujin Wang, Duanfu Xu1, Journal of Applied Polymer Science, 2004, 92, 552.

[29] Sarit Thanomchat, Sarintorn Limpanart, Kawee Srikulkit, Journal of Applied Polymer Science, 2010,117, 1969.

[30] Anton Marcincin, Marcela Hricova, Anna Ujhelyiova, Ondrej Brejka,Peter Michlik,Maria Dulíkova, Zuzana Strecka, Stefan Chmela , fibers & textiles in Eastern Europe 2009, 17, 29.

[31] Natee Srisawat, Manit Nithitanakul, Kawee Srikulkit, Journal of Metals, Materials and Minerals, 2009, 19, 53, 2009.

[32] Gupta VB, Kothari VK, editors, Manufactured Fibre Technology, Chapman and Hall, London, 1997.

[33] Gurudatt K, De P, Rakshit AK, Bardhan M K, J. Appl. Polym. Sci. 2003,90,3536.

[34] Abdolhosein Fereidoon, Morteza Ghorbanzadeh Ahangaria, Seyfolah Saedodina, Journal of Macromolecular Science R , Part B: Physics, 2008, 48,196 .

[35] Wunderlich B, Macromolecular Physics, Acadamic:New York, 1960, 3, 48.

[36] Seung Hwan Lee, Jae Ryoun Youn, Journal of applied polymer science 2008, 109, 1221.

[37] Gilman J W, Applied Clay Science, 1999, 15, 31.

[38] Chgnati Srinivasa Reddy, Chapal Kumar Das, J of Appl Polym Sci, 2006,102, 2117

[39] Sangeetha Hambir, Neelima Bulakh, Jog JP, Polymer Engineering and Science, 2002, 42,1800,

[40] Rezaei F, Yunus R , Ibrahim N A, Materials and Design, 2009, 30, 260.

[41] Arrakhiz F Z, Elachaby M, Bouhfid R , Vaudreuil S, Essassi M , Qaiss A, Materials and Design, 2012, 35,318.

[42] Kumar A P, Depan D, Tomer N S, Singh R P, Prog Polym Sci, 2009, 34,479.

[43] Alexandre M, Dubois P, Mater Sci Eng, 2000, 28, 63.

[44] Ray S S, Okamoto M, Prog Polym Sci, 2003, 28, 1539.

[45] Hasegawa N , Okamoto H , Kato M, Usuki A, J. Appl. Polym. Sci., 2000, 78, 1918.

[46] Danyadi L , Janecska T, Szabo Z, Nagy G, J Moczo, B Pukanszky, Composites Sci Technol., 2007, 67, 2838.

[47] Shahryar Jafari Nejad, Seyed javad Ahmadi, Hossein Abolghasemi, Ahmad Mohadde Spour, J. of appl. Polym Sci.,2007,7, 2480.

[48] Hassan M , El-Dessouky, Carl A Lawrence, J. nanopart. Res., 2011, 13, 1115.

[49] Chih-Wei Chiu, Chin-An Lin, Po-Da Hong, J Polym Res, DOI 10.1007/s 10965-010-9426-0, 2010.

[50] Coats A W, Redfern J P, Kinetic parameters from thermogravimetric data, Nature 1964, 68, 201.

CHAPTER 5

SYNTHESIS, CHARACTERIZATION AND ANTIBACTERIAL PROPERTIES OF TITANIUM DIOXIDE NANOPARTICLES

Contents

Titanium dioxide nanoparticles were prepared by sol gel method and wet synthesis. XRD was used to study the crystalline phase and size of TiO_2 nanomaterials. TiO_2 prepared by sol gel method showed anatase crystal structure when it is calcined at 500^0C and rutile structure is obtained when it is calcined at 1000^0C, but the crystallite size was very high compared to anatase form. TiO_2 prepared by wet synthesis showed rutile form with lower particle size at the calcination temperature 400^0C. SEM showed that TiO_2 prepared by wet synthesis gave spherical nanoparticles of rutile TiO_2. Element analysis was done by energy dispersive X-ray atomic spectrum. Commercially available rutile form (CTO) showed higher crystallite size in XRD. Thermogravimetric analysis was carried out on rutile TiO_2 (both synthesized and commercial powder). TEM images of TiO_2 prepared by wet synthesis method (NTO) showed particle size as low as 7nm. Antibacterial properties of the NTO and CTO were studied using Bacillus aereus (gram positive) and Escherichia coli (gram negative bacteria).

5.1 Introduction

Titanium dioxide, also known as titania, is a naturally occurring oxide of titanium. The properties of titanium dioxide includes high refractive index, light absorption, non-toxicity, chemical stability and relatively low-cost production [1-5]. Titanium dioxide nanoparticles have attracted attention in the fields of environmental purification, solar energy cells, photocatalysts, gas sensors, photo electrodes and electronic devices. It has been widely used as a pigment in paints, ointments, toothpaste etc [6-10]. Surface area and surface-to-volume ratio increase dramatically as the size of material decreases.

The performances of TiO_2 is strongly influenced by the crystalline structure, the morphology and the size of the particles [11–15]. Nanosized TiO_2 particles are of particular interest due to their specifically size-related properties. As the size, shape, and crystal structure of TiO_2 nanomaterials vary, not only does surface stability change but also the transitions between various phases of TiO_2 under pressure and heat. Generally it is in three forms, rutile (tetragonal,a=b=4.58A^0,c=2.95A^0), anatase (tetragonal, a=b=3.78A^0,c=9.5A^0) and brookite (rhombohedral, a=5.43A^0, b=9.16A^0, c=5.13A^0). These crystalline structures consist of $[TiO_6]^{2-}$ octahedral, which share edges and corners in different manners and keeping the overall stoichiometry as TiO_2 [16-19]. Among various phases of titania reported, anatase shows a better photocatalytic activity and antibacterial performance [20-24]. A stable anatase up to the sintering temperature of the ceramic substrates is most desirable for applications on antibacterial self-cleaning building materials like bathroom tile, sanitary ware etc [25-27]. Anatase-to-rutile transformation is usually occurs at 600 to 700°C [28-30]. Phase transition to rutile is nonreversible because of the greater thermodynamic stability of rutile phase [31,32].

Hwu et al observed the crystal structure of TiO_2 nanoparticles depend on the preparation method. For TiO_2 nanoparticles below 40nm, anatase seemed more stable and transformed to rutile at greater than 973K [33]. Banfield et al found that prepared TiO_2 nanoparticles had anatase and/or brookite structures, which transformed to rutile after reaching a certain particle size [34]. Once rutile was formed, it grew much faster than anatase. They found that rutile became more stable than anatase for particle size greater than 14nm. A number of studies have focussed on the synthesis of titanium dioxide nanoparticles [35–43]. Anatase and rutile are commonly obtained by hydrolysis of titanium compounds, such as titanium tetrachloride ($TiCl_4$) [44-46] or titanium alkoxides ($Ti(OR)_4$), in solution [47-50]. Brookite is sometimes observed as a by-product of the precipitation reaction carried out in acidic medium at low temperature [47, 48, 51-53]. Brookite is also obtained as large crystals by hydrothermal methods at high temperature and pressure in aqueous [54] or in organic media [55]. Tianyou Peng et al reported the stability of anatase form up to 800^0C prepared by hydrothermal synthesis [38]. S Mahshid et al reported the formation of anatase phase by hydrolysis of titanium isopropoxide solution and nanoparticles shows anatase to rutile transformation at the temperature lower than 600 °C [40]**.**

There are only a few reports on the synthesis of nanomaterials of rutile TiO_2.Yoichi Ishibai et al reported the rutile nanoparticles in colloidal form by wet synthesis [56]. To achieve both effective UV ray shielding and high transparency in the visible region, they developed a TiO_2 colloidal sol. They investigated sunscreen capability and suppression of photocatalytic activity of rutile form. They have obtained particles with 20-30nm range in TEM.

Synthesis of rutile form by wet synthesis method and anatase form by sol gel technique is reported in this chapter. The material was characterized by

different techniques and compared with commercially available rutile form. Antibacterial properties of NTO and CTO were also studied.

5.2 Experimental

5.2.1 Materials

Aqueous solution of $TiCl_4$ (purity>99.9%), HNO_3 and aqueous ammonia used were analar grade. Titanium (IV) isopropoxide and isopropanol was supplied by alpha chemicals, Cochin.

5.2.1.1 Sol gel method

Titanium (IV) isopropoxide (100g) was added to iso-propanol (200g) and the mixture was stirred for 5min using a magnetic stirrer. After stirring, a mixture of water (25.33g) and iso-propanol (127g) was added dropwise to the alkoxide solution. After adding the water/alcohol solution, the mixture was stirred for about 24 hours at room temperature. The precipitate was dried, at 100^0C in a hot air oven. It was then calcined at 500^0C and 1000^0C in a muffle furnace.

5.2.1.2 Wet synthesis

In this method, both $TiCl_4$ solution (200 g/l) and NaOH solution (64.5 g/l) were added drop wise to water with stirring. After the resulting solution reaches pH to 7, the slurry was filtered, and the filter cake of TiO_2 was washed and redispersed in water to prepare 1 M of TiO_2 slurry. Resulting TiO_2 slurry and an aqueous solution of HNO_3 were refluxed at 95^0C for 2 h, cooled to room temperature and neutralized with 28% of aqueous ammonia. Then, it was filtered, washed and calcined at 400^0C [56]. Details of characterization techniques are given in chapter 2, section 2.2.

5.3 Results and Discussion

5.3.1 X-ray diffraction analysis (XRD)

XRD is used to determine crystal structure and crystallite size can be calculated using Debye Scherrer equation.

$$CS = 0.9\lambda/\beta\cos\Theta \quad \text{---------- (5.1)}$$

where CS is the crystallite size, β is the full width at half-maximum ($FWHM_{hkl}$) of an hkl peak at 2Θ value, Θ is the half of the scattering angle. Crystal size is determined by measuring the broadening of a particular peak in a diffraction pattern associated with a particular planar reflection from within the crystal unit cell. It is inversely related to the FWHM of a individual peak. If the peak is broad, the crystallite size will be small and vice versa. The periodicity of individual crystallite domains reinforces the diffraction of X-ray beam, resulting in a tall narrow peak. If the crystals are randomly arranged and have low degrees of periodicity, the result is a broader peak. This is generally the case for nanomaterials. Figure 5.1 represents the XRD patterns of TiO_2 prepared by sol-gel method. From the XRD pattern it is clear that anatase form of TiO_2 is obtained by this method when it is calcined at 500^0C and rutile form is observed in XRD when it is calcined at 1000^0C. As the crystallite size increases, the diffraction peak becomes narrower as in the case of TiO_2 calcined at 1000^0C. Broadening of peak is observed in the case of TiO_2 prepared by wet synthesis method is an indication of reduction in crystallite size. XRD of TiO_2 prepared by wet synthesis method (figure 5.2) and commercial (figure 5.3) TiO_2 shows the peaks of rutile form. TiO_2 prepared by sol gel method and calcined at 500^0C shows peaks corresponds to the planes (101), (004), (200), (105),(211),(204),(116),(220),(215) indicate anatase form. In figure 5.2, it can be seen the peaks corresponds to the planes (110), (101) (111) (210) (211) and (220) of rutile form. Crystallite size was calculated by

De bye Sherrer equation is given in table 5.1. Least crystallite size is obtained for TiO_2 prepared by wet synthesis method.

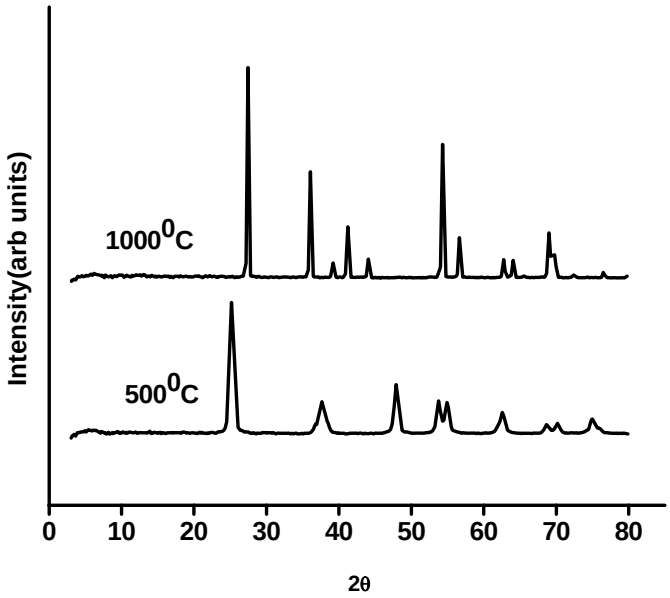

Figure 5.1: XRD pattern of TiO_2 prepared by sol gel method

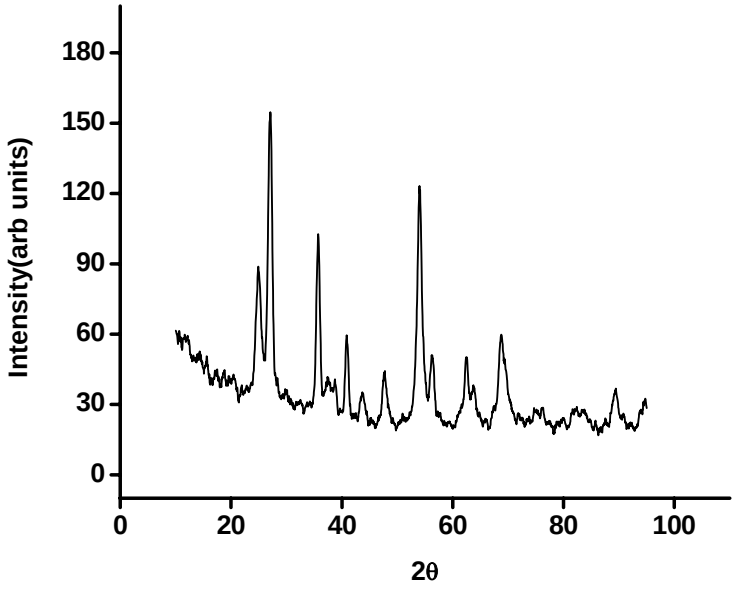

Figure 5.2: XRD pattern of TiO_2 prepared by wet synthesis

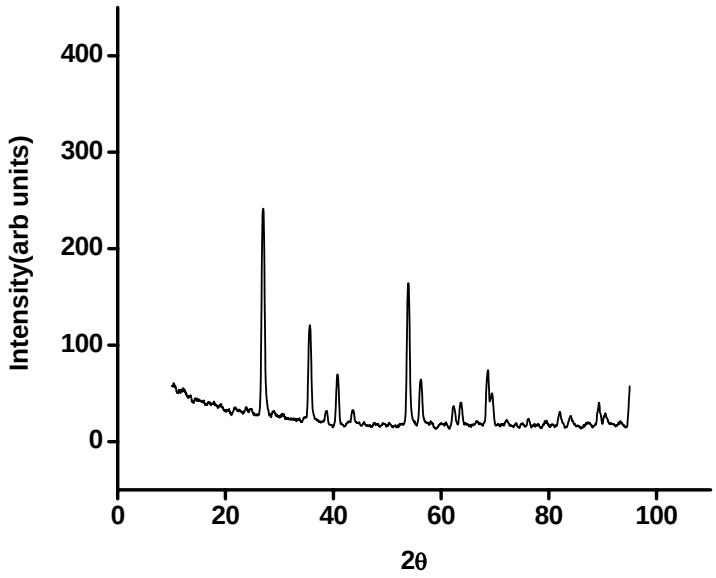

Figure 5.3: XRD pattern of commercial rutile TiO_2

Table 5.1: Crystallite size of TiO_2 prepared by different methods

TiO_2 Prepared by	**Crystallite size(nm)**
Wet synthesis	11.8
Sol gel method (calcined at 500^0C)	17.8
Sol gel method (calcined at 1000^0C)	31.8
Commercial TiO_2	26.45

5.3.2 Scanning electron micrographs

Scanning electron micrographs of TiO_2 prepared by sol gel method (STO), wet synthesis (NTO) and commercial TiO_2 (CTO) are given in figure 5.4a, 5.4b, 5.4c respectively. By changing the method of preparation morphology of TiO_2 also changes. In figure 5.4b small spheres are observed for NTO when compared to CTO and STO. In figure 5.4a large particles are seen due to the high temperature of calcination.

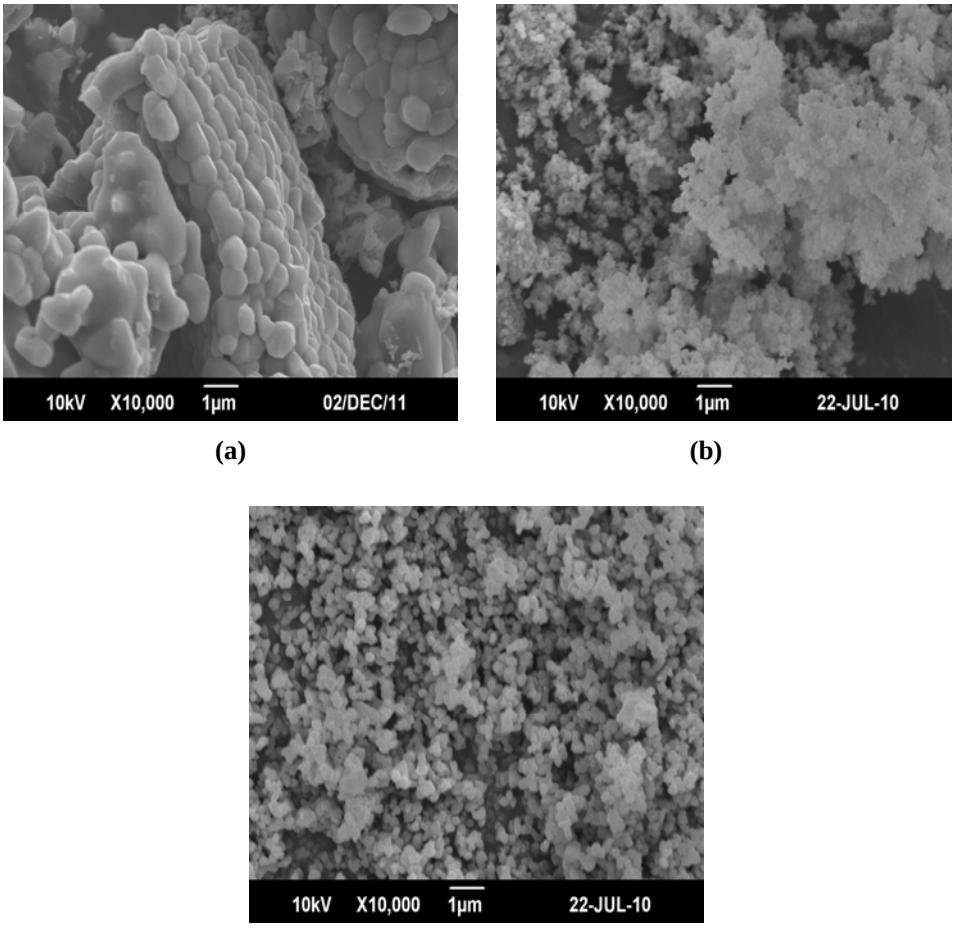

(a) **(b)**

(c)

Figure 5.4: Scanning electron micrographs of TiO_2 prepared by (a) sol gel method (b) wet synthesis (c) commercial rutile TiO_2

5.3.3 Thermogravimetric analysis

TGA is a thermal analysis technique that measures the weight change in a material as a function of temperature and time in a controlled environment. This can be very useful to investigate the thermal stability of a material and to investigate its behaviour in inert or oxidizing atmosphere. It is useful for all types of solid materials, including organic and inorganic materials. The material is heated to high temperature so that one of the components decomposes into a

gas, which dissociates into the air. In this process, heat and stoichiometry ratios used to determine the percent by mass ratio of a solute. If the compounds in the mixture remain are known, then the percentage by mass can be determined by taking the weight of what is left in the mixture and dividing it by the initial mass. The degradation behaviour of NTO, STO and CTO was studied using TGA in nitrogen atmosphere is shown in figure 5.5. Similar degradation behaviour is shown by all samples.

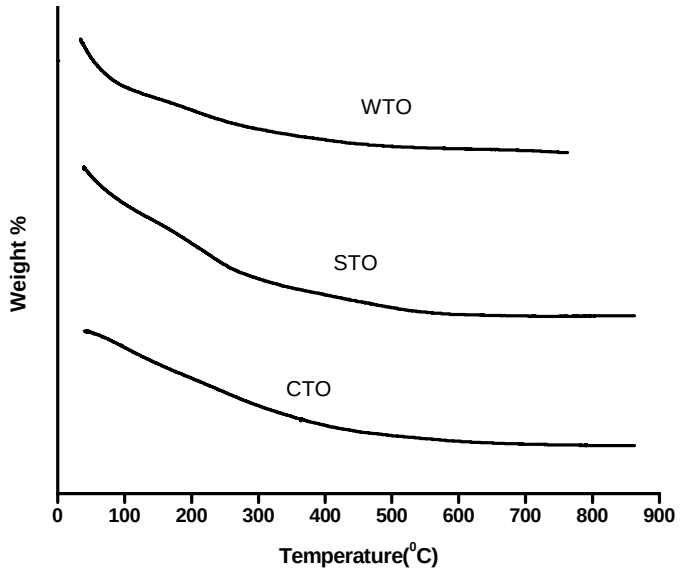

Figure 5.5: Thermogram of TiO_2

5.3.4 Transmission electron microscopy

TEM gives the size and shape of the particles on the scale of atomic diameters. Figure 5.6 shows the TEM image of titanium dioxide prepared by wet synthesis. It is observed that the particles are in the range 5-20 nm and are mostly of elongated shape. Particle size of the smallest particle is found to be as 7 nm. Particle size distribution of TiO_2 is shown in figure 5.7. Most of the particles are in 10-15nm range.

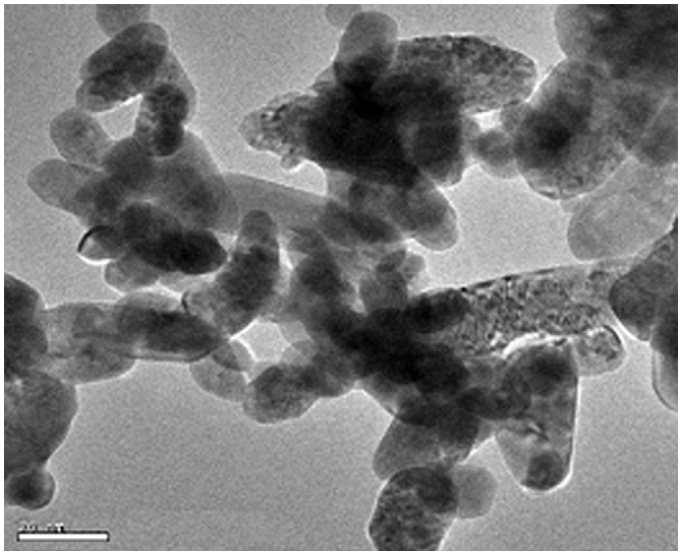

Figure 5.6: Transmission electron micrograph of TiO_2

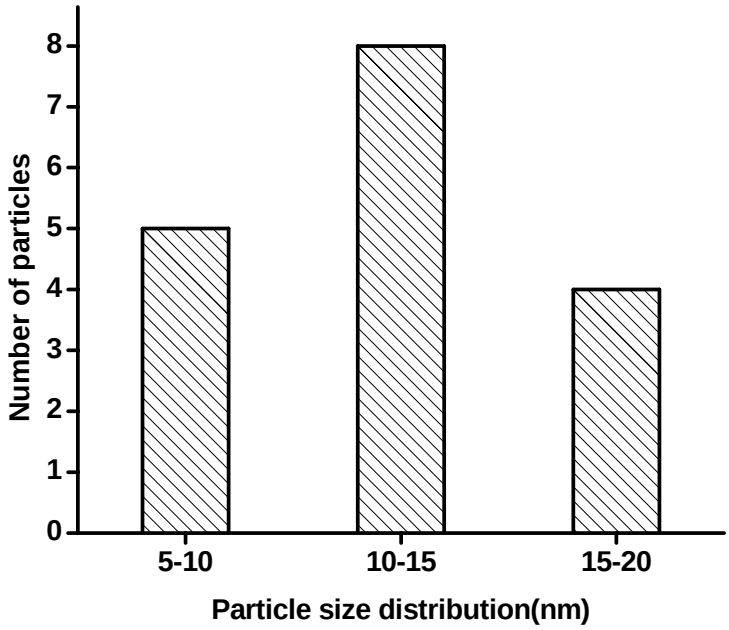

Figure 5.7: Particle size distribution of TiO_2

5.3.5 Energy Dispersive Analysis by X-rays (EDAX)

EDAX is used to analyze the chemical composition of a material under SEM. Figure 5.8 represents the EDAX of TiO_2 nanoparticles prepared by wet synthesis. EDAX shows only peaks of titanium and oxygen. From figure 5.8 it is clear that TiO_2 is free from impurities.

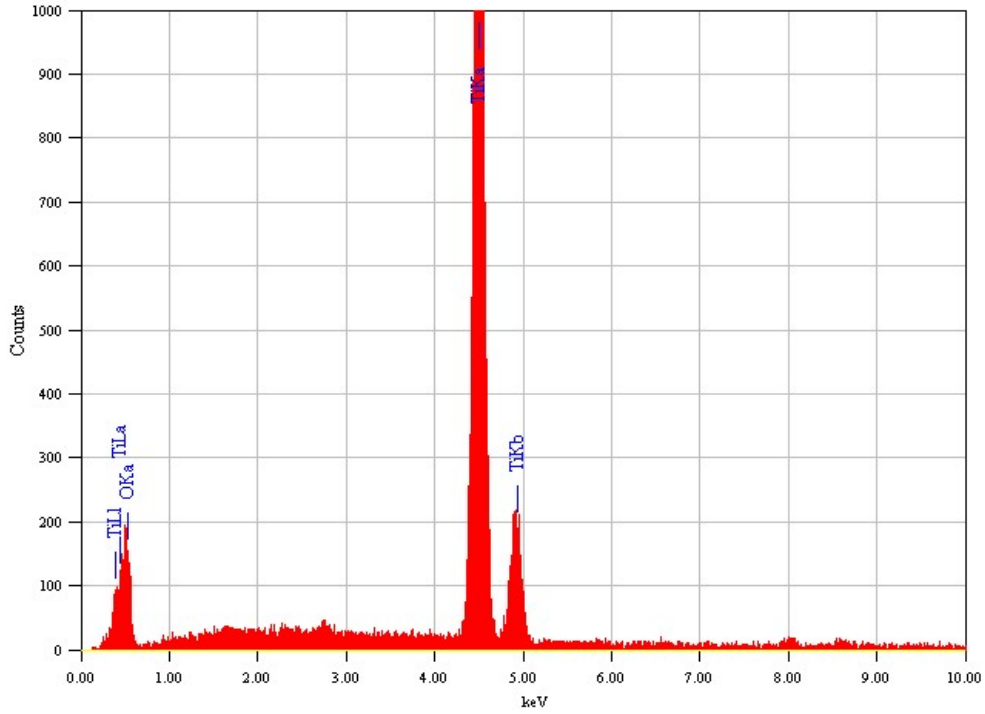

Figure 5.8: Energy dispersive X-ray spectrum of TiO_2 prepared by wet synthesis

5.3.6 Antibacterial properties of TiO_2

Reduction in colony forming units (CFU)

Antibacterial properties of CTO and NTO to Bacillus aereus is shown in table 5.2. Percentage reduction in Bacillus aereus is 99.06% for CTO and for 93.2% for NTO. TiO_2 shows good resistance to Bacillus aereus. From the table it is clear that particle size of TiO_2 has no significant role in the antibacterial properties of TiO_2.

Table 5.2: Colony forming unit using Bacillus aereus (NCIM No:2155)

Sample	Colony forming unit	% of reduction
Control	$75x\ 10^6$	
CTO	$707x10^3$	99.06
NTO	$10x10^6$	93.2

Table 5.3: Colony forming unit using Escherichia coli (NCIM No:2343)

Sample	Colony forming unit	% of reduction
Control	$9x\ 10^8$	
CTO	$31x10^7$	65.6
NTO	$45x10^7$	50

Antibacterial properties of CTO and NTO in E Coli is shown in table 5.3. Percentage reduction in Escherichia coli is 65.6% for CTO and for 50% for NTO. Reduction in particle size do not enhance the resistance to E-Coli.

5.4 Conclusion

Titanium dioxide nano particles can be successfully prepared by wet synthesis method and sol gel method. Rutile TiO_2 is obtained from wet synthesis method and anatase is obtained from sol gel method. TiO_2 preapred by sol gel method is converted to rutile form when it is calcined at 1000^0C, but crystallite size is very high. Titanium dioxide nanoparticles show different morphology according to method of preparation. TEM studies show elongated structure of TiO_2 nanoparticles with size 7nm for smallest particle. EDAX shows the absence of impurities in prepared TiO_2. Thermogravimetric studies show similar degradation behaviour for all TiO_2 particles indicate absence of impurities. Titanium dioxide shows excellent resistance to bacillus aereus.

References

[1] Rammal A, Brisach F , Henry M, Chimie C R, 2002, 5, 59.

[2] Kamat P V, Chem. Rev, 1999, 93,267.

[3] Mills A, Hill G, Bhopal S, Parkin I P, Neill S A O, J.Photochem. Photobiol.A: Chemistry, 2003, 160,185.

[4] Awati P S, Awate S V, Shah P P , Ramaswamy V,Catal.Comm.4,393.

[5] Zhang R, Gao L, Zhang Q, Chemosphere, 2004, 54,405.

[6] Pfaff G, Reynders P, Chem. ReV, 1999, 99, 1963.

[7] Salvador A, Pascual-Marti M C, Adell, J R, Requeni A, March J G, J. Pharm. Biomed. Anal, 2000, 22, 301.

[8] Zallen R, Moret M P, Solid State Commun., 2006, 137, 154.

[9] Braun J H, Baidins A, Marganski R E, Prog. Org. Coat., 1992, 20, 105.

[10] Yuan S A, Chen W, Hu S S., Mater. Sci. Eng. C, 2005, 25,479.

[11] Hadjipanayis G C, Siegel R W, eds., Kluwer Academic Publishers, Dordrecht, Nanophase Materials, NATO ASI Series E 260, 1994.

[12] Bickley R I, Gonzalez-Carreno T, Lees J S, Palmisano L, Tilley R J D, J. Solid State Chem., 1991, 92, 178.

[13] Krol R, Goossens A , J. Schoonman, J. Electrochem. Soc, 1997, 144, 1723.

[14] Moritz T, Reiss J, Diesner K, Su D, Chemseddine A, J. Phys. Chem. B, 1997, 101, 8052.

[15] Kavan L, Gratzel M, Gilbert S E, Klemenz C, Scheel H, J. Am. Chem. Soc., 1996, 118, 6716.

[16] Gopal M, Chan W J M, Jonghe L C D., J. Mater.Sci.,1997,32,6001.

[17] Encyclopedia of Chemical Technology, Mark H F, Othmer D F, Overberger C G, Seaberg G T, Eds, John Wiley, New York,1983,23,139.

[18] Weast R, C Hand book of Chemistry and Physics, CRC Press Boca Raton FL,1984,B-154

[19] Kostov, I Minerology,3rd ed,Nauka, Izkustia,Sofia,1973.

[20] Yang S W, Gao L J, Am. Ceram. Soc., 2005, 88, 968.

[21] Karakitsou K E, Verykios X E, J. Phys. Chem. 1993, 97, 1184.

[22] Addamo M, Augugliaro V, Paola D A, Lopez G E, Loddo V, Marci G, Molinari R, Palmisano L, Schiavello, M. J. Phys. Chem. B 2004, 108, 3303.

[23] Hu C, Lan Y, Hu X, Wang A, J. Phys. Chem. B 2006, 110,4066.

[24] Sakatani Y, Grosso D, Nicole L, Boissiere C, Illia S, Sanchez C, J. Mater. Chem. 2006, 16, 77.

[25] Fujishima A, Rao T N, Tryk D A, J. Photochem. Photobiol, C 2001, 1, 1.

[26] Parkin I P, Palgrave R G, J. Mater. Chem. 2005, 15, 1689.

[27] Mills A, Lee S K, J. Photochem. Photobiol. , A 2006, 182,181.

[28] Zzanderna A W, Rao C N R, Honig , J. M. Trans. Faraday Soc. 1958, 54, 1069.

[29] Yoganarasimhan S R, Rao C N R, Trans. Faraday Soc. 1962,58, 1579.

[30] Kumar S R, Pillai S C, Hareesh U S, Mukundan P, Warrier K G K, Mater. Lett., 2000, 43, 286.

[31] Reidy D J, Holmes J D, Morris M A, J. Eur. Ceram. Soc., 2006, 26, 1527.

[32] Navrotsky A, Kleppla O J, J. Am. Ceram. Soc. 1967, 50,626.

[33] Hwu Y, Yao Y D, Cheng N F, Tung C Y, Lin H M, Nanostruct. Mater. 1997, 9, 355.

[34] Gribb A A, Banfield J F, Am. Mineral., 1997, 82, 717.

[35] Sergio Valencia, Juan Miguel Marin and Gloria Restrepo, The Open Materials Science Journal, 2010, 4, 9.

[36] Anwar N S, Kassim A, Lim H L, Zakarya S A, Huang N M, Sains Malaysiana,2010, 39, 261.

[37] Wei Ning Wang I, Wuled Lenggoro , Yoshitake Terashi , Tae Oh Kim, Kikuo Okuyama, Materials Science and Engineering B,2005, 123,194.

[38] Tianyou Peng, De Zhao, Ke Dai, Wei Shi, Kazuyuki Hirao, J. Phys. Chem. B 2005, 109, 4947.

[39] Xiujuan Yang, Zhifei Dai, Atsushi Miura, Naoto Tamai,Chemical Physics Letters ,2001,334, 257.

[40] Mahshid S, Sasani Ghamsari M, Askari1 M, Afshar N, Lahuti S, Semiconductor Physics, Quantum Electronics & Optoelectronics, 2006. 9, 2, 65.

[41] Azarmidokht Hosseinnia, MansoorKeyanpour-Rad, Mohammad Pazouki, World Applied Sciences journal, 2010, 8,1327.

[42] Agnes Pottier, Corinne Chaneac, Elisabeth Tronc, Leo Mazerolles, Jean Pierre Jolivet, J. Mater. Chem., 2001, 11, 1116.

[43] Monreal H A, Chacon-Nava J G, Arce-Colunga U, Martınez C A, CasillasP G, Martınez-Villafane A, Micro & Nano Letters, 2009, 4, 4, 187.

[44] Santacesaria E, Tonello M, Storti G, Pace R C, Carra S J, J. Colloid Interface Sci,1986, 111, 44.

[45] Matijevic E, Budnick M, Meites L, J. Colloid Interface Sci,1977, 61, 302.

[46] BekkermanL I, Dobrovolskii I P, Ivakin A A, Russ.J. Inorg. Chem., 1976, 21,223.

[47] Chemseddine A, Moritz T, Eur. J. Inorg. Chem., 1999, 2, 235.

[48] Bischoff B L, Anderson M A, Chem. Mater., 1995, 7, 1772.

[49] Arnal P, Corriu J P R, Leclercq D, Mutin P H, Vioux A, J. Mater. Chem.,1996 6, 1925.

[50] Arnal P, Corriu J P R, Leclercq D, Mutin P H , Vioux A, Chem. Mater., 1997, 9, 694.

[51] Music S, Gotic M, Ivanda M, Popovic S, Turkovic A, Trojko R, Sekulie A, Furie K, Mater. Sci. Eng., B, 1997,47, 33.

[52] Bokhimi X, Morales A, Novaro O, Lopez T, Sanchez E, Gomez R, J. Mater. Res.,1995, 10, 2788.

[53] Jalava J P, Heikkila L , Hovi O, Laiho R, Hiltunen E, Hakanen A, Harma H , Ind. Eng. Chem. Res., 1998, 37, 1317.

[54] Keesmann I, Anorg Z, Allg. Chem., 1966, 346, 31.

[55] Kominami H, Kohno M, Kera Y, J. Mater. Chem., 2000, 10, 1151.

[56] Yoichi Ishibai, Takashi Nishikawa and Shigeyoshi Miyagishi, Journal of dispersion science and Technology, 2006, 27, 1093.

.....ꕥ....

POLYPROPYLENE/TITANIUM DIOXIDE NANOCOMPOSITES

Contents

PP/TiO_2 composites were prepared using 0-5wt% of NTO through melt mixing. It was then made in to films by compression moulding process. PP composites with CTO was also prepared under the same conditions. Mechanical, dynamic mechanical, morphology and thermal properties of the composites and neat PP were studied. Transparency of the films were decreased by the addition of TiO_2. However, NTO filled PP composites showed better transparency compared to PP/CTO composites. Melt flow index (MFI) of PP was increased at low concentration of NTO while for CTO filled composites showed a decrease in MFI compared to neat PP. DSC studies showed an increase in crystallinity by the addition of TiO_2. XRD indicated monoclinic crystal form of PP in neat PP and composites. TGA revealed increased thermal stability of PP by the addition of TiO_2. LOI was increased by the addition of nanoparticles. SEM images of the fractured surface of nano composites showed uniform dispersion of the TiO_2 in the nanocomposites. Mechanical, morphological and IR studies were carried out after thermal and UV ageing. NTO filled PP showed better properties compared to that of CTO filled PP composites.

6.1 Introduction

In recent years, materials with sizes 1-50 nm have attracted a great attention because of their versatile applications in polymer/inorganic nanocomposites, optoelectronic devices, biomedical materials etc [1–6]. Polymer nanocomposites prepared by melt mixing have been reported to show enhanced properties compared to neat polymers [7]. Polymer nanocomposites have attracted great attention because of their significant enhancement in mechanical strength and thermal properties at low filler contents [8-15]. This improvement is due to the unique characteristics of the nanofillers [16]. There is a growing trend in using nanoparticles of conventional inorganic fillers in plastic composites. Two major findings in the field of polymer nanocomposites began the investigations of these materials. First, Toyoto researchers observed nylon nanocomposites, for which moderate inorganic loadings resulted in significant improvements of the thermal and mechanical properties. Second, Grannelis reported the possibility of melt mixing polymers and clays without organic solvents. Since then, the high promise of industrial applications of nanocomposites have motivated vigorous research, which has showed remarkable enhancements of properties of the nanocomposites. There are some investigations has been done to improve the properties of polymers by the addition of inorganic nanofillers such as SiO_2 [17], ZnO [18] and $CaCO_3$ [19]. Recently, nanocomposites based on PP constitute a major challenge for industry since they enhance the mechanical and physical properties of PP [20-22]. PP is one of the most widely used thermoplastic due to its good physical and mechanical properties as well as the ease of processing at a relatively low cost. The commercial PP has a wide range of applications in automobiles, textiles, furniture, electrical equipment and packaging industry [23]. Extensive investigations have been conducted to broaden the application of PP by improving properties like strength, impact resistance

and thermal stability [24–54]. PP melts are more viscoelastic than other thermoplastic melts like polyamide and polyester. There is a number of studies on the PP nanocomposites filled with different types of fillers such as carbon nanotubes [55-57], nanoclay [58-60], talc, mica and fibrous fillers like glass, jute, aramid, carbon fibers etc. Reinforcement at nanoscale to enhance properties of polymer including changes in the polymer crystallization behaviour is being investigated [61]. The improved properties may be due to the synergistic effects of nanoscale structure and interaction of fillers with polymers. The size and nanostructure of the dispersed phase markedly influence the properties of polymer nanocomposites [62-65]. To obtain nanocomposites with enhanced performance, nanoparticles are to obtain a fine dispersion of the nano powders in the polymer to promote a strong interface adhesion between matrix and nanofillers. There are some reports on the use of nanoparticles of various geometric shapes, including nano–TiO_2, tubes and silica platelets [66-68]. TiO_2 has been used as white colour pigment due to its high refraction index, chemical stability and nontoxicity. One of the most interesting properties of TiO_2 based cosmetics is UV-ray absorption and UV-ray scattering. Since the extent of light scattering depends on the relationship between the particle size and the wave length of light, decrease in TiO_2 particle diameter achieves high transparency in visible light, while UV-ray absorptivity increases with the extension of the geometric area occupied by TiO_2 [69].

We reported various properties of PP/TiO_2 nanocomposites prepared by melt mixing method in this chapter. PP/TiO_2 composites with 0-5 wt% of TiO_2 (both CTO and NTO) were prepared. Mechanical properties, dynamic mechanical properties, thermal properties, melt flow index, transparency, limiting oxygen index, crystallization, morphology and x-ray diffraction studies of the composites were investigated. Mechanical, morphological and

IR studies were carried out after UV and thermal ageing. Experimental details are same as in chapter 3, section 3.2.

6.2 Results and Discussion

6.2.1 Mechanical properties of PP/ TiO_2 composites

Tensile strength of the PP/NTO composites and PP/CTO composites are shown in figure 6.1. Tensile strength of the composites increases with increase the concentration of TiO_2, reaches a maximum at a concentration of 1wt% of TiO_2. NTO filled PP shows higher tensile strength compared to CTO filled composites. Tensile strength of PP is increased by 26% by the addition of 1wt% NTO and 22.6% by the addition of CTO.

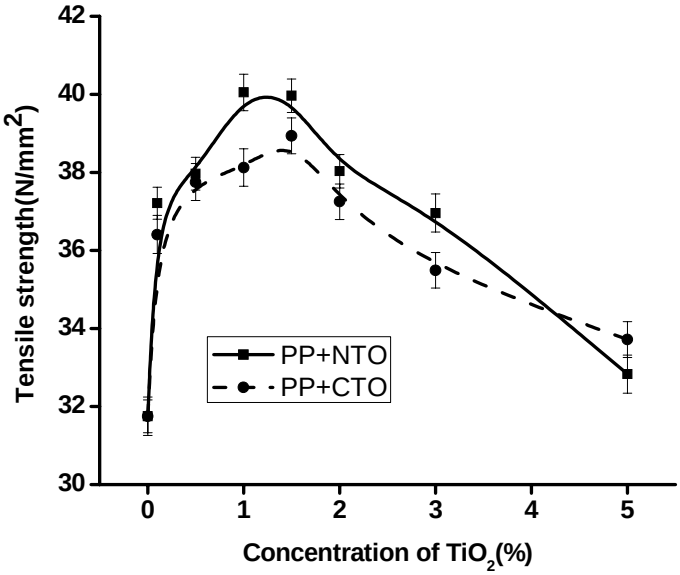

Figure 6.1: Effect of TiO_2 on tensile strength of PP/ TiO_2 composites

The interface between nanoparticles and a polymer matrix can transfer stress, which is beneficial for the enhancement of the tensile strength of composite films. However, on increasing the concentration of nanoparticles, aggregation occurs, which leads to a decrease in the interaction between

particles and polymer resulting in defects in the composites. Therefore, the effective interfacial interaction is decreased and tensile strength of the films also reduced [70].

Tensile modulus of the neat PP and its composites with TiO_2 is shown in figure 6.2. Modulus of PP increases with increasing concentration of TiO_2, reaches a maximum at 1wt% of TiO_2. NTO filled composites show higher modulus compared to CTO filled composites. An increase of 23% in modulus is observed by the addition of 1 wt% NTO and 19.8% by 1wt% CTO. The improvement in modulus of PP/TiO_2 composites is related to increased stiffness, quality of the dispersion of TiO_2 and also to the adhesion between the matrix and TiO_2.

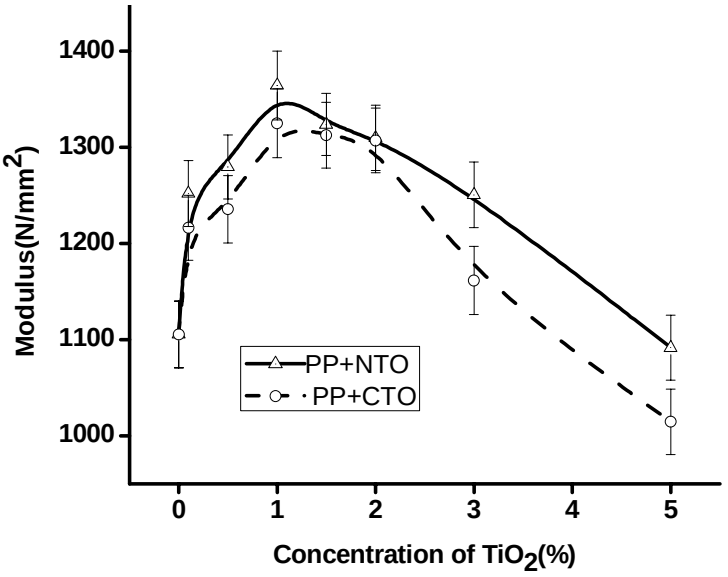

Figure 6.2: Effect of TiO_2 on modulus of PP/ TiO_2 composites

Elongation at break of the composites and neat PP are shown in figure 6.3. Elongation at break decreases with increasing concentration of TiO_2. After 1 wt %, elongation at break of PP is increased. Decrease in elongation at break may be due to the increase in stiffness of the composites.

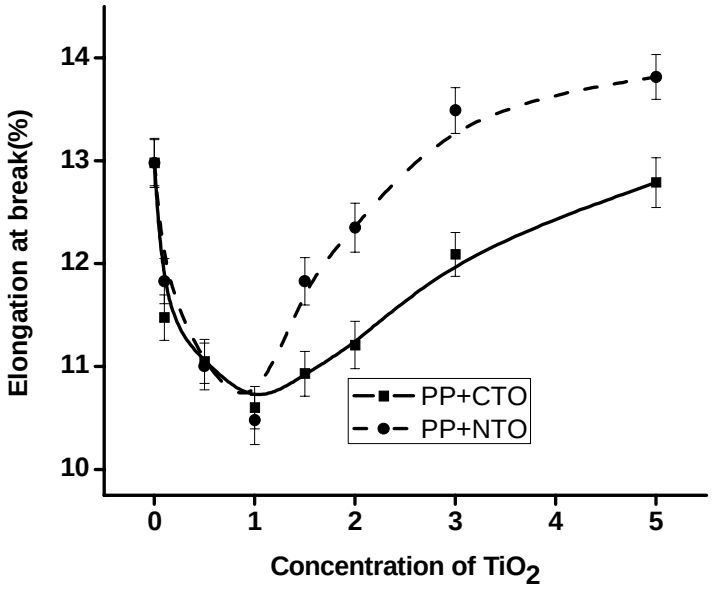

Figure 6.3: Effect of TiO_2 on elongation at break of PP/ TiO_2 composites

6.2.2 Dynamic mechanical analysis

The storage modulus of neat PP and PP/TiO_2 composites as a function of temperature at 1Hz are shown in figure 6.4.

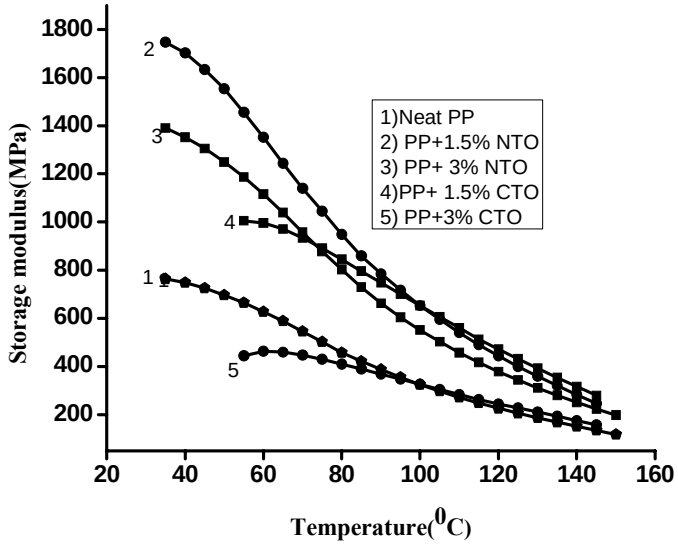

Figure 6.4: Effect of TiO_2 on storage modulus of PP/ TiO_2 composites

Storage modulus of the PP is increased with the addition of TiO_2.This increase is significant at low temperature. The storage modulus of PP increased with increase in TiO_2 concentration due to the stiffening effects of TiO_2, indicating efficient stress transfer between the polymer matrix and TiO_2.

The loss modulus of PP and composites are given in figure 6.5. Loss modulus also increases substantially with TiO_2 concentration. The reinforcing effect of TiO_2 may be due to their specific interactions and the formation of a rigid percolating TiO_2 network within the polymer matrix. Maximum improvement is shown by PP with 1.5 wt% NTO. Composites of PP with NTO show significant improvement compared to PP with CTO.

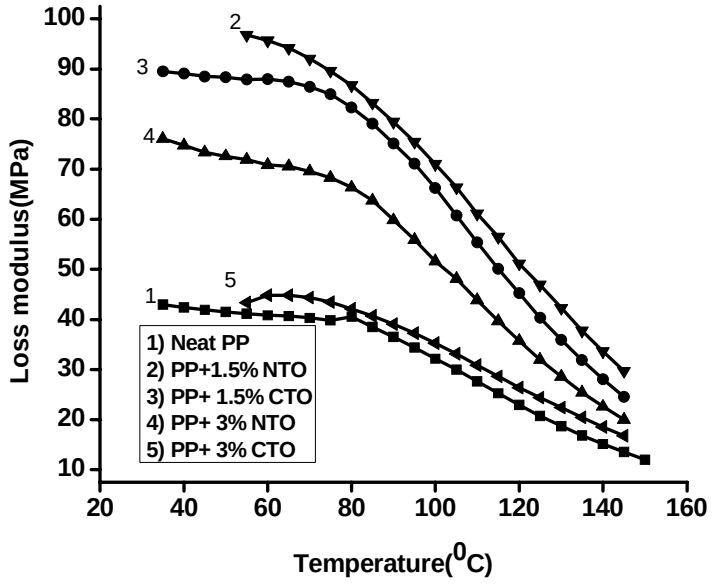

Figure 6.5: Effect of TiO_2 on loss modulus of PP/ TiO_2 composites

The tanδ curves of PP and composites are shown in figure 6.6. It is evident from the figure that there is an increase in tanδ value on addition of TiO_2. This indicates an increase in damping property. It is obtained in many cases that the

improvement of stiffness significantly decreases the ductility. But PP/TiO_2 composites showed increased stiffness without reducing ductility.

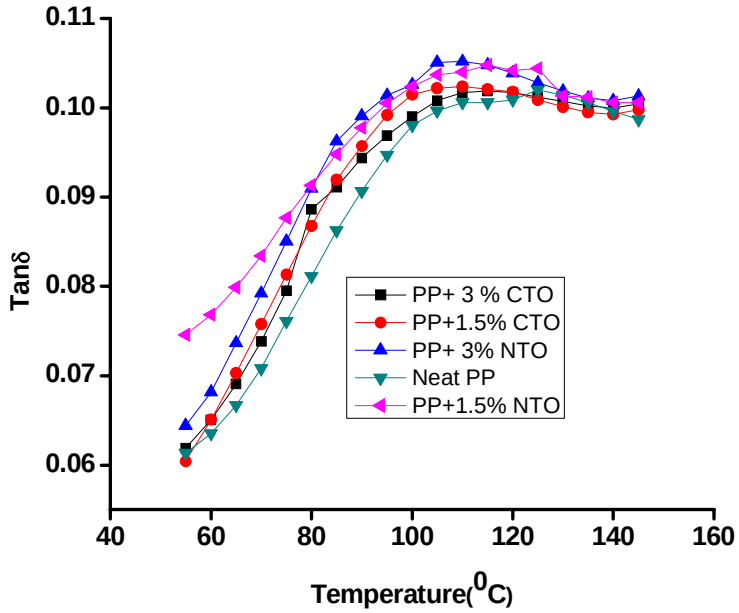

Figure 6.6: Effect of TiO_2 on tanδ of PP/ TiO_2 composites

6.2.3 Torque studies

Figure 6.7 represents the variation of torque with mixing time for the neat PP and PP/NTO composites and PP/CTO composites. Torque is increased rapidly during initial mixing and then dropped to stabilized on increasing the mixing time. This indicates good level of filler dispersion at the specified conditions. Also the torque value of the PP/NTO composites was higher than that of neat PP and PP/CTO composites. This also points towards interfacial interaction between the nanoparticles and polymer [70].

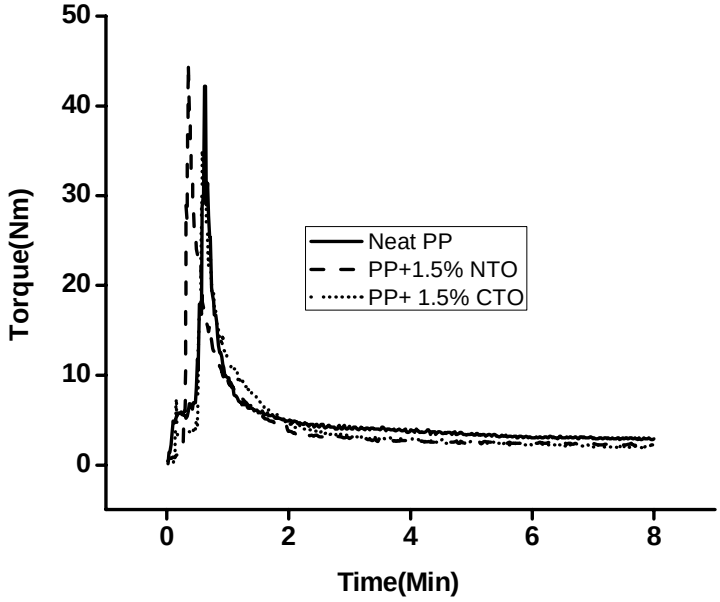

Figure 6.7: Variation of torque with time during mixing

6.2.4 Morphology of the fractured surface

Mechanical properties of a composite depends on the dispersion of filler in the composites [71]. Figures 6.8a, 6.8b, 6.8c, 6.8d, 6.8e, 6.8f and 6.8g show SEM images of tensile fractured surfaces of neat PP, PP/CTO and PP/NTO composites. From SEM images it is clear that the TiO_2 particles are well dispersed in the PP matrix. F.G. Ramos Filho et al. reported the similar fractured surface of PP/modified bentonite nanocomposites. They also observed good dispersion of modified bentonite in PP [72]. NTO particles are more dispersed when compared to CTO particles. At higher concentration of TiO_2, large particles are observed due to the agglomeration of TiO_2.

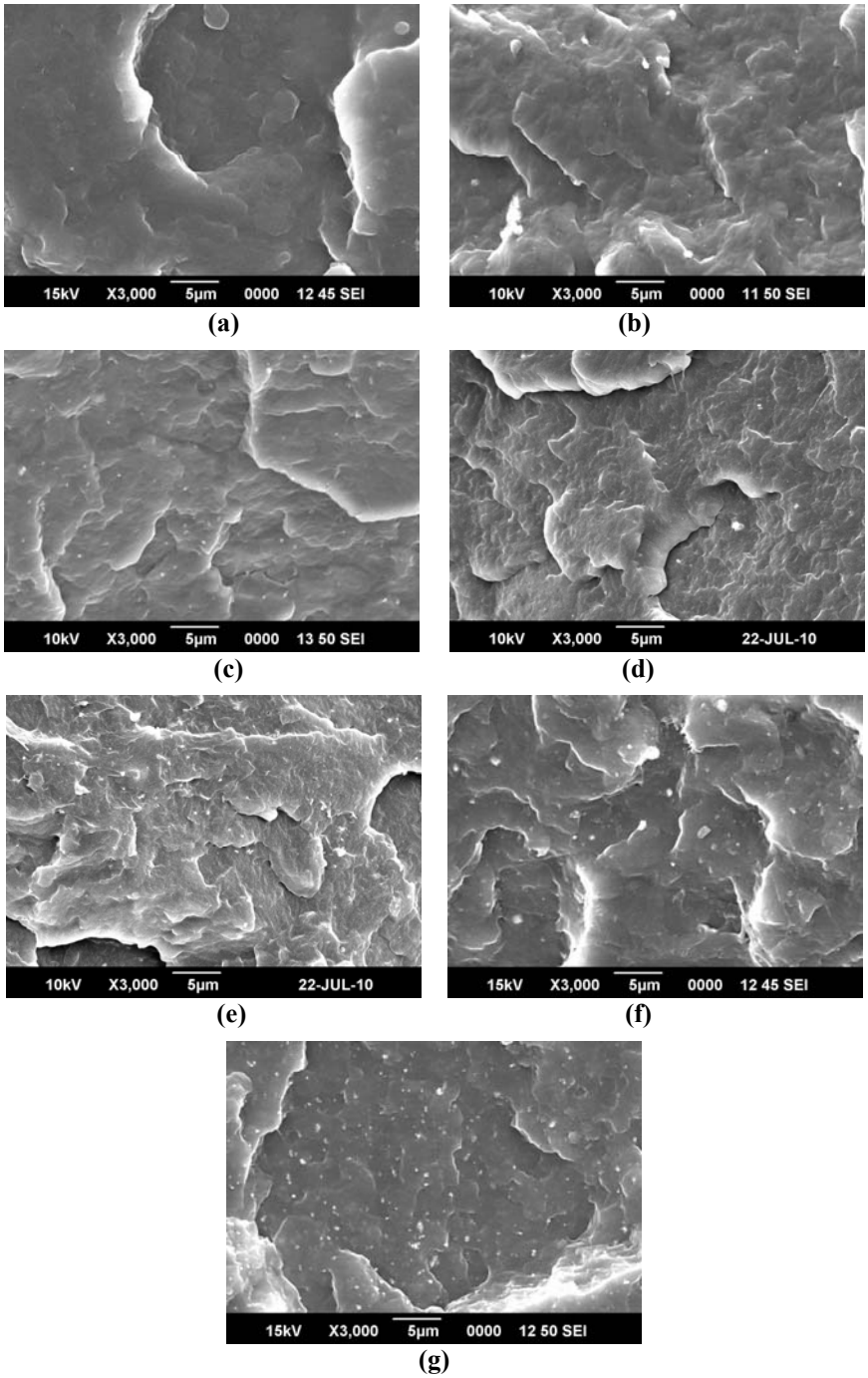

Figure 6.8: SEM images of fractured surface of a) neat PP b) PP+1.5wt% NTO c) PP+1.5wt% CTO d) PP+2wt% NTO e) PP+2wt% CTO f) PP+5wt% NTO g) PP+5wt% CTO filled composites

6.2.5 Energy dispersive atomic X-ray spectrum (EDAX)

EDAX is used for understanding the chemical composition of a material. EDAX shows the presence of TiO_2 in the PP matrix. The EDAX of neat PP and PP/TiO_2 composites are shown in the figures 6.9a, 6.9b and 6.9c respectively.

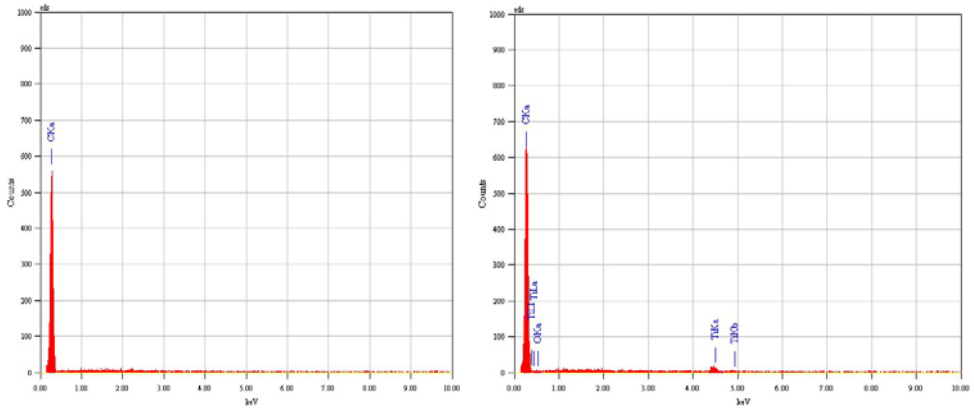

(a) **(b)**

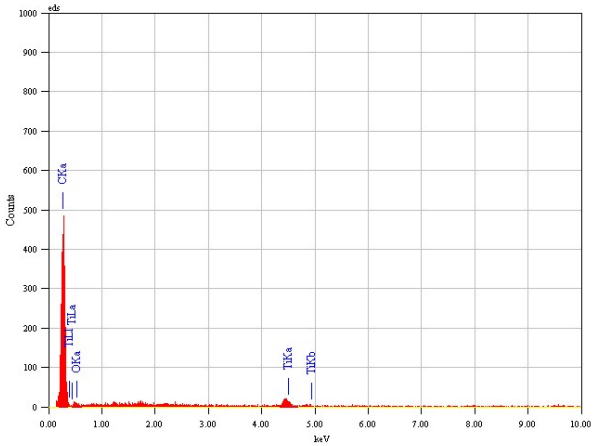

(c)

Figure 6.9: EDAX of a) neat PP b) PP+5wt%NTO c) PP+5wt%CTO composites

6.2.6 X-ray diffraction analysis of Composites

XRD is the most commonly used technique to evaluate the degree of dispersions of nanoparticles in a polymer. XRD studies also provide opportunity to evaluate the crystalline structure, the extent of crystallization and also crystalline orientation. Figure 6.10 shows the XRD of the composites and neat PP. Sharp peaks indicate the crystalline nature of PP. X-ray diffraction pattern of nanocomposites show sharp and highly intense peaks compared to that of neat PP. This is due to the development of crystallinity in the polymer. The peaks obtained are corresponding to the planes (110), (040), (130) represents α– form of monoclinic isotactic PP.

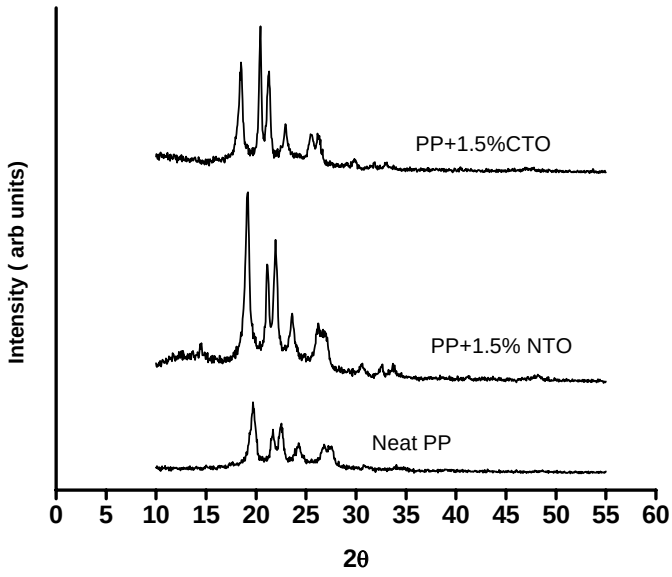

Figure 6.10: X-ray diffraction pattern of neat PP and TiO_2 filled composites

6.2.7 Thermogravimetric analysis

Degradation behaviour of the composites and neat PP was studied using TGA is shown graphically in the figure 6.11 and the data is tabulated in Table 6.1. As shown in figure 6.11 and table 6.1, TiO_2 filled composites show enhanced thermal stability. Thermal stability of PP is increased more

significantly by the addition of NTO compared to CTO filled PP. The onset of degradation is increased by 29.8^{0}C at 1.5wt% of NTO filled PP. The increased endset of degradation also points to the improved thermal stability of the composites. The rate of degradation decreased by 13.42% upon 1.5 wt% of NTO particles. The temperature at which maximum degradation take place is increased by 5.3^{0}C at 1.5 wt% of NTO particles. Enhancement in thermal stability of polymers in presence of fillers is due to the hindered thermal motion of polymer molecular chains [73]. An increase in onset of degradation and maximum decomposition temperature is reported for PP by the addition of intumenescent flame retardant [74]. It is reported that the addition of organoclay to a polymer matrix is expected to slow down the release rate of decomposed products within the nanocomposites, thus increasing the thermal stability [75]. Shahryar Jafari Nejad et al reported an increase in thermal stability of PP with modified bentonite clay. They observed an increase in onset temperature by 22^{0}C at 3 wt% clay loading [76]. An increase in thermal stability of PP/TiO_2 nanocomposite fibers is observed by Hassan M. et al [77].

Table 6.1: Effect of TiO_2 particle size on thermal stability of PP/ TiO_2 composites

Concentration of TiO_2 (%)	Temperature at which maximum degradation take place (^{o}C)		Residue (%)		Degradation rate (%)		Onset of degradation (^{o}C)		Endest of degradation (^{o}C)	
	NTO	CTO	NTO	CTO	NTO	CTO	NTO	CTO	NTO	CTO
0	471.6	471.6	1.3	1.3	56.3	56.3	391.0	391.0	496.9	496.9
0.5	474.1	472.3	1.4	1.4	52.0	54.6	419.4	415.4	498.6	497.1
1.5	476.9	476.9	2.1	2.0	49.3	52.4	420.9	417.3	503.8	500.3
3	476.6	474.1	3.4	3.3	50.2	51.8	416.4	416.1	500.3	499.2

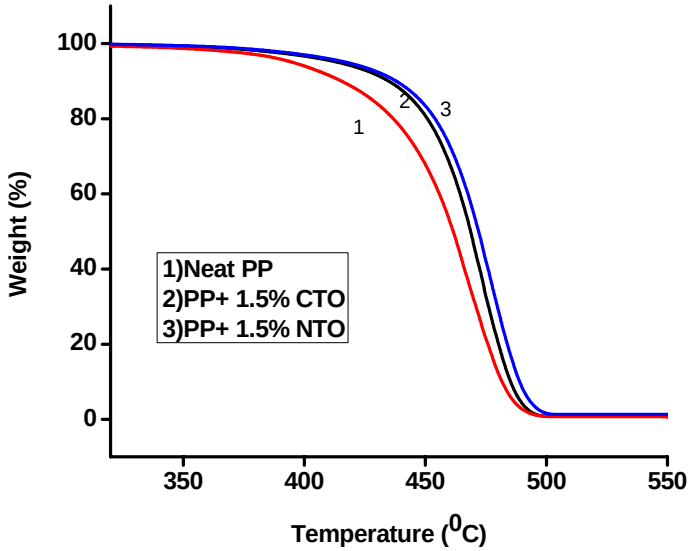

Figure 6.11: Thermogram of PP and PP/ TiO_2 composites

6.2.8 Kinetic analysis of thermal decomposition

Kinetics of degradation behaviour of PP and PP/TiO_2 composites were studied using Coats–Redfern method [78]. Thermal degradation functions used for the Coats–Redfern method were listed in Table 3.3 and detailed description is given in section 3.3.8.

Table 6.2: Apparent activation energy (E) and correlation coefficients(R) for neat PP and PP/ TiO_2 composites by Coats–Redfern method.

Sample name	R	E (kJ/mol)
Neat PP	0.999	126.52
PP+0.5% NTO	0.999	140.69
PP+1.5% NTO	0.999	158.64
PP+3% NTO	0.999	137.25

From the table 6.2 it is clear that the activation energy of PP fiber is increased by the addition of NTO. Activation energy (E) obtained for neat PP is 126.5 kJ/mol, 1.5% NTO added PP is 158.6 kJ/mol. Significant increase in activation energy indicates high thermal stability. Representative plot of

Coats–Redfern equation for neat PP, PP/0.5wt% NTO, PP/1.5wt% NTO nanocomposite and PP/3wt% NTO nanocomposite are shown in figures 6.12a, 6.12.b, 6.12.c and 6.12d respectively.

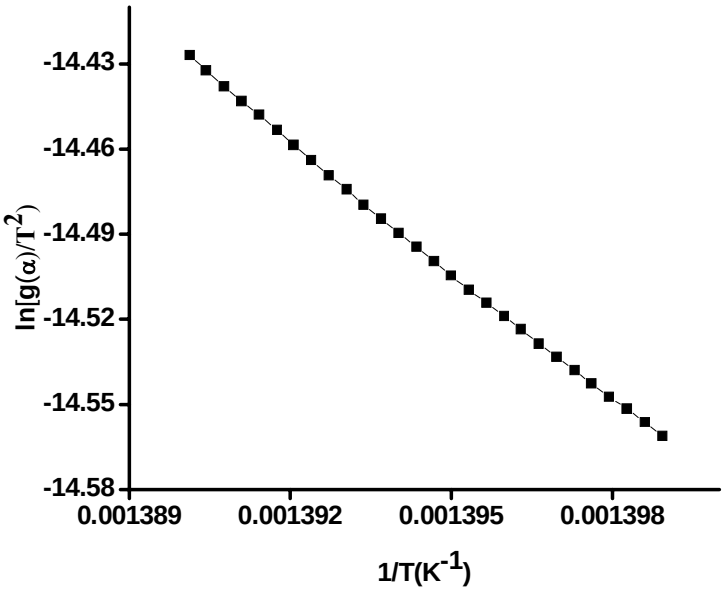

Figure 6.12a: Representative plot of Coats–Redfern equation for neat PP

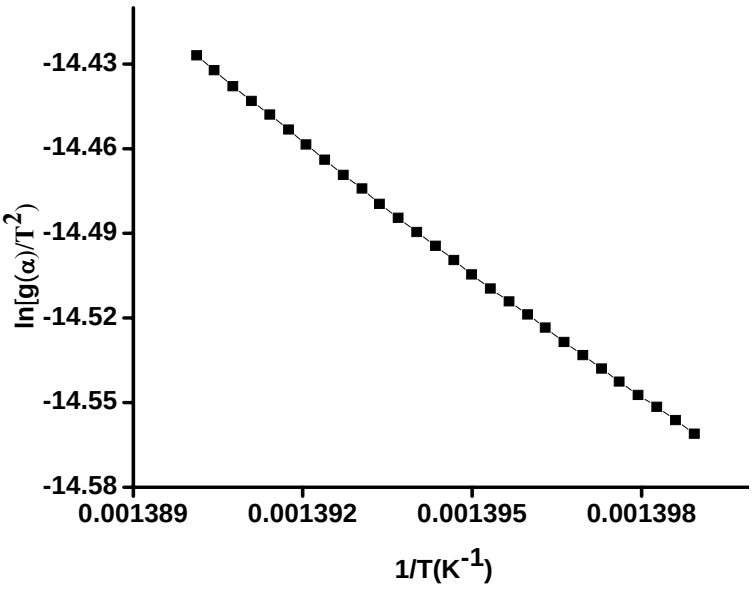

Figure 6.12b: Representative plot of Coats–Redfern equation for PP+0.5% NTO

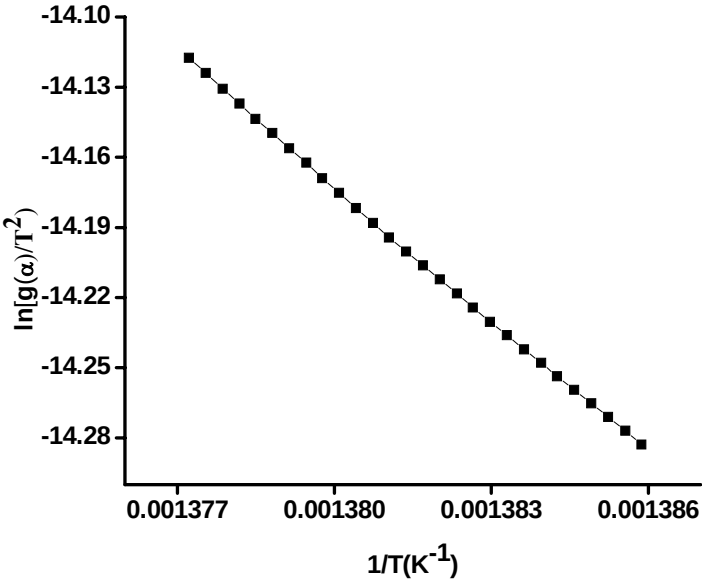

Figure 6.12.c: Representative plot of Coats–Redfern equation for PP+1.5% NTO

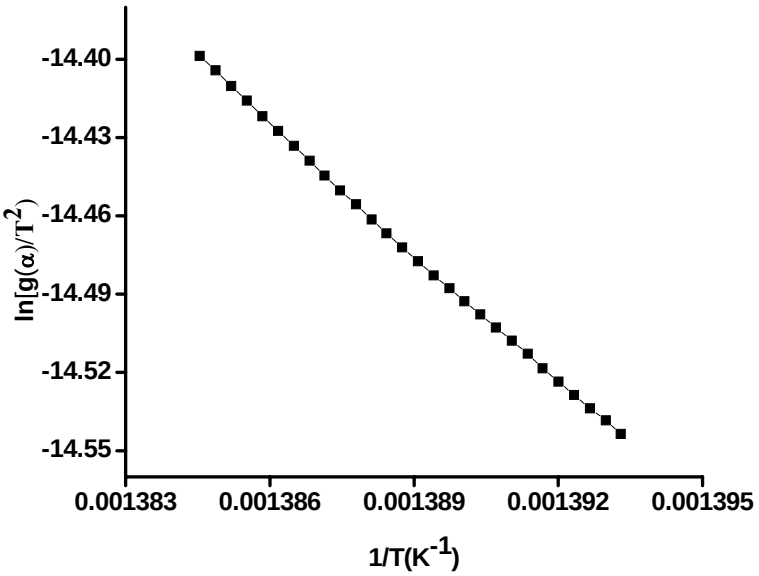

Figure 6.12.d: Representative plot of Coats–Redfern equation for PP+3% NTO

6.2.9 Differential Scanning Calorimetry

Properties of a semicrystalline polymer are related to degree of crystallization and crystallite size [79]. Nucleating agents that have been reported in the literature include metal oxides and hydrides, residual catalysts and diamide segments [80-82]. Several researchers reported the use of nanoparticles, such as organically modified nanoclays and nanotubes as crystallization promoters for different polymers [83-86].

DSC crystallization exotherms of neat PP and composites are shown in figure 6.13. From DSC crystallization exotherms, Tc (the temperature at the crossing point of the tangents of the baseline and the high-temperature side of the exotherm), Tcp (the peak temperature of the exotherm) and ΔH_c (enthalpy of crystallization) can be obtained is shown in table 6.3. Percentage crystallinity (Xc) was calculated using the Equation 3.1. It shows an increase in crystallinity by the addition of TiO_2. The Tc – Tcp values of the composites were smaller than that of neat PP, indicating that addition of TiO_2 increased the crystal growth rate (CGR) of PP.

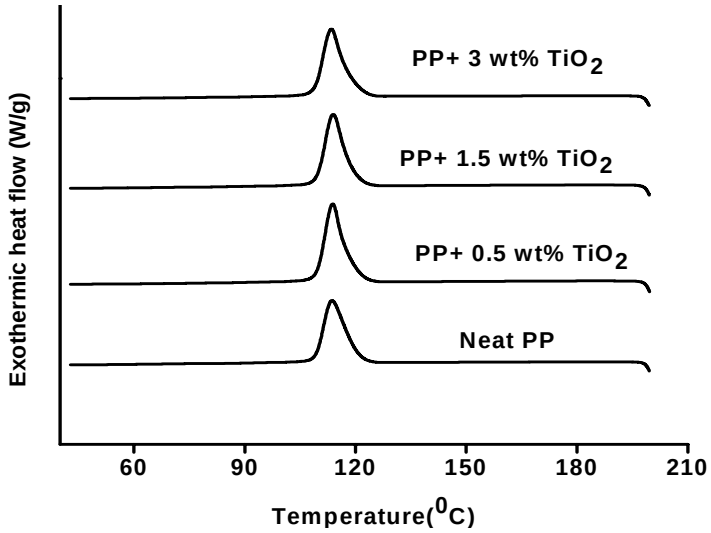

Figure 6.13: Cooling behaviour of neat PP and PP/ TiO_2 composites

Table 6.3: Effect of TiO_2 on the crystallization behaviour of PP

Sample name	Tc(^{0}C)	Tcp(^{0}C)	ΔH_c(J/g)	Xc(%)	Tc-Tcp
Neat PP	120.60	113.64	81.65	39.4	6.96
PP+0.5%NTO	118.5	113.84	98.3	47.5	4.66
PP+1.5%NTO	118.93	113.95	91.28	44.6	4.98
PP+3%NTO	119.25	113.46	92.0	45.5	5.79

Melting behaviour obtained from DSC is shown in figure 6.14 and values are tabulated in table 6.4. From the figure, Tm (designed here as the temperature at the crossing point of the tangents of the baseline of the melting peak), Tmp (the peak temperature of the curve), and ΔHm (heat of fusion) can be obtained. The maximum rate of melting (Tmp) occurred at 163.8^{0}C for pure PP and its Tm is 154.3^{0}C. The Tm value of PP with 3 wt% NTO is increased by about 1.7^{0}C compared with neat PP.

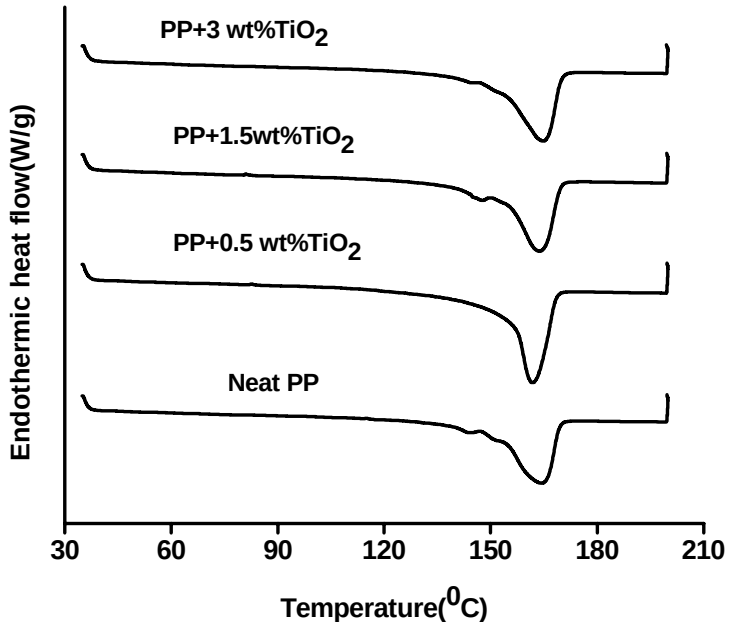

Figure 6.14: Melting behaviour of neat PP and PP/ TiO_2 composites

Table 6.4: Effect of TiO_2 on the melting behaviour of PP

Sample name	Tm(^{0}C)	Tmp(^{0}C)	ΔHm(J/g)
Neat PP	154.37	164.77	48.61
PP+0.5% NTO	156.5	161.95	64.32
PP+1.5% NTO	154.81	164.07	55.46
PP+3% NTO	152.65	164.92	64.89

6.2.10 Melt flow index

Figures 6.15a and 6.15b show the effect of TiO_2 on the MFI of PP at 5kg and 2.16kg respectively. MFI of PP is decreased by the addition of CTO indicate a decrease in flow of the polymers. In nanocomposites, MFI is increased by the addition of low concentration of NTO indicate an increase in the flow of the polymers. A low content of nanoparticles may provide flow favouring orientation due to the small size of NTO as depicted in figure 6.16. An increase in MFI is reported on addition of multi walled carbon nanotube to PP [87]. After adding 1wt% NTO to the PP the MFI value decreases gradually, indicates the structure of nanoparticles was interconnected to hinder the molecular motion of polymer chains [88].

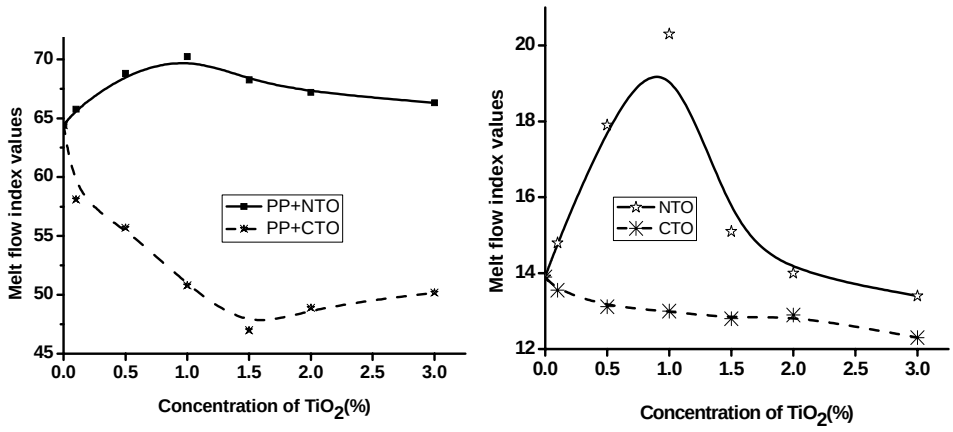

Figure 6.15: Effect of TiO_2 particle size on the melt flow index of PP using (a) 2.16kg and (b) 5 kg weight

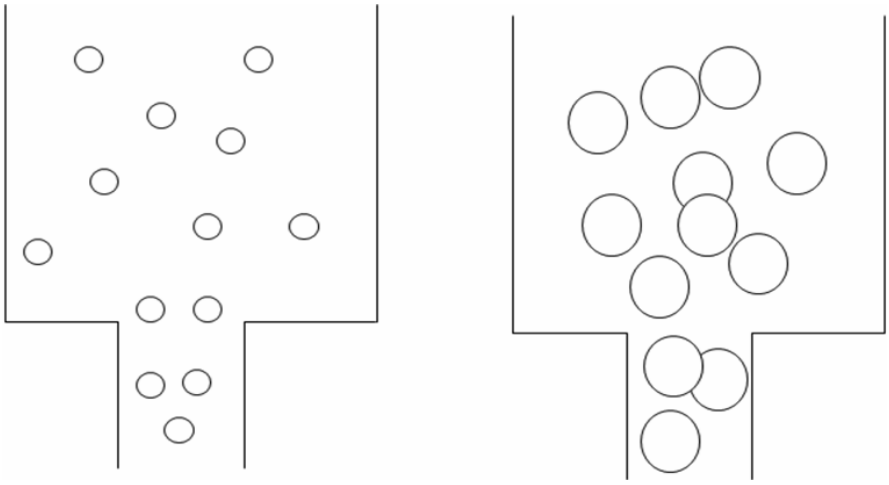

(a) (b)

Figure 6.16: Schematic representation of flow behaviour of (a) PP+NTO (b) PP+CTO composites

6.2.11 Transparency of the films

The percentage transmittance of neat PP and the composites is given in figure 6.17. Transmittance of the film is decreased by the addition of TiO_2. NTO filled PP films show higher transparency when compared to CTO filled PP films. The photographs showing the transparency of the films are given in figure 6.18. From photographs it is evident that the composites based on NTO are much clearer than those containing CTO. This may be due to decrease in spherulite size of PP and also due to smaller TiO_2 particles in the composites.

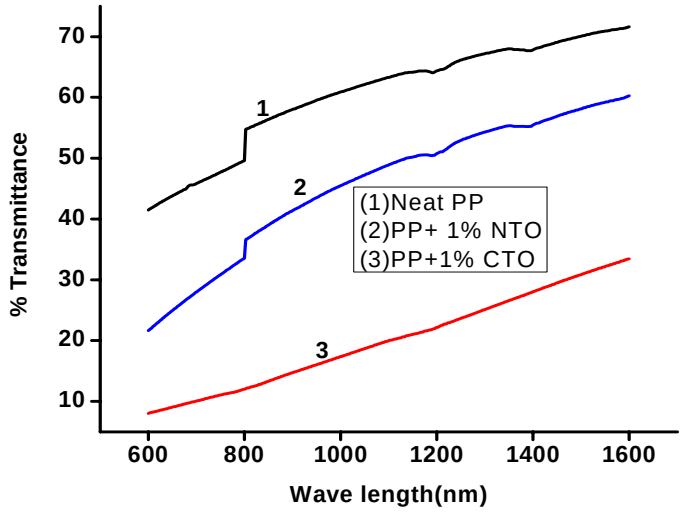

Figure 6.17: Visible-IR transmittance of neat PP and PP/ TiO_2 composites

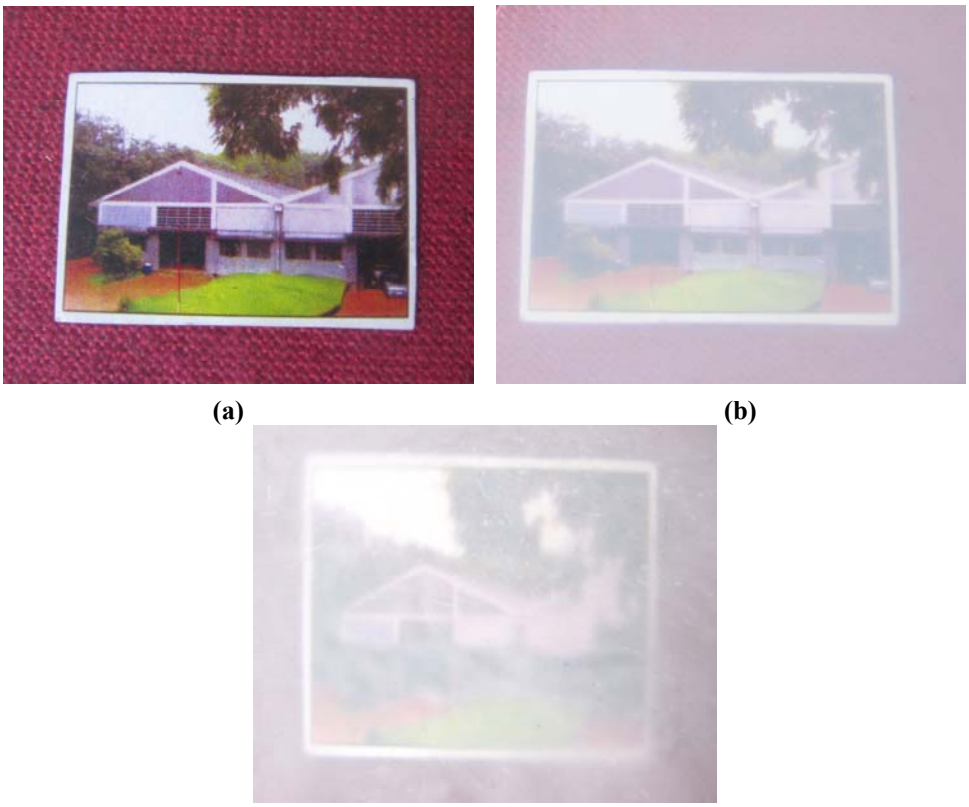

(a) **(b)**

(c)

Figure 6.18: Photographs of a) neat PP b) PP+1wt%NTO c) PP+1wt%CTO films

6.2.12 Limiting oxygen index

Use of nanoparticles in polymers for fire retardant applications help to avoid toxicity of the degradation products compared with the more traditional additives like halogenated compounds and allows the production of light weight products. Figure 6.19 represents the LOI of the neat PP and its composites with NTO. Neat PP shows 18% and the composites show 19% LOI. The improvement in the flame retardancy may be due to the good filler dispersion in the PP matrix because of the addition of TiO_2 [89].

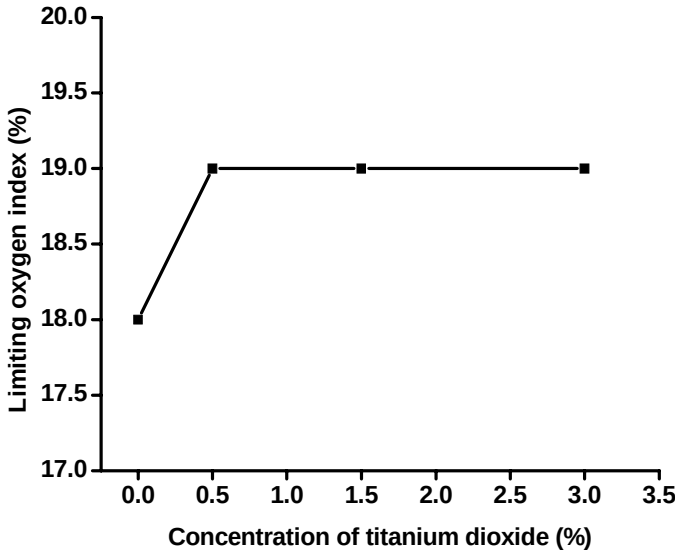

Figure 6.19: Effect of TiO_2 on the limiting oxygen index of PP/ TiO_2 composites

6.2.13 Thermal and Photo Ageing

Degradation of polymeric materials is a commonly encountered problem that causes changes in their chemical, physical and mechanical properties. There are many factors causing polymer degradation: solar light, other high energy radiations, heating, chemicals attack, stress loading, water loading, biological sources etc. Among these factors, ultraviolet radiation and light is the common factors that cause degradation of polymers under outdoor

environments. The degradation mechanism of PP under light and temperature is given in figure 3.19. In this section, mechanical, morphology and IR studies of the neat PP and composites after thermal and UV ageing were discussed.

6.2.13.1 Thermal ageing

6.2.13.1.1 Mechanical properties of PP/TiO_2 nanocomposites

The mechanical properties of the nanocomposites, such as tensile strength and modulus after 24 hrs of thermal ageing have been evaluated and the results are shown in figures 6.20 and 6.21. Mechanical properties of the composites showed higher value compared to neat PP even after thermal ageing. More degradation was observed in the case of composite prepared with CTO and neat PP. This evidences that reduction in particle size of TiO_2 increases the ageing resistance of the composites. Thermal ageing when conducted in an air oven, the degradation takeplace in presence of oxygen, which is the main factor responsible for degradation of PP in the thermal environment [90]. In polymer, there will be a depth profile of degradation, with higher rate of oxidation near the surface, due to the lack of oxygen in the sample interior. Thus, diffusion of oxygen plays a major role in determining the extent of chemical degradation [91, 92]. In nanocomposites, oxygen molecules are concentrated more on the fillers, decreasing the diffusion path through the PP. It helps to resist the degradation of polymer molecules.

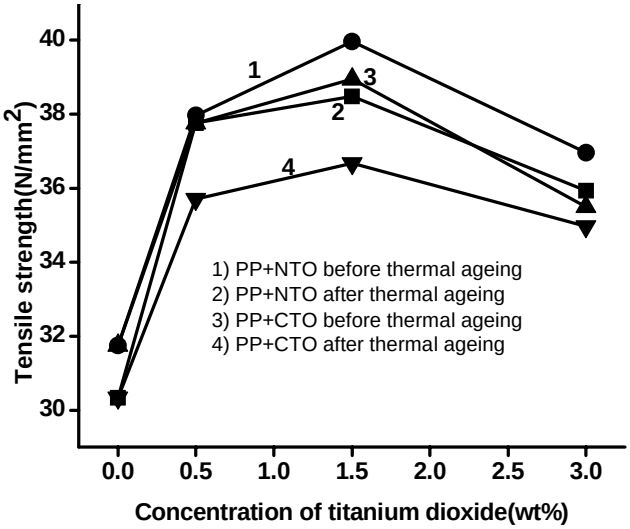

Figure 6.20: Effect of thermal ageing on tensile strength of PP/TiO_2 composites

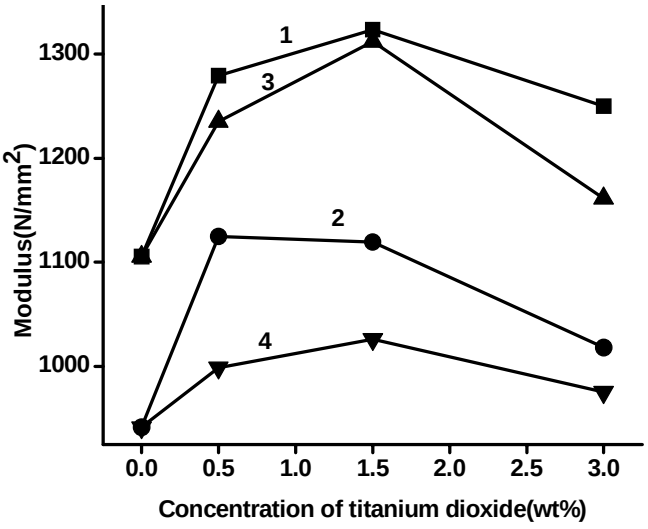

Figure 6.21: Effect of thermal ageing on tensile modulus of PP/TiO_2 composites

6.2.13.1.2. IR studies

Degradation products of neat PP and its composites with NTO after thermal ageing are studied by IR spectroscopy. IR spectrum of neat PP, PP with 0.5 wt% NTO, 1.5 wt% NTO and 3 wt% NTO are shown in figure 6.22.

The degradation of PP results in the formation of hydroperoxides and carbonyl species like ketones, esters and acids. These products give absorption peaks in the wave number range 3200-3600 and 1600-1800 cm^{-1} [93]. IR spectrum of neat PP, PP with 0.5 wt% NTO, 1.5 wt% NTO shows a peak in the range of 3200-3600 cm^{-1} indicating the formation of hydroperoxides. The intensity of this peak is less in case of PP composites with 3wt% NTO. The IR peak in the range 1600-1800 cm^{-1} corresponds to carbonyl group, the intensity of which decreases with increasing NTO concentration, which supports the fact that incorporation of nano TiO_2 reduces thermal degradation of PP. The characteristic peaks for PP in the wave number range of 2800-3000 cm^{-1}, are related to the asymmetric and symmetric C-H stretching vibration. The intensity of this peak increases with increase in the NTO concentration. This indicates an increase in thermal stability of PP in presence of NTO.

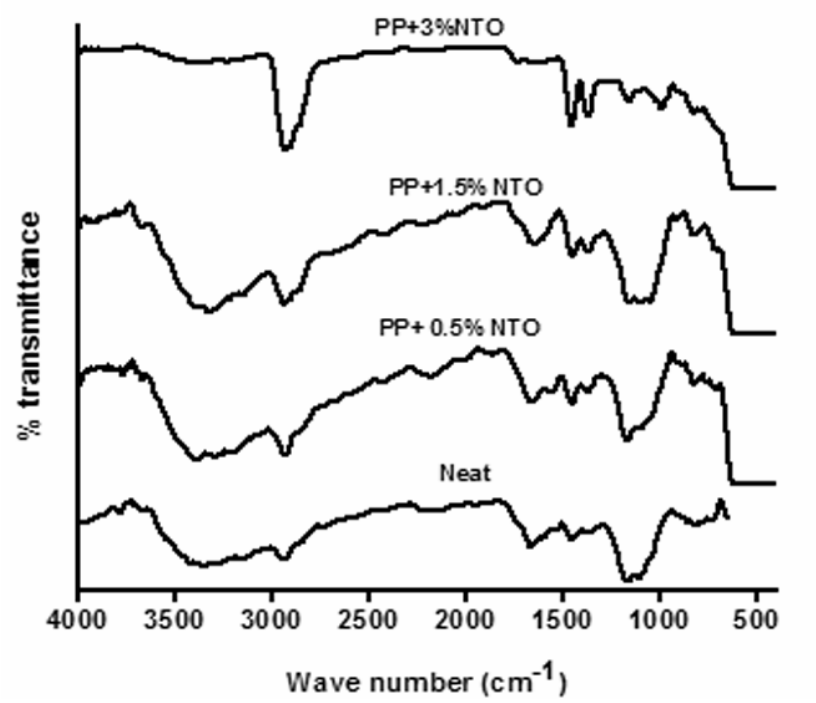

Figure 6.22: IR spectrum of PP/NTO composites after thermal ageing

6.2.13.1.3 Morphology of the tensile fractured surface

The SEM images of the fractured surface of the neat PP, 1.5 wt% of NTO and 1.5 wt% of CTO filled PP after thermal ageing is shown in the figures 6.23a, 6.23b and 6.23c. A well dispersed filler matrix system is observed after ageing.

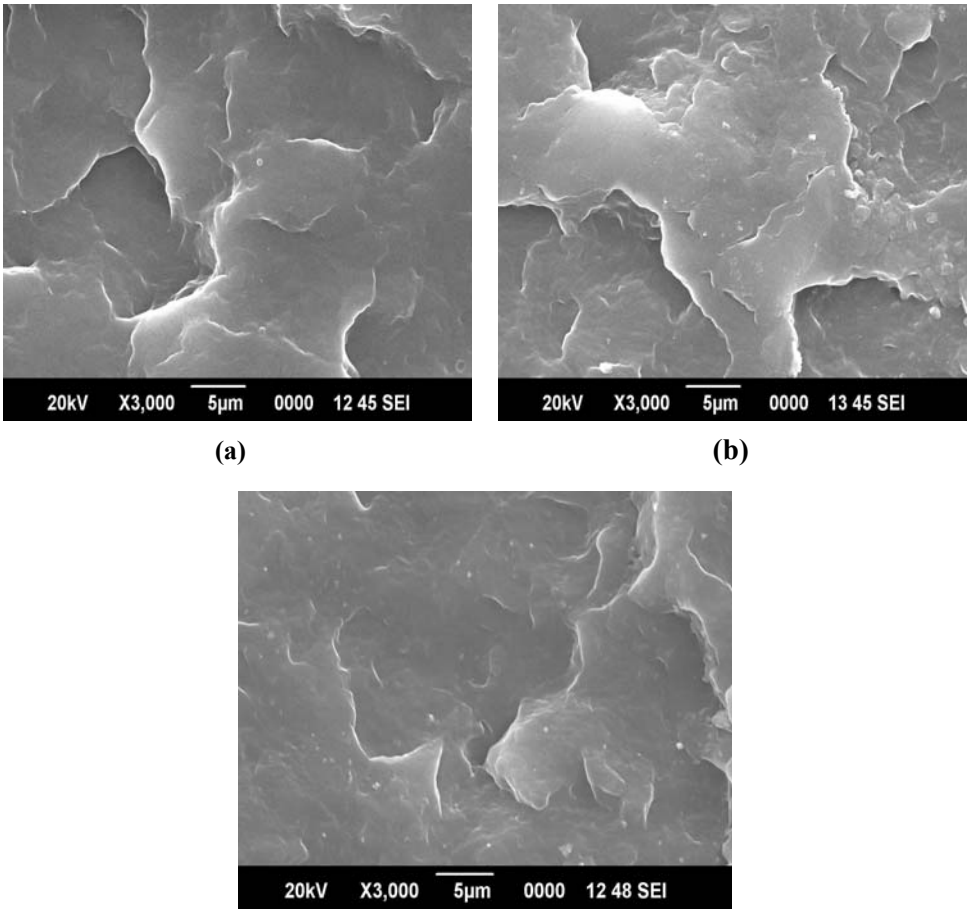

(a) **(b)**

(c)

Figure 6.23: Scanning electron micrographs of (a) neat PP (b) PP+1.5wt%NTO and (c) PP+1.5wt% CTO filled composites after thermal ageing.

6.2.13.2 UV ageing

6.2.13.2.1 Mechanical properties

The mechanical properties of the neat PP and composites, such as tensile strength and modulus before and after 48 hours of UV irradiation are represented in figure 6.24 and 6.25. After UV irradiation, tensile strength and modulus of neat PP and composites decreased. Properties of NTO filled PP after UV irradiation are higher than that of CTO filled PP composites and neat PP. Based on the tensile results, it can be summarized that the presence of TiO_2 particles can act as effective UV screen to resist photodegradation for PP. Hongxia Zhao et al has been observed the stability of PP/ZnO composites after UV irradiation under UV light [93].

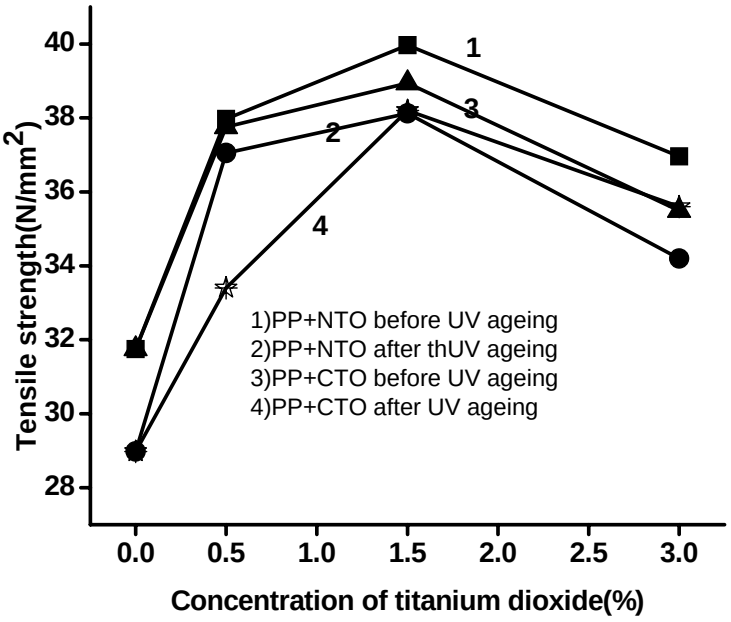

Figure 6.24: Effect of photo ageing on tensile strength of PP/TiO_2 composites.

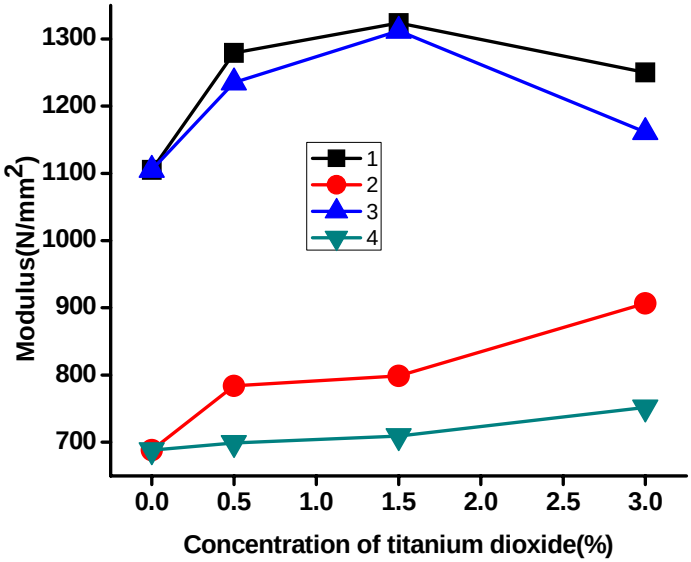

Figure 6.25: Effect of photo ageing on tensile modulus of PP/TiO_2 composites

6.2.13.2.2 Fourier transform infrared studies

Figure 6.26 represents the FTIR spectrum of neat PP, 1.5% NTO filled PP and 1.5% CTO filled PP after UV irradiation respectively. Intensity of the peak due to the formation hydroperoxide in the range of 3200-3600 cm^{-1} decreases significantly by the addition of TiO_2 and this decrease is significant in the case of NTO filled PP composites than CTO filled composites. Intensity of characteristic peak of PP in the range 2800cm^{-1} increased by the addition of TiO_2. PP/NTO filled composite shows intense peak compared to that of PP/CTO composites. TiO_2 nanoparticles may be stabilizing the PP molecules thereby delaying the photodegradation.

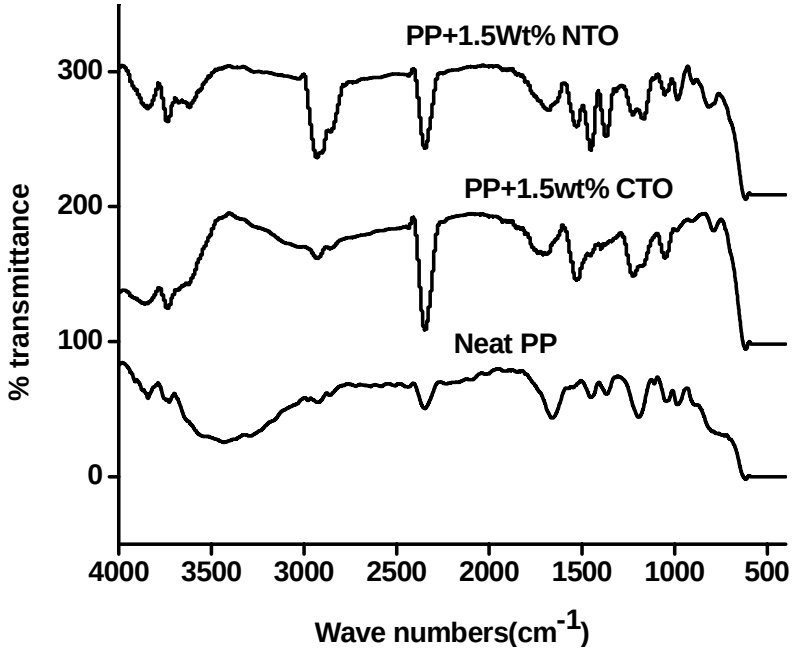

Figure 6.26: IR spectrum of PP/TiO_2 composites after photo ageing

The dominant screening mechanism is that the TiO_2 nanoparticles absorbed the UV radiation and hence reduced the UV intensity that can promote oxidation of the PP. Outstanding photo-stabilization effect of zinc oxide nano particles on PP [93] and LLDPE is reported [94].

6.2.13.2.3. Morphologies of tensile fractured surfaces

Figure 6.27 shows the overviews of the surface morphologies of tensile fractured specimens of PP, PP/NTO and PP/CTO composites after UV irradiation respectively.SEM photographs of neat PP shows holes after UV irradiation. These holes are caused by photo-degradation on the specimen surfaces. When examining the fractured surface of composites such holes are not observed.

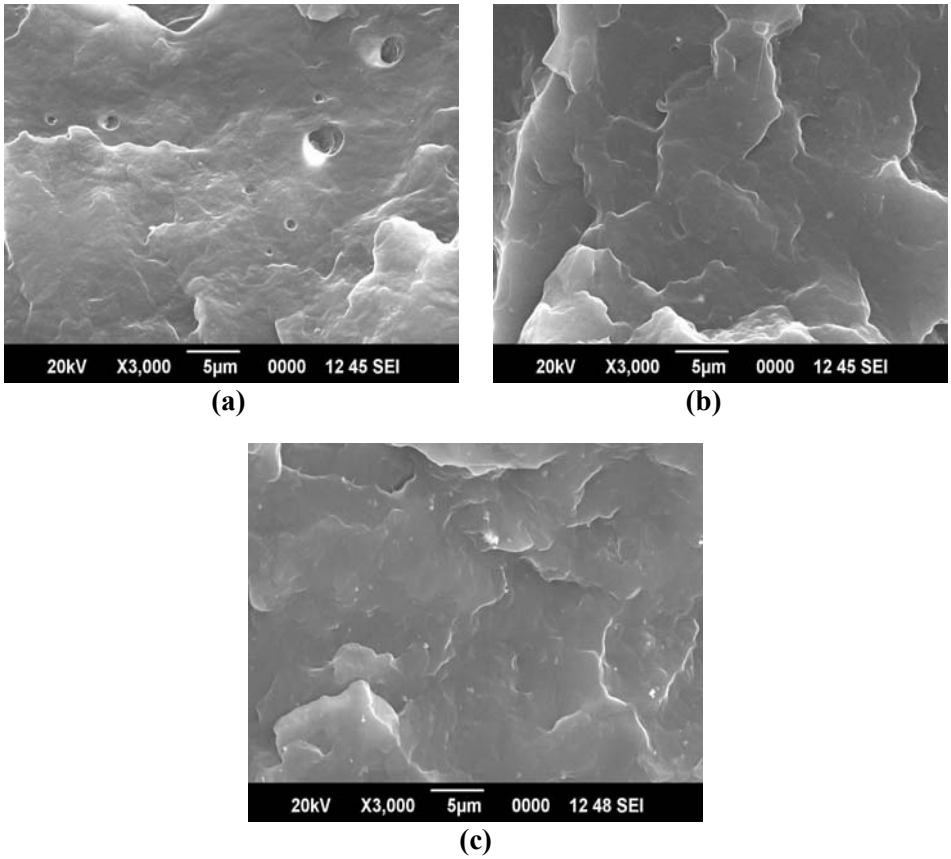

Figure 6.27: Scanning electron micrographs of (a) neat PP (b) PP+1.5wt%CTO and (c) PP+1.5wt% NTO filled composites after photo ageing

6.3 Conclusion

Mechanical and dynamic mechanical properties of PP are improved by the addition of TiO_2. PP shows better thermal stability in presence of TiO_2. Differential scanning calorimetric studies show increase in crystallinity of PP by the addition of TiO_2. X-ray diffraction studies of neat PP and composites indicate the presence of α phase of monoclinic PP. Melt flow index increases by adding low concentration of NTO, whereas CTO added PP shows a decrease in MFI. Transparency of the PP films is decreased by the addition of TiO_2. PP with NTO filled films show higher transparency when compared to CTO filled PP films. Limiting oxygen index of PP is increased by the addition

of TiO_2. Mechanical, morphology and IR studies show improved performance of composites even after thermal and UV ageing when compared to neat PP. NTO filled PP shows better properties than CTO filled composites.

References

[1] Pavlidoua S, Papaspyrides C D , Prog Polym Sci,2008, 33,1119.

[2] Kubacka A, Serrano C, Ferrer M, Lunsdorf H, Bielecki P, Cerrada ML, Fernandez-Garcia M,Nano Lett, 2007,7,2529.

[3] Kagan C R, Mitzi D B, Dimitrakopoulos C D, Science, 1999, 286,945.

[4] Eckle M, Decher G , Nano Lett, 2001,1,45.

[5] Choy J H, Kwak S Y, Jeong Y J, Park J S, Angew Chem Int Ed, 2000, 39,4041.

[6] Cristofaro A D, Violante A , Appl Clay Sci, 2001, 19,59.

[7] Hsu Y G, Lin K H , J Polym Res,2001,8,69.

[8] Fereidoon A, Ahangari M G, Saedodin S, Journal of macromolecular Science, Part B: Physics 2008, 48,196.

[9] Mehta S, Mirabella M, Rufener K, Bafna A, J of Appl Polym Sci, 2004,92,928.

[10] G Mani, Q Fan, Samuel C U, Yang Y, J of Appl Polym Sci, 2005,97,218.

[11] Garcia M, van Vilet G, Jain S, Schrauwen B A, Sarkissov A, van Zyl W E, Boukamp B, Rev.Adv.Mater.Sci, 2004,6,169.

[12] Marosfoi B B, Szabo A, Marosi Gy, Tabuani D, Camino G, Pgliari S, J of Thremal Analysis and Calorimetry, 2006,86,669.

[13] Jiann-Wen Huang, J Appl Polym Sci, 2008,107, 3163.

[14] Pralay Maiti, Pham Hoai Nam, Masami Okamoto, Macromolecules 2002, 35,6.

[15] Maurizio Avella, Simona Cosco, Maria Laura Di Lorenzo, Emilia Di Pace, Maria Emanuela Errico, Gennaro Gentile, Macromol Symp, 2006, 234, 156.

[16] Yang J, Lin Y, Wang J, Mingfang Lai, Jing Li, Liu J, Xin Tong, Cheng H, J.Appl Polym Sci, 2005,98,1087.

[17] Garcia M, van Vilet G, Jain S, Schrauwen B A, Sarkissov A, van Zyl W E, Boukamp B, Rev.Adv.Mater.Sci, 2004,6,169.

[18] Dong Wook Chae, Byoung Chul Kim, Polym. Adv. Technol, 2005, 16, 846.

[19] Shu-Cai Li, Ya-Na Li, J of Appl Polym Sci, 2010, 116, 2965.

[20] Maurizio Avella, Maria Emanuela Errico, Gennaro Gentile, Macromol. Symp, 2007, 247, 140.

[21] Garcıa Lopez D, Merino J C, Pastor J M, J. Appl. Polym. Sci, 2003, 88, 947.

[22] Ellis T S, D Angelo J S, J. Appl. Polym. Sci , 2003, 90, 1639.

[23] Hasegawa N, Okamoto H, Kato M, Usuki A, J.Appl. Polym. Sci, 2000, 78, 1918.

[24] Rumiana Kotsilkova, Evgeni Ivanov, Ekaterina Krusteva, Clara Silvestre, Sossio Cimmino, Donatella Duraccio, J Appl Polym Sci, 2010,115, 3576.

[25] Reyes de Vaaben S, Aguilar A, Avalos F, Ramos de Valle L F, J of Thermal Analysis and Calorimetry, 2008,93,947.

[26] Henry Kuo Feng Cheng, Nanda Gopal Sahoo, Xuehong Lu, Lin Li, J Therm Anal Calorim, DOI 10.1007/s10973-011-1498-5

[27] Liu Z, Gilbert M J, J Appl Polym Sci 1996;59(7):1087–98

[28] Wang Y, Wang J, Polym Eng Sci, 1999,39,190.

[29] Lei SG, Hoa SV, Ton-That MT, Compos Sci Technol, 2006,66,1274.

[30] Chen M, Tian G, Zhang Y, Wan C, Zhang Y, J Appl Polym Sci, 2006,100,1889.

[31] Jeong S H, Yeo S Y, Yi S C, J Mater Sci, 2005, 40, 5407.

[32] Bhattacharyya A R, Sreekumar T V, Liu T, Kumar S, Ericson L M, Hauge R H, Smalley R. E, Polymer 2003, 44, 2373.

[33] Chatterjee A, Deopura B L, Compos A 2006, 37, 813.

[34] Kumar S, Doshi H, Srinivasarao M, Park J O, Schiraldi D A, Polymer, 2002, 43, 1701.

[35] Rottstegge J, Qiao Y K, Zhang X, Zhou Y, Xu D, Han C C, Wang D, J Appl Polym Sci, 2007, 103, 218.

[36] Gordeyev S A, Ferreira J A, Bernardo C A, Ward I M, Mater Lett 2001, 51, 32.

[37] Rong M Z, Zhang M Q, Zheng Y X, Zeng H M , Friedrich K, Polymer 2001, 42, 3301.

[38] Bikiaris D N, Papageorgiou G Z, Pavlidou E, Vouroutzis N, Palatzoglou P, Karayannidis G P, J Appl Polym Sci,2006, 100, 2684.

[39] Huang L, Zhan R, Lu Y, J Reinforc Plast Compos, 2006, 25,1001.

[40] Rubaca M, Zieba J, Fibers Text Eastern Eur 2006, 14, 49.

[41] Yu B, Qi L, Ye J, Sun H, J Polym Res 2007, 14, 107.

[42] Ghasemi A, Hossienpour A, Morisako A, Saatchi A, Salehi M, J of Magnetism and Magnetic Materials, 2006, 302, 429.

[43] Yang H, Zhu S, Pan N, J Appl Polym Sci, 2004, 92, 3201.

[44] Burniston N, Bygott C, Stratton J, Surf Coat Int Part A, 2004, 87, 179.

[45] Tjong S C, Bao S P, Liang G D, J. Polym. Sci. B. Polym. Phys. 2005, 43,3112.

[46] Jose M V, Dean D, Tyner J, Price G, Nyairo E, J. Appl. Polym. Sci., 2007, 103,3844.

[47] Xu W, Ge M, He P, J. Polym. Sci. B. Polym. Phys., 2002, 40, 408.

[48] Amash A, Zugenmaier P, J. Appl. Polym. Sci., 1997, 63, 1143.

[49] Zhou Z, Wang S, Zhang Y, J. Appl. Polym. Sci., 2006, 102, 4823.

[50] Takashi K, Eric G, Jenny H, Richard H, Walid A, Jack D, Macromol Rapid Commun 2002, 13, 761.

[51] Valentini L, Biagiotti J, Kenny J M, Santucci S, J Appl Polym Sci, 2003, 87, 708.

[52] Kearns J C, Shambaugh R L, J Appl Polym Sci, 2002, 86, 2079.

[53] Bhattacharyya A R, Sreekumar T V, Liu T, Kumar S, Ericson L M, Hauge R H, Smalley R E, Polymer 2003, 44, 2373.

[54] Valentini L, Biagiotti J, Kenny J. M, Manchado M A L, J Appl Polym Sci, 2003, 89, 2657.

[55] Thomas S Ellis, Joseph S D Angelo, J Appl Polym Sci, 2003,90,1639.

[56] Masaya Kawasumi, Naoki Hasegawa, Makoto Kato, Arimitsu Usuki, Akane Okada, Macromolecules 1997, 30, 6333.

[57] Quang T, Nguyen, Donald G Baird, Advances in Polymer Technology 2006, 25, 270.

[58] Bhattacharya A R, Sreekumar TV, Tao Liu, Satish Kumar, Ericson M, Robert H. Hauge, Richard E Smalley, Polymer 2003, 44, 2373.

[59] Avella M, Errico M E, Rimedio R, J. Mater. Sci, 2004, 39, 6133.

[60] Avella M, Errico M E, Martuscelli E, Nanoletters, 2001, 1, 213.

[61] Lu S, Melo M, Zhao J, Pearce E M, Kwei T K, Macromolecules, 1995, 28, 4908.

[62] Ahmadi S J, Huang Y D,Li J W, J. Mater. Science, 2004, 39, 1919

[63] Lee D C, Jang LW, J. Appl. Polym. Sci, 1998, 68, 1997.

[64] Fornes T D, Yoon PJ, Keskkula H, Paul D R, Polymer, 2001, 42,9929.

[65] Liu L, Qi Z, Zhu X, J. Appl. Polym. Sci, 1999, 71,1133.

[66] Jakob M, Levanon H, Kamat PV , Nano Lett, 2003, 3,353.

[67] Shi SL, Zhang LZ, Li JS ,J Polym Res, 2009, 16,395.

[68] Chiu F C, Chu P H, J Polym Res, 2006, 13,73.

[69] Yoichi Ishibai, Takashi Nishikawa , Shigeyoshi Miyagishi, Journal of dispersion science and Technology, 2006, 27, 1093.

[70] Shu-Cai Li, Ya-Na Li, Journal of Applied Polymer Science 2010, 116, 2965.

[71] Lin Hongjiao, Yan Hong, Liu Bo, Wei Liqiao, Bingshe Xu, Polym Degrad Stab 2011,96,1382.

[72] Florencio GF, Tomas JAM, Marcelo SR, Suedina MLS, Polym Degrad Stab, 2005,89,383.

[73] Gilman JW, Appl Clay Sci, 1999,15,31.

[74] Dogan Mehmet, Yılmaz Aysen, Bayramli Erdal, Polym Degrad Stab, 2010, 95, 2584.

[75] Danyadi L, Janecska T, Szabo Z, Nagy G, Moczo J, Pukanszky B, Composites Sci Technol, 2007,67,2838.

[76] Jafari Nejad Shahryar, Ahmadi Seyed javad, Abolghasemi Hossein, Mohadde Spour Ahmad, J Appl Polym Sci, 2007, 7, 2480.

[77] Hassan M, El-Dessouky, Carl AL, J Nanopart Res, 2011,13,1115.

[78] Coats AW, Redfern JP. Nature 1964,68,201.

[79] Jiang-Ping He, Hua-Ming Li, Xia-Yu Wang, Yong Gao, European Polymer Journal, 2006,42,1128.

[80] Van Bennekom ACM, Gaymans R J ,Polymer, 1997,38,657.

[81] Bouma K, de Wit G, Lohmeijer JHGM,Gaymans RJ,Polymer, 2000,41,3965.

[82] Agarwal US,G de Wit, Lemstra PJ, Polymer, 2002,43,5709.

[83] Ou CF, J Appl Polym Sci, 2003,89,3315.

[84] Ou CF, J Polym Sci Part B:Polym Phys, 2003,41,2902.

[85] Anoop Anand K,Agarwal US, Rani Joseph, Polymer, 2006,47,3976.

[86] Wu T Ke Y,Thin solid films, 2007,515,13,5220

[87] Chin-Chun Teng, Chen-Chi M Ma,Yen-Wei Huang, Siu-Ming Yuen, Cheng-Chih Weng,Cheng-Ho Chen,Shun-Fua Su, Composites: Part A,39,2008,1869.

[88] Lee S H, Kim M W,Kim S H,Youn J R., Eur Polym J, 2008,44,1620.

[89] Kancheng mai, Zhengjun Li,yuxin qiu, Hanmin zeng, Journal of Applied Polymer Science,2001, 81, 2679 .

[90] Rapoport N Y, Berulava S I, Kovarskii A L, Musayelyan I N, Yershov YuA,Miller V B, Polym Sci USSR (EnglmTrnasl)1975,A17,2901.

[91] Rabello M S, White J R, Polym Degrad Stab 1997,56,55.

[92] Zanetti M, Bracco P, Costa L, Polym Degrad Stab, 2004,85,657.

[93] Hongxia Zhao, Robert K Y Li, Polymer 2006,47,3207.

[94] Yang R, Li Y, Yu J, Polym Degrad Stab 2005,88,168.

.....ooo.....

POLYPROPYLENE/TITANIUM DIOXIDE NANOCOMPOSITE FIBERS

Contents

PP/TiO_2 nanocomposites were prepared by melt mixing method and made in to fiber by melt spinning and drawing. Mechanical properties of the PP fiber was improved by the addition of TiO_2 nanoparticles. Thermogravimetric analysis showed significant improvement in thermal stability. Crystallinity of PP fiber was increased with the addition of TiO_2 nanoparticles. XRD shows there is no change in the crystal structure of PP fibers by the addition of TiO_2. Antibacterial studies were carried out using Bacillus aereus and Escherichia coli.

7.1 Introduction

New fiber technologies have been developed in past years to improve the physical properties and spinnability of polymers by the incorporation of reinforcing fillers into polymer [1]. However, most micro fillers are not suitable for fiber spinning because they cause spinline failure due to their size, which approaches the order of the fiber diameter [2]. As the particle size decreases, their effects increase due to their large total surface area per unit volume [3]. Because of small size, the interaction between the nanofiller and the polymer is maximized by increasing contact area. Hence, the nanofiller loading could be reduced to low loadings compared with conventional composites containing a high loading of fillers. Conventional methods used to modify fibers and fabrics do not, more often, lead to permanent effects and lose their functions after laundering or wearing, however due to their high surface energy, nanoparticles show better affinity for fibers and fabrics and improve the durability of their function. Hence, the studies relating modification of polymeric textile fibers and fabrics by nanoparticles has increased recently [4–6].

PP is widely used thermoplastic for textile application (especially in carpets and nonwovens) and plastics. Nanometer scale particles as nano-sized fillers attract an interest for increasing the properties of polymer [7-14]. Carbon nanotube (CNT) [15, 16, 7, 8] and montmorillonite (MMNT) [17,18] have reported as nano-fillers for plastics as well as fibers. Fibers from PP are usually found in many end-use products due to their properties like light weight, resistance to moisture and chemicals, low cost, sufficiency strength and ease in processing [19-21]. There are some reports on the use of silica for enhancing mechanical properties of PP fibers [22, 23]. Inorganic materials like

metal and metal oxides have attracted great attention over the past decades due to their ability to withstand harsh process conditions. Of the inorganic materials, metal oxides such as TiO_2, ZnO, MgO and CaO are of great interest as they are not only stable under harsh process conditions but also safe materials to human beings and animals.

In this chapter the development of PP/TiO_2 nanocomposite fibers by melt spinning and drawing is reported. Mechanical, thermal, antibacterial, x-ray diffraction analysis and morphological studies of these fibers were also conducted. Experimental details are same as in chapter 4, section 4.2.

7.2 Results and Discussion

Photographs of PP and PP/TiO_2 nanocomposite fibers were shown in figure 7.1. PP/TiO_2 nanocomposite fiber shows white in colour while neat fiber is colourless.

Figure 7.1: Photographs of neat PP fiber and PP/TiO_2 composite fibers

7.2.1 Mechanical properties of the fibers

Mechanical properties of the fiber depend on internal structure, degree of crystallinity and spinning conditions [24]. Tenacity of the PP/CTO and PP/NTO composites are shown in figure 7.2. Tenacity of the PP fiber is increased by the addition of TiO_2 particles indicating reinforcing effect of TiO_2. In the case of filler reinforced fiber, the tenacity is found to depend on the distribution and orientation of the filler. At 3 wt% of NTO, tenacity is increased by 72.69% indicates good orientation of TiO_2 in the PP fiber. At lower concentration, tenacity is decreased, may be due to the lack of good orientation of TiO_2 nanoparticles in PP fiber. A substantial increase in modulus (figure 7.3) is observed at 3 wt% of TiO_2. The increase in modulus of the fibers is related to the inherent stiffness and quality of the dispersion of TiO_2 and also due to adhesion between the matrix and nanoparticles. Variation of elongation at break of the PP fibers with filler loading is shown in Figure 7.4. An increase of 15.79% is observed at 1.5 wt% of NTO. This indicates a decrease in brittle nature of the fiber. Linear density of the fibers is increased by 29.16% at 3 wt% of NTO as is evident from figure 7.5. Increase in linear density indicates increase in the fineness of the fiber. This is also supported by SEM photographs (figure 7.13). Time to rupture of the fiber (figure 7.6) increases, reaches a maximum and then decreases at higher loadings. The maximum value is 46.2, at a loading of 0.5 wt% NTO. These results show that TiO_2 nanoparticles offers significant reinforcement to PP fibers. The improved mechanical properties can be attributed to the effective matrix–filler interaction enabling load transfer from the polymer matrix to the TiO_2 nanoparticles.

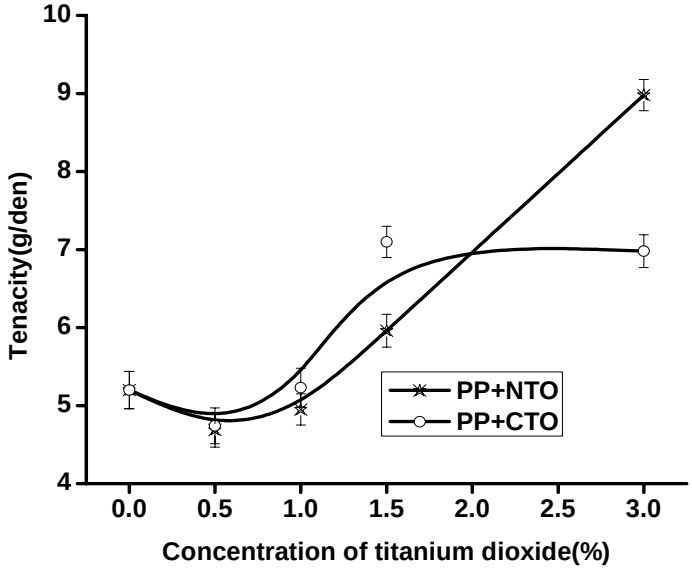

Figure 7.2: Effect of TiO_2 on tenacity of PP/TiO_2 composite fibers

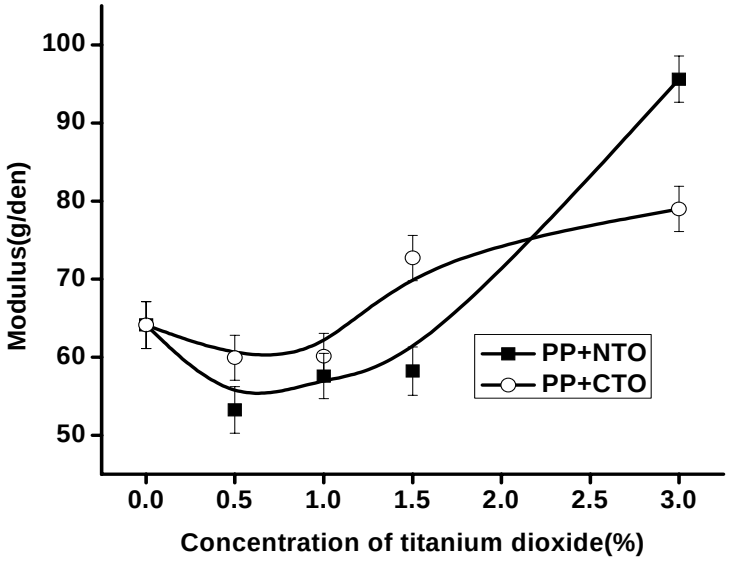

Figure 7.3: Effect of TiO_2 on modulus of PP/TiO_2 composite fibers

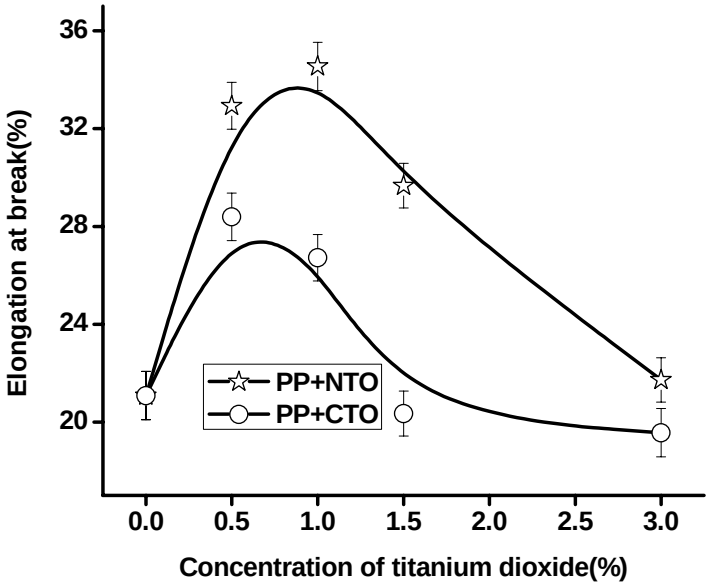

Figure 7.4: Effect of TiO_2 on elongation at break of PP/TiO_2 composite fibers

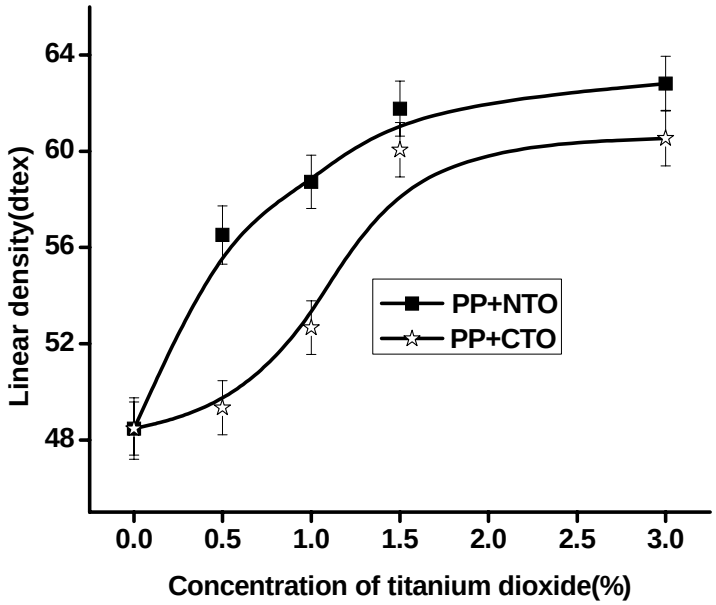

Figure 7.5: Effect of TiO_2 on linear density of PP/TiO_2 composite fibers

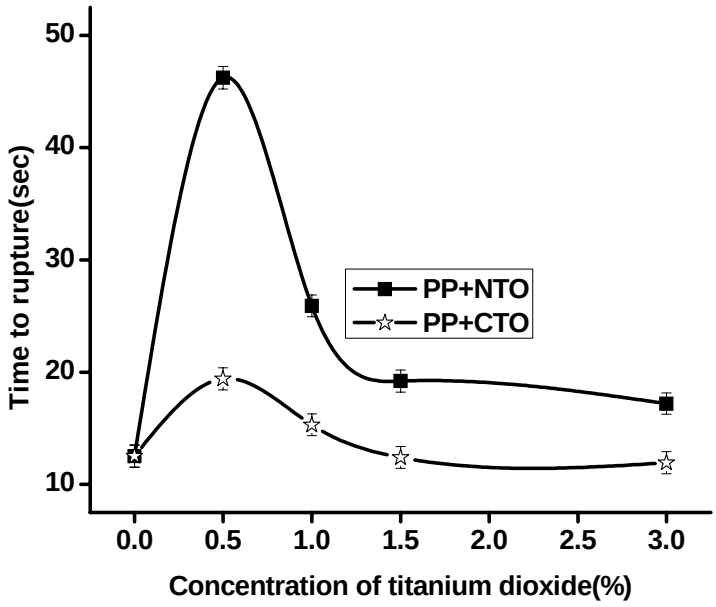

Figure 7.6: Effect of TiO_2 on time to rupture of PP/TiO_2 composite fibers

7.2.2 Thermogravimetric analysis

Figures 7.7 and 7.8 show thermograms and differential thermograms of neat fiber and NTO filled PP fibers and values are given in table 7.1. The neat fibers start to decompose at 324.9 ^{0}C and ends at 473.7^{0}C. The 0.5wt% NTO filled PP begin to decompose at a relatively higher temperature of 377.8 ^{0}C and ends at 499.2 ^{0}C. The increase in onset temperature may be due to the increased adhesion force at PP/TiO_2 interface. In case of good interfacial interaction, particles are capable of restricting the mobility of a polymer chain, making the scission of polymer chains harder at lower temperature. As a result, the degradation temperature of the nanocomposite shifts to higher temperature [25]. The temperature at which maximum degradation take place is increased by 37 ^{0}C at 0.5 wt% of NTO nanoparticles. Residue of unfilled fiber at 800^{0}C was almost close to 0.38%. For filled composites, residue is about 0.68%, 1.33%, 2.81% for 0.5, 1.5 and 3% loadings of NTO respectively. This shows enhanced thermal stability of PP fiber by the addition of NTO nanoparticles.

An increase in thermal stability of PP by the addition of various fillers is reported in literature [26, 27].

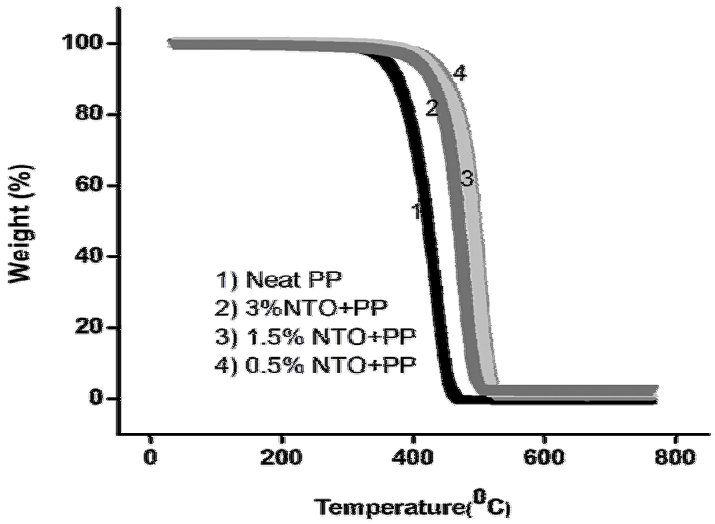

Figure 7.7: Thermogram of PP/TiO_2 nanocomposite fibers

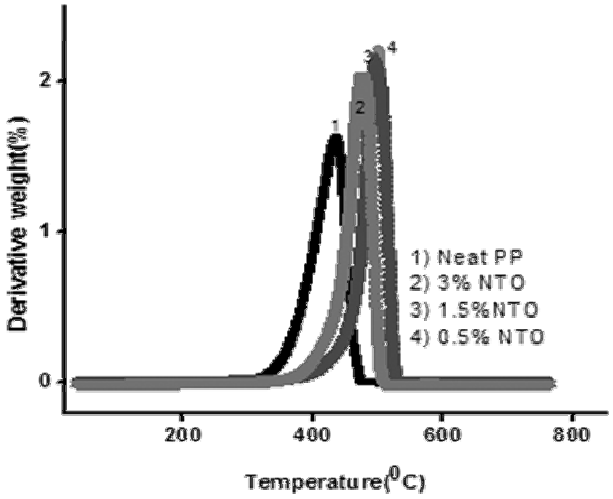

Figure 7.8: Differential thermogram of PP/TiO_2 nanocomposite fibers

Table 7.1: Effect of TiO_2 on the thermal stability of PP/TiO_2 nanocomposite fibers

Sample name	Onset temperature (^{0}C)	Endset temperature (^{0}C)	Residue (%)	Temperature at which maximum degradation(^{0}C)
Neat PP	324.9	473.7	0.38	433.5
PP+0.5% NTO	377.8	499.2	0.68	470.5
PP+1.5% NTO	373.7	499.8	1.33	469.7
PP+3% NTO	372.2	498.9	2.81	469.5

7.2.3 Kinetic analysis of thermal decomposition

Coats–Redfern method was used to evaluate the kinetics of thermal degradation of PP and PP/NTO composites [28]. Thermal degradation functions for the Coats–Redfern method were listed in table 3.3 and details are given in section 3.3.8. From the table it is clear that the activation energy of PP fiber is increased by the addition of TiO_2 nanoparticles. Activation energy (E) obtained for neat fiber is 79.57 kJ/mol, 0.5% TiO_2 added PP fiber is shown E of 141.5 kJ/mol. Significant increase in activation energy indicates high thermal stability. Representative plots of Coats–Redfern equation for neat PP fiber, PP/0.5wt%TiO_2, PP/1.5wt%TiO_2 and PP/3wt%TiO_2 nanocomposite fiber are shown in figures 7.9a, 7.9b, 7.9c and 7.9d.

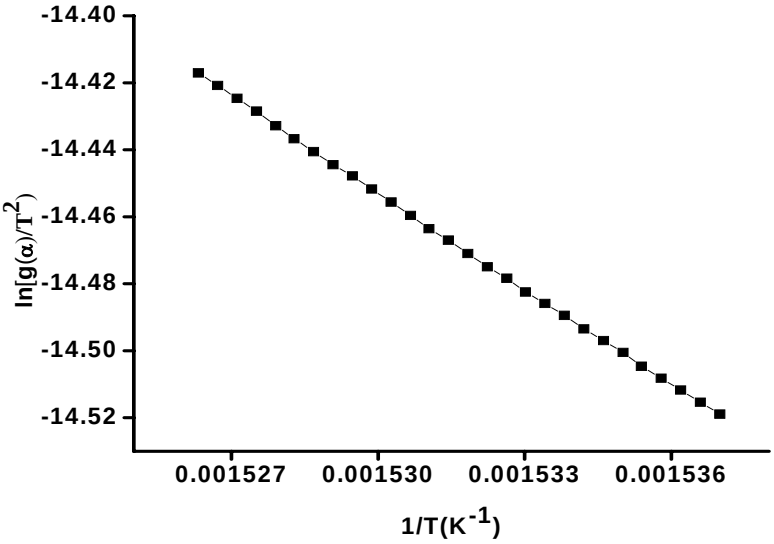

Figure 7.9a: Representative plot of neat PP fiber

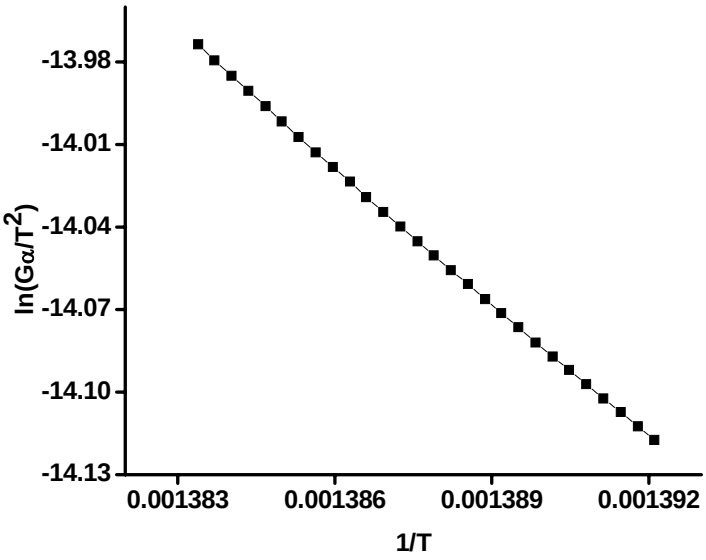

Figure 7.9b: Representative plot of 0.5 wt% NTO added PP fiber

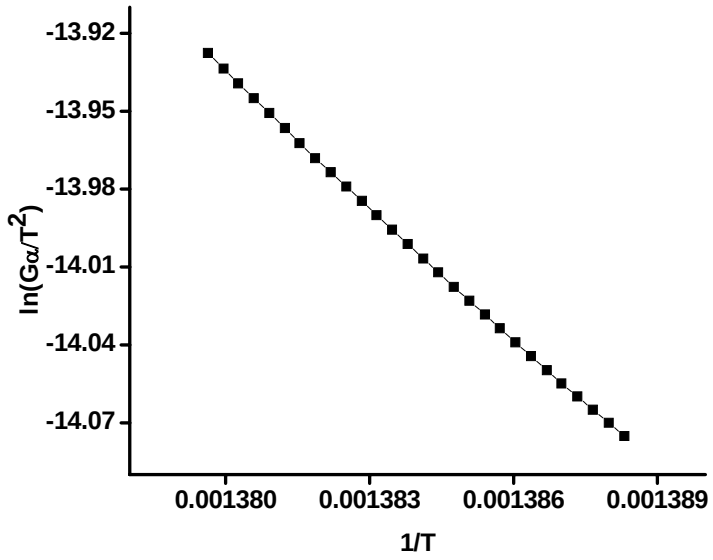

Figure 7.9c: Representative plot of 1.5 wt% NTO added PP fiber

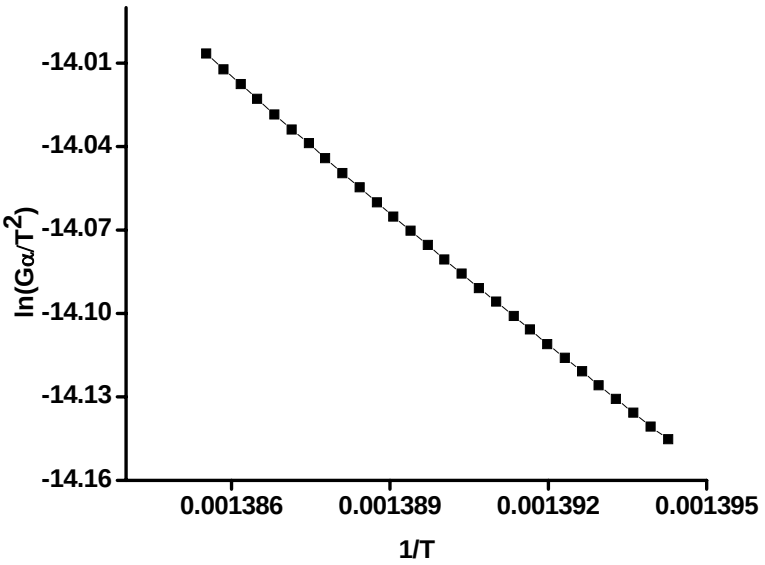

Figure 7.9d: Representative plot of 3 wt% NTO added PP fiber

Table7. 2. Apparent activation energy, E and correlation coefficients (R) of the fibers by Coats– Redfern method

Sample name	R	E(kJ/mol)
Neat PP	0.999	79.57
0.5%NTO+PP	0.999	141.57
1.5%NTO+PP	0.999	136.9
3%NTO+PP	0.999	131.87

7.2.4 Differential scanning calorimetry

The effect of TiO_2 nanoparticles on the crystallization behaviour of PP fiber is studied with DSC. The peak crystallization temperatures (Tcp), the apparent crystallization temperature (Tc), and the corresponding enthalpy (ΔHc) for the samples are shown in table 7.3. Figure 7.10 shows the DSC cooling scans of PP/TiO_2 nanocomposite fiber samples. Percentage crystallinity (Xc) of the fibers can be calculated from the Equation 4.1. The percentage crystallinity increases with NTO loading, reaches a maximum at 1.5 wt% and then decreases. Neat fiber shows 58.48% crystallinity while 1.5 wt% NTO filled fiber shows 61.2% indicating that TiO_2 nanoparticles are acting as nucleating agents for PP crystallization. These findings are most probably due to nucleation role of NTO in the crystallization of PP which results in a higher degree of crystallinity. But it can be inferred that larger aggregates prevent the crystal growth and hence reducing the crystallinity as the NTO content increases up to 3wt%. Since the addition of NTO is not expected to affect the molecular weight or to cause any chain branching in PP, only the nucleating activity of the nanoparticles was considered in accordance with literature [29].

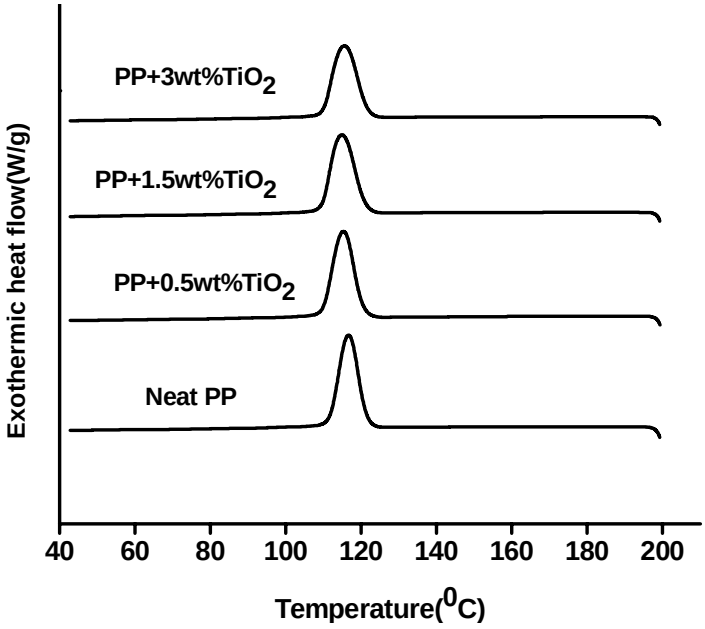

Figure 7.10: Cooling behaviour of neat PP and PP/TiO_2 nanocomposite fibers

Table 7.3: Effect of NTO on the crystallization of PP/TiO_2 nanocomposite fibers

Sample name	Tc (^{0}C)	Tcp (^{0}C)	ΔH_c	Xc(%)
Neat PP	121.43	116 .68	96.5	58.48
PP+0.5%NTO	120.45	115.33	99.78	60.56
PP+1.5%NTO	121.10	114.93	99.46	61.19
PP+3%NTO	121.68	115.57	92.18	57.59

Melting behaviour of neat fiber is shown in figure 7.11. The peak melting temperatures (Tmp), the apparent melting temperature (Tm) and the corresponding enthalpy (ΔH_m) for the samples are shown in table 7.4. The maximum rate of melting (Tmp) occur at 166.6^{0}C for PP fiber and its Tm is 151.5^{0}C. The Tm value of PP fiber with 3 wt% NTO is increased by about 3.2^{0}C compared with neat PP fiber. Tmp of PP is decreased by the addition of NTO nanoparticles. In Figure 7.11, it can be seen that there is a small peak at

lower melting temperature of PP fiber and a peak at higher melting temperature. However, NTO filled PP fiber shows only single peak at high melting temperature. The first peak, with lower melting temperature, indicates the presence of a small amount of β-phase, whereas the second peak indicates the melting of α-phase.

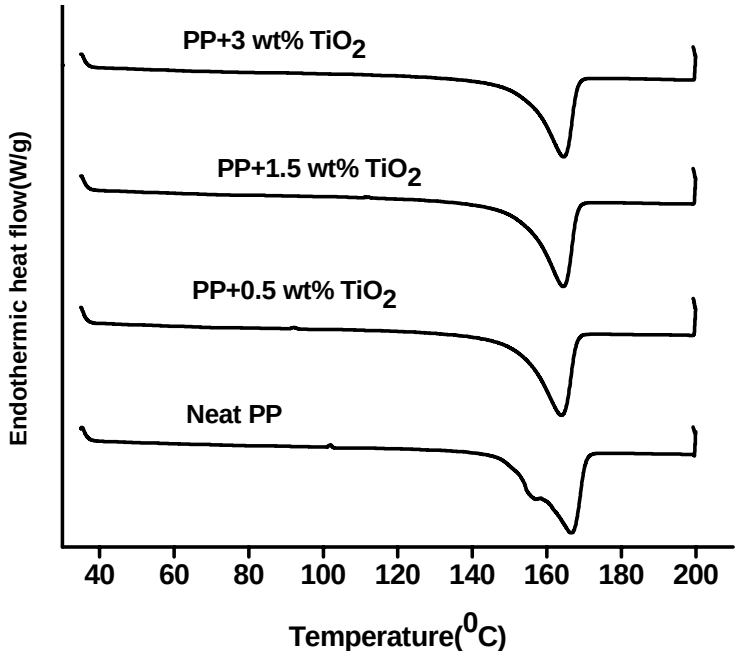

Figure 7.11: Melting behaviour of PP and PP/NTO composite fibers

Table 7.4: Effect of NTO on the melting behaviour of PP/NTO fibers

Sample name	Tm (^{0}C)	Tmp (^{0}C)	ΔH_m(J/g)
Neat PP	151.53	166.66	89.5
PP+0.5%NTO	153.32	163.95	76.58
PP+1.5%NTO	154.26	164.45	78.58
PP+3%NTO	154.74	164.55	69.2.29

7.2.5 X-ray diffraction analysis

X-ray patterns of neat PP fibers and NTO filled PP fibers are shown in Figure 7.12. Usually, iPP is a multicrystalline polymer and has five crystalline forms such as α, β, γ, δ and pseudohexagonal. The XRD study (Figure 7.12) shows TiO_2 do not affect the crystalline form of PP fibers. Same crystalline form is observed for both PP and composite fibers. The peaks observed is corresponds to (110), (040) and (130) and (041) planes of PP, indicate the α– form of iPP.

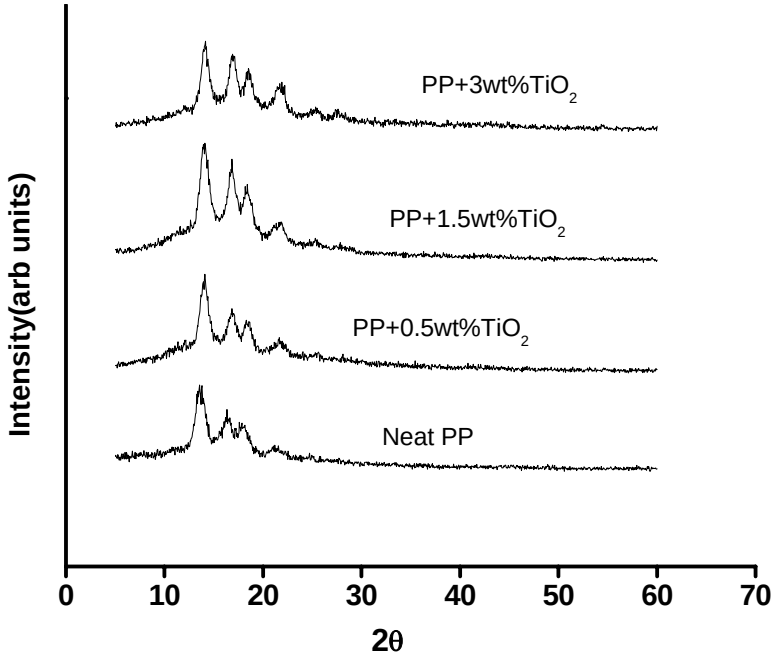

Figure 7.12: X-ray diffraction pattern of PP and PP/NTO composite fibers

7.2.6 Scanning electron microscopy

SEM images of neat PP and PP/TiO_2 fibers with different concentrations are shown in Figure 7.13. The surfaces of the fibers are investigated in terms of their shape and uniformity. PP/TiO_2 nanocomposite fiber surface is smooth in appearance. The crosssection of the fibers is given in Figure 7.14. SEM

photograph of cross section of filled fiber is different from that of neat PP. It shows a uniform dispersion of filler in the matrix, resulting in the good mechanical and thermal properties.

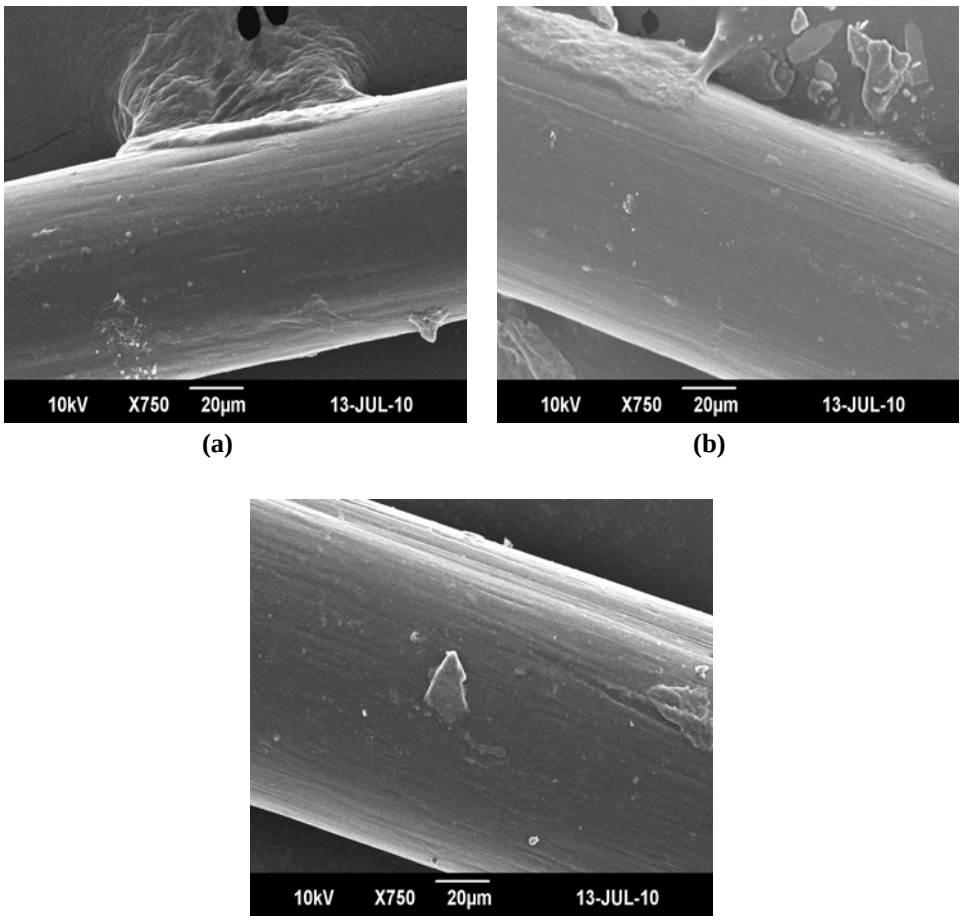

(a) **(b)**

(c)

Figure 7.13: Scanning electron micrographs of (a) Neat PP (b) PP+ 3wt% NTO (c) PP+ 3wt% CTO fibers

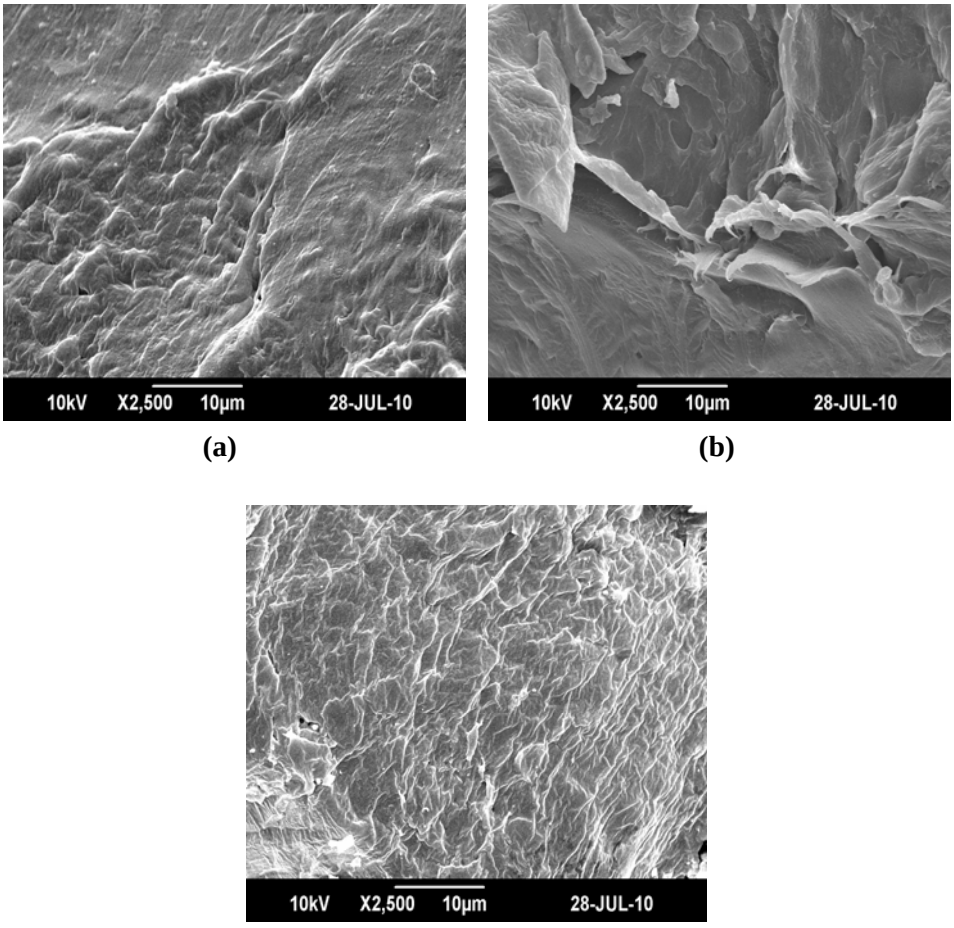

Figure 7.14: Scanning electron micrographs of cross section of (a) neat PP fiber (b) PP+3wt% NTO fiber (c) PP+ 3wt% CTO fiber

7.2.7 Antibacterial properties of fibers

Figure 7.15 shows the SEM of the fibers after putting them in bacterial medium for ten days in Bacillus aereus. Fiber surface is more smooth when compared to morphology of fibers before bacterial attack (figure 7.13). Figure 7.16 shows the morphology of the fibers after putting them in bacterial medium for ten days in E-coli. Fiber morphology is not significantly changed by the attack of E-coli.

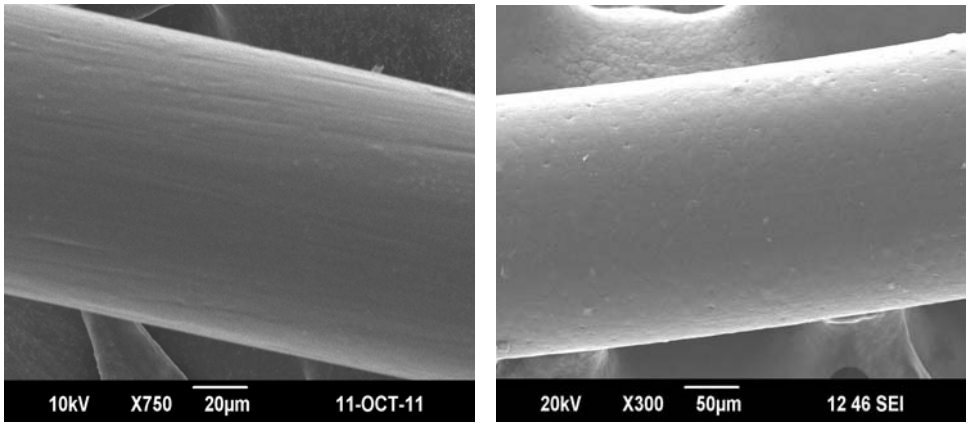

(a) **(b)**

Figure 7.15: Scanning electron micrographs of (a) neat PP (b) PP/3wt%NTO filled fibers after treating with Bacillus aereus.

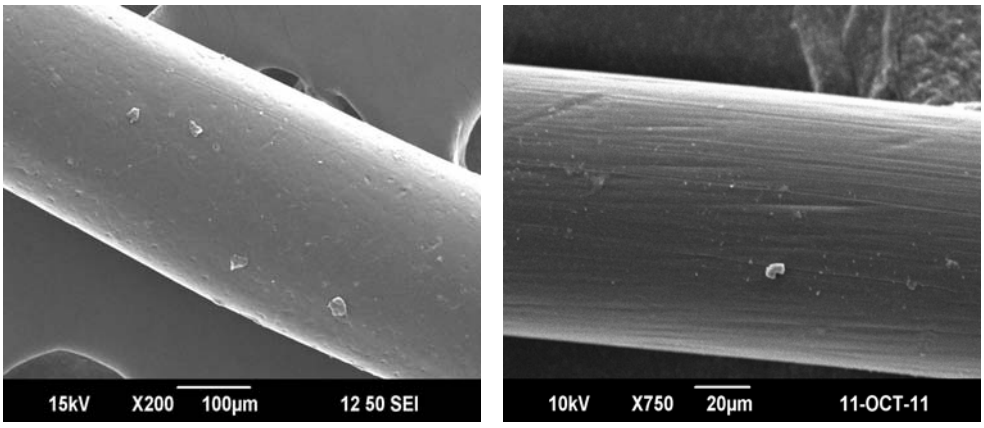

(a) **(b)**

Figure 7.16: Scanning electron micrographs of (a) neat PP (b) PP/3wt%NTO filled fibers after treating with E- Coli.

7.3 Conclusion

Mechanical properties of PP increased with the addition of TiO_2 nanoparticles. Thermogravimetric analysis indicates an increase in onset temperature, maximum degradation temperature and residue indicating improved thermal stability. DSC studies show increase in crystallization indicating that

TiO_2 nanoparticles are acting as nucleating agents for PP crystallization. Surface morphology study of fibers show smooth surface even after the addition of nano TiO_2. Analysis of SEM images of cross section of fibers points to well dispersed system, which is the reason for improvement in mechanical properties. NTO filled PP fiber shows significant improvement in properties when compared to CTO filled PP fiber. PP fiber and NTO filled fiber shows excellent resistance to bacillus aereus.

References

[1] Salem D R,Structure formation in polymeric fibers, Hanser, Munich 2001

[2] Seung Hwan Lee,Jae Ryoun Youn, Journal of applied polymer science, 2008,109,1221.

[3] Jeong S H, Yeo S Y, Yi S C, J Mater Sci, 2005, 40, 5407.

[4] Schadler L S, Ajayan P M, Schadler L S, Braun P V, Eds, Wiley-V C H, Weinheim, 2003, Chapter 2, pp 77.

[5] Wong Y W H, Yuen C W M, Leung M Y S, Ku S KA, Lam H L I, Autex Res J, 2006, 6, 1.

[6] Bhattacharyya A R, Sreekumar T V, Liu T, Kumar S, Ericson L M, Hauge R H, Smalley R E, Polymer 2003, 44, 2373.

[7] Arib R M N, Sapuan S M, Ahmad M M H M, Paridah MT, Khairul Zaman H M D, Mater Des, 2006,27,391.

[8] Karsli Nevin Gamze, Aytac Ayse, Mater Des 2011,32,4069.

[9] Das Arijit, Satapathy Bhabani K, Mater Des, 2011, 32,1477.

[10] Zeng Anran, Zheng Yuying, Guo Yong, Qiu Shangchang, Cheng Lei, Mater Des 2012,34,691.

[11] Zhiping Lv, Kunjun Wang, Zhihua Qiao, Wenjie Wang, Mater Des 2010, 31,3804.

[12] Baniasadi H, Ramazani SA, Nikkhah Javan, Mater Des 2010,31,76.

[13] Bourbigot S, Gilman JW, Wilkie CA, Polym Degrad Stab, 2004,84,483.

[14] Gong F, Feng M, Zhao C, Zhang S, Yang M. Polym Degrad Stab, 2004, 84,289.

[15] Bhattacharyya A R, Sreekumar, T V, Liu T, Kumar S , Ericson L M, Robert H H, Smalley R E, 2003, *Polymer*, 44 ,2373.

[16] Chatterjee A, Deopura, B L, Polym, 2003, 4 **,** 102.

[17] Liu X H, Wu Q J, Polymer,2001,42,10013.

[18] Gao F, 2004, *Mater. Today*, **7,** 50.

[19] Horrocks AR, Anand SC, Handbook of technical textiles, The Textile Institute, Woodhead Publishing Limited, Cambridge, 2000, ISBN1 85573 3854.

[20] Zhang S, Horrocks A R, Prog Polym Sci 2003,28,1517.

[21] Noumowe A, Cement and Concrete Research, 2005,35,2192.

[22] Rottstegge J, Zhang X, Zhou Y, Xu D, Han C C, Wang D, *J. Appl. Polym. Sci*., 2007, 103**,** 218.

[23] Caldas V, Brown G R, Nohr R S, Macdonald J G, Raboin L E, *J. Appl. Polym. Sci. ,*1997,65, 1759.

[24] Lee Seung Hwan, Youn Jae Ryoun, J Appl Polym Sci, 2008,109,1221.

[25] Chatterjee A, Deopura B L, Compos A , 2006, 37, 813.

[26] Rezaei F, Yunus R, Ibrahim N A,Mater Des 2009,30,260.

[27] Arrakhiz F Z, Elachaby M, Bouhfid R, Vaudreuil S, Essassi M, Qaiss A. Mater Des, 2012,35,318.

[28] Coats AW, Redfern JP. Kinetic parameters from thermogravimetric data, Nature 1964, 68,201.

[29] Bikiaris Dimitris N, Papageorgiou George Z, Pavlidou Eleni, Vouroutzis Nikolas, Palatzoglou Paraskevas, Karayannidis George P, J Appl Polym Sci, 2006,100,2684.

.....ൟ.....

SUMMARY AND FUTURE OUTLOOK

PP has been getting much attention over the years because it is a very durable polymer commonly used in aggressive environments including automotive battery casings, fuel containers etc. They are used to make bottles, fibers for clothing, components in cars etc. However, it has some shortcomings such as low dimensional and thermal stability. Materials such as metal oxides with sizes of the order 1–50 nm have received a great deal of attention because of their versatile applications in polymer/ inorganic nanocomposites, optoelectronic devices, biomedical materials, and other areas. They are stable under harsh process conditions and also regarded as safe materials to human beings and animals.

In the present investigation, PP is modified by incorporating metal oxide nanoparticles such as ZnO and TiO_2 by simple melt mixing method. Melt spinning method was used to prepare PP/metal oxide nanocomposite fibers. Various studies have been carried out on these composites and fibers.

In the first part of the study, ZnO nanoparticles were prepared from $ZnCl_2$ and NaOH in presence of chitosan, PVA, ethanol and starch. This is a simple and inexpensive method compared to other methods. Change in morphology and particle size of ZnO were studied. Least particle size was obtained in chitosan medium. The particles were characterized by using XRD, SEM, TEM, TGA and EDAX. Antibacterial properties of ZnO prepared in

chitosan medium (NZO) and commercial zinc oxide (CZO) were evaluated using a gram positive and a gram negative bacteria.

Melt mixing method was used to incorporate ZnO particles in PP. The incorporation of ZnO in PP matrix resulted in an increase in the tensile strength and modulus, reached a maximum at 1.5wt% concentration of ZnO and then decreased. In the case of PP filled with NZO 39.7% increase in tensile strength and 71.6% increase in tensile modulus was observed. CZO filled PP showed 29.5% increase in tensile strength at 1.5 wt% CZO and 28.7% increase in tensile modulus was observed at 0.5wt% of CZO. It is known that the interface between nanoparticles and polymer matrix can transfer stress, which results in an increase of the tensile strength of composite films. However, with increasing content of nanoparticles, aggregation may occur, which resulted in decreased contact area between the nanoparticles. Thus, the effective interfacial interaction is reduced, and the tensile strength of the films decreased at higher concentration. The dynamic mechanical properties of PP were increased with increase in ZnO concentration. Torque value of the PP/NZO composites were higher than that of neat PP and PP/CZO composites. TGA studies indicated an improvement in thermal stability of PP by the addition of ZnO. Enhancement of thermal stability of polymers in presence of fillers may be due to the hindered thermal motion of polymer molecular chains. Coats–Redfern method was used to determine the kinetics of degradation behavior of PP and PP/ZnO composites. Significant increase in activation energy also indicated increase in thermal stability. In NZO filled PP, MFI increased by the addition of low concentration of NZO, indicated an increase in the flow of the polymers. At low concentration nanoparticles may favor orientation and flow due to the small size of NZO. After adding 1wt% NZO to the PP the MFI value decreased gradually. It indicated the structure of nanoparticles was interconnected to hinder the molecular motion of polymer

chains. NZO filled PP films showed higher transparency when compared to CZO filled PP films. This may be due to decrease in spherulite size of PP and also due to smaller ZnO particles in the composites, since larger particle scatter the visible light and product become more opaque. LOI of PP was increased by the addition of ZnO. The improvement in the flame retardancy was attributed to the filler dispersion in the PP matrix. Differential scanning calorimetric studies showed increase in crystallinity of PP by the addition of ZnO. X-ray diffraction studies of neat PP and composites indicated the presence of α phase of monoclinic PP. PP has tertiary carbon atoms and is known to be very vulnerable to oxidative degradation under influence of elevated temperature and sunlight. ZnO nanoparticles play an important role in stabilizing the PP molecules and delay the photodegradation products by acting as screens. Mechanical, morphology and IR studies were carried out before and after thermal and UV ageing. PP/ZnO composites showed improved properties when compared to neat PP. NZO filled PP showed better properties than CZO filled composites.

Melt spinning was used for the preparation of neat PP fiber and PP/ZnO composite fiber. Mechanical properties of the fiber was increased by the addition of ZnO. Tenacity of PP fibers was increased by the addition of ZnO, reached maximum at 0.5wt% and decreases. The increase in tenacity was 71.5wt% at 0.5wt% of NZO and 41.1% for 0.5 wt% CZO added PP fiber. The increase in modulus was about 38.6% for 0.5 wt% of NZO and 36.7% in case of 0.5wt% of CZO compared to that of neat PP fiber. Increase in tenacity may be due to the good orientation of NZO in the fiber. Thermal stability of the PP fiber was increased significantly in presence of NZO. The temperature at which maximum degradation take place was increased by 38.9^0C by the addition of 3wt% NZO. ZnO had no significant effect on the crystallinity of PP fiber. X-ray diffraction studies indicated similar crystal form of PP fiber and

composite fibers. Morphology of the cross section of the neat fiber was different from the morphology of the CZO filled, NZO filled PP fiber indicated difference in dispersion and molecular orientation of the fibers. PP fiber and NZO filled fiber did not attacked significantly by bacteria.

In the second part of work, TiO_2 nanoparticles were prepared by sol-gel method and wet synthesis. Effect of preparation method on the crystal structure and particle size was investigated. Sol gel method gave anatase form and wet synthesis method gave rutile form of TiO_2. The particles were characterized by XRD, SEM, TEM, TGA and EDAX. Antibacterial properties of TiO_2 was evaluated using a gram positive and a gram negative bacteria.

PP was modified with TiO_2 prepared by wet synthesis method (NTO) and commercial TiO_2 (CTO). Mechanical and dynamic mechanical properties of PP were found to be improved by the addition of TiO_2. Tensile strength of PP was increased by 26.1% by the addition of NTO. An increase of 23% in tensile modulus was observed by the addition of 1 wt% of NTO. PP showed better thermal stability in presence of TiO_2. Differential scanning calorimetric studies showed increase in crystallinity of PP by TiO_2 addition. X-ray diffraction studies of neat PP and composites indicated the presence of α phase of monoclinic PP. MFI of PP was increased by adding low concentration of NTO, whereas CTO added PP showed a decrease in MFI. Transparency of the PP films were decreased by the addition of TiO_2. PP with NTO filled films showed higher transparency when compared to CTO filled PP films. LOI of PP was increased by the addition of TiO_2. Mechanical, morphology and IR studies showed improved performance of composites even after thermal and UV ageing compared to neat PP. NTO filled PP showed better properties than CTO filled composites.

PP/TiO_2 nanocomposites fibers were prepared by melt spinning method. Mechanical properties of PP fiber increased by the addition of TiO_2 nanoparticles. At 3 wt% of NTO, tenacity were increased by 72.7% indicated good orientation of TiO_2 in the PP fiber. At lower concentration, mechanical properties decreased and may be due to the lack of orientation of TiO_2 nanoparticles in PP fiber. Thermogravimetric analysis showed an increase in onset temperature, maximum degradation temperature and residue indicating high thermal stability. The temperature at which maximum degradation occured was increased by 37 ^{0}C at 0.5 wt% of NTO nanoparticles. DSC studies showed an increase in crystallization indicating that TiO_2 nanoparticles are acting as nucleating agents. Surface morphology study of fibers showed smooth surface even after the addition of nano TiO_2. SEM images of cross section of fiber show good dispersion of nanoparticles, which was the reason for improvement in mechanical and thermal properties. NTO filled PP fiber showed significant improvement in properties when compared to CTO filled PP fiber. PP fiber and NTO filled fiber showed excellent resistance to bacillus aereus.

It could be concluded that ZnO and TiO_2 are promising candidate to modify the performance of PP matrix and its fibers.

Future work

- Melt mixing of various matrix with this metal oxide reinforced PP fiber and evaluation of its properties, optimization of fiber length etc.
- Coating of conducting polymers to this PP/metal oxide nanocomposite films and fibers for conducting applications.
- Modification of various polymer matrix using these metal oxides.
- Modification of ZnO and TiO_2 for better properties

Applications of PP/metal oxide nanocomposite and its fibers

PP/metal oxide nanocomposites can be used for high strength applications. PP/metal oxide nanocomposites fibers can be used for making cloths, baby diapers etc. It can be used for making defense clothings because of its bacterial resistance and high strength. It can be used to make fishing net, ropes etc due to its improved properties.

Abbreviations and Symbols

ASTM	American Society for Testing and Materials
BCF	Bulked Continuous Filament
$CaCO_3$	Calcium Carbonate
CF	Continuous Filament
CFU	Colony forming unit
CNT	Carbon nano tube
CS	Crystallite size
CTO	Commercial titanium dioxide
CVD	Chemical Vapour Deposition
CZO	Commercial Zinc Oxide
DMA	Dynamic Mechanical Analysis
DNA	De oxy ribo nucleic acid
DPA	Diphenylamine
DSC	Differential Scanning Calorimetry
EDAX	Energy dispersive X ray analysis
FTIR	Fourier Transform Infrared
GPa	Giga Pascal
gpd	gram per denier
iPP	isotactic polypropylene
kJ/mol	Kilo Joule per mole
LDPE	Low density poly ethylene
LOI	Limiting Oxygen Index

MFR	Melt flow rate
MHz	Mega Hertz
mm/min	Milli meter per minute
N/mm^2	Newton per millimetre squre
NCIM	National collection of industrial organisms,Pune.
nm	nanometer
NTO	Titanium dioxide prepared by wet synthesis
NZO	Zinc oxide prepared in chitosan medium
PP	Polypropylene
PVA	Polyvinyl alcohol
SEM	Scanning Electron Microscopy
SWNT	Single walled carbon nanotube
TEM	Transmission Electron microscopy
Tex	Textile
TGA	Thermo gravimetric analysis
TiO_2	Titanium dioxide
UV	Ultraviolet
Xc	Percentage crystallinity
ZnO	Zinc oxide

List of Publications

Publications in international journals

[1] Saisy K Esthappan, Suma K K, Rani Joseph, Effect of titanium dioxide on the thermal ageing of polypropylene, *Polymer Degradation and stability*, 97 (2012), 615-620.

[2] Saisy K Esthappan, Suma K K, Rani Joseph, Thermal and mechanical properties of polypropylene/titanium dioxide nanocomposite fibers, *Materials and Design*, 37, (2012), 537-542.

Publications in Conferences

[1] Saisy K Esthappan, Suma K K, Sreejesh P.R, Sinto Jacob and Rani Joseph, "Use of nano titanium dioxide for the improved mechanical and thermal properties", International conference POLYCHAR 19,2011, Kathmandu, Nepal.

[2] Saisy K Esthappan, Suma K K, Sreejesh P.R, Sinto Jacob and Rani Joseph "Effect of metal oxides on the Mechanical properties of polypropylene", International conference ICMF 2011,Thrissur,India.

[3] Saisy K Esthappan, Sreejesh P R, Sinto Jacob, Anuraag Srivastav, Mukesh Kumar Sinha, nanocomposite fibers through melt spinning", International conference,Functional Polymers, 2011,Calicut, India.

[4] Saisy K Esthappan, Suma K K, Sreejesh P.R, Sinto Jacob and Rani Joseph; "Melt spinning and mechanical properties of polypropylene /titanium dioxide nanocomposite fibers", International conference on Polymer Science and Engineering Emerging Dimensions, 2010, Chandigarh, India **[Best poster award]**.

[5] Saisy K Esthappan, Suma K K and Rani Joseph; “Effect of titanium dioxide on the properties of polypropylene” International conference on Advancements in Polymeric Materials 2010, Bhubaneswar, orissa, India.

[6] Saisy K Esthappan and Rani Joseph; “Polypropylene nano zinc oxide composites”, International conference on Advances in Polymer Technology, 2009, Kochi, India.

[7] Saisy K Esthappan, Shiny Palaty, Honey John and Rani Joseph; “Studies on the conductivity and tensile properties of polyaniline blended natural rubber latex”; International conference on Advances in Polymer Technology,2008, Kochi, India.

[8] Saisy K Esthappan and Rani Joseph; “Mechanical properties of epoxy polymer filled with nano silica”, Annual research symposium, CHEMFERENCE, 2009, Chennai, India.

[9] Saisy K Esathappan and Rani Joseph,“Modification of Polyester resin using nanosililca” UGC sponsored National seminar on Quantum chemistry and Nano Techniques, 2009, Kochi, India.